3 8006 10104 7184

42/446

CRANFIELD INSTITUTE OF TECHNOLOGY

SCHOOL OF MECHANICAL ENGINEERING

Ph.D. THESIS

Session 1988-89

SALIM ABID TABASSUM

SOLAR REFRIGERATION
Evaluation Of Technical Options and Design Of A Solar-Generator-Adsorber For A Novel Adsorption Refrigerator

(Volume I)

SUPERVISOR PROF. BRIAN NORTON

SEPTEMBER 1989

This thesis is submitted for the degree of DOCTOR OF PHILOSOPHY

ABSTRACT

Various technical options for developing a solar operated refrigerator have been discussed. Their suitability for being used as a vaccine store for the conditions specified by the World Health Organization Expanded Programme on Immunization (EPI) have been evaluated.

A model to predict the performance of a photovoltaic refrigerator have been developed and used to identify factors which influence its performance. It was concluded that it can be more competitive in areas where insolation is high and sunshine hours are long. It has been proposed that ice-lined refrigerators, which would run during the day, may be more economical and eliminate the need for a battery storage.

The option of operating an 'Electrolux' absorption refrigerator with evacuated tube heat pipe collectors has been assessed. It was concluded that the operation was not possible without a major re-design of the commercially available models. However, it was proposed that coordination of the EPI with other development programmes may be useful. It is proposed to build, with this coordinated effort, biogas plants. Biogas can then fuel the modified burner of the kerosene fueled absorption refrigerators. This may well prove to be a cheaper option.

Characterization of various adsorption pairs has been done using the experimental rig developed for the purpose. The influence of various properties of adsorption pairs on the performance of an adsorption

refrigeration cycle has been studied. It was observed that the generation temperature in an adsorption refrigeration cycle (or a bivariant absorption system), for a specified operating regime, was only a function of the refrigerant.

A relationship between the refrigerant properties and the generating temperature for specified operating conditions was developed. Using this relationship it was established that ammonia and methanol cannot be generated at temperatures below 120°C for WHO/EPI specified operating conditions, if the condenser was air-cooled.

A novel idea of direct absorption of solar radiation into the activated carbon bed is put forward to combat the temperature differential of 24°C, in a conventional design of SGA, between the carbon and the metal container. The idea was practically implemented by replacing the top of the metal box by transparent glass sheet. The seal between the metal container and glass imposed practical difficulties in that design but the tests proved that the idea had potential. A new tubular design of the SGA is proposed finally which is hoped to bring improvement to the performance of activated carbon adsorption refrigerators.

ACKNOWLEDGMENTS

I would like to express my very deep gratitude to Prof Brian Norton, my supervisor, without whose warm and enthusiastic support the completion of this work might not otherwise, have been reached.

I would also like to thank all SME staff and other friends who were always there to help in every moment of need.

My thanks go as well for the test area staff who afforded me much technical help and advice during the experimental work.

This work could not have even started without the enormous support and sacrifices of my parents, wife and children. My special thanks go to my wife who, despite her ill health, was able to support me, both finacially and morally, during the last 8 months after my financial assistance was terminated.

I am indebted to the Overseas Development Administration who were able to sponsor me, for over two years, to carry out the research work. I hope this would prove to be a significant contribution towards building a better future for my country, Pakistan.

Over and above all, I am grateful to Almighty Allah for bestowing upon me the ability to bring this work to a logical conclusion.

SUMMARY OF CONTENTS

TABLE OF CONTENTS VOLUME I

LIST OF FIGURES VOLUME I

LIST OF TABLES VOLUME I

NOMENCLATURE

A	area	m^2
A_C	collector area	m^2
AMx	air mass x	
C_x	specific heat capacity of material x	$Jkg^{-1}K^{-1}$
d	diameter	m
$_x$	emittance of material/surface x	
Gr	Grashof number	
g	gravitational constant	mS^{-2}
h_c	convective heat transfer coefficient	$Wm^{-2}K^{-1}$
h_r	radiative heat transfer coefficient	$Wm^{-2}K^{-1}$
I	average monthly irradiation	Jm^{-2}
k_x	thermal conductivity of material x	$Wm^{-1}K^{-1}$
L	length	m
m	concentration of refrigerant	$kgkg^{-1}$
m_0	maximum adsorbable amount of refrigerant	kgS^{-1}
Nu	Nusselt number	
p	pressure of vapours	Nm^{-2}
p_s	saturation pressure of vapours	Nm^{-2}
Pr	Prandtl number	
Q	energy per unit time	W
q	enrgy per unit time per unit area	Wm^{-2}
q_{st}	heat of adsorption	$kJkg^{-1}$
Ra	Raleigh number	
Re	Reynold number	
T	temperature	K
t	time	S
t_x	thickness of component x	m
U	overall heat transfer coefficient	$Wm^{-2}K^{-1}$
V	velocity	mS^{-1}
v	specific volume	m^3kg^{-1}
W	adsorption space	m^3
x	ratio of vapours to liquid in a mixture	

GREEK

α	absorptance,thermal diffusivity	m^2S^{-1}
β	volumetric coefficient of expansion	K^{-1}
η	efficiency	
θ	slope	degrees
λ	wavelength	micron
μ	absolute viscosity	$kgm^{-1}S^{-1}$
ν	kinematic viscosity	m^2S^{-1}
ρ	density of material x	kgm^{-3}
σ	Stefan-Boltmann constant	$Wm^{-2}K^{-4}$
τ	transmittance	

SUBSCRIPTS

a	ambient, air
b	battery
c	charcoal, condenser, collector
e	evaporator
eff	effective
g	generator
i	inverter
m	methanol, maximum
sky	sky
t	top
vc	vapour compression cycle

CHAPTER ONE

Introduction

1.1 Objectives

The current study evaluates the technical options for utilizing solar energy for the refrigerated storage of vaccines and puts forward design proposals for the most appropriate option. Local manufacturing is given the most importance in selection. The vaccines contain live organisms, thus it is of utmost importance that these should be maintained at the prescribed temperatures during their transit from the manufacturer to the ultimate place of application. The term 'cold chain' describes the infrastructure which ensures this.

1.2 Expanded Programme on Immunization (EPI): aims and hurdles

Effectiveness of the cold chain is the key to the ultimate success of the World Health Organization's 'Expanded Programme on Immunization' (EPI) which aims at achieving, by the year 1990, the effective routine immunization of all children and expectant mothers against the six major diseases: diphtheria, measles, whooping cough, poliomyelitis, tetanus and tuberculosis [1,2]. The greatest difficulty faced by the EPI is in the developing countries where 80% of the population lives in rural areas often unconnected by rail or even satisfactory road links and not served by a national electricity grid. The major energy source in these parts of the world is generally animal dung and/or firewood. The most dominant logistics problem of the EPI is to transfer successfully the heat-sensitive vaccines from the port of entry to the vaccinators in such remote rural health centres.

The cold chain is specific to the country in which it operates. However, many of the major levels involved, from the manufacturer to the vaccinator, are common. The major difficulties being faced by the EPI are at the last level of the cold chain i.e a rural health clinic. The traditional alternatives to electricity - kerosene and bottled gas - are now becoming less practical as the escalating prices of oil makes these fuels more expensive and beyond affordable limits of the developing nations. Even if kerosene supplies are available readily, the refrigeration units which run on this fuel are unreliable and their performance falls short of providing a refrigerated vaccine store [3]. Another major problem with kerosene is the level of purity. Contaminated kerosene can seriously affect the efficiency of the burner. There are other hazards associated with kerosene fueled refrigerators as well. For instance, as pointed out in [4], contaminated oil can block the supply pipe, or a break in the pipe can be a potential fire hazard, the wicks need constant cleaning and the glass acting as a windsheild is not too strong.

Solar-operated refrigeration provides an answer to these problems. The household vapour compression refrigerator powered by the solar electricity generated through the photovoltaic panels has been on the market for quite some time. But high initial cost, recurrent expenditure on the maintenance and replacement of storage batteries and the need for high technology photovoltaic cells and associated control equipment have been prohibitive to their widespread acceptance. In this report a low cost, 'low' technology, rugged and reliable refrigeration system suitable for a rural health clinic (i.e. the lowest level in the cold chain) is proposed. It is based

on an adsorption refrigeration cycle employing activated carbon as the adsorbent and methanol as the refrigerant. A novel design for a solar-generator-adsorber (SGA) is proposed in which the solar radiation is absorbed directly by the activated carbon bed.

1.3 Structure of this thesis

This thesis has been written with the intention;

a) specific to describe the up-to-date research of solar refrigeration

b) to serve as a comprehensive guide on the technology and art of solar refrigeration, for its prospective users, for individuals and organizations alike.

c) to identify the areas for further development and putting forward some proposals for the future researchers.

The report has been divided into nine chapters; each one fully comprehensive and equipped with a list of references at the end of each one.

Chapters two and three present the review of refrigeration and solar energy harnessing techniques respectively. In chapter four the fundamentals of adsorption process have been discussed with a specific view to its application to refrigeration. The process is quite complicated and yet not completely understood. An attempt has

been made to present, in a simple manner, the basic theory of gas adsorption at solid surfaces. Various models representing the adsorption equilibrium have been assessed and compared. A set of equations has been developed to ascertain the thermodynamic performance of adsorption refrigeration cycle and subsequently employed to compare the performance of various adsorption pairs.

Various alternative techniques to build a solar refrigerator has been discussed in chapter five. A criterion has been devised to assess the feasibility of an option for vaccine storage. After initial survey three alternative proposals have been chosen for their further detailed evaluation. An up-to-date survey of prototypes and commercial units has been presented at the end of the chapter.

Chapter six deals with the further evaluation of the three selected options. It is subdivided into three parts. Part one deals with the photovoltaic vapour compression refrigeration units. For the assessment of the system a detailed but simple mathematical model has been developed. The model enables one to work out the size of photovoltaic array and the capacity of battery storage system for the given refrigeration capacity on the basis of monthly averaged weather data.

In part two of the sixth chapter the option of operating an 'Electrolux' absorption refrigerator by the heat collected through Thermomax evacuated tube heat pipe collectors has been evaluated. Intermittent solid sorption refrigeration is the subject of the

third part of the chapter six. Using the basic thermodynamics of adsorption, a new relation for the generation temperature has been developed in terms of various cycle temperatures. This relation provided a basis to ascertain the suitability of a refrigerant for the solar operated adsorption refrigerators. Various absorption and adsorption pairs were evaluated and activated carbon and methanol was found to be the most suitable.

Chapter seven narrates the design, construction, operation and results of the adsorption pair characterization rig. The detailed assessment of the results has been carried out. The results have been compared with those from other sources. Arguments have been put forward when the results differed. The anomalies arisen out of the results have been explained.

Chapter eight of the report deals with the implementation of the novel idea of absorbing the solar radiation directly by the activated carbon bed. A new design of a solar collector/generator/ adsorber (SGA) has been tested and the results reported here. The results provided a qualitative evidence that the idea was practical. The design of the SGA was not satisfactory and alternatives were proposed.

The final chapter of the thesis, i.e. chapter nine, summarizes the whole work described in this report and takes inferences out of it. Proposals for future work has been put forward in this chapter which include an elaborate design of a novel SGA for activated carbon methanol adsorption refrigerator.

REFERENCES

1 World Health Organization, 'Expanded programme on immunization', WHO chronicle, 33, Geneva, 1979.

2 United Nations Children's Fund, 'Universal child immunization by 1990', Assignment Children, 69/72, 1985.

3 World Health Organization, 'Solar powered refrigeration for vaccine storage and icepack freezing, status summary, June 1985' WHO document EPI/CCIS/85.4, 1985

4 Perkins, F.T., 'The need for stable vaccines in the developing countries', Proceedings, Symposium on Stability and Effectiveness of Measles, Poliomyelitis, and Pertussis vaccines, 28 & 29 september 1976, Yugoslav Academy of Sciences and Arts, Zagreb, 1976.

CHAPTER TWO

Refrigeration : An Overview

2.1 The process of refrigeration

Refrigeration is the thermodynamic process by which the temperature of a space or an article is reduced and maintained below the ambient. A refrigerator achieves this by absorbing heat at a lower temperature from the cooled space and transforming it so that it is rejected at a higher temperature to the surroundings.

A variety of techniques have been devised to produce refrigeration to cater for a wide range of applications. Though they differ, all these techniques extract heat from the cooled space by evaporating a saturated or subcooled liquid called a refrigerant. Where they differ is in the thermodynamic process employed to enable the refrigerant to reject that heat at a higher temperature to the surroundings.

2.2 An ideal cycle: the Carnot refrigerator

An ideal reversible thermodynamic refrigeration cycle is the reversed Carnot cycle, which consists of two isothermal and two isentropic processes. Figure 2.1a shows a layout of system components, and fig 2.1b represents the cycle processes on a T-s (i.e., Temperature-entropy) diagram. The processes trace out an area in an anti-clockwise sense indicating a negative net work. This means it is a cycle which requires external work to be done for its completion. The cycle uses a wet vapour as a refrigerant. This vapour is compressed isentropically in a compressor from a low pressure and temperature (state 1) to a higher pressure and

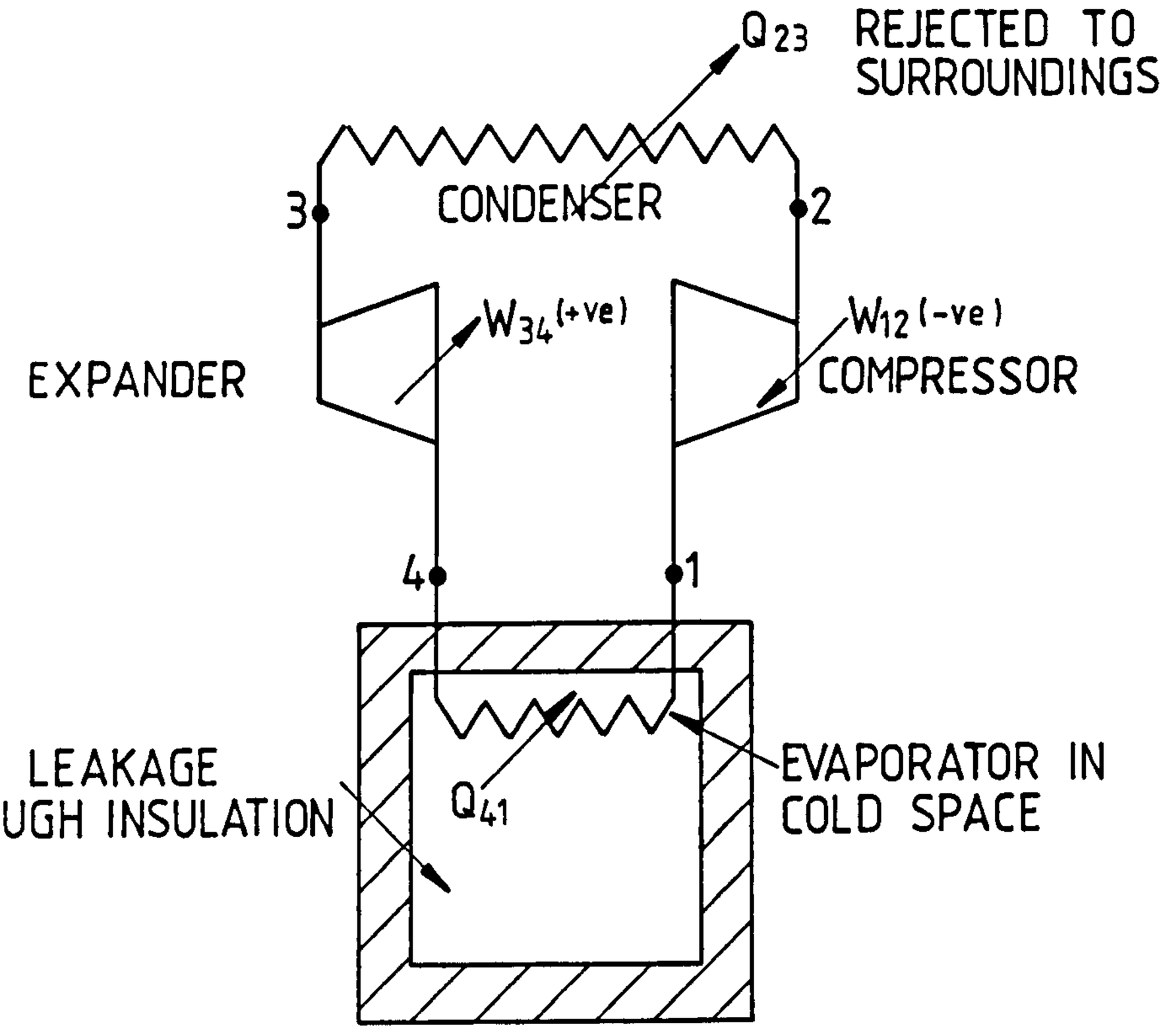

(a)

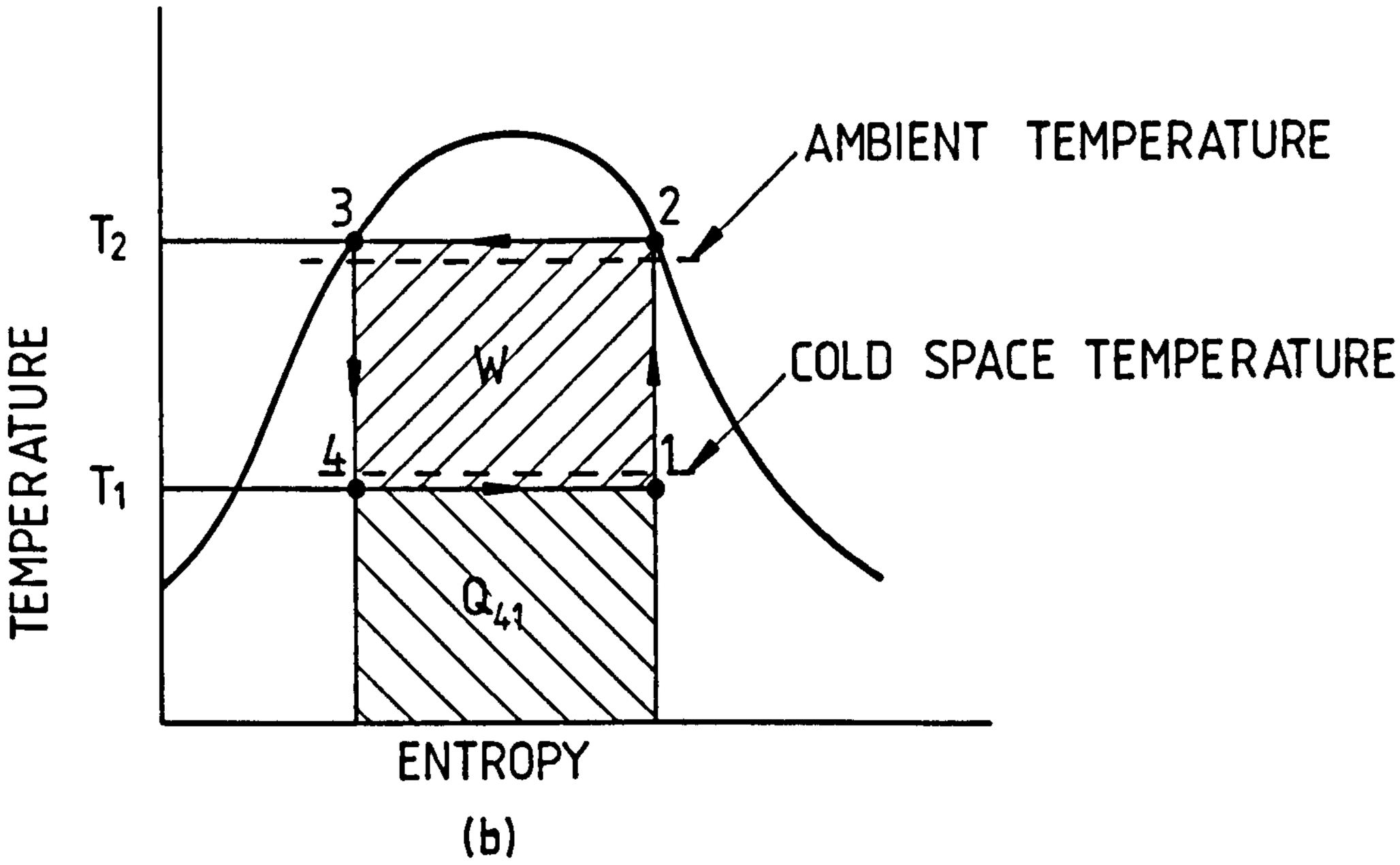

(b)

Fig 2.1 Carnot refrigerator: a) system layout
b) thermodynamic cycle represented on a T-s diagram

temperature (state 2). It is passed through a condenser in which it is condensed at a constant pressure to state 3. The fluid is then expanded isentropically in an expander, which is coupled to the compressor, to its original pressure (state 4), and is finally evaporated at constant pressure to state 1.

Coefficient of performance (COP) of a refrigerator indicates its effectiveness and is defined as

$$COP = \frac{\text{refrigerating effect}}{\text{energy input}} = \frac{Q_{41}}{W} = \frac{T_1}{T_2 - T_1}$$

Figure 2.2 shows the variation of COP of a Carnot refrigerator with typical values of T_1 and T_2. It is clearly evident from the figure that the COP reduces greatly with the increase in heat rejection temperature. Taking a practical situation where heat rejection is at ambient temperature of 40°C and and heat extraction is at -10°C, the Carnot COP will be 5.26. In an actual refrigerator, due to process irreversibilities and finite size of components, COP is much less than the ideal Carnot COP.

Due to incorporation of impossibly idealized processes, this cycle is not practical. However,

(i) It sets the upper performance bounds for a practical refrigerator.

(ii) It provides a basis for rating the performance of practical systems.

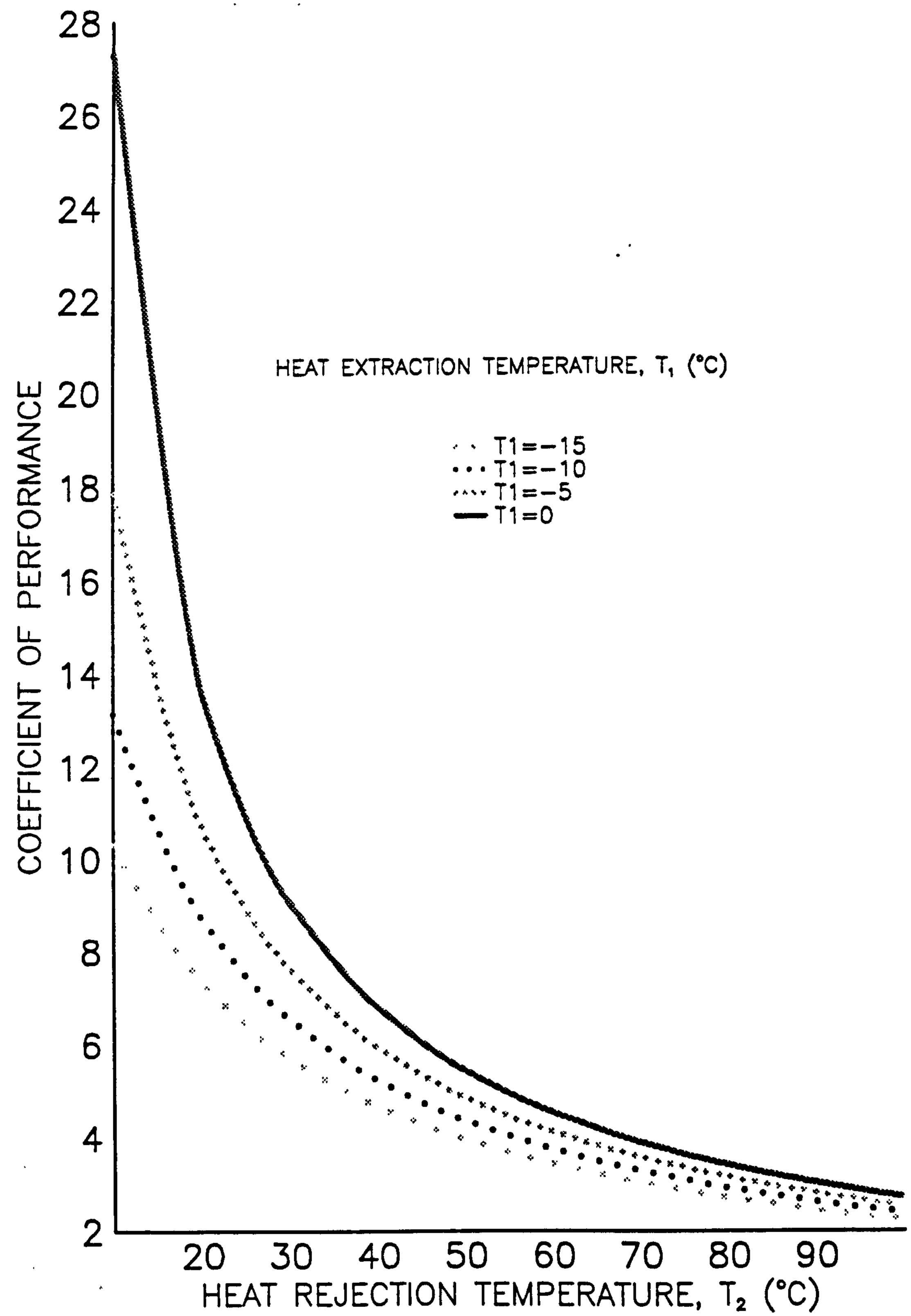

Fig 2.2 Performance curves of a Carnot refrigerator

2.3 Practical refrigeration techniques

An ideal refrigerating cycle has just been described above which is not possible practically. Working limitations of compression and expansion devices and the rates of heat transfer which are expected in practical devices restrict the selection of thermodynamic processes which can be used practically in working refrigerators. For instance no expansion or compression is possible practically without heat transfer due to friction. This fact turns the reversible isentropic processes 1-2 and 3-4, shown in figure 2.1, into irreversible polytropic processes. Therefore, where a practical refrigeration cycle will try to duplicate the ideal reversed Carnot cycle, it will have to employ the practical processes reducing its performance considerably below that of the ideal cycle.

The different refrigeration techniques which has so far been put into practice are discussed in the next sections.

2.3.1 Open cycle evaporation

The underlying principle is that the refrigerant, by evaporating under ambient conditions, extracts its latent heat of vaporization from its surroundings; consequently the surrounding temperature is reduced. The centuries old technique of producing chilled drinking water by storing them in unglazed porous pots, in suitable climates, relies on this principle. Small scale cabinets fitted with wicks onto the side walls and equipped with a water storage tank had been used to keep food cool.

Being an open cycle process this needs a cheap and readily available refrigerant e.g. water. But climatic conditions impose the greatest limitation of all. Wet-bulb temperature is the limit of refrigeration produced by evaporation of water.

2.3.2 Vapour-compression cycle

A standard vapour-compression cycle is shown in fig 2.3. This is a practical version of the reversed Carnot cycle. Comparing it with figure 2.1, following differences can be spotted:

(i) process 3-4 does not take place a) isentropically and b) in an expander,

(ii) state 1 is moved from wet region to the saturated vapour line, and

(iii) state 2 lies in the superheated region.

All these changes have been forced upon by the practical working limitations inherent in the devices which carry out these processes. Let us consider the modifications one by one.

Energy is consumed overcoming friction, thus the process 3-4 cannot take place isentropically in an expander. Furthermore, much of the expansion work would be dissipated by mechanical friction. Under these circumstances, a simple throttling expansion would not result

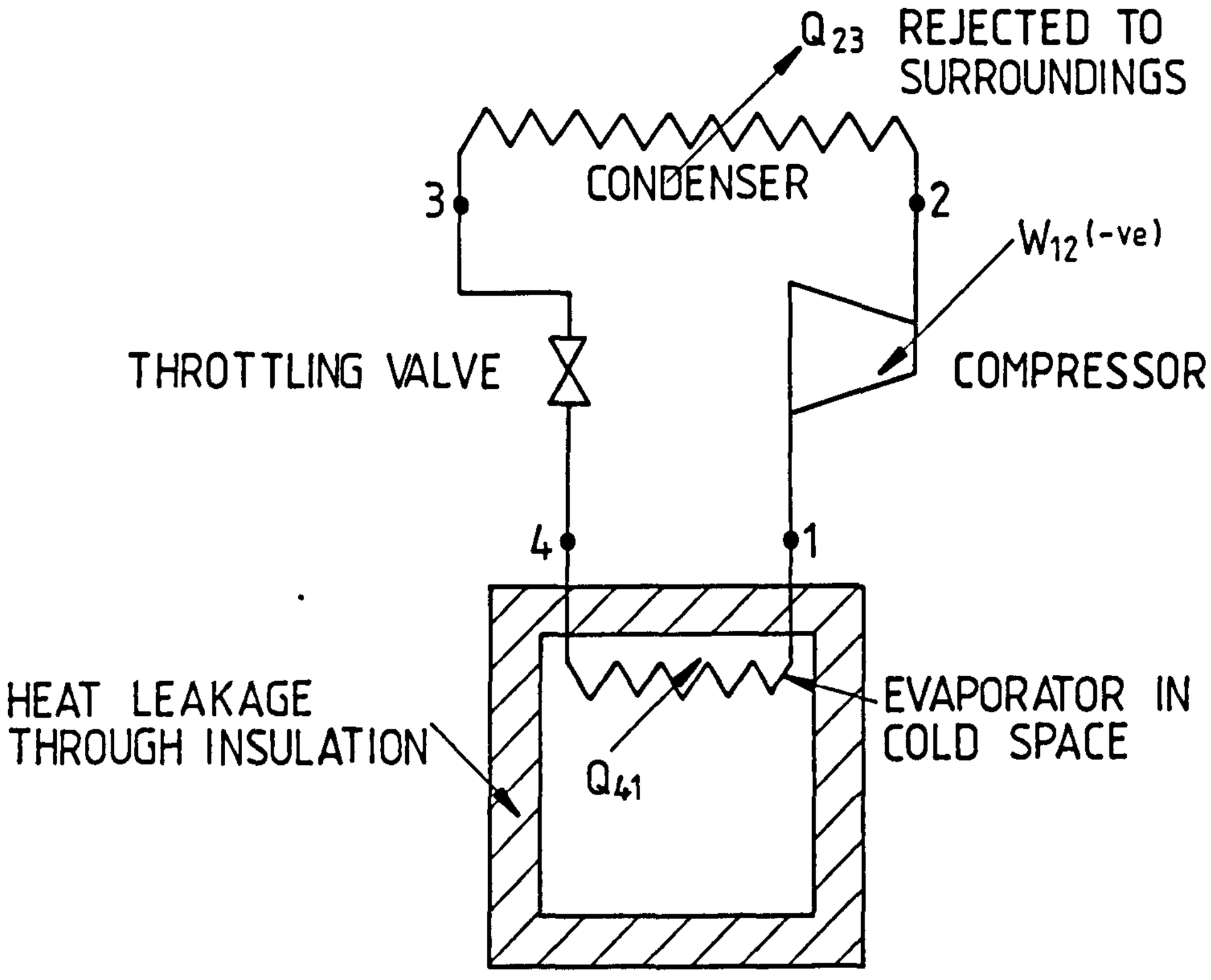

(a)

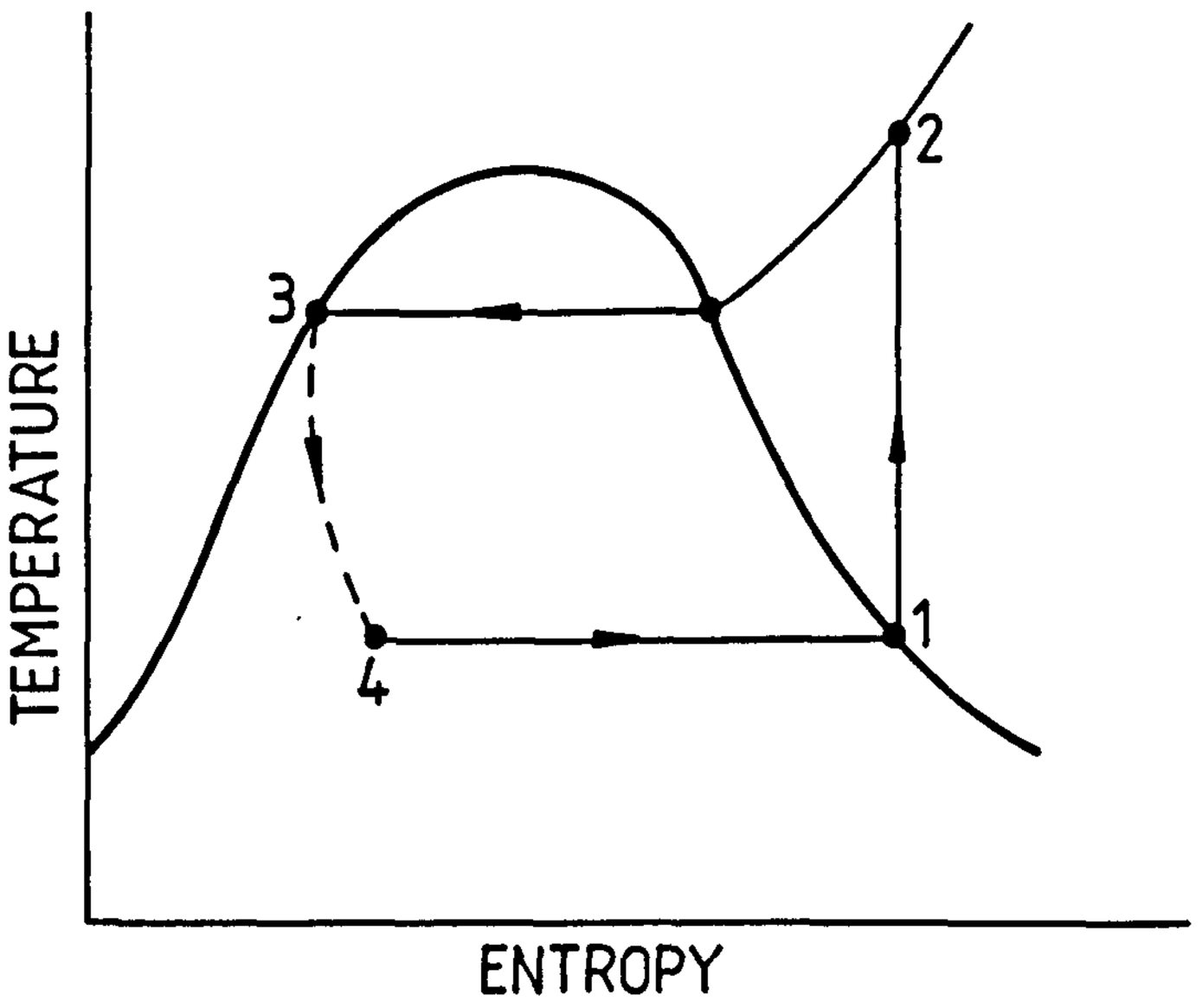

(b)

Fig 2.3 Vapour compression refrigerator: a) basic components
b) thermodynamic cycle represented on a T-s diagram

in a significant reduction in the performance of the real cycle, though it would introduce a worthwhile mechanical simplification of the plant. Thus, the expansion process 3-4 is not isentropic but is a constant enthalpy expansion process taking place in a simple throttling valve (see fig 2.3a). It is represented by a broken line on the T-s diagram (i.e fig 2.3b)indicating that no work transfer takes place through this process.

The reason for moving state point 1 onto the saturation line is two-fold. Firstly, due to varied nature of cooling load, it will be difficult to arrange for the evaporation process 4-1 to cease at state 1 in the wet region as shown in fig 2.1b. Secondly any liquid refrigerant, which will be part of the wet vapour, passing into the compressor would tend to wash away the lubricating oil. This is undesirable if the compressor is of a conventional reciprocating or positive-displacement rotary type. Moreover the oil would be carried to the evaporator where it might form a film on the tube surface imparing the heat transfer process. It is usual, therefore, to transfer a saturated or slightly superheated vapour into the compressor.

The shift in the position of state 2 is a consequence of moving the state point 1 onto the saturated vapour line.

2.3.2.1 Actual vapour-compression cycle

In an actual vapour compression system, the processes are further modified (see fig 2.4a) for practical reasons. The factors which force these changes are listed below.

a) The pressure drop occuring in the pipe-work and other components move the state points 1 and 2 to 1' and 2'.

b) To maintain the physical size of condenser within reasonable limits, most of the heat transfered in the condenser (process 2-3) must be rejected by virtue of an appreciable temperature difference. It is therefore possible to subcool the liquid after condensation to within a few degrees of surrounding temperature. This shifts the state point 3 into the liquid region to state 3'.

c) As a precaution against ingesting liquid into the compressor, vapours are always superheated in the evaporator. For this reason the state 1 is sketched in the superheated region as state 1'.

Pressure-enthalpy (p-h) diagram is another more convenient way of displaying the thermodynamic cycles. Both the standard (i.e. 1-2-3-4-1) and the actual (i.e. 1'-2'-3'-4'-1') vapour-compression cycles have been sketched on p-h diagram in fig 2.4b.

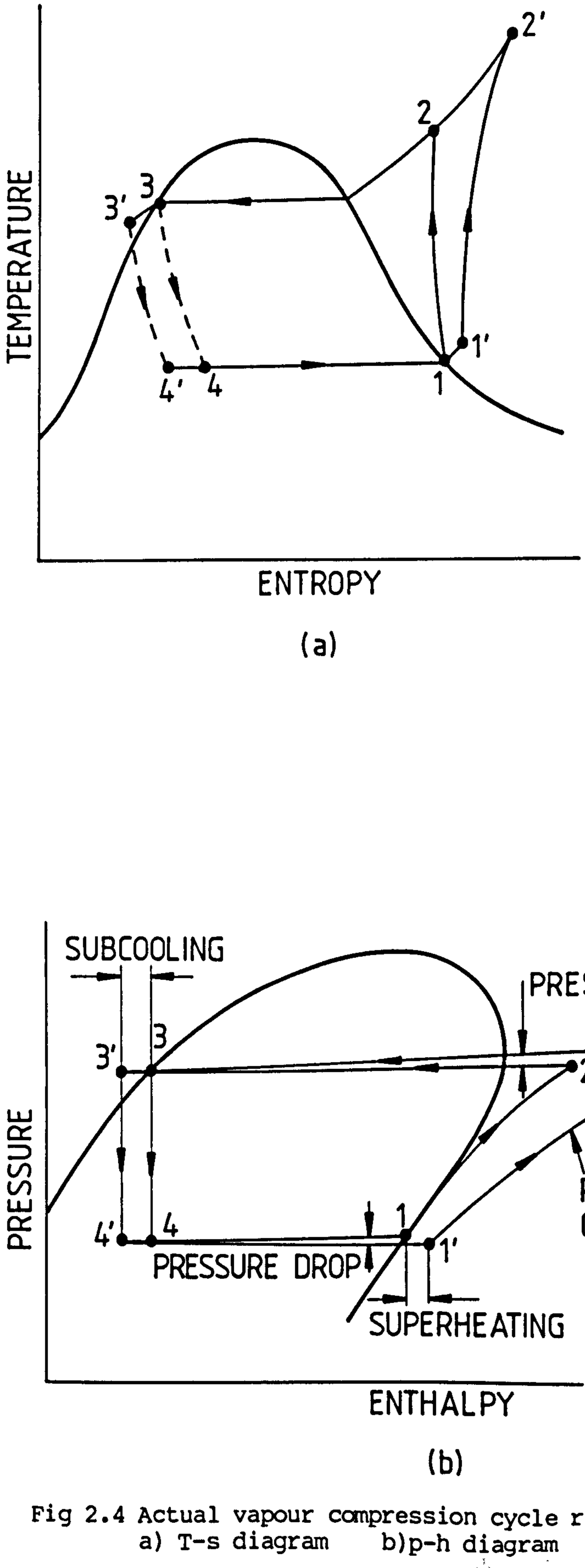

(a)

(b)

Fig 2.4 Actual vapour compression cycle represented on
a) T-s diagram b)p-h diagram

The p-h diagram of fig 2.4b clearly indicates that compression work 1'-2' is greater than the work done in process 1-2. This lowers the COP of the actual vapour-compression cycle. In general it is in the region of 3-5.

2.3.3 Vapour sorption cycle

Certain liquids and gases can be dissolved into certain liquids and solids. The amount of vapours dissolved is a strong function of temperature and pressure of the 'mixture'. Large quantities of vapours can be dissolved at low temperature and on subsequent heating of the 'mixture' the vapours can be removed from the sorbent. This principle forms the basis of a vapour sorption refrigerator.

This process of dissolution of vapours into liquids and solids is catagorized further into two broader catagories namely; absorption and adsorption. Absorption of vapours by liquids and solids generally involves some kind of chemical bondage between the molecules of the two species involved in the process. Whereas adsorption is a purely physical phenomenon in which the binding energy is very much similar to the forces of cohesion.

In a vapour compression cycle, discussed above, the vapours are compressed in a compressor, and the work of compression is comparable with the the other energy transfer processes in the cycle. The compression work can be considerably reduced, however, if the vapour is dissolved in a suitable liquid or solid before

compression. After compression the vapour can be driven off by heating the solution and then throttled and evaporated in the usual way. This principle is employed in a sorption refrigerator.

Vapour sorption cycles are further divided into two catagories; i.e. the continuous cycles and the intermittent cycles.

2.3.3.1 Continuous vapour sorption cycle

A continuous vapour sorption cycle refrigerator is diagramatically shown in fig 2.5a. Comparison of fig 2.3a and fig 2.5a reveals that the compressor of a vapour compression refrigerator has been replaced by three components; i.e. a generator, an absorber and a solution pump. The system in general is partitioned into a high pressure side, comprising of a generator and a condenser, and a low pressure side which include an evaporator and an absorber. The pressure gradients between the two sides are balanced through two expansion valves and a solution pump.

Refering to fig 2.5b, the processes of condensation (i.e.2-3), throttling (i.e.3-4), and evaporation (i.e.4-1) take place in conventional components. After evaporation to state 1, the refrigerant vapour is fed into an absorber where it is dissolved (or absorbed) in another liquid called absorbent. This process takes place at a low pressure and a little above ambient temperature. The process of solution is exothermic and therefore is accompanied by the rejection of heat, Q_s, to the surroundings. This solution is then pumped to the required pressure, by a solution pump, to a

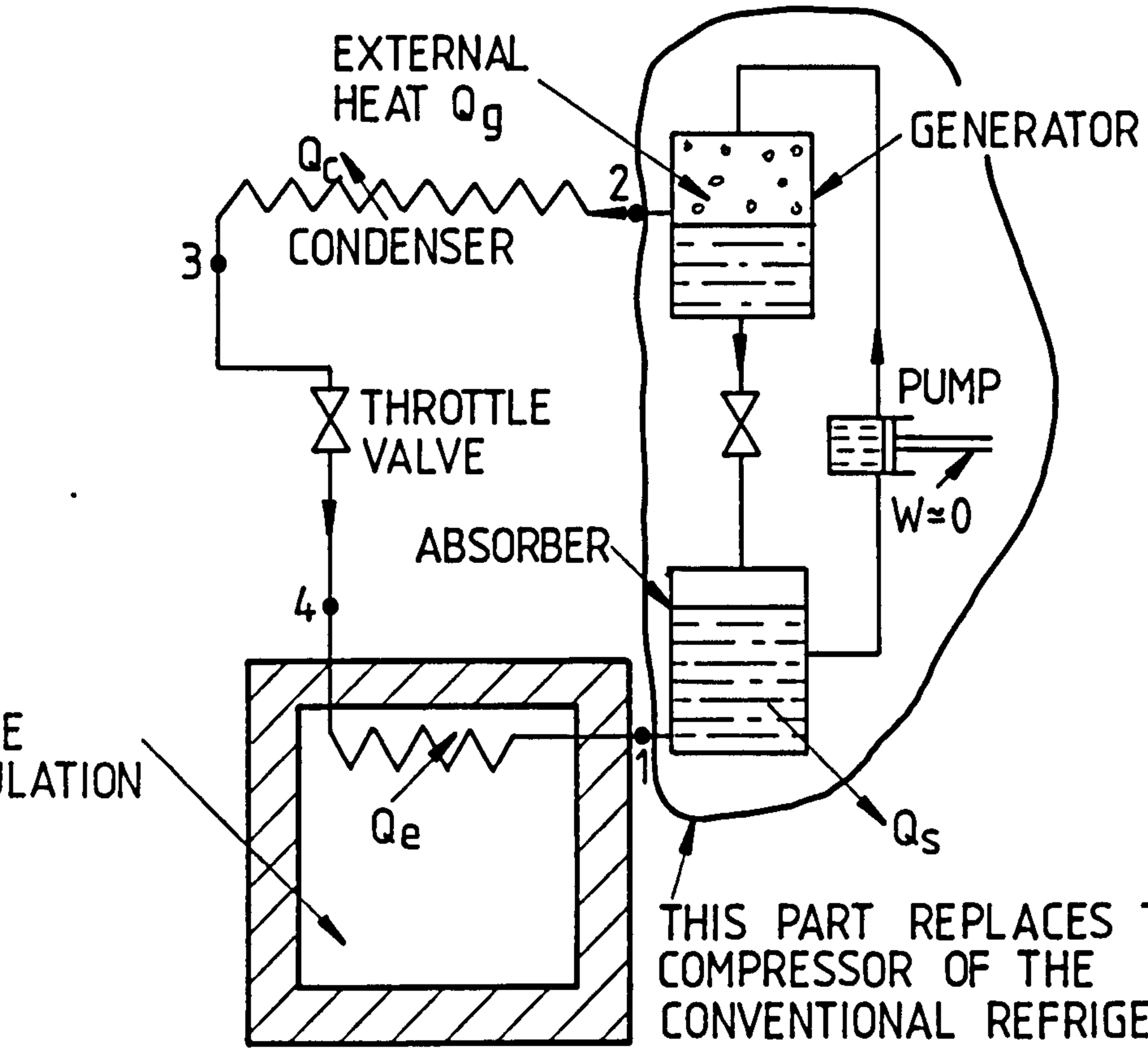

(a)

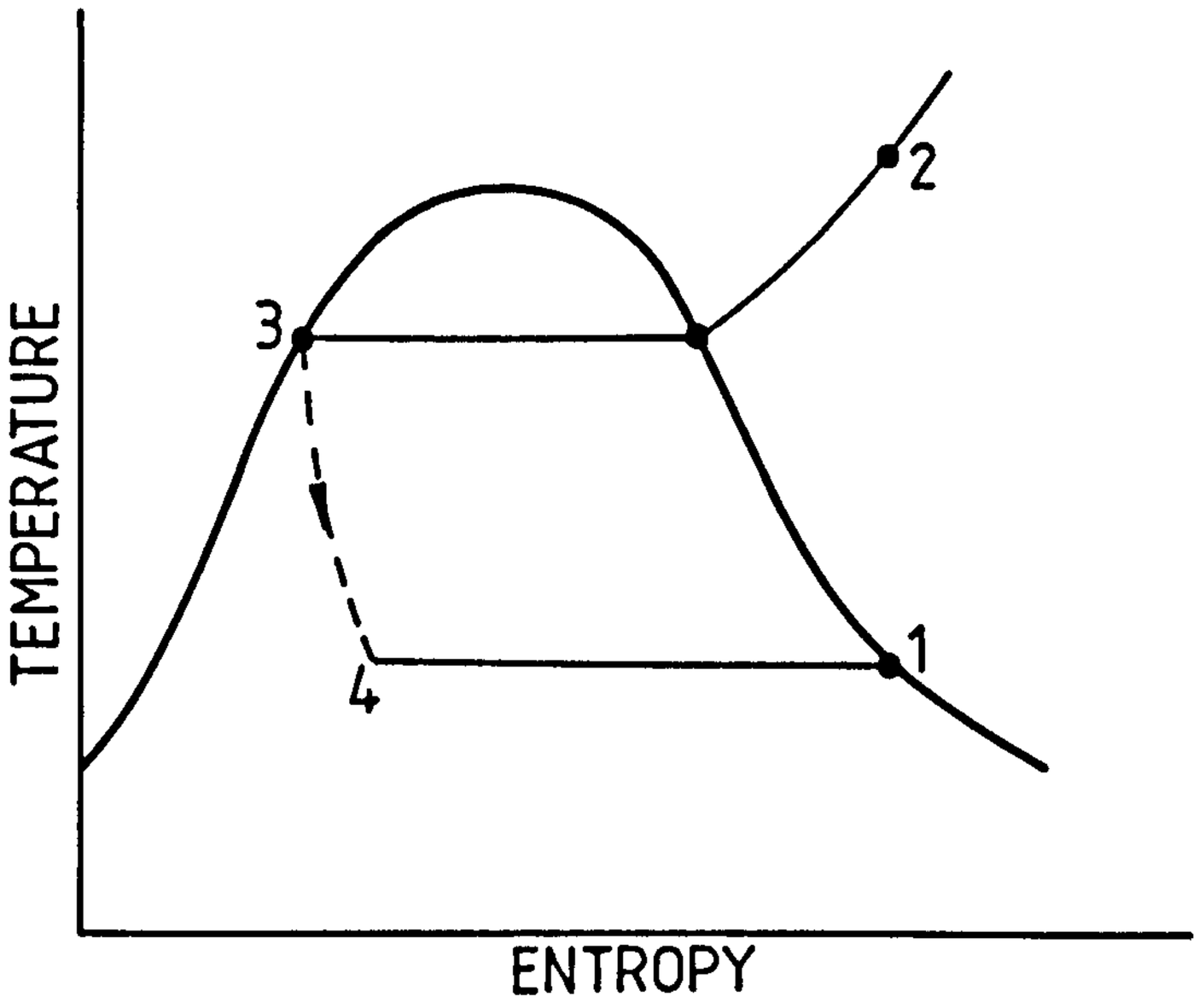

(b)

Fig 2.5 Continuous vapour sorption refrigerator: a) major parts
b) thermodynamic cycle represented on a T-s diagram

generator which is maintained at a temperature T_g. At a higher temperature solubility of a refrigerant in an absorbent is appreciably reduced. Thus the heat, Q_g, received in a generator removes the vapour from the solution. The process is called desorption. The high pressure high temperature vapour at state 2 is then fed into a condenser to complete the main cycle, while the remaining weak solution is returned to an absorber after reducing its pressure via a throttle valve. The thermodynamic analysis of the cycle can be performed as follows.

The energy is transferred in the form of heat at three temperature levels: 1) ambient temperature T_a at which heat is rejected during condensation and absorption, 2) temperature T_e at which heat is absorbed at the evaporator, and 3) the temperature T_g at which heat is supplied to the generator. The small amount of energy supplied to the solution pump can be neglected when compared to the above mentioned energy transfers. This whole picture is represented in fig 2.6 by the combination of a reversible carnot refrigerator and a reversible heat engine. The heat engine receives a quantity of heat Q_g at a temperature T_g and rejects heat at T_a while producing a quantity of work W_g. The efficiency of the heat engine is

$$W_g/Q_g = (T_g - T_a)/T_g$$

The refrigerator receives a quantity of heat Q_e at T_e and rejects heat at T_a while absorbing a quantity of work W_e. The coefficient of performance of the refrigerator is given by

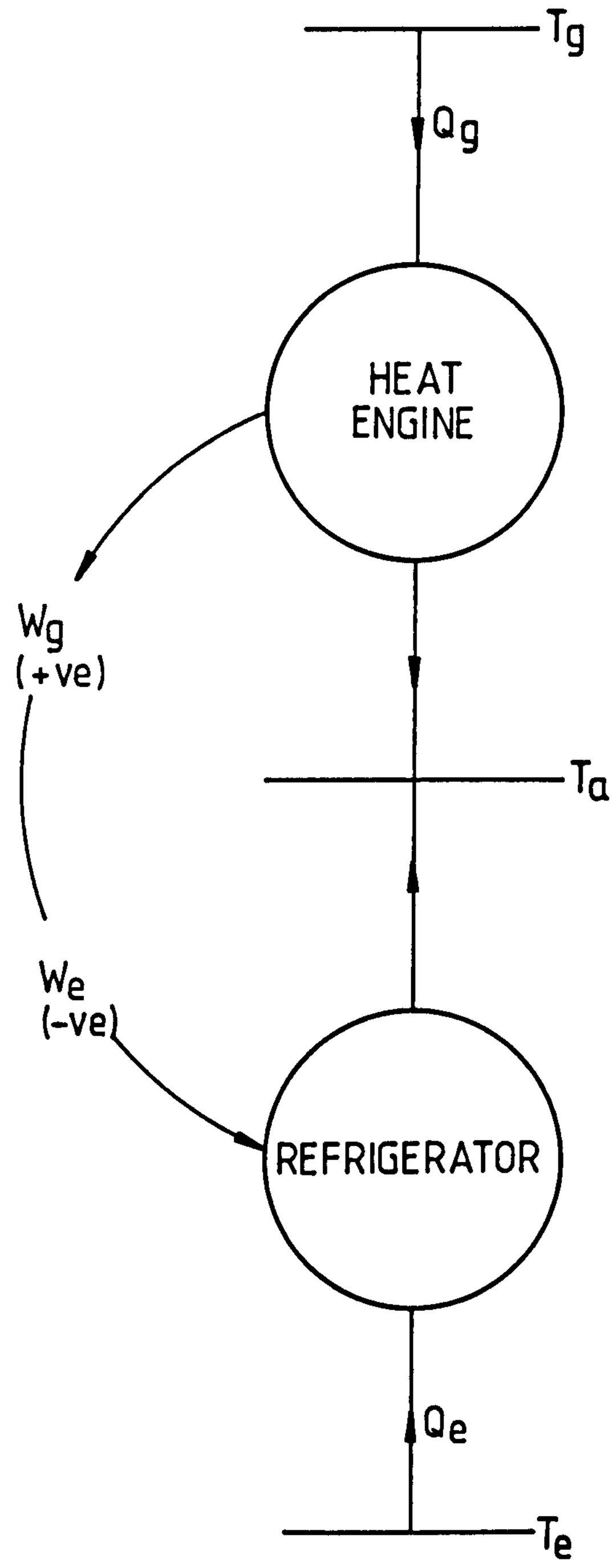

Fig 2.6 A reversible equivalent of a sorption refrigerator

$$-Q_e/W_e = T_e/(T_a - T_e)$$

The work produced by the engine is made equal to the work absorbed by the refrigerator so that the combination is equivalent to an absorption refrigerator with pump work equal to zero. Thus the coefficient of performance of absorption refrigerator, which is defined by Q_e/Q_g, will be

$$COP = T_e(T_g - T_a)/T_g(T_a - T_e)$$

Under the ideal assumptions of reversible processes this gives the limiting coefficient of performance for an absorption refrigerator. With normal operating temperatures it gives a value of more than one. But in practical situations the coefficient is always less than unity.

The most widely used absorption pairs are ammonia-water and lithium bromide-water. The later is used mainly in airconditioning plants because, water being the refrigerant, sub-zero temperatures cannot be produced using this pair. The one major drawback of using the ammonia-water absorption pair is the evaporation of water during the generation of ammonia. The undesired evaporation of water, on one hand, represents a wasted amount of heat supplied to the generator. On the other hand the presence of any water vapours in the condenser and evaporator is detrimental to their optimum performance. Two main effects attributable to the presence of water vapours in the concentrated ammonia vapours can be summarized as below:

(i) Partial pressure of ammonia vapours inside the condenser will be slightly lowered raising the working pressure of the refrigerant and subsequently raising the generation temperature.

ii) If the condensed water vapours reach the evaporator these will keep on accumulating in there and may freeze if the evaporation temperature is too low. This will bring the working of the refrigerator to a halt.

This necessitates the removal of water vapours from the ammonia vapours desorbed from the rich solution in the generator of a vapour sorption refrigerator. The water content of the generated ammonia vapours, being less superheated, will be condensed by cooling before the pure ammonia vapours. This fact is utilized in two different ways to achieve the desired results.

a) An open heat exchanger called an 'analyzer' is introduced between the hot stream of vapours from the generator and cold stream of rich solution from the absorber. This process condenses the undesired water vapours and pre-heats the rich solution thus reducing the generator input, and/or

b) The generated vapours are passed through a heat exchanger using an external supply of cold water. This is called a 'rectifier' or a 'dehydrator'. This arrangement can give almost anhydrous ammonia.

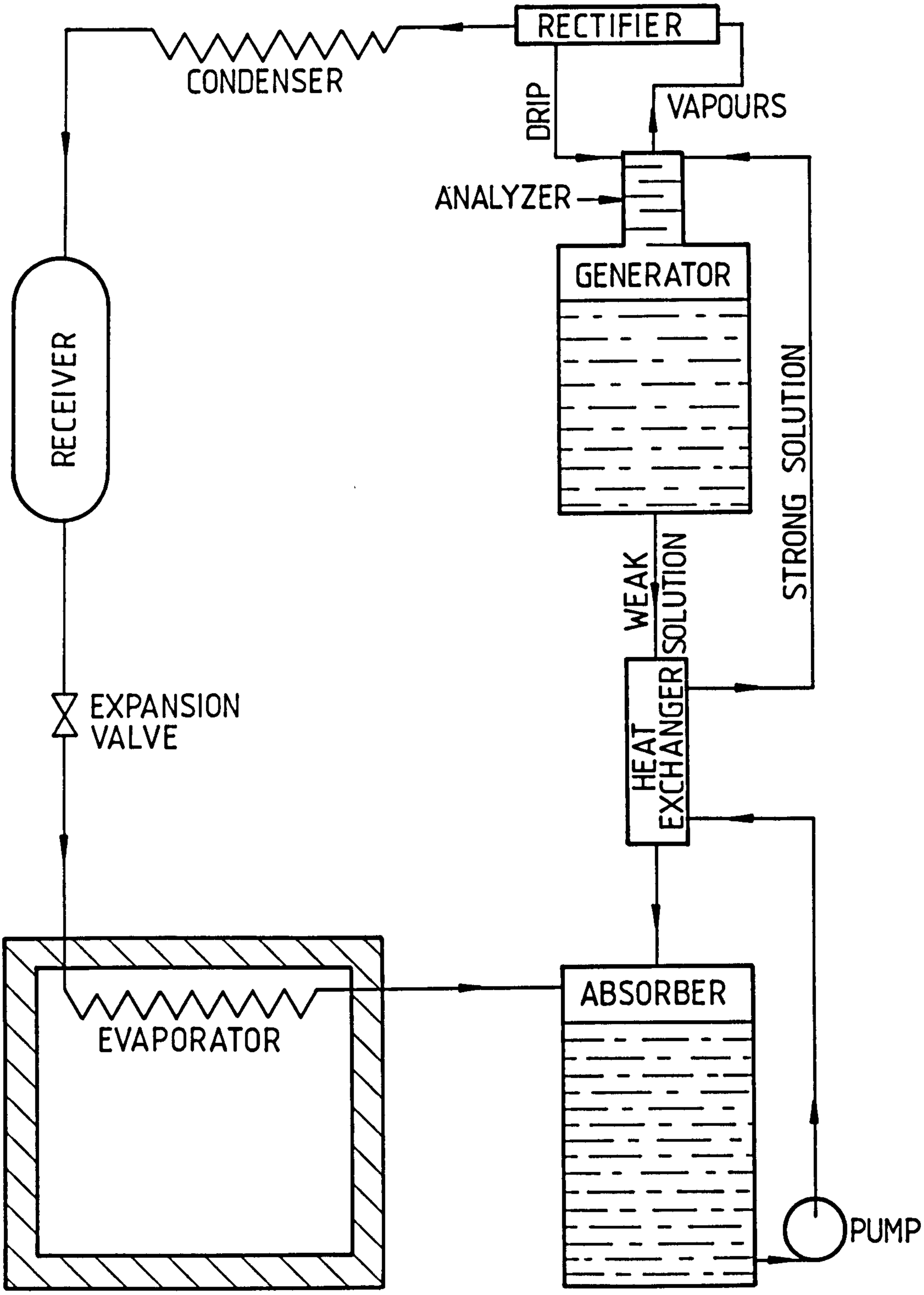

Fig 2.7 Schematic representation of an aqua-ammonia refrigerator

Studying the heat transfer operations at different levels carefully we find that the hot weak solution from the generator needs to be cooled down before entering into the absorber. At the same time the strong solution formed in the absorber is to be heated to generate ammonia. Therefore it makes sense to introduce a heat exchanger to transfer the rejected heat from weak solution to pre-heat the rich solution. The system incorporating all these modifications is shown in fig 2.7. .

The process of water vapour rectification brings complexity to the system and reduces its efficiency. Alternative systems with ammonia as refrigerant and lithium nitrate and sodium thiocyanate has been proposed and tested to overcome this barrier.

2.3.3.2 The Platen-Munters refrigerator

The evaporation of the refrigerant is achieved generally by reducing its pressure by passing it through an expansion device. But the same effect can be produced if the liquid refrigerant is fed into an inert atmosphere, which is not saturated with the refrigerant. According to Dalton's law of partial pressures, exposure of small amount of refrigerant in an inert atmosphere will lower its partial pressure and will evaporate.

This principle was used by von Platen and Munters [1], in what is now generally known as the 'Electrolux' refrigerator, after the firm who first developed it commercially. A schematic diagram showing the essential features of this refrigerator is shown in fig 2.8. The

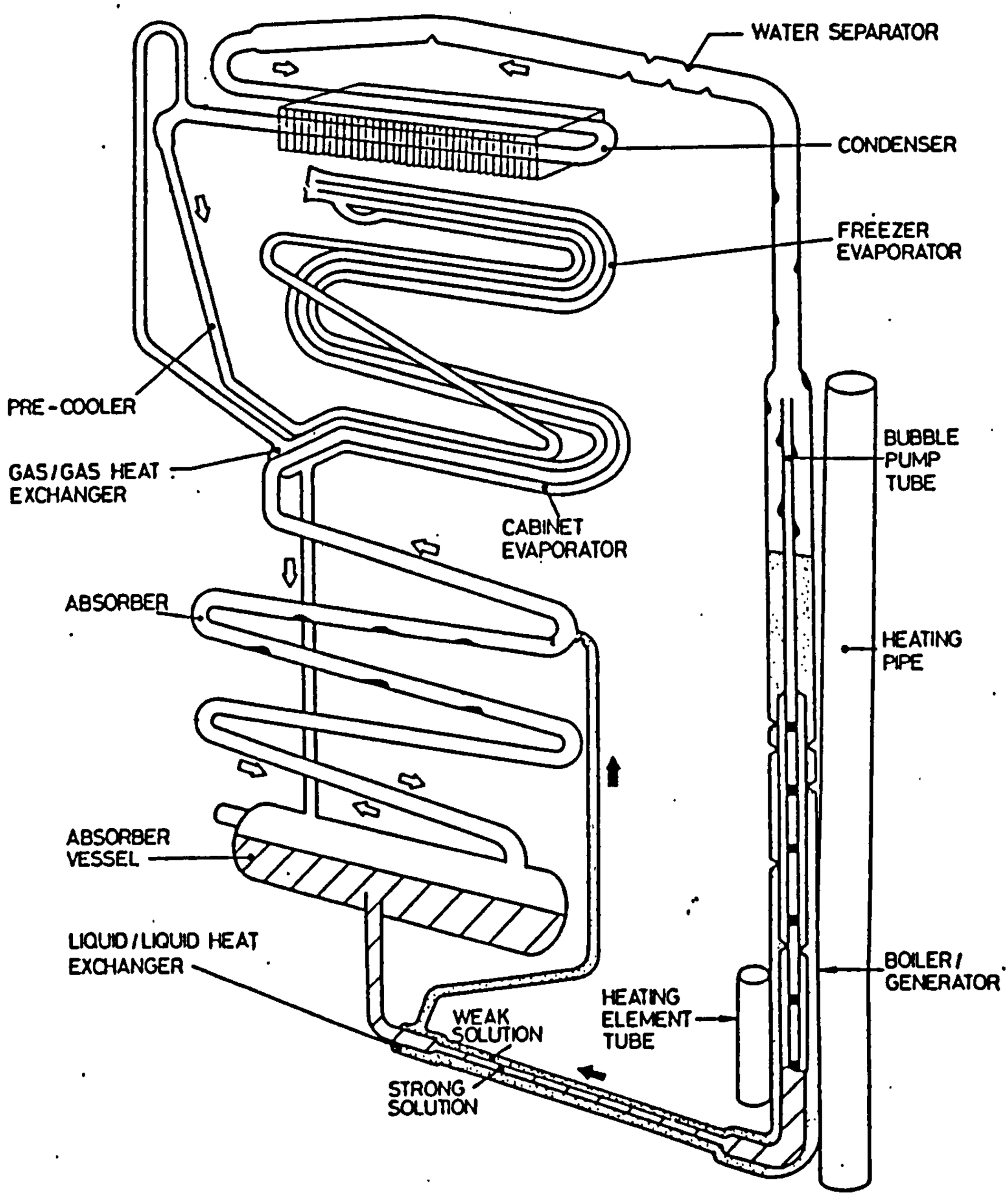

Fig 2.8 Schematic representation of Platen-Munters refrigerator

inert gas is hydrogen which is concentrated in the parts of the circuit where ammonia pressure is to be low i.e. in the evaporator and absorber. The total pressure is effectively uniform throughout the circuit. Thus the circulation of fluid can be accomplished by convection currents set up by density gradients. This means that there is no moving parts in the refrigerator and hence is both very quiet and reliable.

The layout of such a system is complex due to special operational requirements. For instance the inert gas hydrogen must be confined to the correct areas of the circuit. The relative placement of the absorber and the generator is important for the vapour pump to be able to produce the required circulation with minimum heat input. Because of these constraints the operational tolerances quoted by Electrolux for their product are $\pm$ 3^{o} on the tilt and $\pm$ 10% on the input power [2].

Hydrogen gas present in the evaporator tend to absorb a fair proportion of the cooling produced by the evaporation of ammonia. This cold mixture of hydrogen and ammonia flows down to the absorber where ammonia is absorbed into the weak solution coming from the generator and hydrogen rises up towards the evaporator. The two gas streams, the cold mixture of hydrogen and ammonia and the hot hydrogen rising towards the evaporator, pass through a heat exchanger. Heat transfer in this gas heat exchanger is not very effective thus affecting the cop of the refrigerator. A typical coefficient of performance as quoted by Electrolux is 20-25% [2].

2.3.3.3 Intermittent vapour sorption cycle

In a continuous vapour sorption cycle all the four main processes i.e. generation, absorption, condensation and evaporation take place at the same time in parallel. The system can be simplified if some of the processes take place in turn; to be more specific if all the four processes are carried out in two phases. Figure 2.9 illustrates the principle.

In fig 2.9a vessel 'A' contains the sorbent and vapour 'mixture' which is being heated. The vapours at high temperature and pressure are driven off and are condensed into the vessel 'B' after loosing latent heat to the ambient. This is the first phase of the complete cyclic operation in which generation and the condensation processes have taken place.

Figure 2.9b represent the second phase of this cyclic operation. Vessel 'A' which, now, contains less of the dissolved vapours is cooled. The vapour pressure is lowered, as a result of it and the weak mixture is ready to sorb more vapours. The lowered vapour pressure will force the condensed refrigerant in vessel 'B' to evaporate which the cold 'mixture' in vessel 'A' is now ready to dissolve. Thus the processes of evaporation and sorption, which take place in this second phase, complete the refrigeration cycle.

The fact that generation and sorption processes are taking place at different times can lead to big advantages. This means that there is

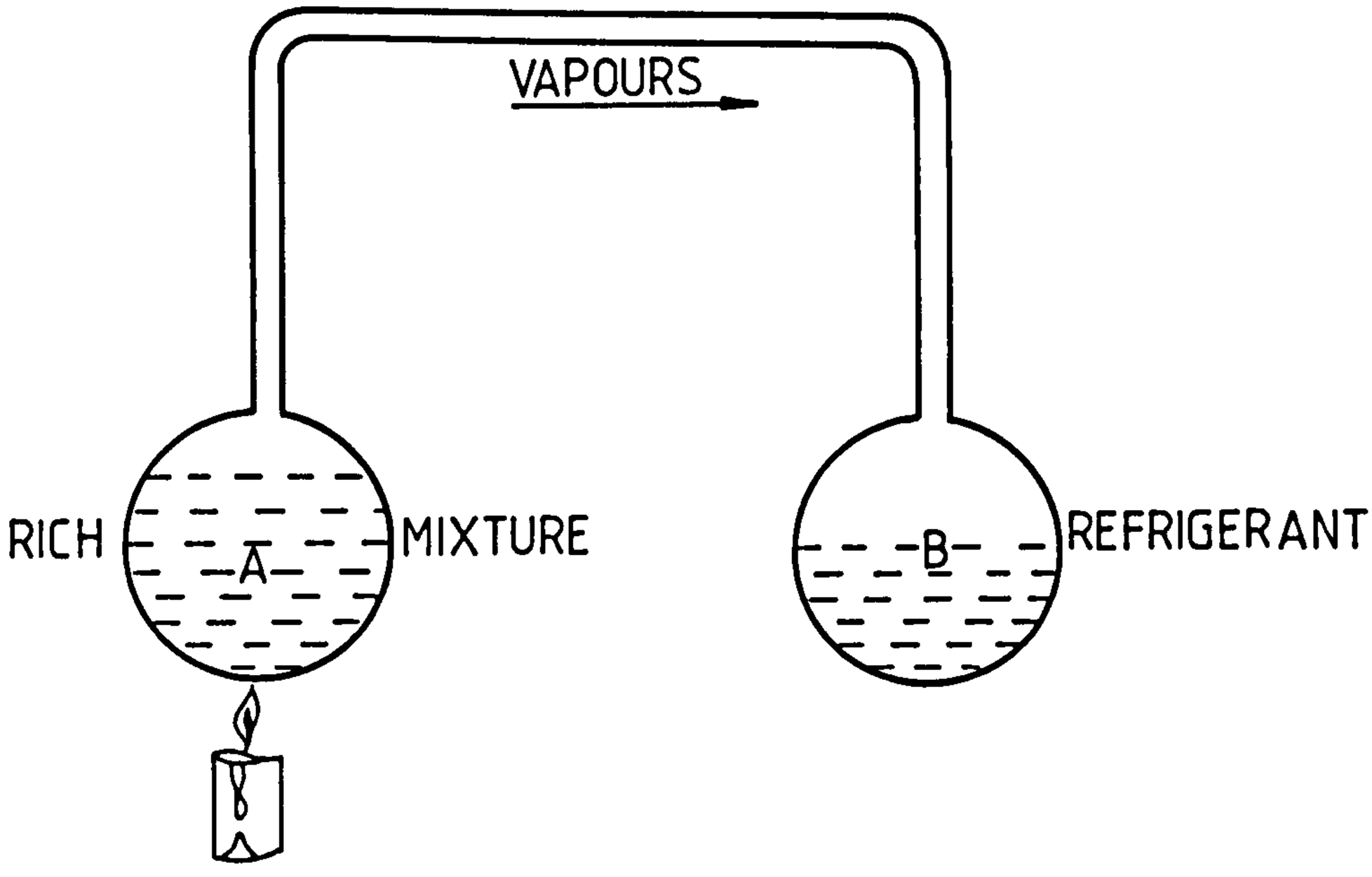

GENERATION PROCESS

(a)

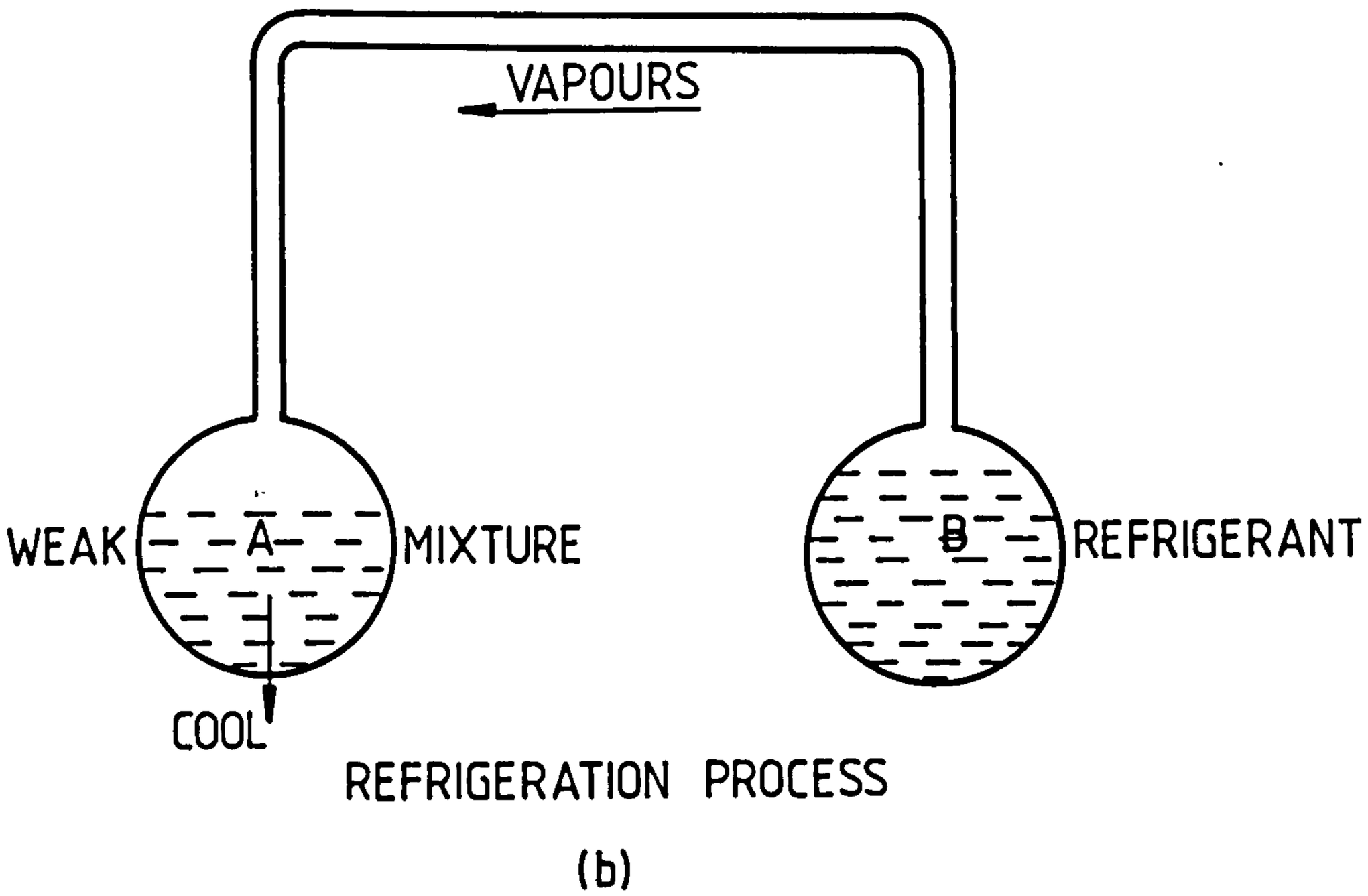

REFRIGERATION PROCESS

(b)

Fig 2.9 Working principle of intermittent sorption refrigerator
a) generation process b) refrigeration process

no need to transport the weak 'mixture' created during generation process to another vessel for sorption operation. It gives the following advantages:

a) the circulation pump is no longer needed, rendering the system more reliable in the absence of any moving parts,

b) as the pump is dispensed with the system can be powered wholly by thermal input.

c) generation and sorption can be accomplished in the same vessel, and

d) solids can be employed as sorbent materials.

A practical intermittent operation vapour sorption refrigerator will normally consist of three components; namely, a generation-cum-sorption vessel, a condenser, and an evaporator. Though additional components my be required on specific systems.

2.3.4 Thermoelectric refrigeration

The thermoelectric effect was first observed by Seebeck in 1822. It was noticed that on making a closed loop of two dissimilar metals, an emf was produced in the circuit when the two junctions were maintained at different temperatures. Later, in 1834, Peltier observed the inverse effect: on passing an electric current through a junction of two dissimilar metals the temperature of the junction can be varied. It can be hot or cold depending on the direction of current. Kelvin pointed out a third effect in 1851. It relates heat absorbed or rejected by a single conductor to the temperature gradient along it and the current flowing through it. This effect takes place in addition to the Joule (i.e $P=I^2R$) heating . However in thermoelectric cooling materials the Kelvin effect is second order compared with those of Peltier and Seebeck, and will not be considered in further study of the subject.

At the turn of the century Altenkirch [3] gave the first serious consideration to the use of these effects for refrigeration. He made the effort to identify and quantify the essential characteristics of materials to be suitable for thermoelectric cooling. For many years practical applications of these thermoelectric effects was restricted to temperature measurements by thermocouples. The reason for this restricted application is the comparitively small thermoelectric effect in metals. However, this effect is quite pronounced in semiconductors. The advent of transistor in 1949 and other semiconductor devices later revived the intrest in the subject. The research activities into semiconductor materials led to the

development of materials in which thermoelectric effects were of sufficient magnitude to realise the fabrication of a useful device.

Principles of solid-state physics have shown that energy level change in electrons is responsible for the transport of thermal energy in a thermoelectric cooling operation. Electrons flowing across a junction of two dissimilar thermoelectric materials, i.e. materials with different available electron energy levels, must undergo an energy change which results in either the evolution or absorption of heat. The direction of current flow determines which will occur. Figure 2.10a shows such a thermoelectric element. Two dissimilar semiconductor materials, n which has a negative Seebeck coefficient and an excess of electrons and p which has a positive Seebeck coefficient and is deficient in electrons, are linked as shown giving hot and cold junctions. A number of such elements can be connected together, as shown in fig 2.10b, to produce a system suitable for a particular application.

The performance of an ideal thermoelectric circuit is limited by two additional effects which are always present: 1) the Joule heating effect which occur throughout the two materials and, 2) the inevitable heat conduction between the two junctions which are at different temperatures. Fig 2.11 shows the performance of a typical commercial module. The coefficient of performance for such modules under normal operating conditions would be in the range of 0.15. These are, in general,less efficient than vapour compression units but with the decrease in size the cop of the latter falls. Goldsmith [4] suggested that the system showed equal efficiencies at

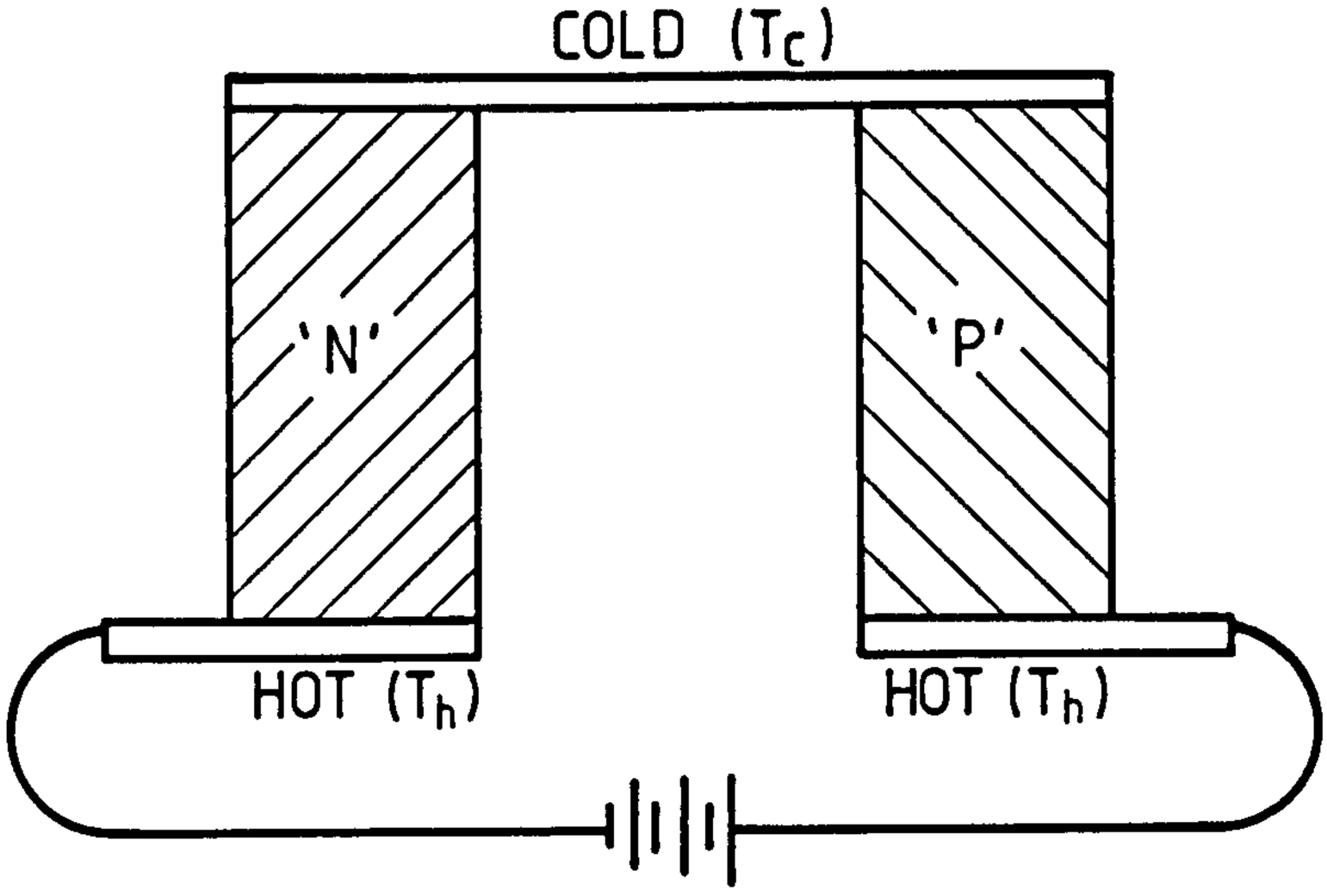

(a)

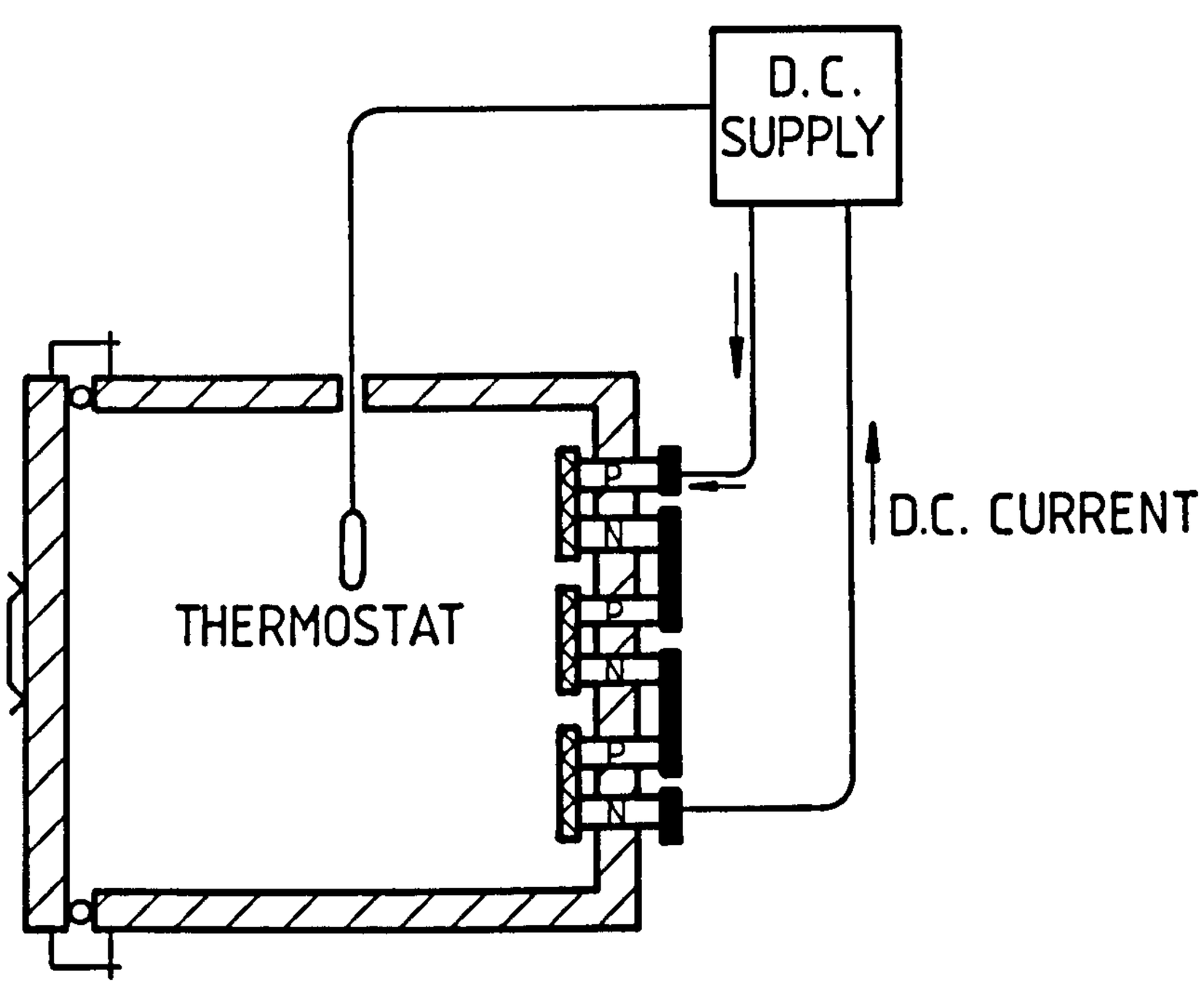

(b)

Fig 2.10 a) A thermoelectric element b) essential elements of a thermoelectric refrigerator

Performance Characteristics
Thermoelectric Module 801-2003
Cambion Inc. Cambridge, Massachusetts, USA

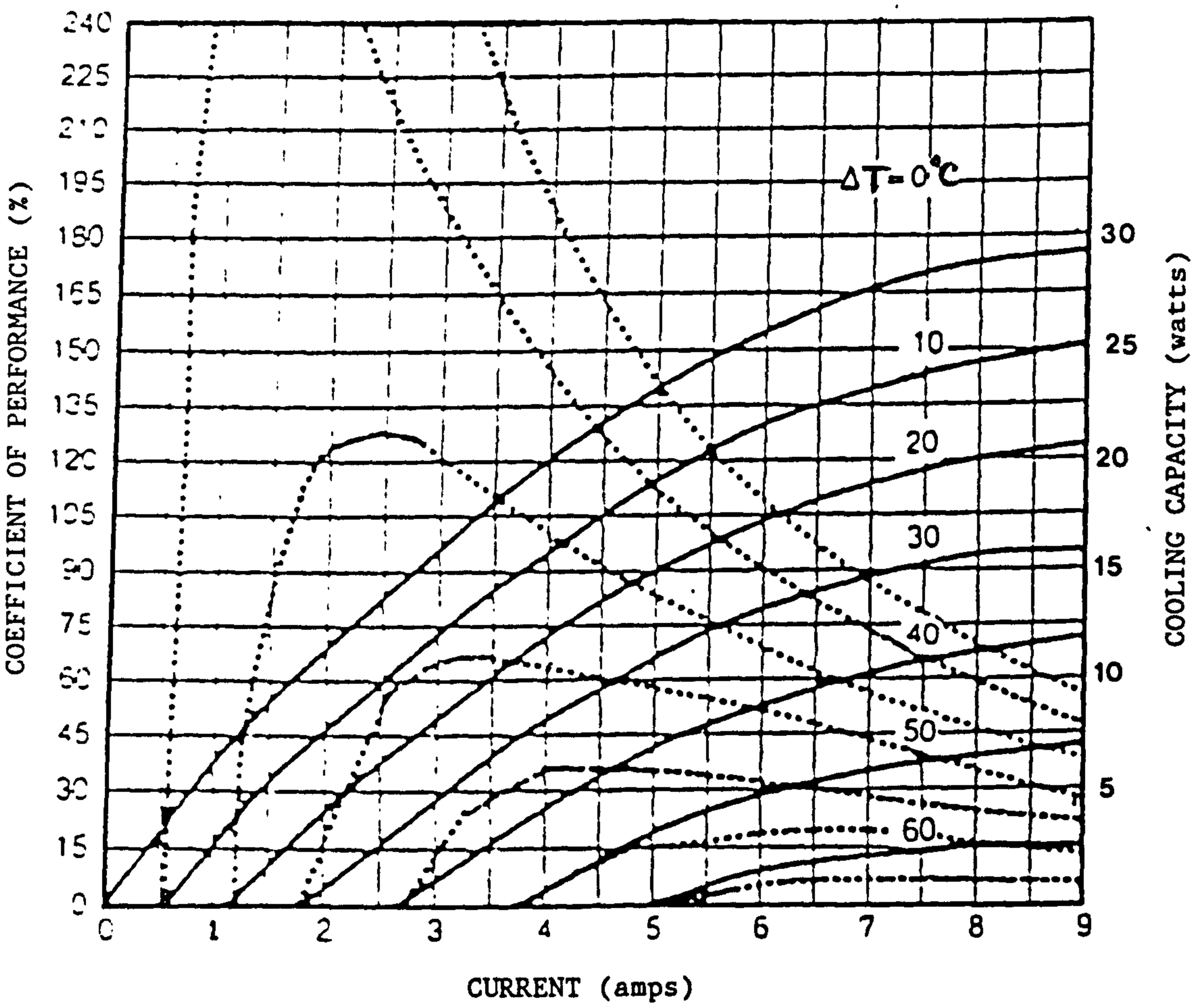

Fig 2.11 Typical performance curves of a commercial thermoelectric module

cooling loads of 10 watts whereas ASHRAE [5] quotes that vapour compression units became economical as the refrigeration capacity increased above 60 to 90 watts.

There are certain advantages of thermoelectric cooling which outweigh its low performance in specialist application areas. Because of its ruggedness, lack of vaporizing refrigerant, and absence of moving parts and thus a longer life this has been applied in the military applications, cooling of medical instruments, electronic equipment and cold junctions, and for humidity control in instruments.

There are various ways in which the temperature and capacity of a thermoelectric refrigerator can be controlled. By varying the applied voltage to the unit its capacity can be varied. The temperature in these units is generally controlled by three different methods:

1- the capacity of the refrigerator is varied through a feedback control circuit to control the temperature. A wheatstone bridge circuit incorporates a variable resistor in one arm which presets the cabinet temperature. The other arm contains a thermistor which sense the temperature in the cabinet. Any imbalance in the bridge output is used to reduce or augment the input power by modulating the current.

2- the hot and cold junctions swop their role if the polarity of the power supply is reversed. This fact is utilized to control the temperature by heating (or cooling) the cabinet when the inside temperature goes below (or above) the set

value. Thus the cabinet temperature remains oscilating about a mean.

3- simplest of all controls is the on-off switching of the power supply to the unit. This is inefficient because heat is conducted into the cabinet during off period through the thermally linked hot and cold junctions. The switching operation can be carried out by a simple bellows, for example, using change of volume of water on freezing.

2.3.5 Steam jet refrigeration

Water is a safe refrigerant abundantly available and has a high latent heat of vaporization. Yet it is quite unsuitable for application in vapour compression plants. The reason for this is its high specific volume at the low evaporation pressures encountered in the process of refrigeration. For instance at $7^{o}C$ the vapour pressure is about 0.01 bar and the corresponding specific volume is about 129 m^3/kg. Such high volume flow rates are not suitable for reciprocating compressors. This has led to the use of steam jet ejector in place of a usual compressor. The working principle of an ejector pump is illustrated in fig 2.12a. High pressure steam is expanded through a convergent-divergent nozzle, to form a high-speed jet at low pressure, into the converging part of ejector pump. The high speed steam entrains the water vapours from the vacuum chamber. The combined stream from the mixing chamber is then diffused in the divergent part of the nozzle until the required exhaust pressure is reached. Such a pump has no moving parts but is in-efficient. The

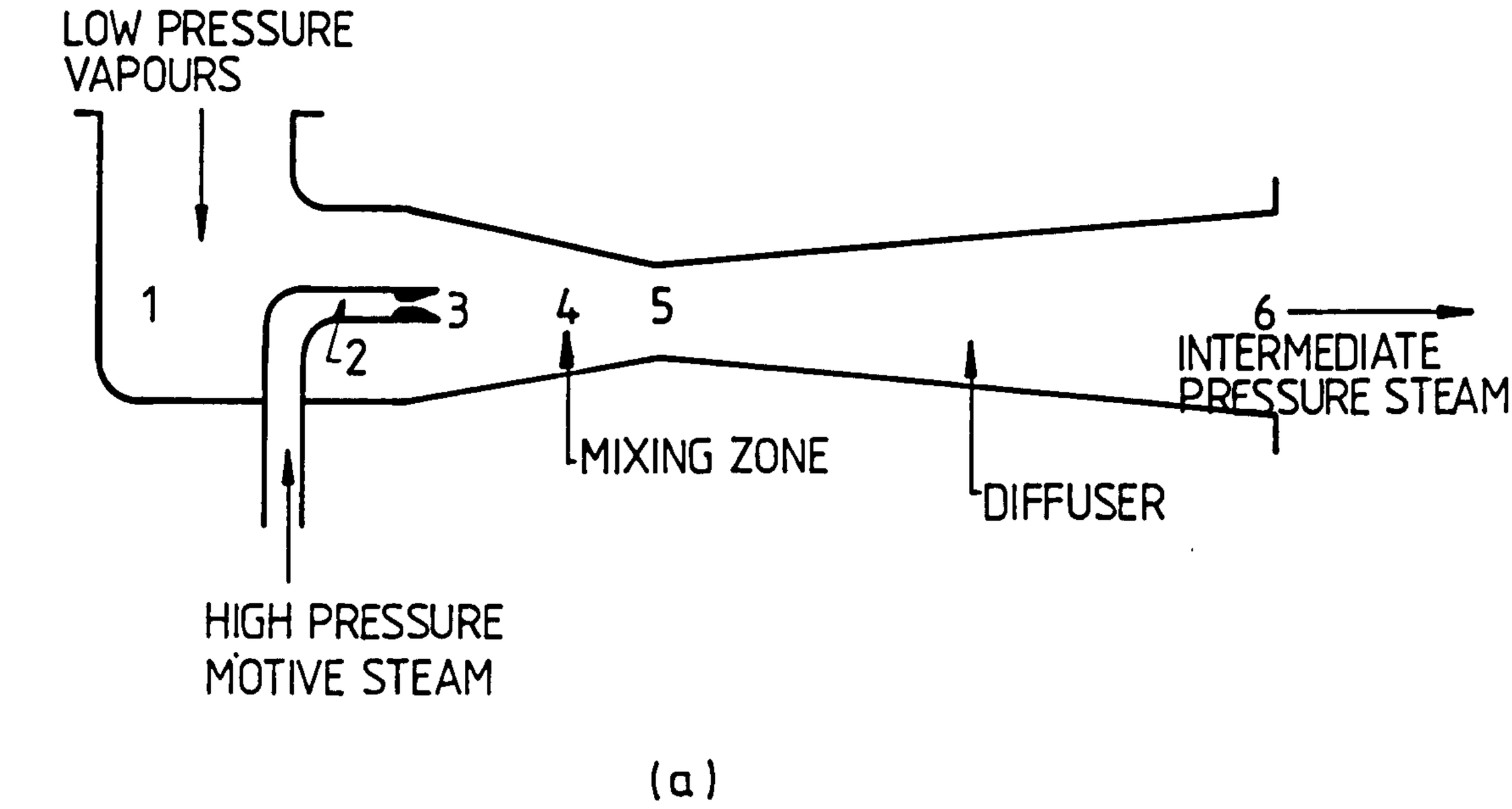

(a)

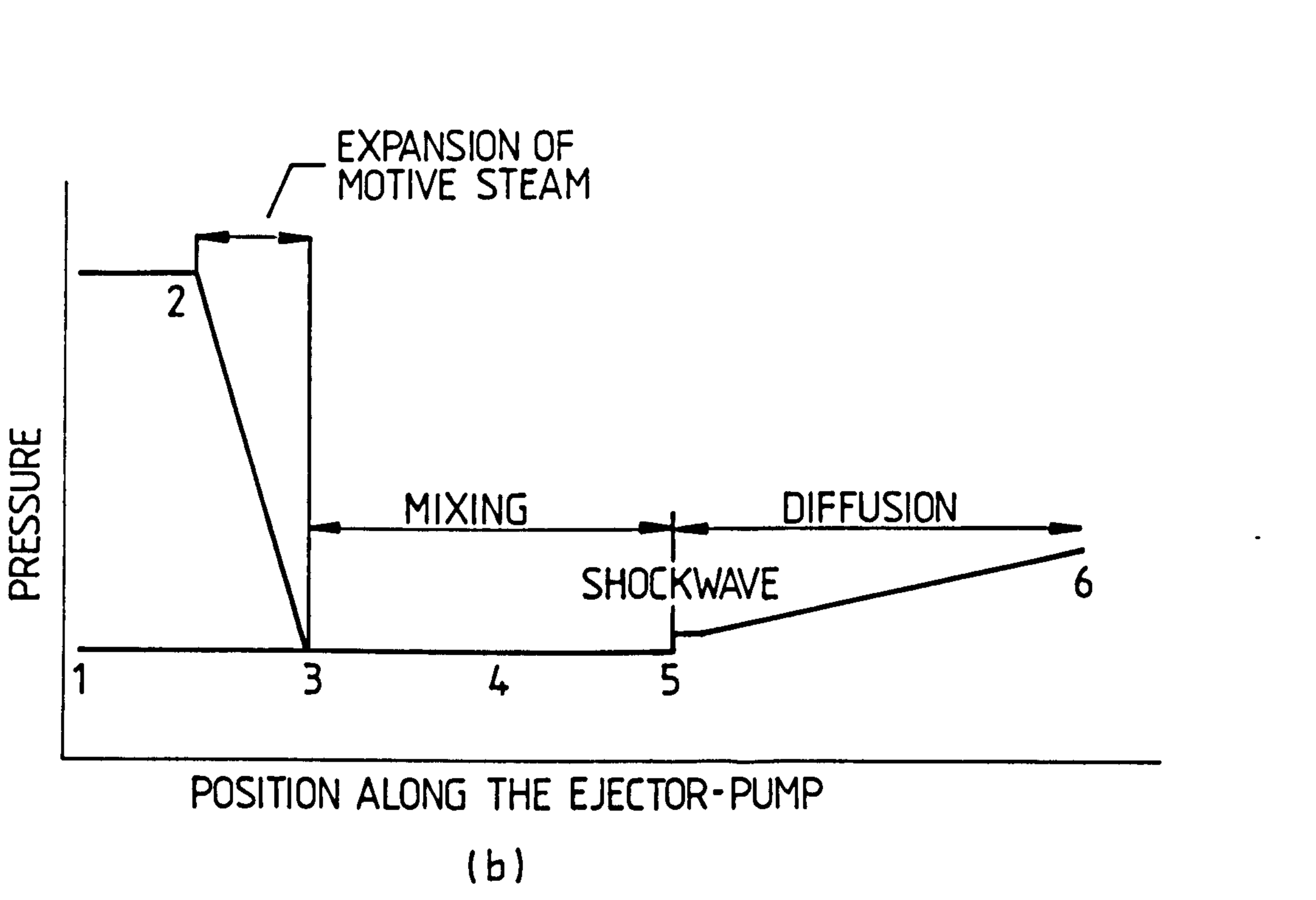

(b)

Fig 2.12 a) Working principle of a vapour ejector pump
b) pressure variations taking place inside the pump

whole process occuring inside an ejector pump is shown in fig 2.12b in a pressure-distance plane.

A vapour compression refrigeration system using an ejector pump is shown in fig 2.13. High pressure steam, typically 70-700 kPag [6], is generated in a boiler expanding in the converging part of the venturi, where the water vapours evaporated in the evaporator are entrained and mixed with the steam from the boiler. The mixed steam, consisting now of both the refrigerant and motive water vapours, is then diffused through the divergent part of the venturi until the condenser pressure is reached. The refrigerant lost in the evaporator is made up by a controlled bleed from the condenser and rest of the condensate is fed back to the boiler by a feed pump. The system demands a high cooling load and the coefficient of performance for larger plants is about 0.35 [6].

The ejector pump was initially designed to utilize water as the refrigerant. But there is no reason that the principle cannot be used for other refrigerants. Martynowsky [7] built a closed cycle plant, similar to the one shown in fig 2.13, using a halogenated hydrocarbon as the refrigerant. These alternative refrigerants give the advantages like higher evaporation pressures and low specific volumes producing lower flow velocities in the mixing chamber and reducing the losses. Sub-zero temperatures are also achievable.

These refrigerator units require only the heat input to operate and a small feed pump for the boiler system.

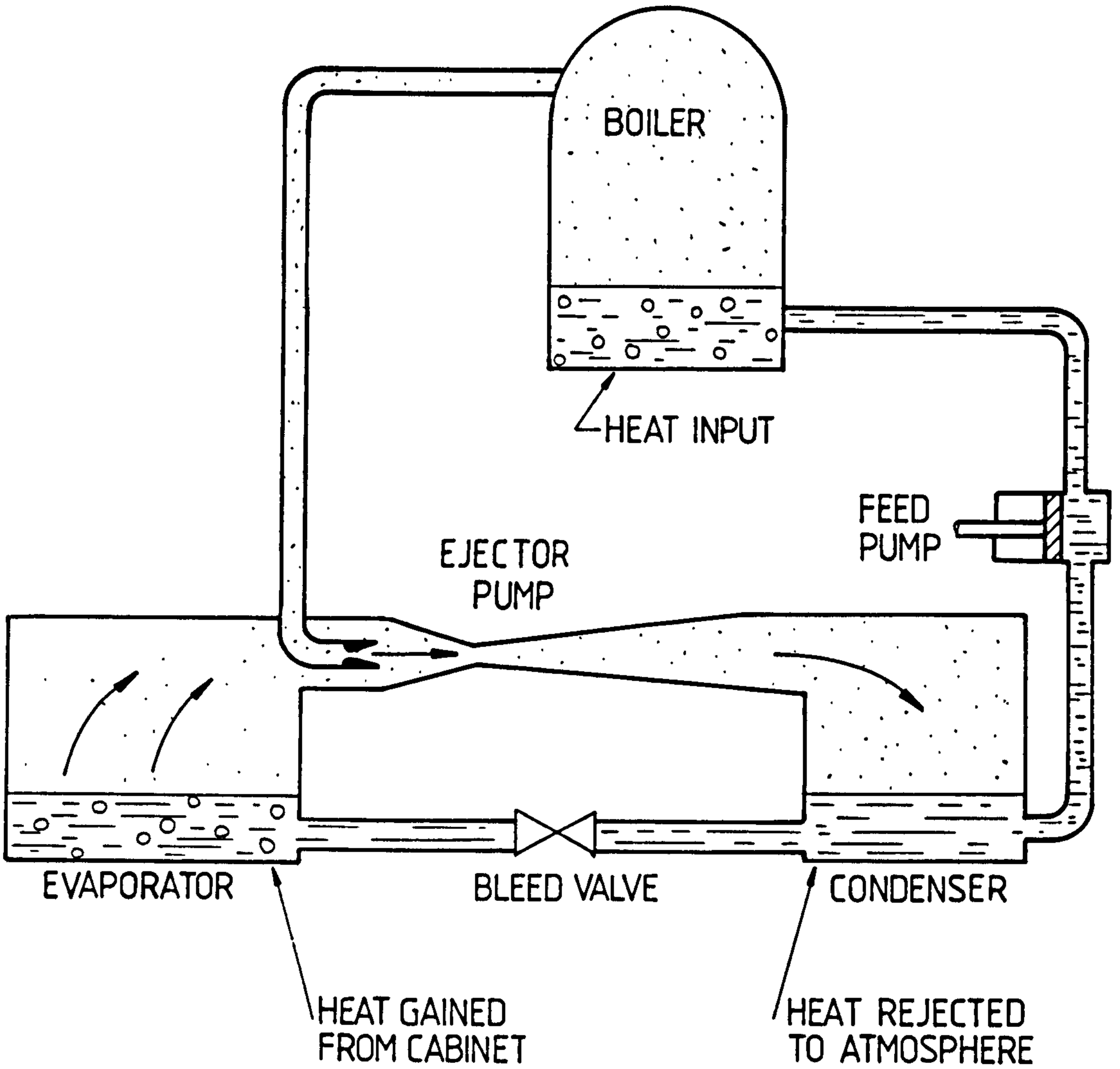

Fig 2.13 A schematic representation of a closed cycle vapour ejector refrigerator

REFERENCES

1 von Platen, B.C. and Munters, C.G. Platen-Munters refrigerating system AB Absorptionskylapparat Patent no. 57398, 18th August 1922.

2 Private communication, Electrolux, Luton, U.K.

3 Altenkirch, E., Physikalische Zeitschrift, 12, 920, 1911.

4 Goldsmith, H.J., 'Thermoelectric Refrigeration', Heywood, London, 1964.

5 ASHRAE Handbook of Fundamentals, American Society of Heating, Refrigeration and Air-conditioning Engineers, 1972.

6 Macinteri, H.J., and Hutchinson, F.W., 'Refrigeration Engineering', John Wiley and Sons, 1950

7 Martynowskey, W., 'Use of waste heat for refrigeration', Refrigeration Engineering, vol 62, no 3, p 51, 1954.

CHAPTER THREE

Solar Energy Collection

3.1 Solar Energy

The earth is a planet of 1.27×10^7 m radius revolving around its sun in an oval orbit, at an average distance of 1.5×10^{11} m completing one rotation each year. The sun is a sphere of intensely hot gases, with a diameter of 1.39×10^9m which appears to spin , to an observer on the earth, about its axis every four weeks. However, it does not rotate as a solid body; the equator takes about 27 days and polar regions take about 30 days for each rotation. It radiates a huge amount of energy generated by continuous fusion reactions taking place in its core. Table 3.1 summarizes the important characteristics of the sun.

The amount of this energy reaching the earth is defined by the solar constant G_o. It is the amount of energy from the sun, per unit time, received on a unit area perpendicular to the direction of propagation of of the radiation, at the earth's mean distance from the sun, above earth's atmosphere. The currently accepted value of solar constant is 1367 Wm^{-2} [1]. Recent satellite and rocket data [4,5] has confirmed that the previously used 1353 Wm^{-2} [2,3,7] value was low. It is generally believed that the discrepancy arose from instrument calibration errors [6]. The data confirms that there are daily and monthly variations of not more than $\pm$0.25% and changes over the 11-year sunspot cycle of by about 1%. None of these variations are of prime importance to the design of solar energy systems.

TABLE 3.1

Characteristics of the sun (adapted from ref [6])

Present age	4.5×10^9 years
Life expectancy	10×10^9 years
Mean distance from earth	1.496×10^{11} m
Diameter (photosphere)	1.39×10^9 m
Angular diameter (from earth)	9.6×10^{-3} radians
variation	$\pm 1.7\%$
Volume (photosphere)	1.41×10^{27} m^3
Mass	1.987×10^{30} kg
Composition	
Hydrogen	73.46%
Helium	24.85%
Oxygen	0.77%
Carbon	0.29%
Iron	0.16%
Neon	0.12%
Nitrogen, silicon, magnesium, sulphur, etc.	<0.1%
Density	
Mean	14.1 kgm^{-3}
centre	1600 kgm^{-3}
Solar radiation	
Entire sun	3.83×10^{26} W
Per unit surface area	6.33×10^7 Wm^{-2}
At air mass zero	1367 Wm^{-2}
Temperature	
Centre	15,000,000 K
Surface (photosphere)	6050 K
Chromosphere	4300 - 50,000 K
Corona	800,000 - 3,000,000 K
Rotation	
Solar equator	26.8 days
30^o latitude	28.3 days
60^o latitude	30.8 days
75^o latitude	31.8 days
Energy source	$4H \rightarrow He + 2e + 2 +$
Rate of mass loss	4.1×10^9 kgs^{-1}

Figure 3.1a (adapted from [7]) shows a graph of spectral irradiance of the sun. It can be noted from the tabulated values of spectral distribution in [7] that 45% of the sun's energy comes to us at wavelengths in the visible spectrum (i.e. between 0.3 and 0.7 micron). Also worth noting is that a little more than 1% of solar constant has wavelengths shorter than 0.3 micron (i.e UV and X-rays) and the rest 54% is in the infrared (IR) region. 96% of the solar constant is associated with wavelengths less than 2.5 micron.

3.1.1 Available solar energy

The solar radiation while passing through the earth's atmosphere undergoes attenuation and modification. Absorption of certain wavelengths ensues because of the presence of gases like H_2O, CO_2, O_3, and O_2 in the earth's atmosphere. Owing to the scattering and reflection in the atmosphere a portion of the collimated beam of solar radiation is diffused. The principal factor which determines the degree of attenuation is the distance through which the radiation travels when in the atmosphere. This distance is minimum when the sun is directly overhead and, at the sea level, is defined as 'air mass' 1. The air mass traversed at a particular location changes as the earth rotates diurnally. When the angle between the zenith and line of sight is 60° the distance traveled by the beam is doubled, i.e. the air mass is equal to 2. Figure 3.1b (adapted from [7]) shows the solar spectrum under 'air mass 1' condition. Parts of the spectrum absorbed by the atmospheric gases are clearly identified in this diagram.

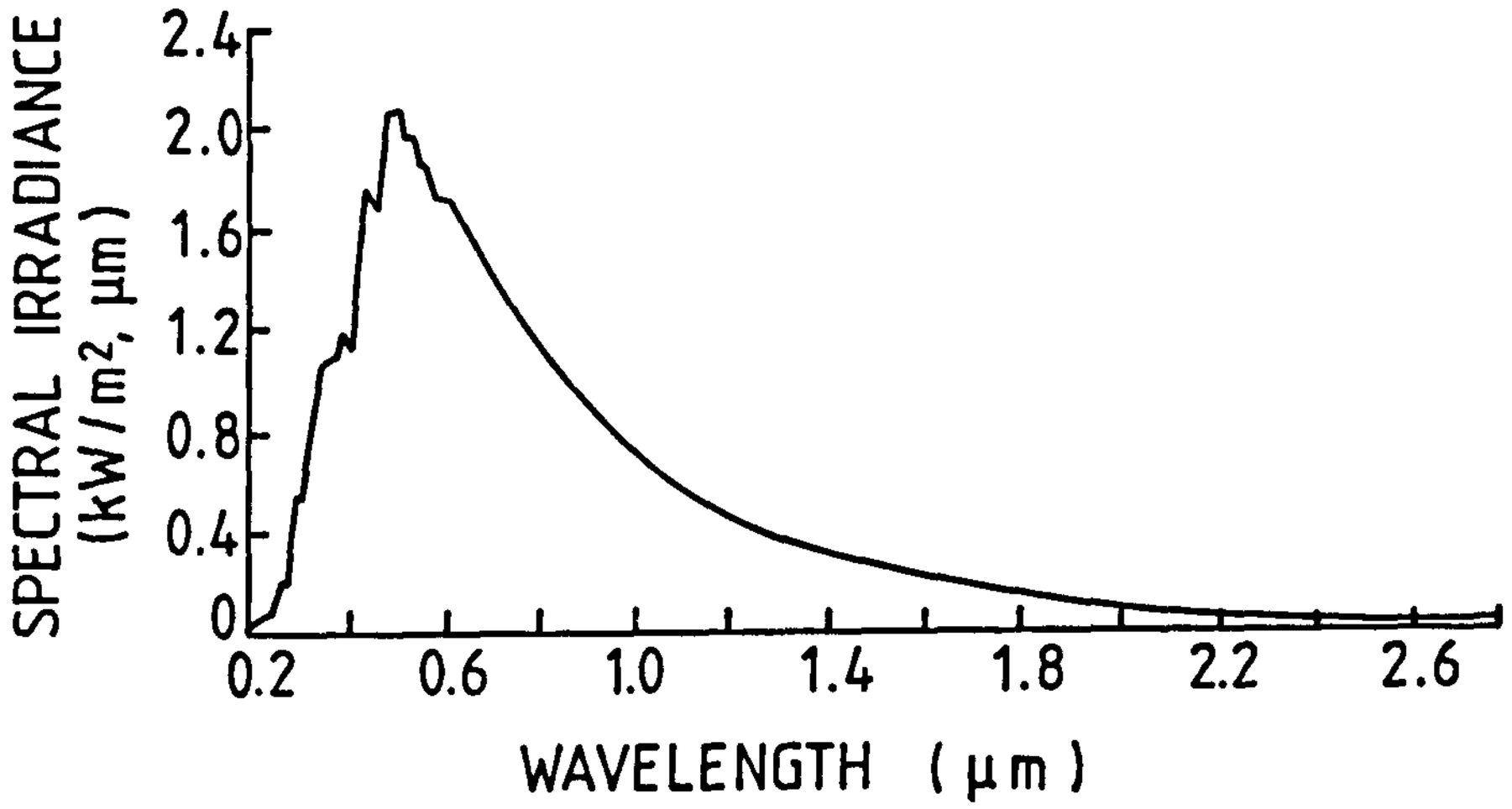

(a)

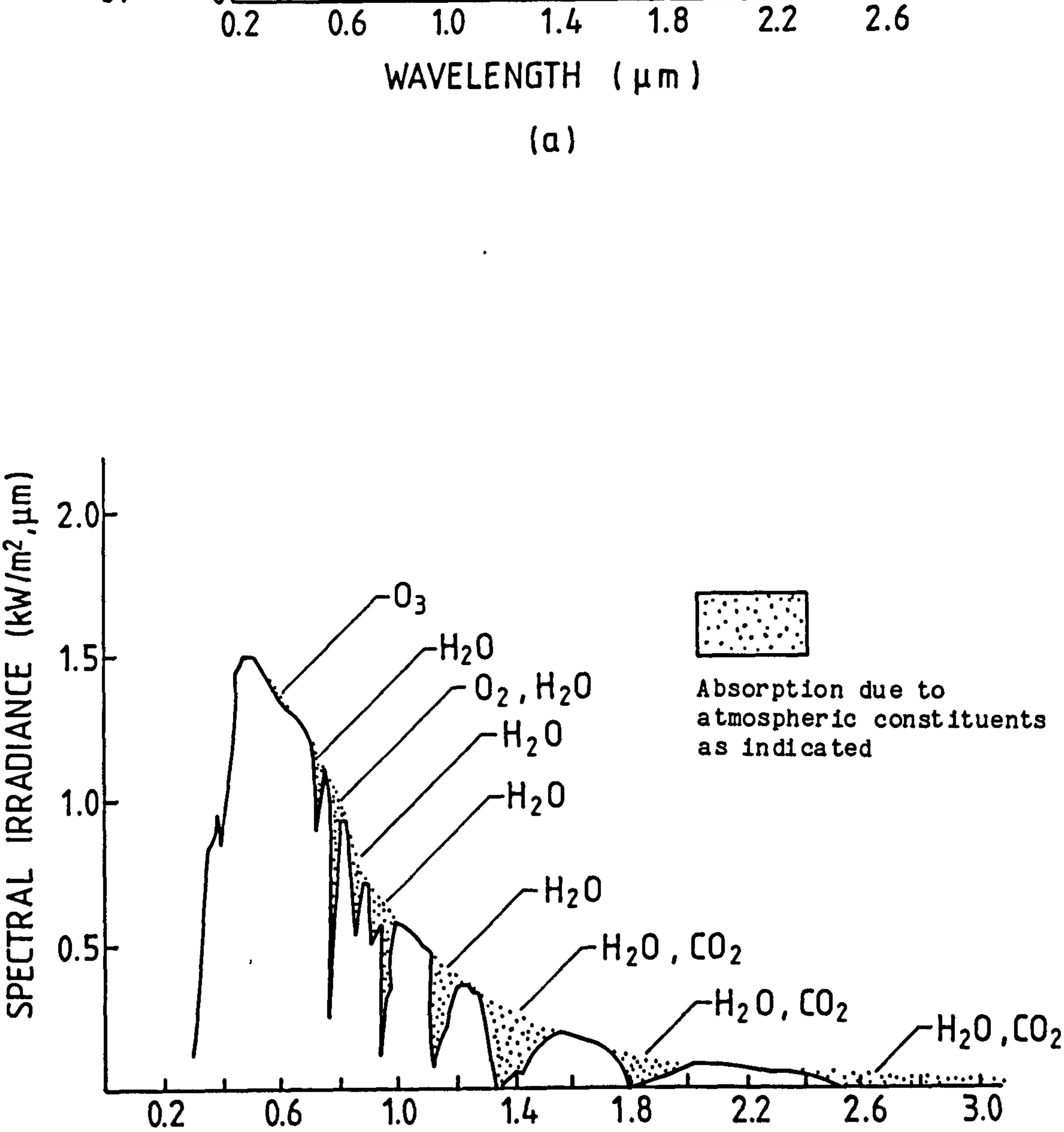

(b)

Fig 3.1 Solar spectral energy distribution
(a) air mass 0 (b) air mass 1

The amount of solar energy available for collection at a particular location is variable. In general there are diurnal and seasonal variations due to earth's rotation both about its axis and around the Sun. This is further complicated by geographical location, latitude, the orientation of the collection device and the prevailing atmospheric and ground conditions. Methods are available to calculate the amount of insolation falling on a surface. Detailed information about different calculation procedures is available in [2], [8]. Insolation levels are also measured and recorded by meteorological services around the world.

A further limitation on the maximum amount of useful energy collected is imposed by the type and design of the collection device and the temperature at which the collected energy is used. This is the subject of the next sections of the chapter where some chosen devices relevant to the refrigeration applications are discussed.

3.2 The flat-plate solar-energy collector

A typical flat-plate collector consists of a large plane area (i.e. the plate) over which the solar insolation falls and is absorbed. The energy so collected is removed from the plate by circulating a gaseous or liquid heat-transfer fluid. As the temperature of the absorbing plate is higher than the ambient there are heat losses from the front and rear of the plate. Thermal insulation is usually placed behind the plate to reduce the heat losses from the rear. Heat losses from the front are reduced by covering it with some material which reduces convective heat losses and is transparent to the incident sun rays but is opaque to the longwave thermal radiation emitted by the plate.

3.2.1 Construction of the collector

A typical flat-plate collector is shown in fig 3.2. The main components are: an insulated box which provides the structure, an absorber plate, and transparent cover sheets. The box is usually made from thin sheet metal or thin planks of wood e.g. plywood. The boxed is lined with a blanket of insulating material which is thicker at the bottom than the sides.

The absorber plate is usually constructed from a high thermal conductivity metal with channels for the flow of heat-transfer fluid. These channels are either formed as integral part of the plate or constructed by attaching pipes to the plate. These channels are connected at the top and bottom by header manifolds. The

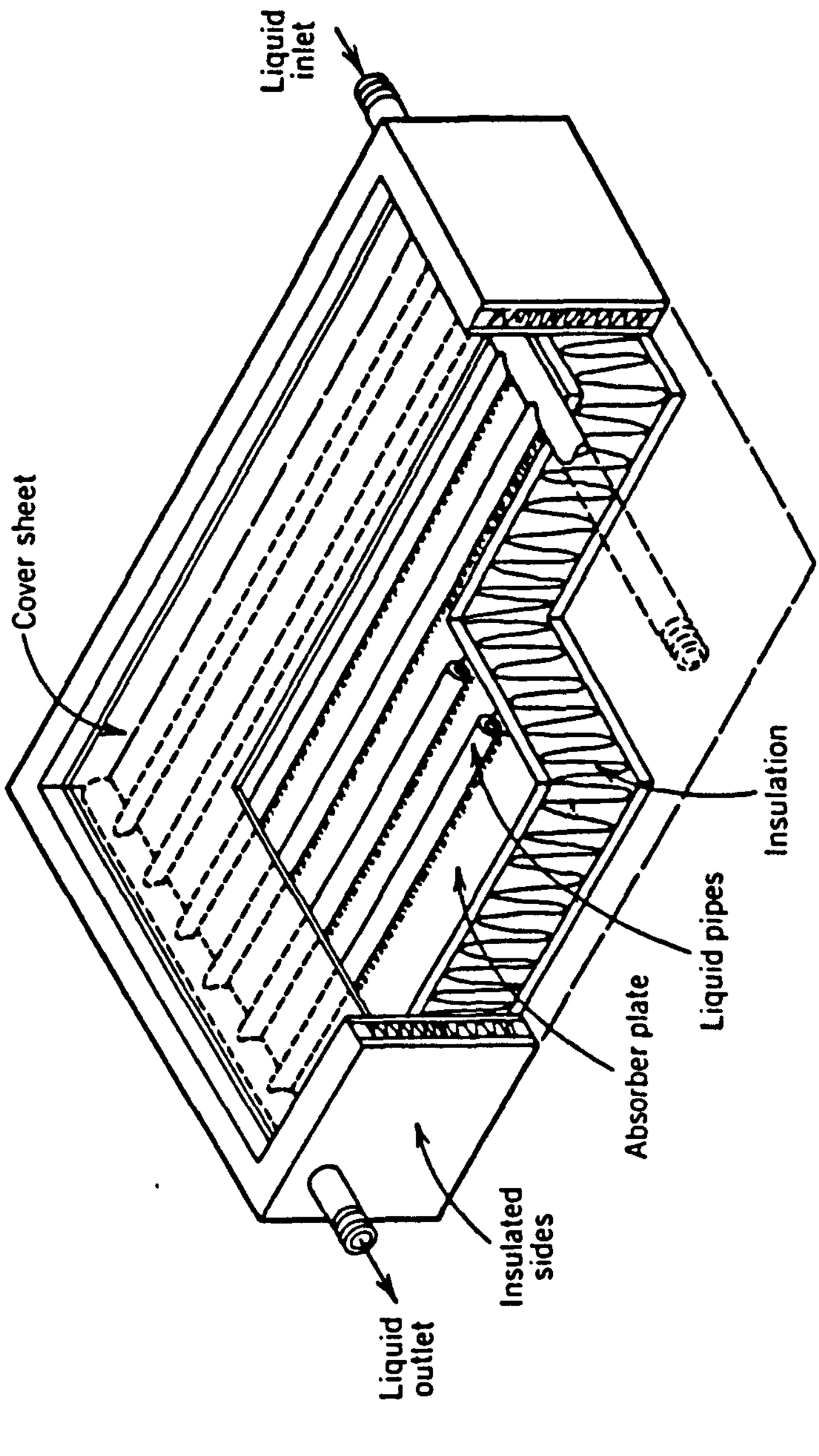

Fig 3.2 Construction features of a typical flat plate solar energy collector

manifolds are generally of larger cross-section than the riser channels. This ensures a steady balanced flow from the channels into the header. The heat-transfer fluid enters and leaves through the headers. The plate surface is usually painted or coated to maximize the absorption of solar insolation and in some cases to minimize the infrared emissions. Matt black paints are generally employed after preparing the surface with an appropriate primer. The primers are normally self-etching type which avoid the peeling of the paint after repeated expansions and contractions. Some coatings are electrochemically plated on the surface of the plate and some special selective coatings, which come in the form of a thin film, are glued to the surface.

The transparent covers can be either glass or plastic sheet. Glass is the most used material for outer covers because of its superior resistance to the environment. The glass sheets used are usually low iron content and about 3-6 mm thick. The surface of glazing can be smooth or patterned. In any case the transmittance of the covers is around 0.9 at normal incidence. Plastic sheets are used normally as a second cover under the glass cover. This protects the plastic from the environment. Furthermore glass does not transmit ultraviolet rays and thus saves the plastic, which is sensitive to these radiations, from deteriorating. The plastic materials used generally for this purpose are acrylic- or fibreglass-reinforced polymers and stretched films of polyvinyl flouride.

3.2.2 Collector performance

The thermal efficiency of a flat-plate collector is described as the ratio of the useful heat extracted to the total solar insolation falling on the aperture area. This can usually be evaluated by performing a heat balance on the collector-plate. As the temperature of the collector plate rises the heat losses to the ambient increase. Thus, at higher operating temperatures, the efficiency is less. A development of this energy balance by a number of authors [9,10,11] has resulted into the Hottel-Whillier-Bliss (HWB) formulation. Though this model involves a number of simplifications concerning the temperature distribution across the collector-plate and the coupled boundary conditions between the water and the tube surface, it can give a fairly accurate comparison of the performance of different designs. More elaborate analyses have also been presented which take into account the temperature variations along the water tube, variation of the thermal capacitance of the system and the effect of radiation properties of surfaces [12-16].

Figure 3.3 is a general representation of a HWB characteristic curve. X-axis gives a general parameter in the shape of ratio of the temperature difference to the solar insolation. Mathematically the curve can be represented by the following equation

$$\eta = (\tau\alpha)_{eff} - U_l(T_i - T_a)/I$$

The intercept of the equation gives the optical efficiency of the collector. It is clearly evident from the figure that the efficiency

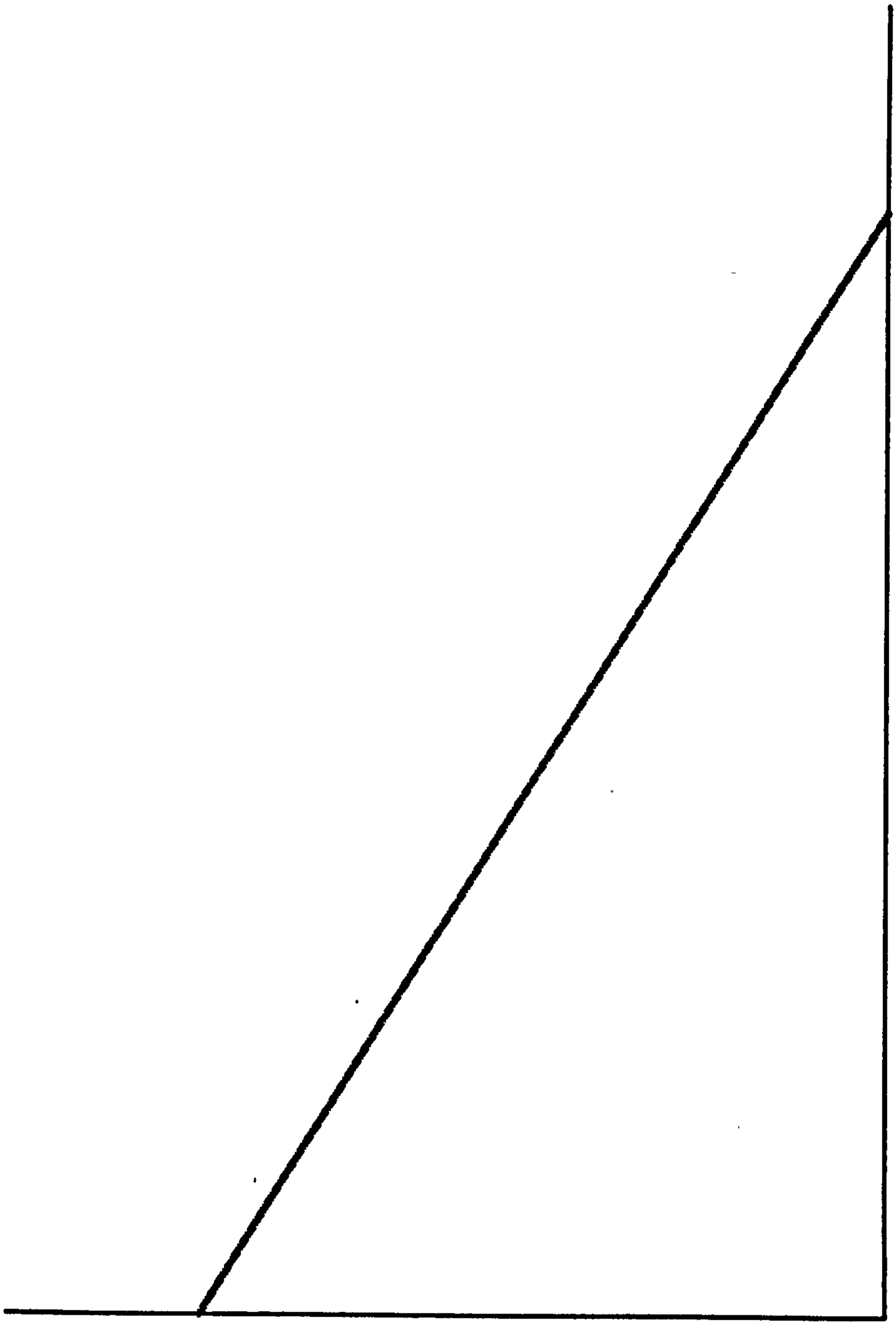

Fig 3.3 Graphical representation of Hottel-Whillier-Bliss formulation

of the collector decreases as the temperature difference increases. This is because the convective and radiative losses from the plate increase as the temperature increases. There are number of ways in which these losses can be reduced at higher temperatures and the efficiency of the collector can be improved. For instance,

a) by increasing the number of transparent covers the radiation losses from the collector plate can be reduced. This enhances the performance at higher operating temperatures although there will be a loss of optical efficiency. Fig 3.4 shows the effect of increasing the number of glass covers. The collector performance improves at higher operating temperatures as the number of covers is increased (the data for this figure has been adapted from [17]; the parameters are: inter-plate spacing=9.5 mm, absorber solar absorptance and infrared emittance=0.95).

b) by using a selective absorber coating on the plate. These coatings have the special radiation property that they absorb a very high percentage of radiation in the solar spectrum (e.g. 85%-95%) but in the infrared band their emittance is very low (e.g. 0.9-0.15). Thus, while the most of solar radiation impinging on the plate is absorbed, the longwave radiation losses from it are reduced to a minimum level. The result is a higher performance of the collector.

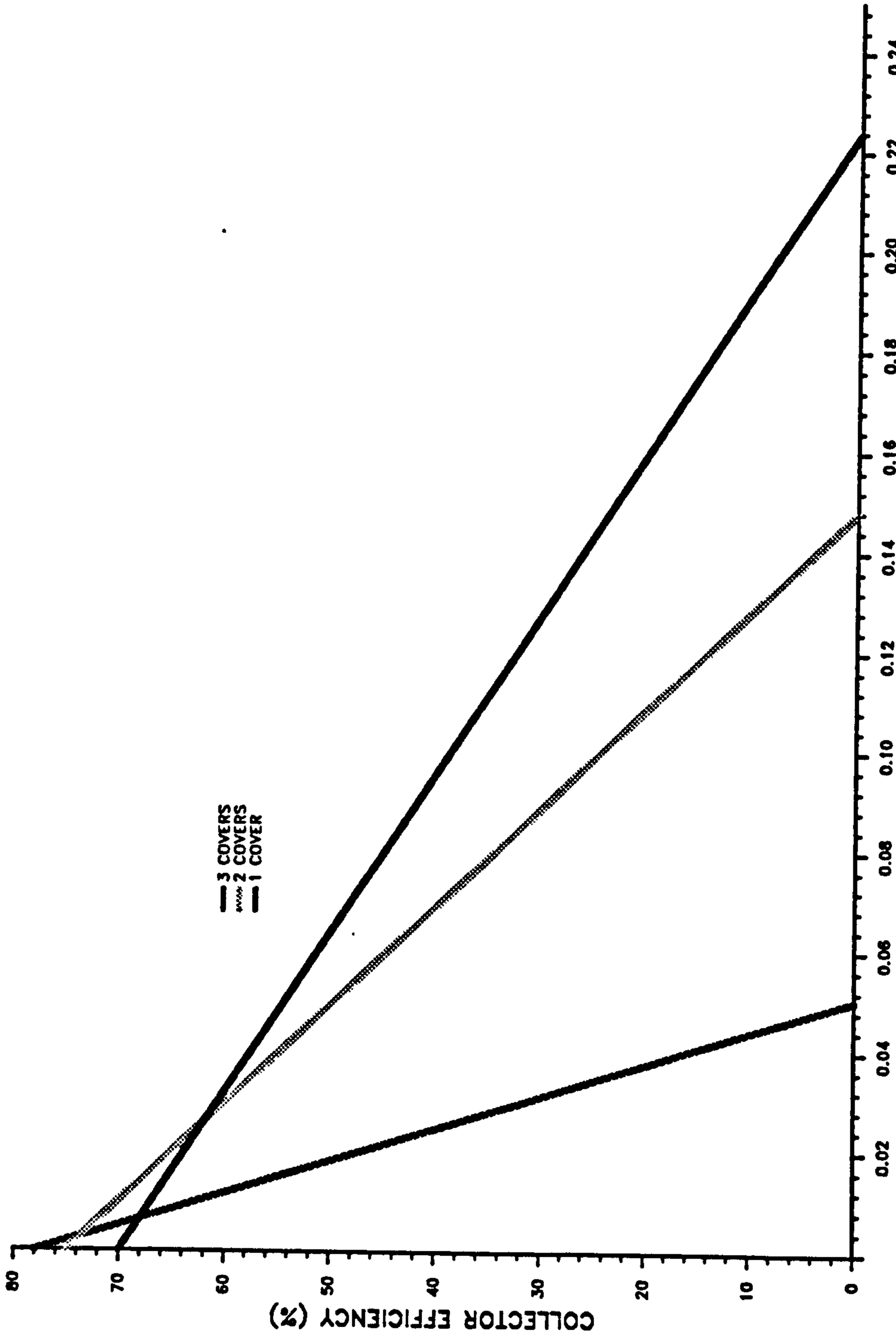

Fig 3.4 Improvement in collector efficiency by increasing number of covers

c) by evacuating the space between the plate and glass covers or putting in some honeycomb structure can reduce the convective and conductive losses thereby improving its performance.

Fig 3.5 shows a qualitative comparison of different measures described above to enhance the performance of a flat-plate collector.

3.3 Evacuated-tube collector (ETC)

This can be described as a cluster of many flat-plate collectors incorporating different performance enhancing features described earlier. The absorber surface in this case can be a long and narrow plate, or a concentric tube, with a selective coating, enclosed in an evacuated tubular glass envelope. The evacuated glass envelope reduces the convection and conduction losses; thus increasing the limit of achievable stagnation temperature (i.e the temperature at which heat losses from the absorber are equal to the heat gains). Different methods for removal of heat from the absorber are employed in different designs.

Fig 3.6a shows a Corning Glass Company's collector; the evacuated envelope was a 102 mm pyrex glass tube holding a flat-plate absorber, with a selective coating, to which a U-shaped tube was attached through which the heat-transfer fluid was circulated. Fig 3.6b illustrates another variation produced by Owens Illinois

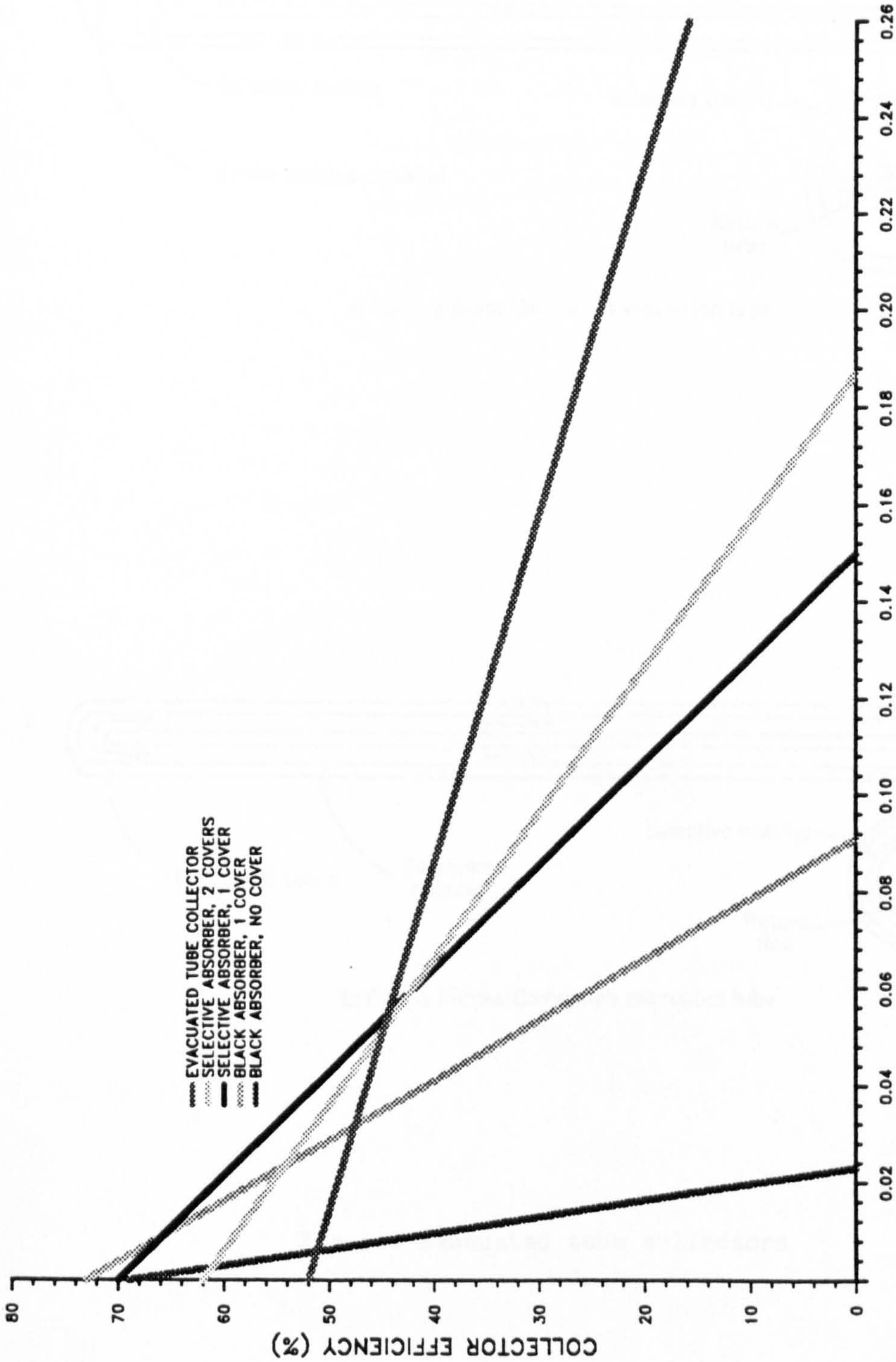

Fig 3.5 Efficiency curves for different types of flat plate collectors

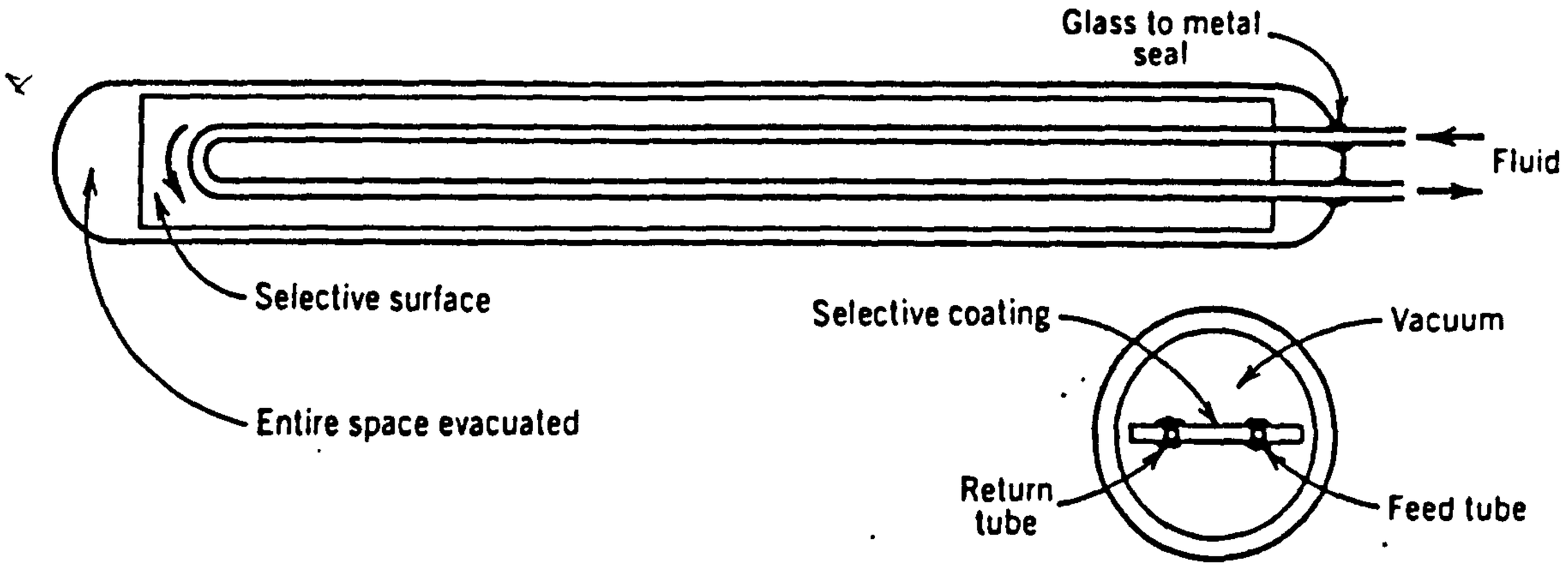

a) Corning Glass Company's evacuated tube

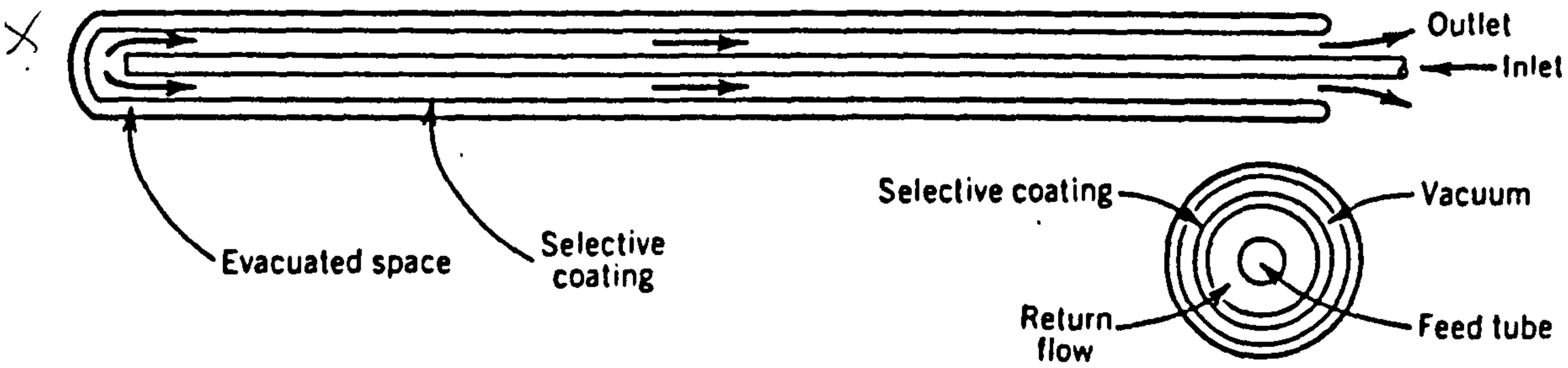

b) Owens Illinois Company's evacuated tube

Fig 3.6 Evacuated tube collectors

Company. This design had three concentric glass tubes. The outercover tube was 53 mm diameter and the overall length is 1067 mm. inner most tube was the delivery pipe through which the heat-transfer fluid entered and returned after circulating through the middle tube. This tube had a selective coating on its outer surface and is hermetically sealed with the outer cover. The space between the two was evacuated.

The two commercial designs discussed above are representative of two basic configurations used for evacuated tubes, i.e. the metal-in-glass arrangement and all-glass configuration respectively. In case of the metal-in-glass type the collectors are connected in series making a serpentine-passage for the heat-transfer fluid through the ETC module. The all-glass ETCs are all connected to one or two manifolds, which carry the streams of heat-transfer fluid. The major drawback in these arrangements is that the failure of one ETC makes the whole module inoperative. The ETCs are high performance collectors but are not used for temperatures in excess of 150^{o}C. The limit is imposed upon by the selective coating, differential thermal expansion and degradation of elastomeric seals. Thus the system designs involving ETCs must incorporate the provision to circumvent the possibility of overheating. An extensive review of the status of ETCs may be found in [18] and [19].

3.3.1 Evacuated tube heat pipe collectors (ETHPC)

This is a variation of metal-in-glass ETCs and differ from the main class by the way the heat is removed from the plate. Instead of heat-transfer fluid getting in direct contact with the plate a heat pipe is used to transfer the collected heat from the plate and transfer it to a manifold through which the heat-transfer fluid is passed. The main advantages of this arrangement are:

a) inherent frost protection

b) low heat capacity

c) high heat-transfer rates

d) thermal diode effect protects against undesired cooling of heating media

e) failure of one tube does not make the whole module inoperative

Fig 3.7 shows a typical ETHPC module manufactured by Thermomax limited [20,21]. In this design the collector plate is coated with a selective coating and is spot-welded to a heat-pipe. The condenser of the heat pipe transfers the heat by direct contact to the fluid flowing in the manifold. There are other variations of ETHPCs commercially available. A few designs have incorporated a concentrating reflector behind the heat pipe (e.g General Electric of USA and Sanyo of Japan). Others transfered heat from the condenser to the manifold by directly clamping it to the manifold (e.g. Fournelle). A detailed analysis of ETHPC was done in order to identify the parameters which would enhance their performance. This is presented in appendix A.

EVACUATED HEAT-PIPE SOLAR COLLECTOR

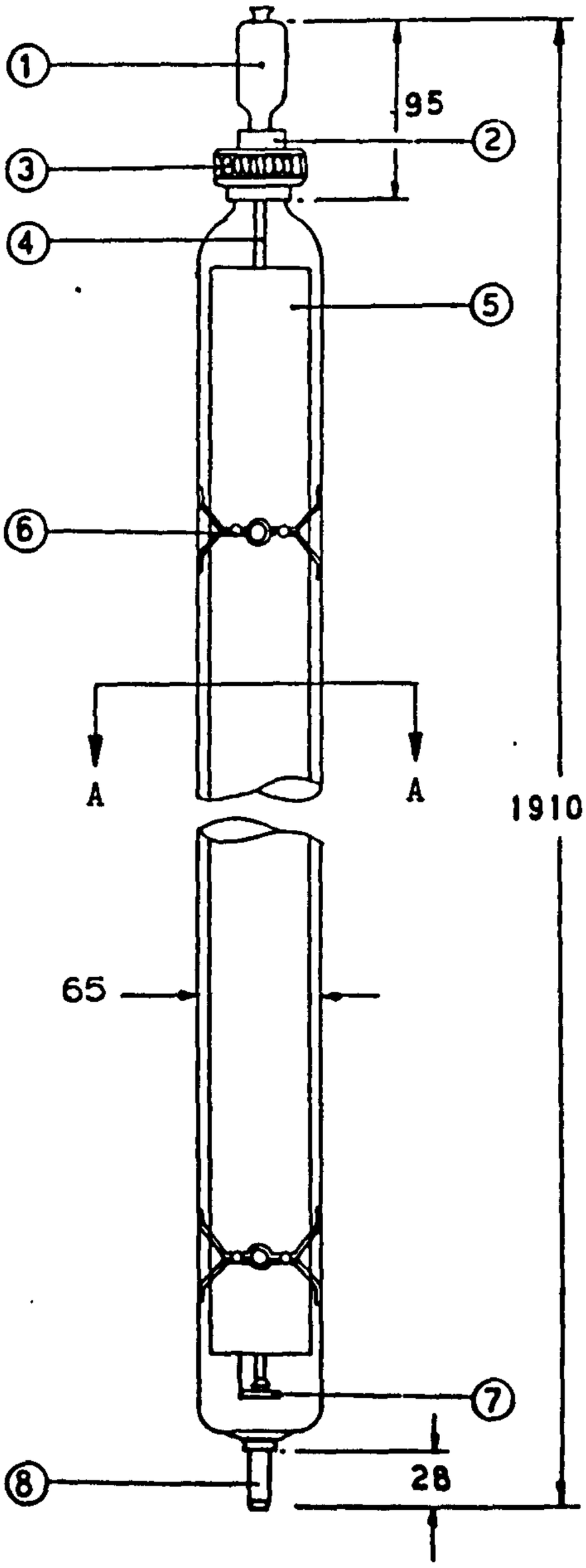

(1) Condenser

(2) Frost Protection Ring

(3) Retaining Cap

(4) Heat Pipe

(5) Absorber Plate

(6) Absorber Support

(7) Getter

(8) Bottom Support

A - A

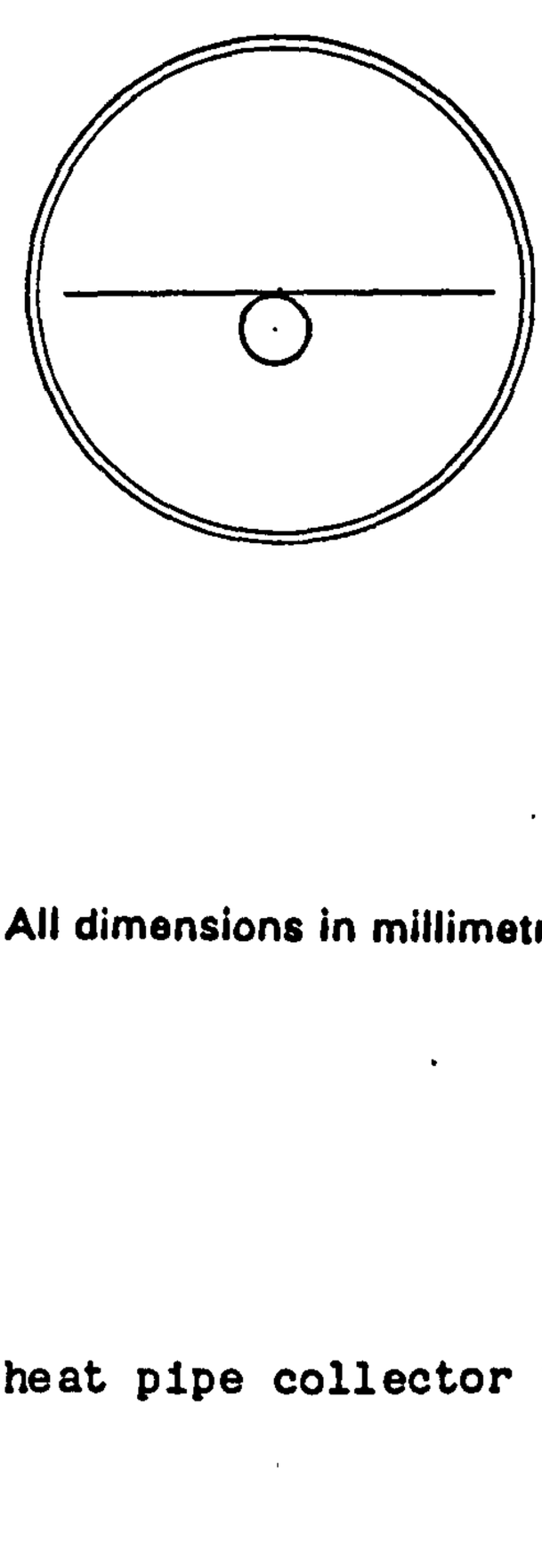

All dimensions in millimetres

Fig 3.7 A THERMOMAX evacuated tube heat pipe collector tube

3.4 Photovoltaic cells

The photovoltaic phenomenon was first observed by Bacquerel in 1839. He observed that more e.m.f. could be generated from an electrolytic cell if the light is allowed to fall on it. He discovered further that increase in the output of cell was dependent on the wavelength of the light. This was observed in an all-solid-state system in 1876 for the case of selenium. Later this material was used with cuprous oxide to develop a solar cell. The silicon solar cell was reported in 1941 but their widespread use as an energy source began in 1958 in spacecrafts.

By early 1970s silicon cells with improved efficiency reawakened the interest in their terrestrial application. By the end of 1970s, the volume of cells produced for terrestrial application had outstripped that for space use.

3.4.1 Properties of semiconductors

Semiconductors according to their electrical properties lie between metals and insulators. Metals have free electrons in their outer shell whereas insulators have a closely packed outer shell with seven or eight electrons. Semiconductors, being in the middle of two extremes, can contain three, four or five electrons in their outer shell.

Most of the semiconductors have a crystalline structure, at least, at microscopic level. At low temperatures and equilibrium state all the available states upto a certain energy level are occupied by two electrons of opposite spin (according to Pauli exclusion principle). This energy level is known as the Fermi level. Electrons may jump to higher energy levels if their energy level is raised. After this electron migration some levels in the originally completely filled band (valance band) would be vacant and some in the next higher band (conduction band) would be occupied. Vacant states in the valence band can be regarded as a physical particle of positive charge commonly known as a hole. The electrons in the conduction band have an abundance of vacant energy states and thus can contribute to current flow. The current flow can be regarded as being due to the sum of the motion of electrons in the conduction band and holes in the valance band. This phenomenon is illustrated in fig 3.8.

Semiconductors are clssified into three catagories .

1 Intrinsic semiconductor in which the electron-hole pairs are produced purely as a result of thermal excitation across the band gap.

2 Extrinsic semiconductors in which additional electrons are present in the conduction band due to ionized donor imperfections (these are called n-type materials), or in which additional holes are present in the valance band due to ionized acceptor imperfections (these are known as p-type materials).

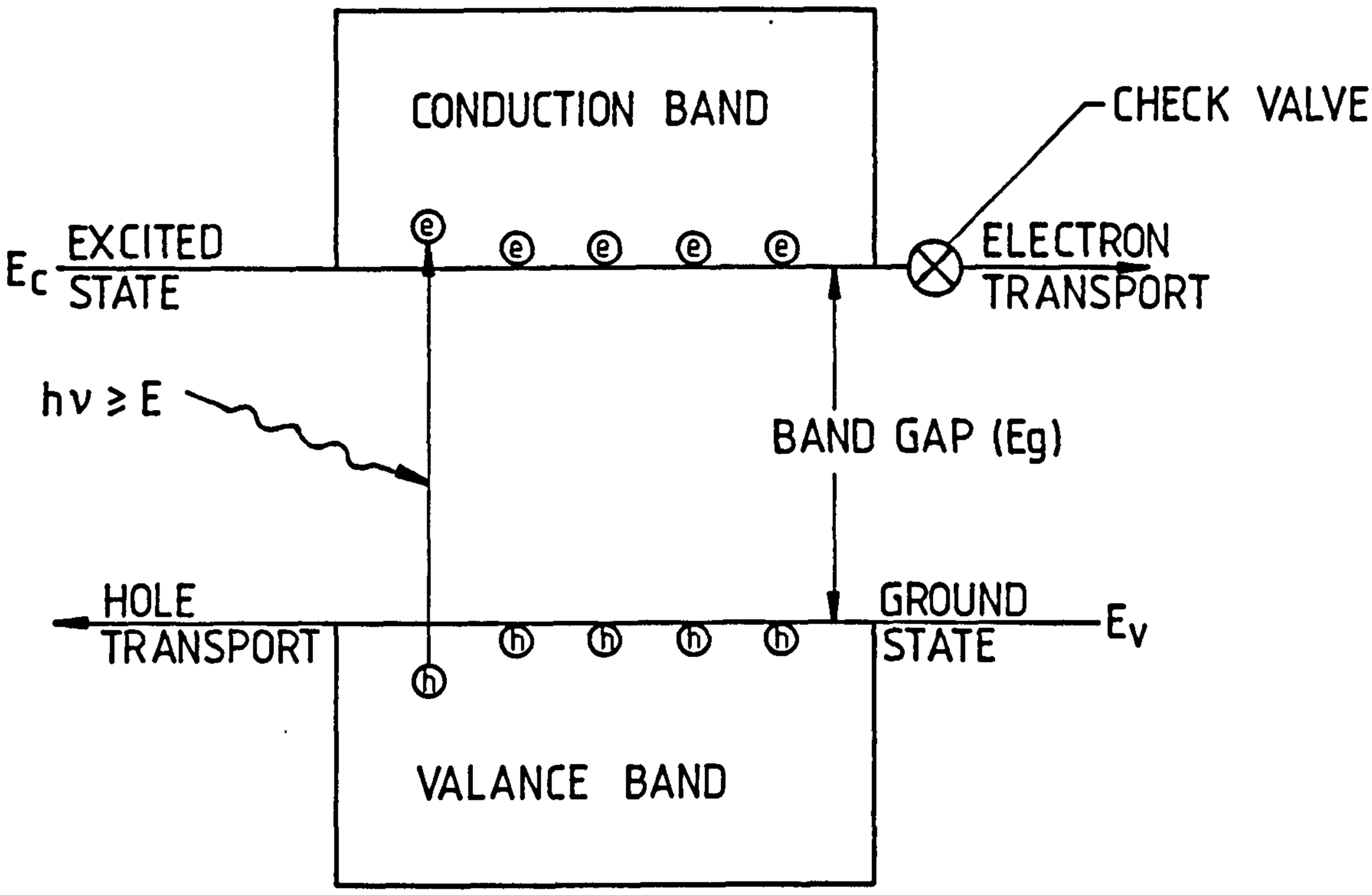

Fig 3.8 Mechanism of conversion of solar energy into electricity

3 Degenerate semiconductor is the one in which so many donor (or acceptor) imperfections are present that states at the bottom of conduction band are almost occupied with electrons (or states at the top of valance band are totally occupied with holes) and Fermi level lies within the conduction (or valance) band.

The energy band diagrams for these cases are shown in fig 3.9.

3.4.2 Principle of photovoltaic conversion

The process of photovoltaic conversion involves absorption of light rays from the solar spectrum. A certain fraction of the incident energy is reflected and the remainder transmitted into the semiconductor. The transmitted light can be absorbed within the semiconductor by using its energy to excite electrons from occupied valance bands to unoccupied conduction bands. Since the two bands are separated by forbidden band, absorption is particularly likely when the energy of photons, making up the light, is greater than the energy of forbidden band gap, E_g, of the semiconductor.

The solar-thermal conversion process, limited by the temperature difference between absorber and ambient, utilizes total spectrum of irradiation. Photovoltaic conversion process due to the quantum electronical transitions involved is sensitive to the spectrum of irradiation and thus is affected by spectral distribution of solar radiation.

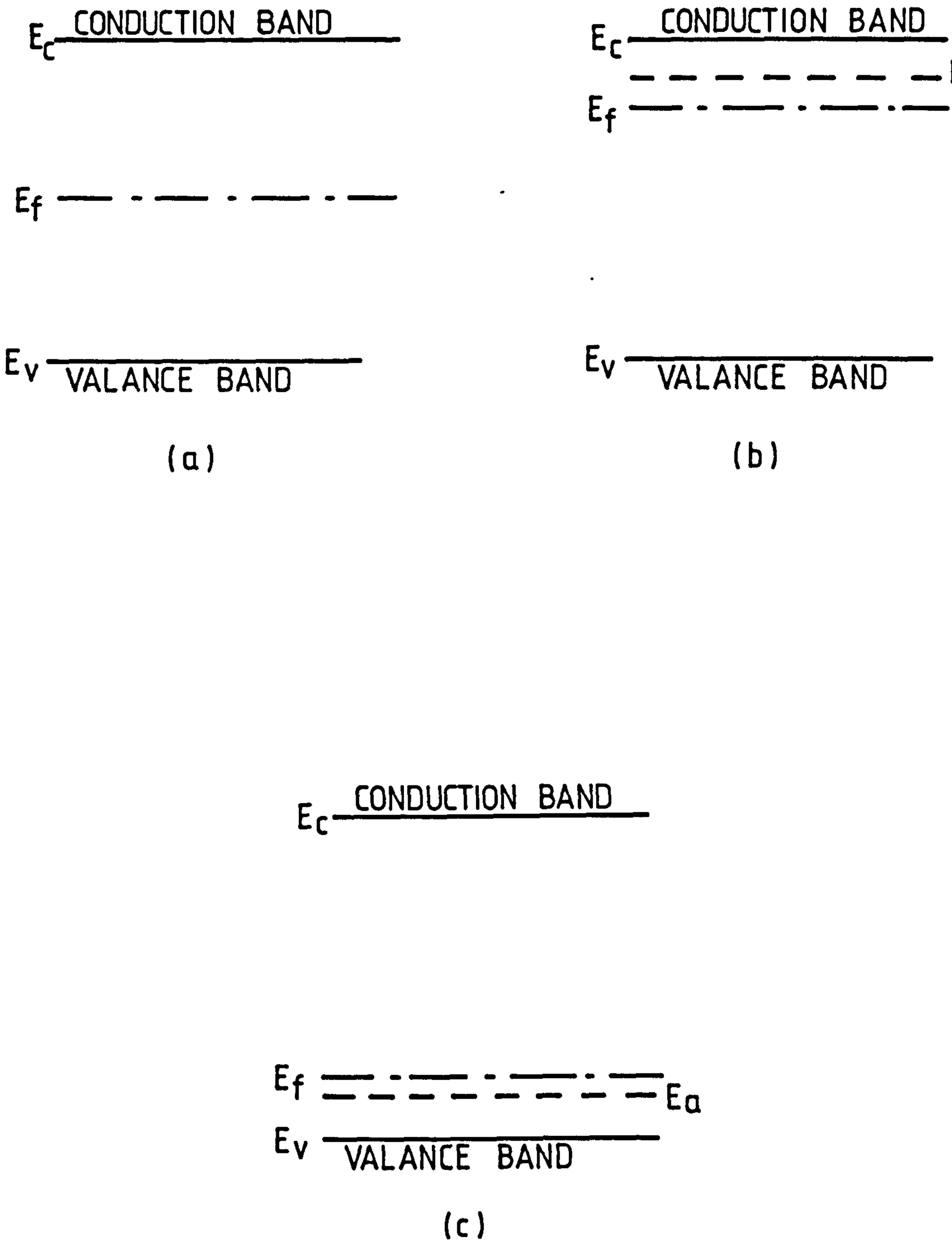

Fig 3.9 Energy band diagrams for three principal types of semiconductors
(a) intrinsic (b) extrinsic (c) degenerate

3.4.3 Structure of solar cells

Regions of semiconductors doped with donor impurities have an increased number of electrons in the conduction band at normal temperatures and are known as n-type material. Those doped with acceptors are known as p-type. The most common solar cells are made by forming a junction between n-type and p-type regions.

There are three common construction features in present day solar cells.

a) An optical absorber which converts photons to electron-hole pairs i.e. the semiconductor;

b) an internal potential energy barrier which separates these charges before they can recombine; and

c) contacts at the ends of the semiconductor to make connection with an external load.

These are not necessarily separated physically within the cell. The four most common type potential energy barriers employed are;

1 Homojunctios : p/n junctions within the same semiconductor material produced by doping process.

2 Hetroface structures : similar to homojunctions but with a window layer of a larger band-gap semiconductor material added to reduce surface recombination losses.

3 Heterojunctions : p/n junctions constructed from two different semiconductor materials.

4 Schottky barriers : the barrier is constructed from a junction between a metal and a semiconductor.

Fig 3.10 illustrates each type and one can see readily that cells have layered structure. In the case of homojunctions the light falls on to a thin layer of, usually, n-type material through a contact grid. For heterojunctions two possible configuration are shown: frontwall mode where the light falls through a contact grid on to a thin layer of the smaller band-gap material and backwall configuration where the light is incident through a contact grid on the larger band-gap material. Schottaky barrier can again have two possible configurations. Incident light can fall on the semi-transparent metal film (i.e frontwall illumination mode) or through the semiconductor (i.e backwall illumination mode).

3.4.4 Expected efficiencies of solar cells

Table 3.2 gives the photon energy levels in different spectral bands of solar spectrum. It can be seen from the table that significant amount of solar irradiance is available in the far infrared region, i.e. wavelength greater than 1.15 micron. The photon energy available in this spectral band is very low and cannot be used by a solar cell. This is one of the reasons for their lower efficiency.

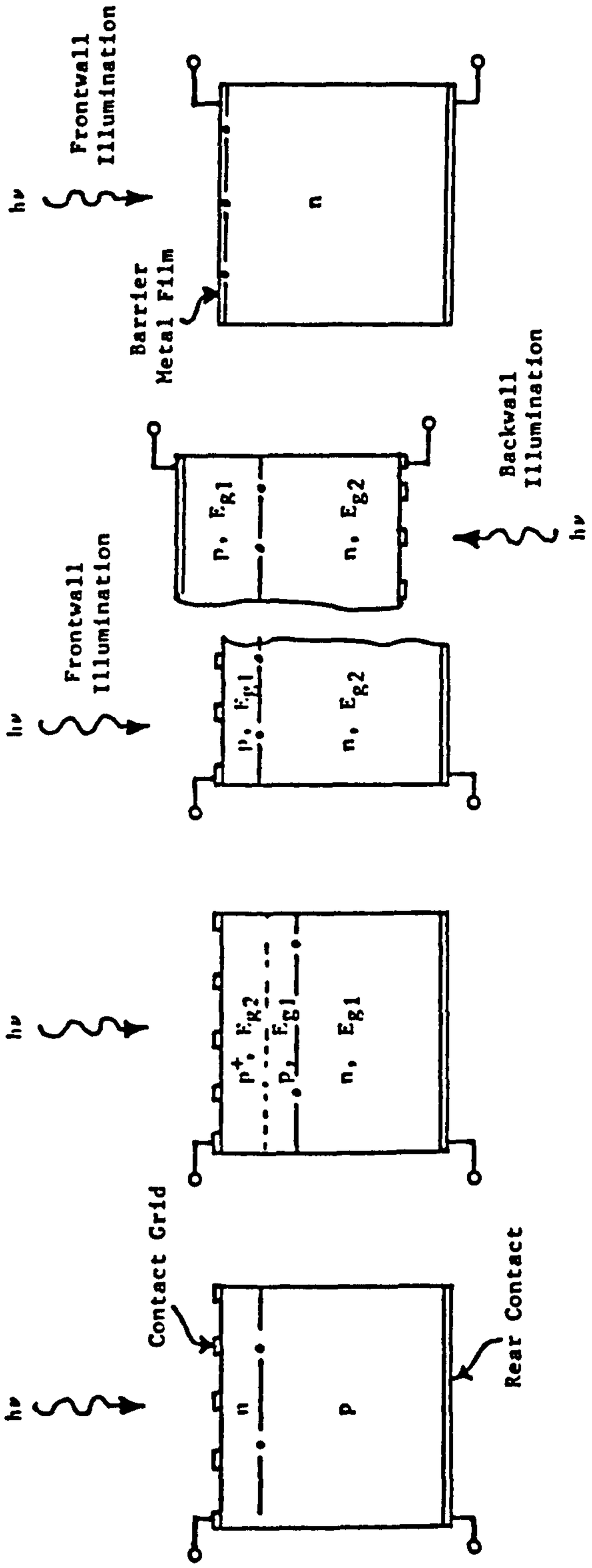

Fig 3.10 Types of potential energy barriers employed in solar cells

TABLE 3.2

Photon energy and solar spectral irradiance
in different spectral bands

Wavelength (micron)	Energy (eV)	Solar spectral irradiance (Wm^{-2})	
		AM0	AM1
- 1.15	0.00 - 1.08	317.7	252.4
1.15 - 1.00	1.09 - 1.24	95.1	84.1
1.00 - 0.90	1.25 - 1.38	82.9	60.2
0.90 - 0.80	1.39 - 1.55	99.3	83.5
0.80 - 0.70	1.56 - 1.78	123.7	80.5
0.70 - 0.60	1.79 - 2.07	151.5	132.5
0.60 - 0.50	2.08 - 2.49	177.0	143.0
0.50 - 0.40	2.50 - 3.11	187.7	151.0
0.40 - 0.30	3.12 - 4.14	101.7	79.1
0.30 - 0.20	4.15 - 6.22	16.3	3.7
0.20 - 0.00	6.23 -	0.1	0.0
	Total	1353.0	1070.0

Different materials used in solar cells have different band gaps and absorption coefficients. Thus the spectral energy available from the sun would be utilized in different proportions by different materials. Neville [22] computed the theoretical maximum power available from six commonly used semiconductors as solar cells. Data for band gaps and absorption coefficients was picked from the available literature. The calculations were based on the assumption of complete absorption of the photons having greater energy than the band gap E_g. Table 3.3 lists his results.

Interaction of radiation with semiconductors is characterized by absorption coefficient. The phenomenon of absorption is wavelength dependent and thus the coefficient of absorption vary with the wavelength. Fig 3.11 shows, for different materials, the variation of absorption coefficient with photon energy. It is evident from the diagram that slopes (on logrithmic scale) for some materials (i.e. direct band gap materials) are much higher than others. This implies that different materials would require different thickness to absorb the same energy. Crystalline silicon cells are usually between 50 and 100 micron thick whereas amorphous silicon cells can be made with thickness below 1 micron [23].

The inefficiency of solar cells can be attributed to many factors such as reflection and transmission losses, nonideal junctions, cell resistances, collection efficiency, etc. But the major limitation comes from the photovoltaic conversion efficiency which is a characteristic of the material itself. Fig 3.12 shows maximum achievable conversion efficiencies of solar cells produced from

TABLE 3.3

Solar spectral power and usable energy ($mWcm^{-2}$)
for six common solar cells

Wavelength (micron)	Sun		Si		InP		GaAs		CdTe		AlSb		CdSe	
	AM0	AM1	AM0	AM1	AM0	AM1	AM0	AM1	AM0	AM1	AM0	AM1	AM0	AM1
- 1.15	31.77	25.04	0.00	0.00	0.00	0.00	0.00	0.00	0.00	0.00	0.00	0.00	0.00	0.00
1.14 - 1.00	9.51	8.41	6.20	5.43	0.00	0.00	0.00	0.00	0.00	0.00	0.00	0.00	0.00	0.00
0.99 - 0.90	8.29	6.02	6.98	5.33	4.97	3.66	0.00	0.00	0.00	0.00	0.00	0.00	0.00	0.00
0.89 - 0.80	9.93	8.35	7.41	5.95	8.71	6.92	8.24	6.84	6.98	4.80	0.00	0.00	0.00	0.00
0.79 - 0.70	12.37	8.05	8.29	5.20	9.60	6.09	10.35	6.65	10.63	6.81	7.35	4.38	3.90	2.72
0.69 - 0.60	15.15	13.25	8.66	7.49	10.18	8.79	10.97	9.47	11.32	9.81	12.75	11.02	13.38	11.58
0.59 - 0.50	17.70	14.30	8.64	7.20	10.09	8.38	10.88	9.05	11.12	9.38	12.62	10.53	13.25	11.00
0.49 - 0.40	18.77	15.10	7.53	5.88	8.80	6.87	9.49	7.40	9.82	7.67	11.02	8.61	11.58	9.05
0.39 - 0.30	10.77	7.91	3.24	2.00	3.78	2.34	4.08	2.52	4.24	2.61	4.75	2.94	4.99	3.07
0.29 - 0.20	1.63	0.56	0.42	0.13	0.49	0.15	0.53	0.16	0.55	0.17	0.62	0.19	0.65	0.20
0.19 - 0.10	0.01	0.01	-	-	-	-	-	-	-	-	-	-	-	-
Total	135.90	107.00	57.37	44.61	56.62	43.20	54.54	42.09	54.66	41.25	49.11	37.67	47.75	37.62
Fraction absorbed of maximum possible	1.00	1.00	0.42	0.42	0.42	0.40	0.40	0.39	0.40	0.39	0.36	0.35	0.35	0.35

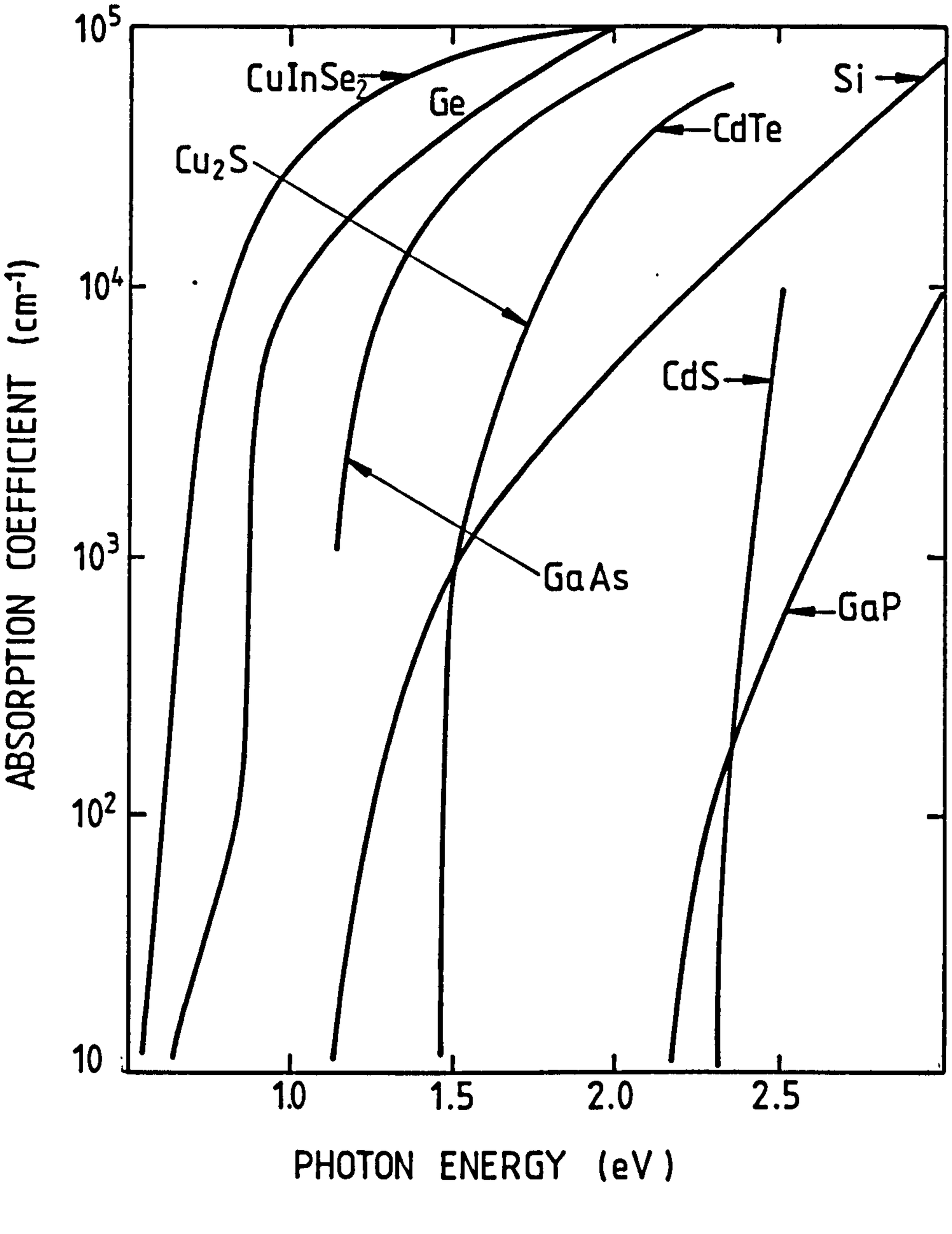

Fig 3.11 Optical absorption coefficient curves for different semiconductors used in solar cells

different materials. These theoretical efficiencies do not take into account the above mentioned factors. The efficiency shows a great dependence on the operating temperature and energy band gap. The optimum band gap varies as the operating temperature changes. Thus, under different environmental conditions, different materials would show an optimum performance.

The actual efficiencies of commercially produced solar cells are lower than the theoretical efficiencies. Efficiencies, cited in the literature, for some cell types, which are considered economical for photovoltaic power production, are listed below;

single crystalline Si	0.12-0.15
poly-crystalline Si	0.10-0.12
single crystalline GaAs	0.16-0.20
thin film CdS-Cu_2S	0.08-0.10
thin film CdS-$CuInSe_2$	0.08-0.10
amorphous Si	0.06-0.08

Subject of solar cells is too vast and diversified to be covered in a few pages. In the previous few sections essential theoretical and technical aspects have been discussed. However, bibliographical references at the end of the chapter are provided for the readers who wish to obtain a deeper understanding and knowledge of the subject.

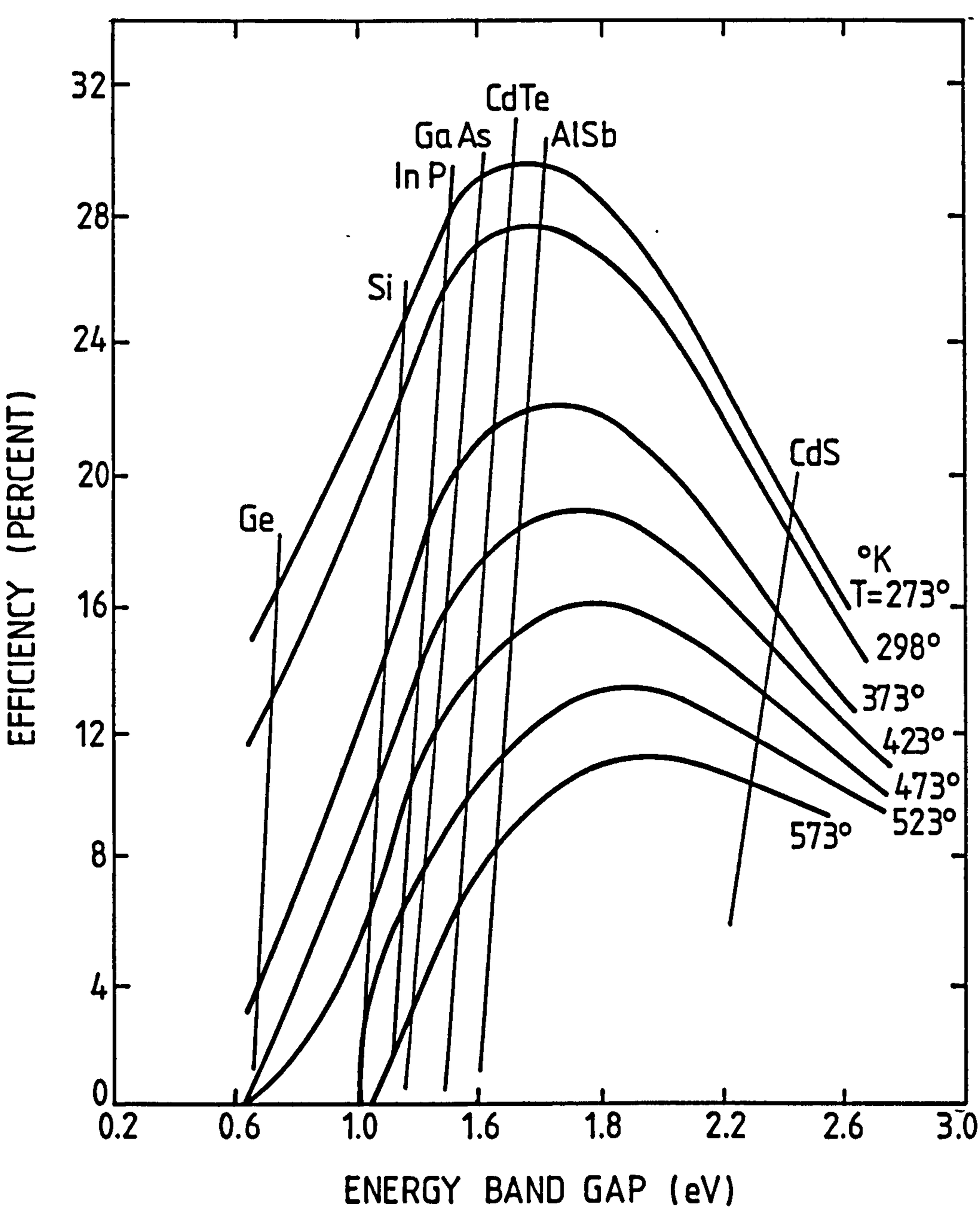

Fig 3.12 Variation of theoretical conversion efficiency of an ideal homojunction with band gap and operating temperature

REFERENCES

1 Frolich, C. and Brura, R.W., 'Solar radiation and its variation in time', Solar Physics, vol 74, pp 209-, 1981.

2 Duffie, J.A. and Beckman, W.A., 'Solar Engineering of Thermal Processes', John Wiley and Sons, N.Y., USA, 1980.

3 Thekaekara, M.P. and Drummond, A.J., 'Standard values for solar constant and its spectral components', National Physical Science, vol 229, pp 6, 1971.

4 Duncan, C.H., Willson, R.C., Kendall, J.M., Harrison, R.G. and Hickey, J.R., 'Latest rocket measurements of the solar constant', Solar Energy, vol 28, no 5, 1982.

5 Hickey, J.R., Alton B.M., Griffin, F.J., Jacobwitz, H., Pellegrino, P., Maschhoff, R.H., Smith, E.A. and Von der Harr, T.H., 'Extraterrestrial solar irradiance variability, two and one-half years of measurements from Nimbus 7', Solar Energy, vol 29, no 2, pp 125-, 1982.

6 Eddy, J.A., 'A new sun, the results from skylab', NASA report SP-402, 1979.

7 Thekaekara, M.P., 'Solar radiation measurement: technique and instrumentation', Solar Energy, vol 18, pp 309, 1976.

8 Stine, W.B. and Harrigan, R.W., 'Solar Energy Fundamentals and Design with Computer Applications', John Wiley and Sons, 1985.

9 Hottel, H.C. and Whillier, A., 'Evaluation of flat plate collector performance', Transactions of the conference on the use of solar energy, Tucson, vol II, part 1, pp 74-104, University of Arizona Press, 1958.

10 Whillier, A., 'Design factors influencing solar collector performance', Low Temperature Applications of Solar Energy, ASHRAE, 1967.

11 Bliss, R.W., 'The derivation of several plate efficiency factors useful in the design of flat plate solar heat collector', Solar Energy, vol 3, no 4, pp 55-64, 1959.

12 Bougard, J., Lagneau, J. and Boussemaere, C., 'Determination of the thermal capacity of CEC-4 collector by several methods', Centre de Recherches sur l'Energie Solaire, Faculte Polytechnique de Monds, Belgium, May 1979.

13 Prapas, D.E., Norton, B. and Probert, S.D., 'Variation of the effective thermal capacitance in a solar energy collector', International Journal of Ambient Energy, vol 8, no 2, pp 59-72, 1987.

14 Garg, H.P. and Datta, G., 'The top loss calculation for flat plate solar collectors', Solar Energy, vol 32, pp 141-143, 1984.

15 Hassan, K., 'Heat transfer through collector glass covers', Proceedings International Solar Energy Society Silver Jubilee Congress, Atlanta, Georgia, USA, pp 312-36, 1979.

16 Tal-Tarlo, I. and Zvirin, Y., 'The effects of radiation properties of surfaces and coatings on the performance of solar collectors', ASME Journal of Solar Energy Engineering, vol 110, pp 217-225, 1988.

17 Altman, M., et al, 'Conservation and better utilization of electric power by means of thermal energy storage and solar heating', Report No. NSF/RANN/SE/GI/27976/pr73/5, University of Pennsylvania, Philadelphia, 1973.

18 Window, B. and Harding, G.L., 'Progress in materials science of all-glass evacuated collectors', Solar Energy, vol 32, no 5, pp 609, 1984.

19 Collins, R.E. and Duff, W.S., 'Principles of evacuated collectors', Solar World Congress, Proceedings of Eighth Biennial Congress of International Solar Energy Society, Perth, Australia, 14-19 August, vol 2, pp 804-809, 1983.

20 Mahdjuri, F., 'Vacuum solar collector equipped with heat pipe', paper presented at International Solar World Congress, Perth, Australia, 1983.

21 Sales literature Thermomax Limited, Bangor, UK.

22 Neville, R.C., Solar Energy Conversion: The Solar Cell, Elsevier Scientific Publishing Company, Amsterdam, 1978.

23 Garg, H.P., Advances in Solar Energy Technology, vol 3, D. Reidel Publishing Company, Holland, 1987.

BIBLIOGRAPHY

1 Fonash, S.J., Solar Cell Device Physics, Academic Press, Inc. N.Y., USA, 1981.

2 Green, M.A., Solar Cells, operating principles, technology, and system applications, Prentice-Hall, Inc., Englewood Cliffs, N.J., USA, 1982.

3 Fahrenbruch, A.L. and Bube, R.H., Fundamentals of Solar Cells, Academic Press, Inc., N.Y., USA, 1983.

4 Hu, C. and White, R.M., Solar Cells : from basics to advanced systems, McGraw Hill, N.Y., USA, 1983

5 Merrigan, J.A., Sunlight to Electricity : photovoltaic technology and business prospects, MIT Press, Cambridge, Massachussets, USA, 1982.

6 Bloss, W.H., 'Photovoltaic energy converters', in Performance of Solar Energy Converters : thermal collectors and photovoltaic cells, D. Reidel Publishing Company, Holland, 1983.

7 Open University, Solar Cell, unit TS251 (10 and 11), Open University Press, Milton Keynes, UK, 1973 and later.

8 Twidell, J. and Weir, T., Renewable Energy Resources, E. & F.N. Spon Ltd, London, UK, 1986.

9 Loferski, J.J., 'Photovoltaic Materials' chapter 18 in Solar Energy Technology Handbook, editors: Dickenson, W.C. and Cheremisinoff, P.N., Marcel Dekker Inc. N.Y., USA, 1980.

10 Proceedings of IEEE Photovoltaic Specialists Conferences held at 18 months intervals.

11 Takakaski, K. and Konagai, M., Amorphous Silicon Solar Cells, North Oxford Academic Publishers Ltd., London, UK, 1986.

12 NASA, Space Photovoltaic Research and Technology 1988, report no NASA CP-3030, proceedings of a conference held at NASA Lewis Research Centre, Cleveland, Ohio, USA, April 19-21, 1988.

CHAPTER FOUR

Adsorption of Vapours on Solids and its Application to Refrigeration

4.1 Adsorption process

When two materials are in contact, there is an interfacial region, the composition of which is different from that of the bulk of either phase. The increase in the concentration of a substance at the interface as compared with its bulk concentration is known as adsorption.

4.1.1 Classification of adsorption

The process of adsorption is classified usually according to (i) the phases constituting the interface, and (ii) the type of forces acting at that surface. Depending on the type of phases in contact four types of adsorption processes can be considered, i.e.

a) liquid/gas
b) solid/gas
c) solid/liquid
d) liquid/liquid

Kiselev [1], Everett [2], and Barrer [3] have classified the process qualitatively, on the basis of molecular interaction at the interface, into specific or non-specific. For detailed study of the subject reader is referred to Oscik [4].

This study is concerned with the adsorption of a gaseous phase on to a solid. The solid in this case is termed as the adsorbent, and the gas, both in bulk and adsorbed phase, is called the adsorbate.

4.1.2 Distinction between adsorption and absorption

Adsorption is a phenomenon which takes place at the external surfaces and, in case of a porous solid, at the internal surface formed by the walls of the pores as well. It is a surface phenomenon that does not involve any changes in the chemical or lattice structure of the solid. Absorption occures if the molecules of adsorbate do not remain on the surface but penetrate into the structure of the solid. In some cases both adsorption and absorption can take place simultaneously. The general term for the latter process, irrespective of the mechanism, (given by McBain [5]), is sorption. The solid in this case is termed as sorbent while, according to some definitions [6], the adsorbed molecules may be considered as a separate adsorbed phase.

4.2 Adsorption from the gaseous phase

The process of adsorption of gases by solids can be broadly classified into two catagories, namely,

(i) physical or van der Waals adsorption;

in which the chemical nature of the adsorbed molecules remains unchanged. The adsorbate molecules are held by the surface molecules of the solid by relatively weak forces; which are same in nature as the forces of attraction which act, for example, in condensation of vapours, and are responsible for the deviations of the behaviour of real gases from the ideal gas behaviour.

(ii) chemisorption;

wherein a chemical reaction takes place between adsorbate and adsorbent surface. A bond is formed between the gas and the solid molecules by exchanging or sharing electrons at the outer orbit. Therefore forces of attraction in this case are much stronger than physical adsorption.

4.3 Physical adsorption of gases

Physical adsorption, is the mechanism by which most of the porous solids and refrigerants of interest herein interact with each other.

As explained above, there are no special adsorption forces. The forces acting in physical adsorption are identical to the intermolecular forces of cohesion, the van der Waals forces (i.e. dispersion-repulsion), which operate in different material phases [7-10]. These electrostatic forces are known to be produced by three effects i.e., Keesom's orientation effect, Debye's induction (polarization) effect, and London's dispersion effect.

The orientation effect contributes significantly towards the mutual interaction of those molecules which have permanent dipole; the magnitude of the effect is inversely proportional to the temperature. The induction effect is caused by induced polarization of molecules in the proximity of a permanent dipole; it is independent of temperature.

These effects are also observed during the interaction of molecules which do not possess permanent dipoles. The effect is explained by putting forward, and subsequently proving its existance experimentally [11-13], the concept of quadrupole. According to the concept a molecule with permanent quadrupole will induce a dipole in a neighbouring molecule and the resulting interaction of the effect produces van der Waals attraction. The energy of this interaction is, however, small and thus the London's dispersion effect is the major contributor towards van der Waals forces between the molecules without electric moment.

London's dispersion effect arises from fluctuating dipole moments. If an atom is without a measurable permanent dipole, this only means that its mean dipole is zero. However, such an atom may have a fluctuating dipole moment about that mean value. This fluctuation being the result of variation with time of the distribution density of electrons round the nucleus. Such a fluctuating dipole, whose orientation in one direction is as probable as its orientation in the opposite direction, gives rise to a fluctuating electric field. When two molecules with fluctuating dipoles come close to one another their total energy decreases and they are attracted to each other. This dispersion effect is also independent of temperature.

A comprehensive review of adsorption fundamentals is beyond the scope of this study. The reader is, instead, referred to earlier discussions by Ruthven [14], Gregg and Sing [15], Cookson [16] and Bikerman [17] and the extensive references cited within these works.

4.4 Adsorption equilibrium

The 'time of adsorption' is defined as the period during which a molecule in adsorbed state remains attached to an adsorption site. This time varies for physical adsorption of different gases and vapours on various porous solids. For instance for activated carbon at room temperature the time of adsorption is in the range from 10^{-12} to 10^{-2} seconds [19], and is determined by the properties of adsorption site, the nature of molecule and its surface, the temperature of the surface and kinetic energy of the molecule. After a longer or shorter period an equilibrium is established when the number of molecules entering and leaving the adsorbed state are equal. This is known as adsorption equilibrium.

Adsorption equilibrium is specified by three properties;

(i) amount of adsorbate m,

(ii) pressure p of bulk phase gas or vapour, and

(iii) the temperature T of the adsorbent-adsorbate complex.

If the temperature is maintained constant during adsorption and only the pressure is varied, the resulting relation between equilibrium pressure and amount adsorbed is known as the adsorption isotherm, whose general equation is

$$m = [f(p)]_T \qquad 4.1$$

Isotherms can have many shapes indicating different structures of adsorbents. Figure 4.1 shows the five basic types of isotherms according to the classification of Brunauer [8]. The diagram shows examples of materials and description of their structure for each type as well. Most of the adsorbents used in refrigeration show I or II type isotherms.

When the pressure is kept constant and the temperature is varied an adsorption isobar is obtained which is represented graphically as in fig 4.2 and mathematically by the relation

$$m = [g(T)]_p \qquad 4.2$$

The data used in constructing the fig 4.2 is from [18] and represent adsorption equilibrium of ammonia on charcoal.

A third type of representation, called isostere, is obtained when equilibrium pressure is determined at different temperatures for constant concentration of the adsorbate. The equation for an isostere is

$$p = [h(T)]_m \qquad 4.3$$

Figure 4.3a is an isosteric representation of the same data which has been used to construct fig 4.2.

TYPE	SHAPE	STRUCTURE & PROPERTIES OF ADSORBENT	EXAMPLES	REFERENCES
I	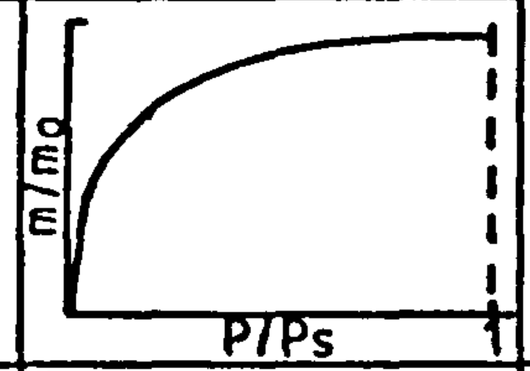	Micrporous structure; pore size is not very much greater than adsorbate molecule diameter. This shape is usually known as Langmuir isotherm.	Ammonia on charcoal Ethyl chloride on charcoal Methanol on activated carbon Methanol on zeolite 13X Water on Zeolite 13X	18, 38 39 38 38 40
II	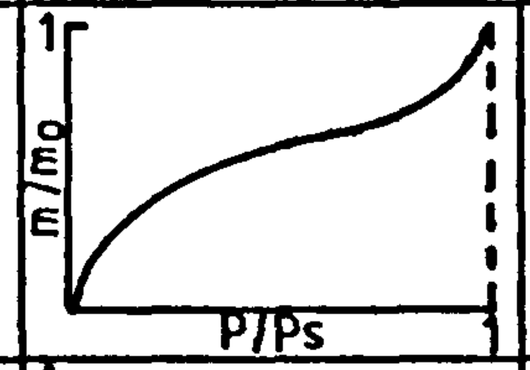	A very common type associated with porous structure; varying pore sizes, generally greater than that of adsorbate molecules; indicates multilayer adsorption.	Various gases e.g. N_2, O_2, argon, on silica gel, activated carbon, soil samples, chromic oxide, etc. Benzene vapours on graphatized carbon black.	8 41
III	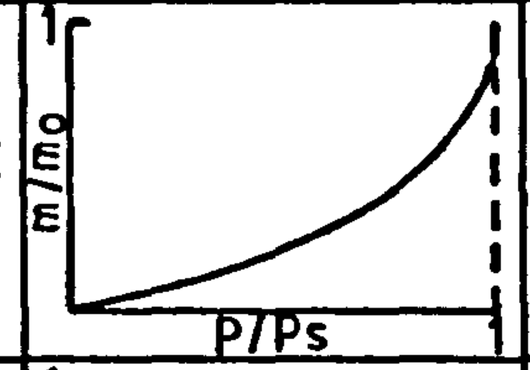	This is rather uncommon. Absolute value of heat of adsorption is equal to or smaller than latent heat of vaporization [4].	Bromine on silica gel. Iodine on silica gel.	42 42
IV	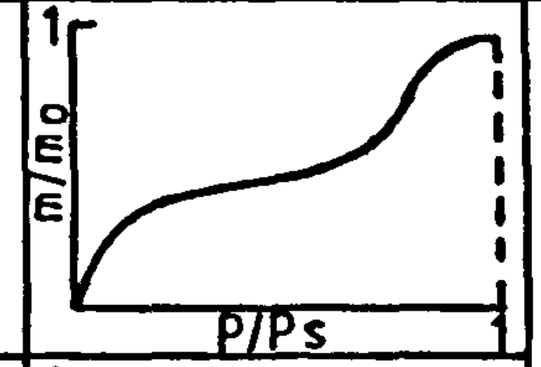	Type IV and V correspond to type II and III, with the difference that adsorption reaches its maximum at a pressure lower than the saturation pressure of adsorbate. The reason is believed to be capillary condensation. Adsorbent possesses variety of pore sizes. Type IV specifically indicate a two-layer adsorption	Benzene on ferric oxide gel.	43
V	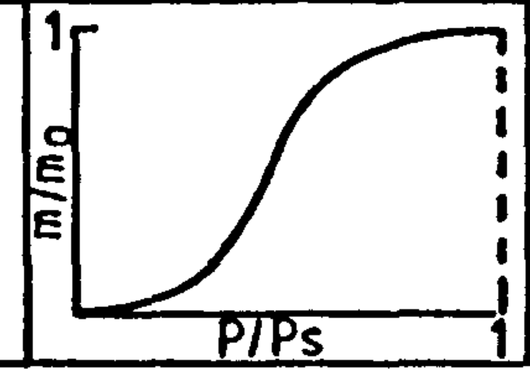		Water on charcoal.	44

Fig 4.1 Brunauer's classification of isotherms

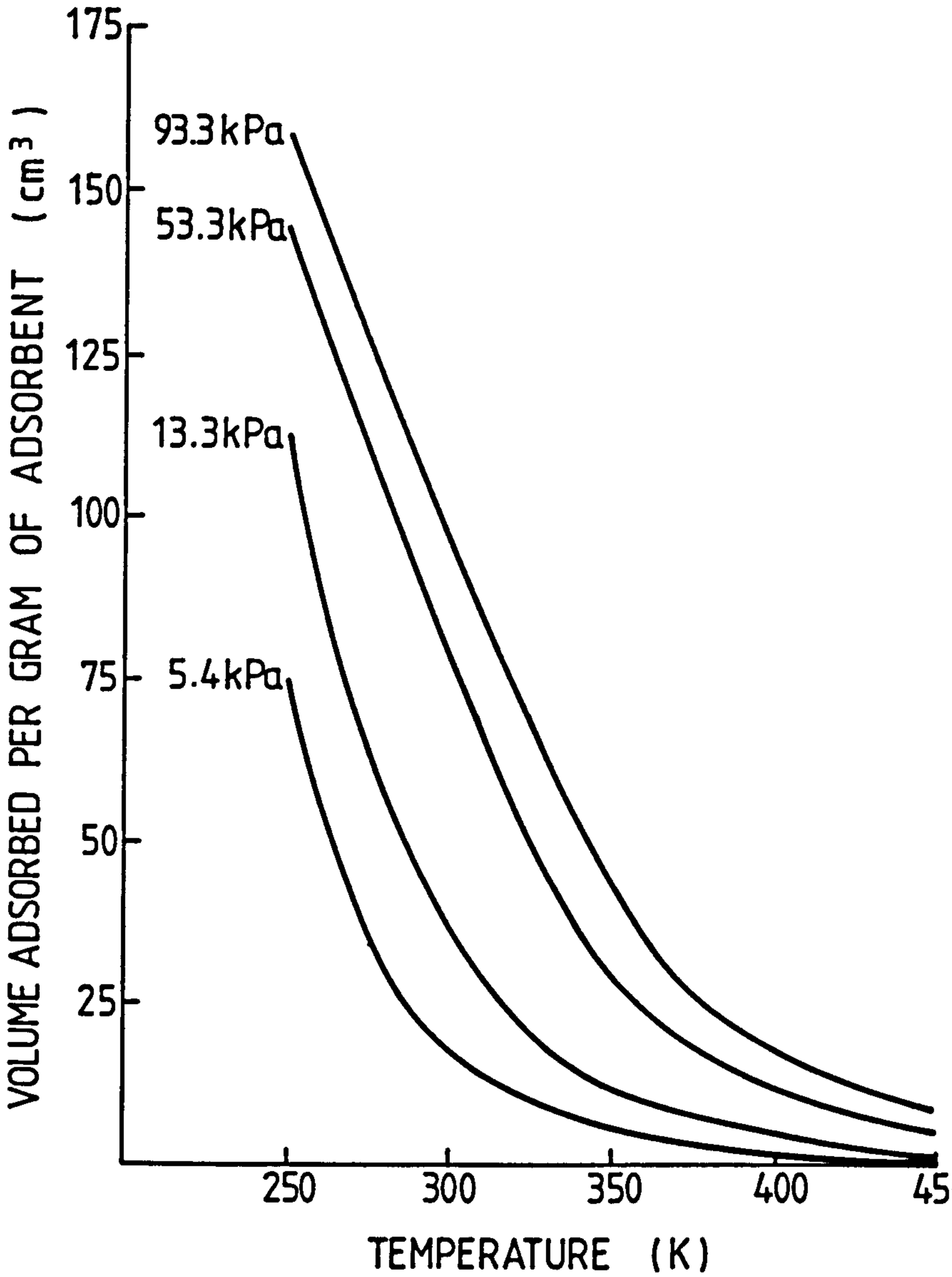

Fig 4.2 Adsorption isobars of ammonia on charcoal [18]

Isosteres resemble the vapour pressure curves of liquids. For a fixed concentration of the adsorbate the pressure rises at first slowly then rapidly with temperature. Thus the curves are concave with respect to pressure axis.

The resemblance of isosteres with vapour pressure curves is more than superficial. Like the vapour pressure curves each point on the isostere represents a unique set of adsorbent-adsorbate temperature and adsorbate bulk pressure at which both are in equilibrium.

Clausius-Clapeyron equation governs the equilibrium between different phases and allows one to calculate the amount the heat involved in the transition from one phase to another,

$$d(\ln p)/d(1/T) = -q/R$$

where q is the change in enthalpy of the system during the phase-change which is assumed to be temperature invariant.

It is customary to plot isosteres as shown in fig 4.3b; i.e. the logarithm of pressure against the reciprocal of absolute temperature. This representation produces a straight line plot of isosteric data. This type of plot is more meaningful as the slope of each isostere represent the left hand side of Clausius-Clapeyron equation 4.4. Thus the heat of adsorption can be readily calculated.

Adsorption isotherm is the usual way of representing the equilibrium. Adsorption refrigeration cycle involves isosteric

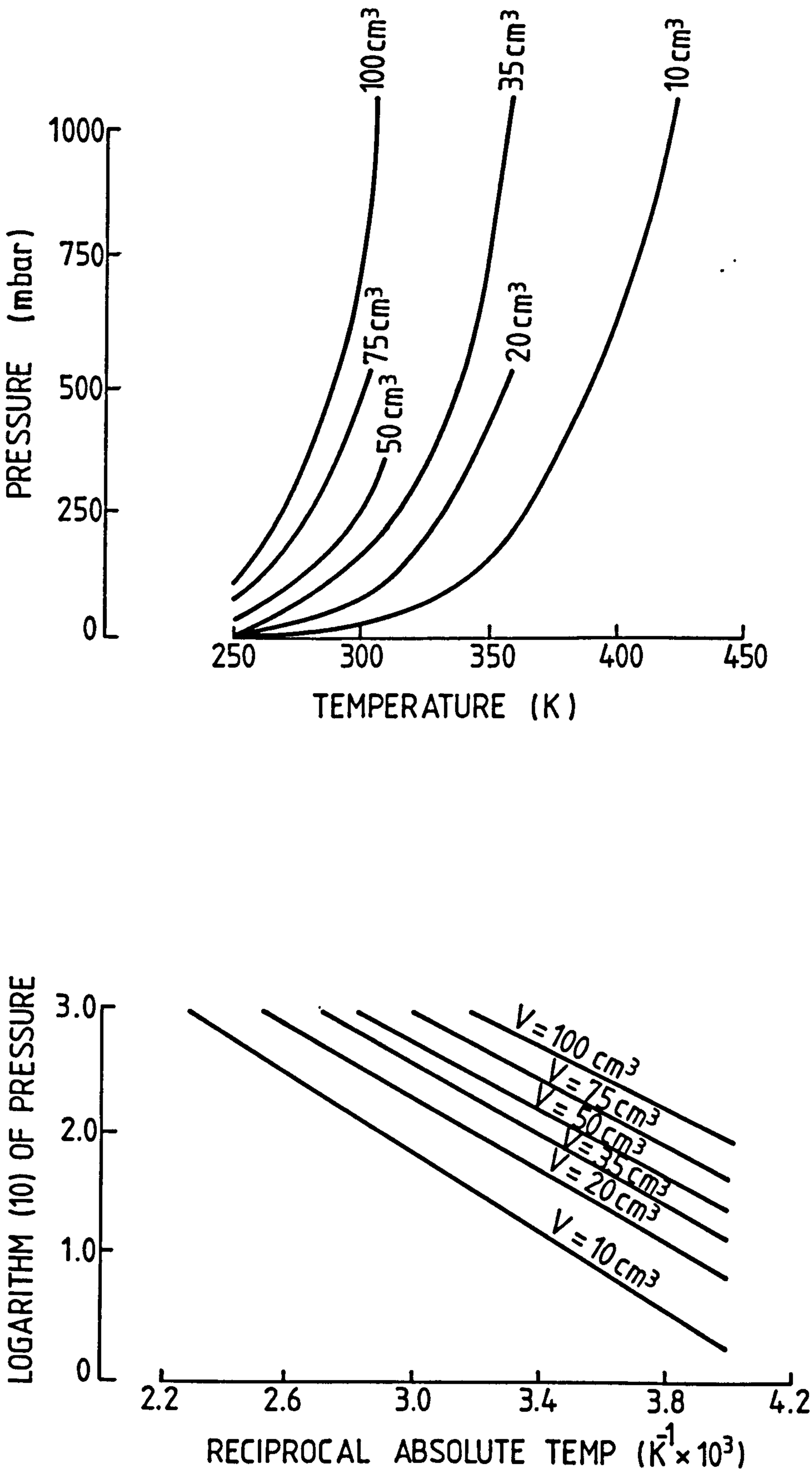

Fig 4.3 Isosteric representation of adsorption data of fig 4.2
(a) linear scale for temperature and pressure
(b) logrithmic pressure and inverse temperature scales

heating and cooling and constant pressure condensation and evaporation processes. Thus for the analysis of adsorption refrigeration cycle, isosteric representation is more suited. Besides, isosteric equilibrium can be established more accurately with simpler apparatus.

4.5 Adsorption equilibrium theories and models

Review of adsorption equilibrium theories and models is relevant to this study. In order to predict the performance of a refrigerator working on adsorption process an accurate description of equilibrium states must be provided.

The adsorbents, on the basis of distribution of potential energy at the adsorption sites (i.e. points corresponding to maxima of potential energy), are catagorized into three types.

(i) Homogeneous

This catagory of solids have same potential energy at all adsorption sites.

(ii) Heterogeneous

If the potential energy varies from site to site these are termed as heterogeneous adsorbents.

(iii) Homotattic

If the variation of potential energy from site to site forms a pattern and districts or patterns of sites having same potential energy can be identified on the surface then the solid is termed as homotattic adsorbent.

Most adsorbents used in refrigeration processes (e.g. activated carbons, zeolites, silica-gel, etc.) are heterogeneous in nature. Thus this section will cover the theories and models describing the adsorption equilibrium of gases and vapours on heterogeneous surfaces.

The complete theoretical calculation of the adsorption equilibrium, from physical properties of adsorbent and adsorbate only, is very difficult. Many models have been put forward so far. Some are very extensively used in industry. But the calculation of adsorption equilibrium for particular systems by these models is semiempirical, because the constants used in these models are determined experimentally for individual solid/gas equilibrium system.

Adsorption equilibrium is, most frequently, represented in the shape of an isotherm. Although when assessing a refrigeration system based on this phenomenon isosteric representation is more informative. Thus the models discussed in the next few sections are equations representing the adsorption isotherm. But isosteric equilibrium, which is more relevant to an adsorption refrigeration system, can easily be deduced from these isotherm equations.

4.5.1 The Langmuir equation

During second world war Langmuir put forward his kinetic theory of adsorption which led to the derivation of the first equation of adsorption isotherm developed theoretically. Many other equations proposed later fit the experimental data better or over a wide range. But all of these equations either use the Langmuir equation as the basis or the theoretical concept for derivation of these equations is the same.

The theoretical principle of Langmuir's molecular-kinetic derivation is the dynamic concept of equilibrium, in which the rates of adsorption and desorption are equal [8,20,21]. He made three other simplified assumptions, which are:

a) Adsorption takes place in a monolayer on the surface of adsorbent and thus the molecules can be adsorbed only on the free surface of the adsorbent. If a molecule strikes an occupied area of the surface it is reflected elastically.

b) The surface of the adsorbent is energetically homogeneous and so the probability of a striking molecule to be adsorbed is equal throughout the surface.

c) Adsorbate-adsorbate interaction is negligible and as such the probability of an adsorbed molecule to leave the surface does not depend on whether the neighbouring sites are occupied or vacant.

The final form of the Langmuir equation is;

$$v = v_m[bp/(1+bp)] \qquad 4.4$$

where v is the volume adsorbed at pressure p and v_m is the volume adsorbed when the surface is covered with a complete monolayer of molecules and b is the adsorption coefficient. For detailed derivation of the equation readers are referred to [8,20,21]. The Langmuir equation was later derived from thermodynamical and statistical principles as well.

Although Langmuir's equation, due to its over-simplified assumptions cannot interpret every kind of experimental data yet its significance remains for expressing the adsorption equilibrium on dynamical principles.

4.5.2 Potential theory of adsorption

This theory was developed by Polanyi at the same time when Langmuir put forward his kinetic theory. The basic idea which forms the basis of potential theory is that at the surface of a solid adsorbent the molecules of the gas are compressed by the forces of attraction acting from surface to a certain distance into the surrounding space. This idea is completely opposite to that of Langmuir's monolayer adsorption. Polanyi [22] characterized the field of the forces of attraction of the adsorbent surface by adsorption potential. He defined the adsorption potential as the work done by the surface adsorption forces in transferring the molecules from gaseous phase to the given point. Fig 4.4 gives a diagramatic representation of potential theory showing the lines of equipotential whose magnitude decreases as distance from the surface increases until it falls to zero. The adsorption potential is given by the equation

$$\varepsilon = RT \ln(p_s/p) \qquad 4.5$$

where R is the gas constant for the vapour, T is the temperature and p is the pressure of the vapour and p_s is the saturation pressure of the vapour at temperature T. To account for non ideal behaviour of real vapours pressures are sometimes replaced by fugacities.

The fundamental postulate of Polanyi's potential theory is the assumption that the adsorption potential is independent of the temperature:

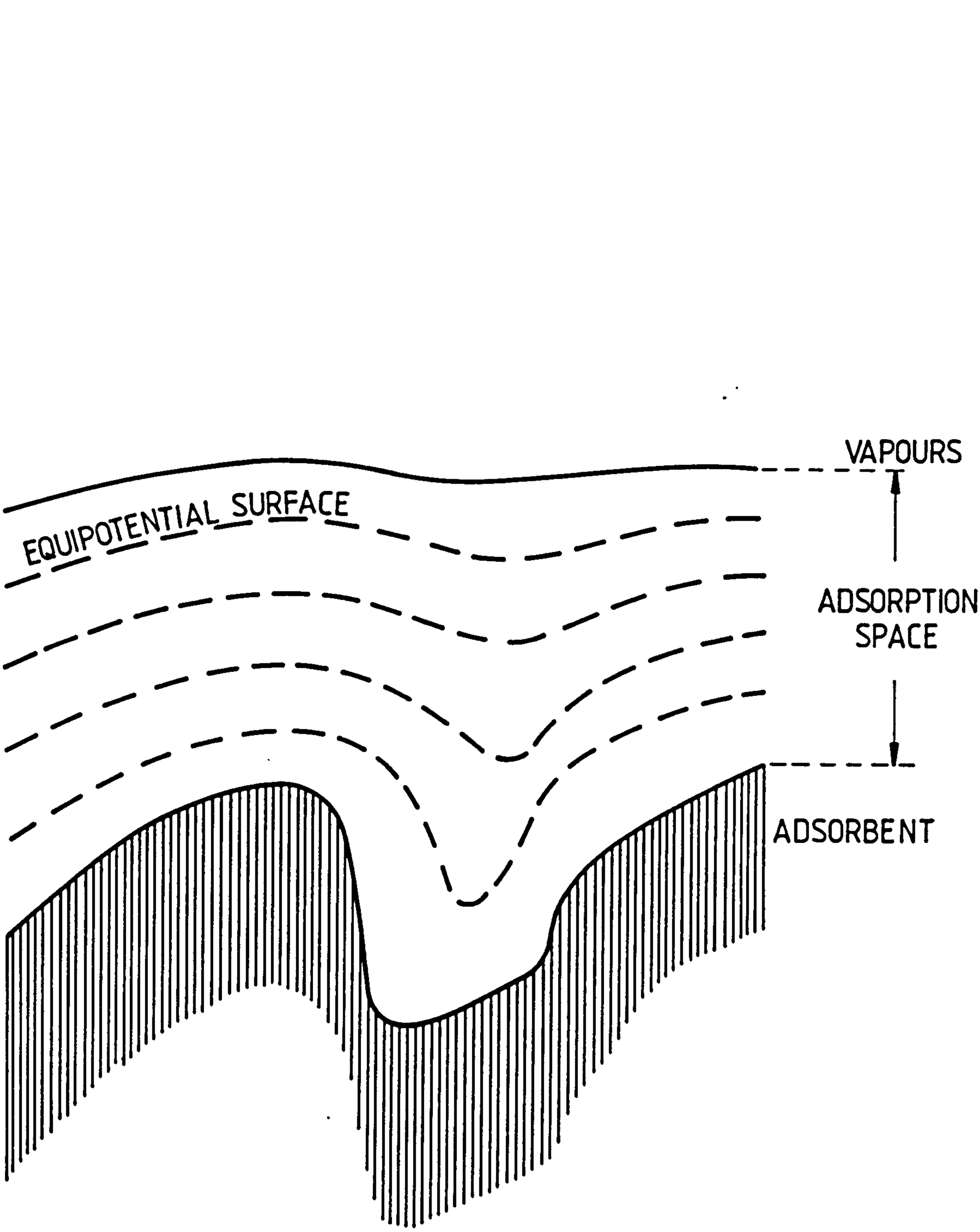

Fig 4.4 Polanyi's equipotential surfaces in adsorption space

$$[\partial\varepsilon/\partial T]_W = 0 \qquad 4.6$$

This gives a unique characteristic curve to an adsorbent-adsorbate pair expressing adsorption potential in terms of the amount adsorbed for all temperatures (see fig 4.5).

Thus the potential theory does not yield a definite adsorption isotherm. Instead the characteristic curve is developed from the experimental isotherm and then isotherms at different temperatures are determined from it.

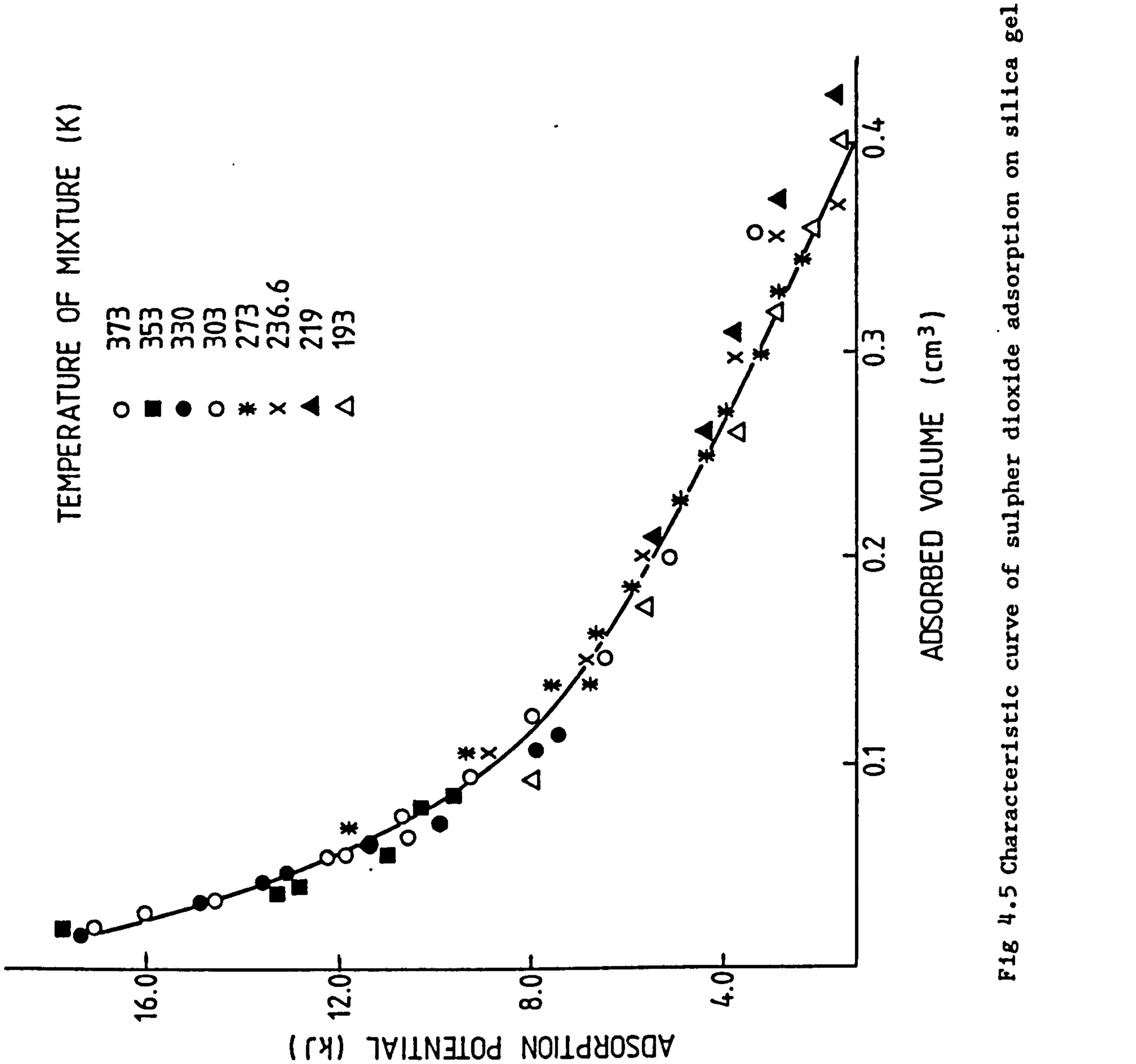

Fig 4.5 Characteristic curve of sulpher dioxide adsorption on silica gel

4.5.3 The BET equation

Brunauer, Emmett and Teller [8,23] extended the Langmuir's idea of monolayer adsorption to multilayer adsorption. They assumed that

a) the adsorption forces, arising as a result of interaction between the adsorbent surface and the adsorbed molecules, act only within the first layer of adsorbed molecules which are in direct contact with the adsorbent surface (this is contrary to the assumption made in the potential theory - see above).

b) the adsorbed layers beyond the first one are not affected by the forces of adsorption and as such the molecules in these layers possess the properties as in the liquid state.

As a result of the assumption (b) the heat of adsorption for the second and layers beyond is constant and equal to the latent heat of evaporation. If it can be further assumed that under saturation pressure of a given vapour an infinite number of layers can be adsorbed on the surface (i.e. if it is not limited structurally, as for instant by its micropores) the BET equation can be written in the form

$$\frac{V}{V_m} = \frac{Cx}{(1-x)(1-x+Cx)} \qquad 4.7$$

where x is the relative pressure, C a constant related to the heat of adsorption, V the volume of the gaseous substance adsorbed, and

V_m is the volume of gaseous substance needed to form a monolayer.

The quantity V_m is the same which appeared in the Langmuir equation. However, the concept of monolayer has been treated in a statistical sense, as under a certain pressure some of the adsorption sites are occupied by more than one molecule, whereas the others remain unoccupied. This happens because of the energetically heterogeneous nature of actual adsorption surfaces. In the development of the BET equation, adsorbate-adsorbate interaction is assumed to sufficiently compensate for the effects of heterogeniety and the mean heat of adsorption is used for the first layer [23]. The constant 'C' in equation 4.7 is determined from the relation

$$C = \exp[(q_{st}-h_{fg})/RT] \qquad 4.8$$

where q_{st} is the heat of adsorption for the first molecular layer and h_{fg} is the latent heat of condensation of the adsorbate.

Equation 4.7 can be written in its linear form as

$$\frac{x}{V(1-x)} = \frac{1}{V_m C} + \frac{C-1}{V_m C}x \qquad 4.9$$

which is a straight line when plotted in so called 'BET coordinates' i.e. x and x/[V(1-x)]. From the slope and intercept of the straight line values of C and V_m are calculated. The applicability of the BET equation is limited over the range of relative pressures from 0.05 to 0.35 and the equation is true for non-porous and macroporous adsorbents. The adsorbents generally used for refrigeration cycles

are microporous and heterogeneous energetically, and quite often structurally as well. The other limitation of the equation 4.7 is that it is based on the concept of infinite number of adsorption layers which fails in case of microporous structure where the size of the pores is often on molecular scale.

To cover this type of adsorbents, the authors [8,23] derived another equation for multilayer adsorption on the walls of micropores. Here they assumed that maximum number of n layers are formed on the wall before they meet the layers on the opposite wall. The derived expression is

$$\frac{V}{V_m} = \frac{Cx[1-x^n(n+1)+nx^{n+1}]}{(1-x)[1+x(C-1)-Cx^{n+1}]} \qquad 4.10$$

Despite the fact that equation 4.10 gives a better fit to the isotherm data, it lacks universal application. It still suffers from the same limits of range of pressure over which it is applicable. The value of n is taken as constant indicate that all the pores are assumed to be of the same dimensions and structure which is not true for many adsorbents (e.g. activated carbon). The other criticism about equation 4.7 apply to equation 4.10 as well because of the same basic concepts used in its formulation.

4.5.4 Dubinin's theory

Polanyi's theory has been very successful in representing adsorption isotherms for physical adsorption but did not provide analytical expression for its determination. Dubinin and co-workers solved this problem (for a comprehensive analysis of Dubinin's equation, readers are referred to [24,25]). First they discovered [26-29] that over a wide range of values of the amount adsorbed, the characteristic curves of different vapours on the same type of adsorbing surface are affine i.e. if we multiply by a certain constant the adsorption potential corresponding to a chosen volume of adsorption space W on the characteristic curve for one vapour we obtain the adsorption potential corresponding to the same value of W on the characteristic curve of another vapour. The multiplication constant was termed as the affinity coefficient whose value can be determined with respect to a standard vapour which is generally taken as benzene.

The function $(RT\ln(p_s/p)$, which was defined to be adsorption potential by Polanyi, was interpreted thermodynamically by Dubinin [30] as

> 'a decrease in the free adsorption energy if the adopted standard state is the state of a normal liquid, which is, at temperature T, in equilibrium with its saturated vapour at pressure p_s. This decrease in free energy represents differential molar work of adsorption.'

Dubinin represented the adsorption amount $_W$ by the following empirical equation;

$$W = W_o \exp[-B/\beta^2(T\ln(p_s/p))^2] \qquad 4.11$$

where W is the volume of liquid like adsorbate, present in the micropores, at a temperature T and pressure p. B is a constant representing the structure of the adsorbent only, β is the affinity coefficient describing the particular adsorbate, W_o is the total adsorption space in the adsorbent, and p_s is the saturation vapour pressure of adsorbate at temperature T.

4.5.4.1 Limitations of Dubinin-Radushkevich equation

Equation 4.11 is known generally as the Dubinin-Radushkevich (D-R) equation. This is applicable at temperature well below the critical temperature and below the relative pressure of 0.4 of the adsorbate.

Taking logarithms on both sides of D-R equation, it can be presented in a linearized form

$$\ln W = \ln W_o - B/\beta^2[T\ln(p_s/p)]^2 \qquad 4.12$$

By plotting lnW against the square of the function $T\ln(p_s/p)$ we should get a straight line. The slope of this line represents the value B/β^2 and the intercept gives the value of total micropore volume W_o. Deviations from this straight line behaviour, however, have frequently been observed. Rand [31] has classified these deviations into three types namely type A, type B and type C. Fig 4.6 shows the general representation of these deviations.

In case of type A deviation (see fig 4.6a) the D-R curve shows two linear portions. Thus the extrapolation of low relative pressure data will result in an erroneous value of micropore volume. Toda and others [32] have attributed this deviation to an activated diffusion effect but Rand [31] contests their point on the basis that their data did not cover the point where the change of slope occures for that system (i.e. carbon dioxide adsorbed on polyfurfuryl alcohol carbons). Zeolites and many other ultramicroporous carbons show type A deviations.

Type B deviation (see fig4.6a) is such that the plot is curved over the whole range of the function $T\ln(p_s/p)$. Thus no extrapolation can sensibly be made. Adsorption of CO_2 and N_2O on activated carbons [33], for example, show this type of deviation. Marsh and Rand [33] suggested that this type of deviation is a result of a distribution of adsorption potential which tends towards a log-normal type. (For specific examples readers are referred to [33] and [34]).

Type C deviation is difficult to explain and complex to linearize. These deviations have been observed for nitrogen and argon adsorbed on certain activated carbons [33]. As shown in fig 4.6b at low values of the function $T\ln(p_s/p)$ the plot deviates upwards. There are two inflexion points on the curve indicating bimodal distribution of adsorption potential. The reasons for this distribution is not very clear.

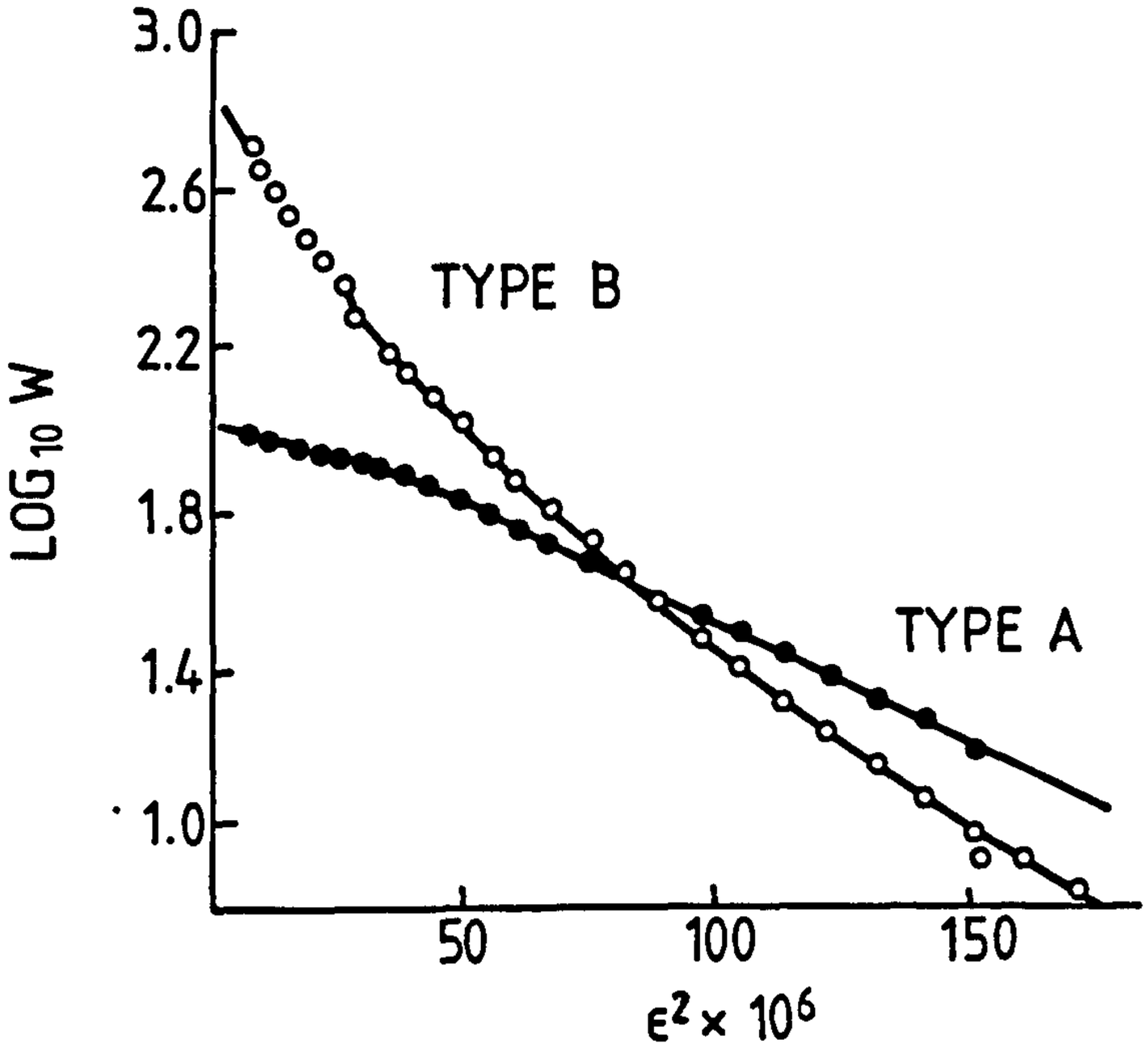

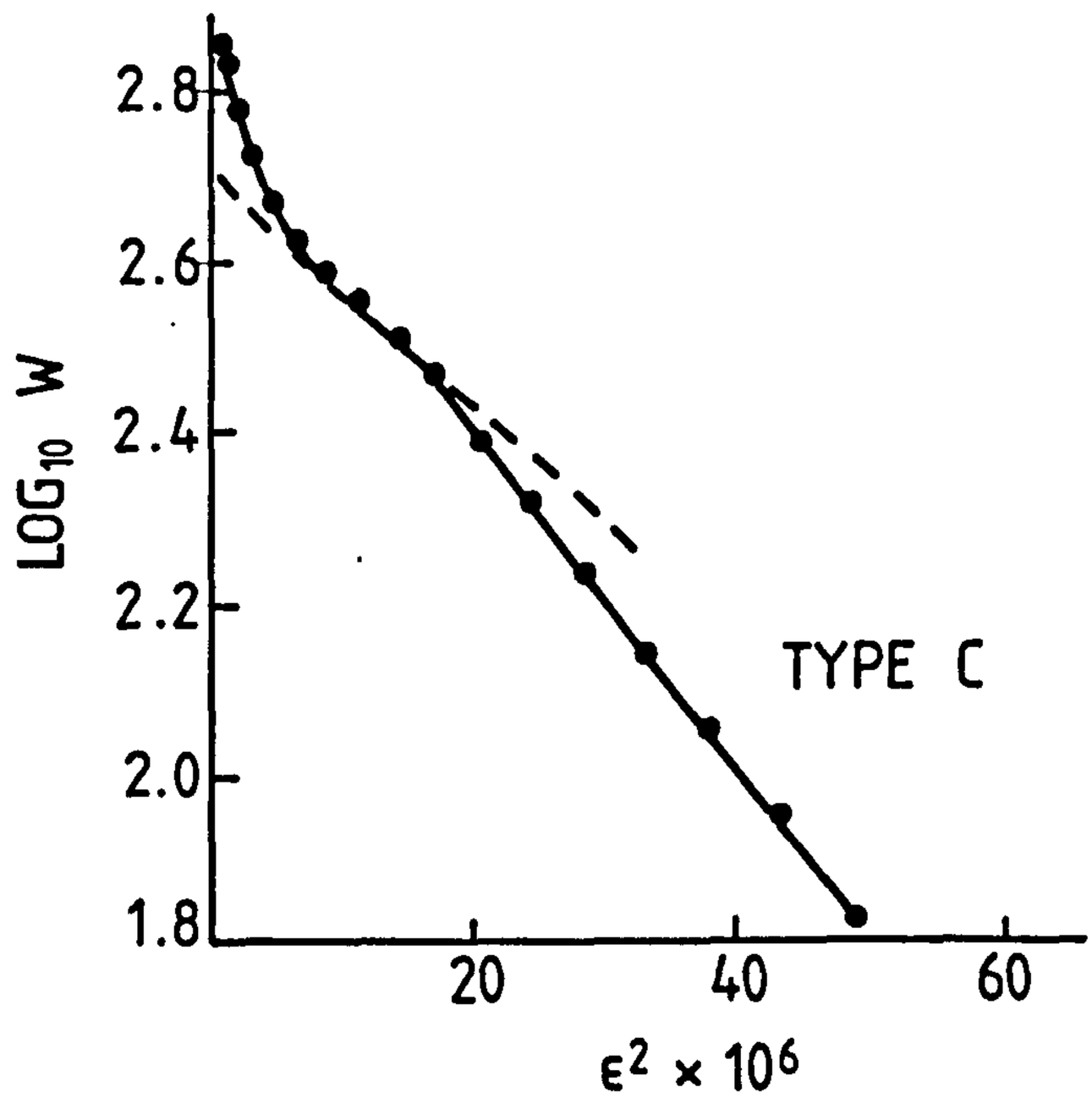

Fig 4.6 Rand's classification of deviations from straight line D-R plot

Dubinin and Astakhov [35] presented a more generalized form of D-R equation which overcame this problem in many cases. The Dubinin-Astakhov (D-A) equation is

$$W = W_o \exp[-(D/E)^n] \qquad 4.13$$

where n is a constant unique to the adsorbent-adsorbate system and W_o is the total micropore volume of the adsorbent. D is the change in Gibbs free energy on adsorption, defined by [35]

$$D = -\Delta G = RT\ln(p_s/p) \qquad 4.14$$

E is specific to the adsorbent and is defined as the characteristic energy of adsorption of the reference vapour, usually benzene.

When n = 2, equation 4.11 and 4.13 are identical and the quantities B (the so called structural constant) and E are related by

$$E = 0.01915(1/B)^{1/2} \quad \text{(kJ/mole)} \qquad 4.15$$

By introducing a variable exponent n they added flexibility into the D-R equation and many of the deviations pointed out above were corrected by selecting an appropriate value of n.

At low coverage and at pressures near to the saturation pressure, Polanyi's postulates are not verified and thus the D-A equation fails to predict the equilibrium correctly in these regions. The suggested range of application by the authors [35] is between

relative equilibrium pressures of 10^{-6} and 0.1. Dubinin and Stoeckli [36] have proposed a two-term equation as alternative to D-A equation. They have shown that adsorption equilibrium of microporous solids, especially activated carbons with high burn-off and extreme activation, can be very precisely represented by the equation, which is modified form of D-A equation, they have proposed in ref [36].

From the point of view of analyzing an adsorption refrigeration cycle D-A equation seems quite appropriate as the regions of inadequacy normally fall outside the cycle's operational domain .

4.5.4.2 Determination of affinity coefficient (β)

The value of affinity coefficient is independent of temperature and almost independent of nature of porosity of the adsorbent. It characterizes therefore the adsorbability of a given vapour on a given adsorbent with respect to a standard vapour.

Theoretical calculation of affinity coefficient is generally based on the nature of forces which cause adsorption of molecules. In the case of non-polar adsorbates the adsorptive interaction is strongly dependent on the polarizability (P) of molecules and the affinity coefficient can be expressed in terms of polarizability [37].

$$\beta = \frac{P}{P_{ref}} \qquad 4.16$$

More precisely, the affinity coefficient can be expressed, as suggested by Dubinin [30], in terms of molecular parachor, Ω

$$\beta = \frac{\Omega}{\Omega_{ref}} = \frac{\left[\frac{\gamma^{\frac{1}{4}} M}{\rho}\right]}{\left[\frac{\gamma^{\frac{1}{4}} M}{\rho}\right]_{ref}} \quad \text{where} \begin{cases} \gamma = \text{surface tension} \\ M = \text{molecular weight} \\ \rho = \text{density of liquid} \end{cases} \qquad 4.17$$

Polar adsorbate molecules possess a permanent dipole moment and as such electrostatic interactions may play greater role in determining the total adsorptive interactions. In case the adsorbent is nonpolar there will be contribution from dipole-induced dipole forces. If the adsorbent is polar in nature there will be an additional contribution due to ion-dipole forces.

Dipole energy is usually evaluated in terms of square of dipole moment. Therefore when electrostatic forces predominantly determine the adsorptive interaction the affinity coefficient (which represent that interaction) may also be expressed in terms of square of dipole moment (μ^2) [37].

$$\beta = \frac{\mu^2}{\mu^2_{ref}} \qquad 4.18$$

Reucroft and co-workers [37] concluded that equation 4.16 gives a good agreement between experimental and theoretical values of affinity coefficient for polar and nonpolar adsorbates alike and the agreement is better when the reference compound is also of a similar polar nature. They also concluded that equation 4.18 or any other equations involving dipole moments give worse agreements between theoretical and experimental values of affinity coefficient for

polar adsorbates. In their words, 'although the affinity coefficient does not depend explicitly on the dipole moment, there is an implicit dependence of affinity coefficient calculated from polarizations on the "polarity" of adsorbate molecule'. Table 4.1 gives experimental values of affinity coefficient derived from ref [29,45,46,47].

4.5.5 Closure

To summarize it may concluded that:

(i) it is possible to deduce the adsorption equilibrium of one vapour from the experimental data of another for the same adsorbent;

(ii) whereas the equilibrium so deduced would provide a good insight into the expected behaviour of the pair, there would always be an element of uncertainty; and thus

(iii) for reliable adsorption equilibrium data, the undertaking of an experimental investigation of each individual pair is inevitable.

4.5.5.1 Implications

Ab initio theoretical design using (for example), locally sourced activated carbon or mineral chabasite is impossible currently without associated experimental evaluation/characterization of those

TABLE 4.1

Affinity coefficient for some vapours and gases on activated carbon

VAPOUR/GAS	AFFINITY COEFFICIENT	REFERENCE
Benzene	1.00	29
Propane	0.78, 0.715	29, 45
n-Butane	0.90, 1.065	29, 45
Methanol	0.40	29
Methyl chloride	0.56	29
Methyl bromide	0.57, 0.565	29, 45
Ethyl chloride	0.76	29
Ethyl ether	1.09	29
Carbon disulphide	0.70	29
Ammonia	0.28	29
Nitrogen	0.33	46
Krypton	0.37	47
Ethanol	0.61	29
Tetrafluorpethylene	0.59	47

materials. The procedure that should be adopted is described in chapter seven. The cost of establishing and running a facility to undertake such tests presents a significant economic barrier to the local design and manufacture of such units.

4.6 Thermodynamic performance of an adsorption refrigerator

The adsorption refrigeration cycle is best understood when sketched on a Clapeyron diagram. Fig 4.7 is a general representation of the cycle. For clarity refrigerant saturation line and low and high concentration isosteres are shown. It is assumed that:

a) the latent heat of vaporization of the refrigerant and isosteric heat of adsorption can be evaluated by the Clausius-Clapeyron equation.

b) isosteres in the range of interest can be represented accurately by the D-A equation which is linear in the coordinates lnP v 1/T.

The operating conditions are described in terms of evaporation temperature, T_e, condensation temperature, T_c, and maximum generation temperature T_g. The evaporation and condensation temperatures set the pressure limits within which the cycle will operate. Thus the two isobars at P_e and P_c can be drawn representing the evaporation and condensation conditions respectively. When the low and high concentration isosteres are located in the diagram the whole cycle is fixed.

The state 1 in the cycle is fixed by the evaporation isobar and the adsorption temperature representing the maximum concentration in the cycle. Thus the isostere passing through this point is the high concentration isostere. The low concentration is fixed by the

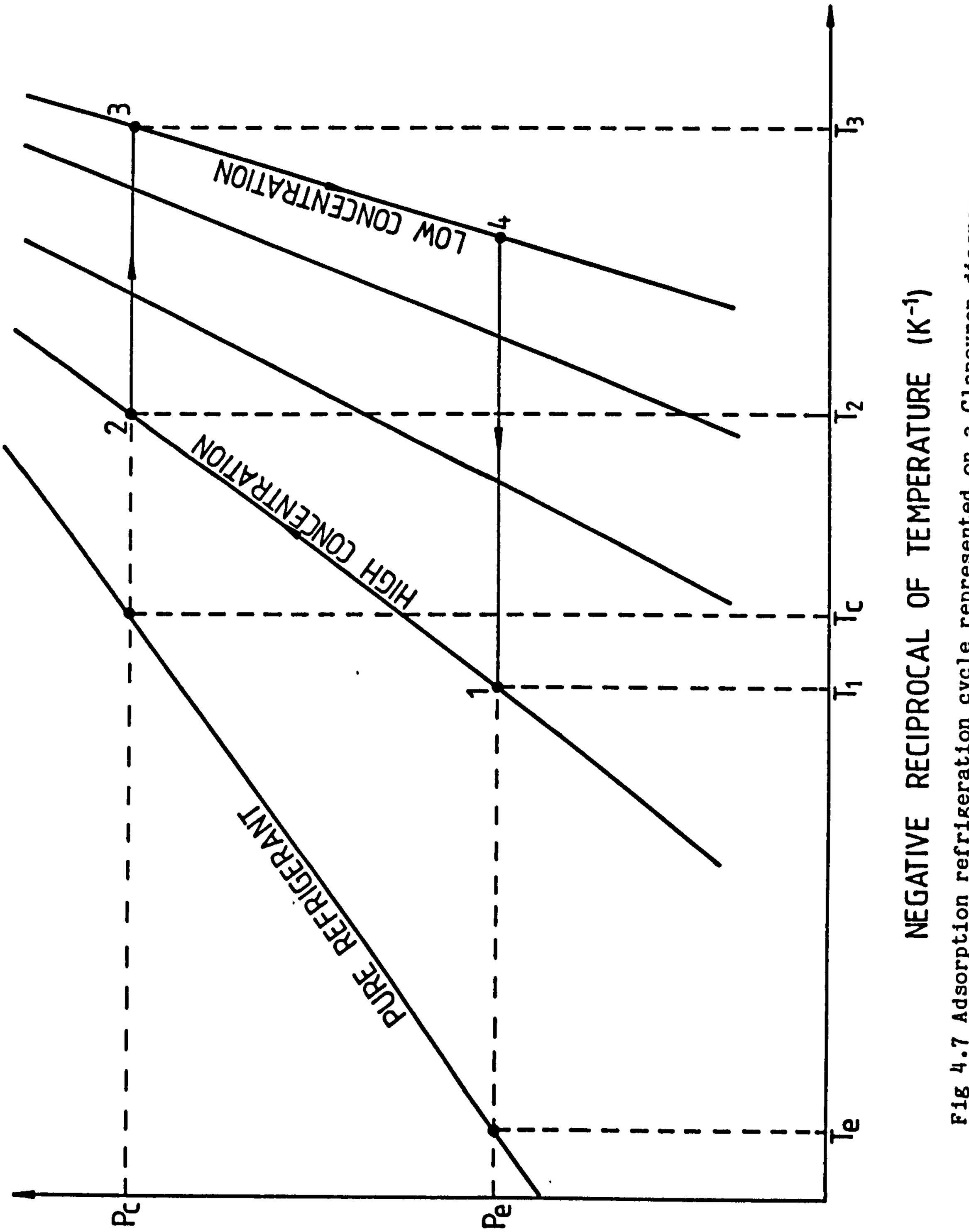

Fig 4.7 Adsorption refrigeration cycle represented on a Clapeyron diagram

condensation isobar and the maximum generation temperature. Thus state 3 locates the low concentration isostere. The two other state points, 2 and 4, are then automatically fixed. The temperature T_2 defined by the state 2 is the temperature at which desorption begins and the state 4 gives the temperature of the mixture at which evaporation starts.

Now that the cycle limits are completely defined, we can proceed further and evaluate the performance in terms of pressure, temperature and concentration of the mixture.

4.6.1 Heat of vaporization and heat of adsorption

The Clausius-Clapeyron equation for phase equilibrium is:

$$d(\ln p)/dT = -Q/RT^2 \qquad 4.19$$

Integrating equation 4.19 along the equilibrium line between two states a and b we get

$$Q = (R\ln(p_b/p_a))/(1/T_b-1/T_a) \qquad 4.20$$

If the states a and b corresponds to evaporation and condensation of the refrigerant then Q will represent the latent heat of vaporization, h_{fg}. Thus,

$$h_{fg} = (R\ln(p_c/p_e))/(1/T_c-1/T_e) \qquad 4.21$$

and if the integration is processed along an isostere then Q will be isosteric heat of adsorption, q_{st}. Therefore integrating equation 4.19 along the low and high concentration isosteres gives,

$$(q_{st})_{low} = (R\ln(p_c/p_e))/(1/T_3-1/T_4) \qquad 4.22$$

and

$$(q_{st})_{high} = (R\ln(p_c/p_e))/(1/T_2-1/T_1) \qquad 4.23$$

4.6.2 Coefficient of performance

Coefficient of performance for a refrigeration cycle is defined by the ratio of the cooling effect produced to the heat supplied to achieve that. In this section a simple mathematical model will be derived which will enable us to compare the performance of different refrigerant-adsorbent pairs. According to fig 4.7 heat is supplied during process 2-3. The process 1-2 is an isosteric process during which the temperature and pressure of the mixture of adsorbent and refrigerant is raised by absorbing sensible heat. The amount of heat Q_{1-2} can thus be evaluated by

$$Q_{1-2} = (C_A+m_hC_R)(T_2-T_1) \qquad 4.24$$

The desorption process 2-3 is an isobaric process. The temperature of the mixture, whose concentration decreases from m_h to m_l due to desorption, rises from T_2 to T_g. Thus during this process the total heat supplied consists of sensible heat and heat of desorption. The continuously changing equilibrium conditions between states 2 and 3 require a more rigorous analysis of this process than is presented

here. However the use of average values of refrigerant concentration and heat of desorption should give estimates accurate enough for comparing the performance of different pairs. Thus,

$$Q_{2-3} = [C_A+C_R((m_h+m_l)/2)](T_3-T_2)+(m_h-m_l)[((q_{st})_h+(q_{st})_l)/2] \quad ....4.25$$

So the total heat supplied to the mixture is,

$$Q_s = Q_{1-2}+Q_{2-3} \quad 4.26$$

The cooling effect is produced by evaporation of refrigerant desorbed during the process 2-3. Refrigerant is at the condensation temperature at the start of evaporation period. It has to cool down to evaporation temperature before it can evaporate. Thus part of the cooling effect produced by evaporation is lost in reducing the refrigerant temperature. Hence the net available cooling effect is given by the equation,

$$Q_c = (m_h-m_l)[h_{fg}-C_R(T_c-T_e)] \quad 4.27$$

Therefore,

$$COP = Q_c/Q_s \quad 4.28$$

Equations 4.24, 4.25 and 4.27 require the value of concentration m to be known before hand. This can be achieved by utilizing the D-A equation which has been discussed in section 4.5.4.

4.6.3 Shortcomings of the analysis

Equations 4.19-4.28 form a good 'tool' for comparing the thermodynamic performance of different adsorbent-refrigerant pairs. Though it has been used in subsequent chapters to evaluate and compare the performance of various pairs, it has inherent drawbacks. These stem mainly from the nature of adsorption forces at the solid-gas interface, which is not completely understood. The accuracy of result can no longer be better than the accuracy of the input data. For instance, the model requires information concerning the adsorption equilibrium of the pair which, if deduced theoretically (see section 4.5.4.2), may possess a high degree of uncertainty, thus inducing errors in the output from the model.

Whereas the model using equations 4.19-4.28 provides a good rating of relative performance, due to analytical simplifications (see section 4.6.2) its output should be regarded as optimistic in absolute terms.

REFERENCES

1 Kiselev, A.V., 'Non-specific and specific interaction of molecules of different electronic structures with solid surfaces', Disc. Faraday Society, vol 40, pp 205-218, 1965.

2 Everett, D.H., 'Interaction of gases and vapours with solids', in Gas Chromatography, Ed: A. Goldup, The Institute of Petroleum, London, pp 219-237, 1965.

3 Barrer, R.M., 'Specificity in sorption', Journal of Colloid and Interface Science, vol 21, pp 415-34, 1966.

4 Oscik, J., 'Adsorption' English translation by I.L. Cooper, Ellis Horwood Limited, Chichester, UK, 1982.

5 McBain, J.W., The Sorption of Gases and Vapours by Solids, George Routledge & Sons, Limited, London, 1932.

6 Hill, T.L., 'Relation between different definitions of physical adsorption', Journal of Physical Chemistry, vol 63, pp 456-460, 1959.

7 de Boer, J.H., in Advances in Colloid Science, vol III, Interscience Publications, New York, USA, p 1, 1950.

8 Brunauer, S., The Adsorption of Gases and Vapours, Princeton University Press, Princeton, 1948.

9 Kiselev, A.V.,'Surface chemistry, adsorption energy, and adsorption equilibria', Quarterly Reviews London, vol 15, pp 99-124, 1961.

10 Dubinin, M.M., Bering, B.P. and Serpinsky, V.V., 'Physical adsorption at gas-solid interface', in Recent Progress in Surface Science, Ed. Danielle, J.F., Pankhurst, K.G.A. and Riddiford, A.C., Academic Press, New York, vol 2, pp 1-55, 1964.

11 Drain, L.E., 'Permanent electric quadrupole moments of molecules and heats of adsorption', Transactions Faraday Society, vol 49, pp 650-654, 1953.

12 Kington, G.L., in The Structure and Properties of Porous Materials, Ed. Everett, D.H., and Stone, F.S., Butterworths, London, p 59, 1958.

13 Kington, G.L. and MacLeod, A.C., 'Heats of sorption of gases in chabazite, energetic heterogeneity and the role of quadrupoles in sorption', Transactions Faraday Society, vol 55, pp 1799-1814, 1959.

14 Ruthven, D.M., Principles of Adsorption and Adsorption Processes, Willey-Interscience, N.Y., USA, 1984.

15 Gregg, S.J. and Sing, K.S.W., Adsorption, Surface Area and Porosity, 2nd edition, Academic Press, London, UK, 1982.

16 Cookson, J.T., Jr., 'Adsorption mechanisms : the chemistry of organic adsorption on activated carbon', in Carbon Adsorption Handbook, Ed: P.N. Cheremisineff and F. Ellerbusch, Ann Arbor Science Publishers Inc. Ann Arbor, USA, 1978.

17 Bikerman, J.J., Physical Surfaces, Academic Press, Inc., N.Y., USA, 1970.

18 Tittof, A., Z. phys. Chem., vol 74, p 641, 1910.

19 Smisek, M. and Cerny, S., Active Carbon, Manufacture, Properties and Applications, Elsevier Publishing Company, 1970.

20 Young, D.M. and Crowell, A.D., Physical Adsorption of Gases, Butterworths, London, 1962.

21 Langmuir, I., 'Adsorption of gases on plane surfaces of glass, mica and platinum', Journal of American Chemical Society, vol 40, p 1361, 1918.

22 Polanyi, M., Verh. deut. phys. Ges., vol 18, p 55, 1916.

23 Brunauer, S., Emmett, P.H. and Teller, E., 'Adsorption of gases in multimolecular layers', Journal of American Chemical Society, vol 60, p 309, 1938.

24 Dubinin, M.M., 'Adsorption in micropores', Journal of Colloid and Interface Science, vol 23, pp 487-499, 1967.

25 Dubinin, M.M., 'The potential theory of adsorption of gases and vapours for adsorbents with energetically nonuniform surfaces', Chem. Revs, vol 60, p 235, 1960.

26 Dubinin, M.M. and Chmutov, K., 'Fiziko-khimicheskie osnovy protivogazovovo dela', Voy. Akad. Khim. Zashch., Moscow, 1939.

27 Zaverina, E.D. and Dubinin, M.M., Zhur. fiz. khim., vol 13, p 151, 1939.

28 Dubinin, M.M. and Timofev, D.P., Dokl. Akad. nauk. SSSR, vol 54, p 705, 1946.

29 Dubinin, M.M. and Timofev, D.P., Zhur. fiz. khim., vol 22, p 133, 1948.

30 Dubinin, M.M., 'Porous structure and adsorption properties of activated carbons', in Chemistry and Physics of Carbon, volume 2, Ed: Walker, P.L. Jr., Marcel Dekker Inc., New York, pp 51-120, 1966.

31 Rand, B., 'On the empirical nature of the Dubinin-Radushkevich Equation of adsorption', Journal of Colloid and Interface Science, vol 56, no 2, pp 337-346, 1976.

32 Toda, Y., Hatami, M., Toyoda, S., Yoshida, Y. and Honda, H., 'Fine structure of carbinized coal', Carbon, vol 8, pp 565-571, 1970.

33 Marsh, H. and Rand, B., 'Microporosity in carbonaceous materials', Proceedings of 3rd conference on industrial carbon and graphite, London, Society of Chemical Industry, pp 172-183, 1970.

34 Hubber, U., Stoeckli, F. and Houriet, J.P., 'A generalization of the Dubinin-Radushkevich equation for the filling of heterogeneous micropore systems in strongly activated carbons', Journal of Colloid and Interface Science, vol 67, no 2, pp 195-203, 1978.

35 Dubinin, M.M. and Astakhov, V.A., Adv. Chem. Series, vol 102, p 69, 1970.

36 Dubinin, M.M. and Stoeckli, H.F., 'Homogeneous and heterogeneous micropore structures in carbonaceous adsorbents', Journal of Colloid and Interface Science, vol 75, no 1, pp 34-42, 1980.

37 Reucroft, P.J., Simpson, W.H. and Jonas, L.A., 'Sorption properties of activated carbon', The Journal of Physical Chemistry, vol 76, no 23, pp 3526-3531, 1971.

38 Current research (see chapter 7)

39 Goldmann, F. and Polanyi, M., Z. phys. Chem., vol 132, p 321, 1928

40 Tchernev, D.I., 'Solar energy application of natural zeolites', in Natural Zeolites: Occurrence, Properties, Use, Editors: Sand, L.B. and Mumpton, F.A., Pergamon Press, N.Y. USA, pp 479-485, 1977.

41 Fowler, R.H. and Guggenheim, E.A., 'Statistical Thermodynamics', Cambridge University Press, Cambridge, 1939.

42 Reyerson, L.H. and Cameron, A.E., Journal of Physical Chemistry, vol 39, p 181, 1935.

43 Lambart, B. and Clark, A.M., Proceedings of Royal Society, vol A122, p 497, 1929.

44 Coolidge, A.S., 'The adsorption of water vapour by charcoal', Journal of American Chemical Society, vol 49, pp 708-721, 1927.

45 Dubinin, M.M., Zaverina, E.D. and Timofev, D.P., Izv. Akad. nauk. SSSR, otd. khim. nauk., p 670, 1957.

46 Dubinin, M.M. and Zhukovskaya, E.G., Izv. Akad. nauk. SSSR, otd. khim. nauk., p 535, 1958.

47 Dubinin, M.M., Zhur. fiz. khim., vol 39, p 1305, 1965.

CHAPTER FIVE

Solar Refrigeration : Practical Options

5.1 Introduction

In the previous chapters different methods for solar energy collection and the production of cold (i.e. refrigeration) have been discussed and their performance limitations considered. This chapter looks generally into the possible ways in which both these processes can be integrated to produce an autonomous solar-operated refrigerator. The options will be evaluated specifically with a view to their application as a system for vaccine storage. Therefore the logical first step in this direction will be to understand the requirements and operational constraints of such a vaccine store.

5.1.1 The WHO Expanded Programme on Immunization

After the success of World Health Organization (WHO) smallpox eradication programme and a record of successful mass-immunization campaigns in the developed countries, the organization in collaboration with United Nations Children's Fund (UNICEF) launched their Expanded Programme on Immunization (EPI). This aimed at reducing, in children, the incidence of death and occurence of disease due to six causes: measles, poliomyelitis, tuberculosis, tetanus, diphtheria and whooping cough. The campaign aims to cover a very high percentage of the potential population. In developing countries, the programme must reach most geographical areas of the country, however remote, as frequently around 80% of the population live in the least developed rural areas.

The infrastructure for the distribution and storage of vaccines from the place of production to the utility point, i.e. a primary health

centre, is often referred to as 'the cold chain'. Table 5.1, reproduced from [1], enlists the temperature and storage requirements at different levels of the cold chain. This study is concerned with the last level, i.e. a primary health centre. A representative clinic serving a population of 100,000 people will require a vaccine storage capacity of 15 litre. In addition to vaccine storage the refrigerator is expected to freeze 3 kg of ice in 24 hours from water at 22°C.

5.2 Selection criterion and operating constraints

The envisaged application of solar refrigerator is at a primary health clinic level which would, in general, be located in remote parts of the developing countries. A criterion, for the selection of a particular system in preference to others, is developed here which suggests the desirable features of such a refrigerator. These are:

a) Manufacturing

The most preferable thing would be that the units are manufacturable with the local technology and skills. The construction material should be also available locally.

b) Maintenance

The units should be repairable at local maintenance centre without waiting for material or technical help to arrive from a developed country.

TABLE 5.1

Level	Temperature of storage Deg.C	Population served	Type of equipment needed	Gross storage volume needed*
NATIONAL OR REGIONAL STORES (4 months stock)	0 to +8	Up to 8 million	Refrigerators	300 litres/ million
	0 to +8	Over 8 million	Cold room	0.75 m3/ million
	-15 to -20	Up to 30 million	Freezers	164 litres/ million
	-15 to -20	Over 30 million	Cold room	0.41 m3/ million
TRANSPORT TO REGION (Quarterly deliveries to all regions simultaneously)	0 to +8	No limits	Cold boxes	30 litres/ million
TRANSPORT TO LOCAL STORES (Monthly deliveries to all stores simultaneously)	0 to +8	No limits	Cold boxes	12 litres/ hundred thousand
LOCAL STORES INC. HEALTH CENTRES (6 weeks stock)	0 to +8	Up to 15 million	Refrigerator with icepack freezing	1.50 litres/ ten thousand

* Based on the following assumed targets;

1-3.5% population growth rate

2-2.6% children enter school (age group 5-6 years)

3-3.5% expectant mothers receiv 2nd doze of tetanus toxide

4-every new born baby (i.e. 3.5%) is immunized

5-100% immunization is effected

c) Ruggedness

The units should be quite robust and rugged so as to withstand the strain of traditional transport methods, e.g. on horse or camel backs. The body of the refrigerator should be corrosion resistant to DIN 8985 (as per WHO specification E3/RF5 contained in appendix B)

d) Service

Ideally speaking, once installed the units should not demand any special attention. These should be able to complete their useful life (e.g. fifteen years) without any rigorous service except the usual daily upkeep.

The operating constraints for photovoltaic refrigerators as derived from [2] and for solar-thermal refrigeration systems as laid down in the WHO specification E3/RF5 (see appendix B) are:

i) The internal temperature of the refrigerator, under continuous ambient temperatures of 22°C, 32°C and 43°C, shall not exceed the range of 0°C to 8°C when fully packed with vaccine vials. This temperature range shall be maintained when the ice packs containing water at 22°C are placed in the freezing compartment and frozen solid.

ii) The design of the system shall permit a minimum of three days continuous operation in the absence of solar energy. During this time the conditions prescribed in (i) above must be met.

The first thing which comes to light is that the required vaccine store will have two, a high temperature and a low temperature, compartments. The low temperature compartment can be referred to as the freezer which will be used for freezing the icepacks. Because of the varied requirements at primary health centres throughout different parts of the world, it is difficult to specify a single suitable size of refrigerator. Nevertheless, a 30 litre capacity refrigerator is considered to be flexible enough to preserve vaccines, freeze icepacks and to hold some additional life saving drugs as well.

5.2.1 Minimum criterion for feasibility

Most developing countries already have established markets for refrigeration equipment, even where the local industry lack the manufacturing capability. It is therefore assumed on this basis that the basic maintenance and repair skills are available in this field, though perhaps not very widespread.

Thus it is proposed that if a solar refrigerator is manufacturable by assembling the conventional mass produced equipment without the involvement of specialized skills and that if the conditions in clause c and d of the criterion in section 5.2 are fulfilled, then the proposed system is considered as a feasible option.

5.3 Solar refrigeration

Figure 5.1 illustrates the different options or methods to integrate the solar collection and refrigeration systems into one autarkic solar refrigerator. Each of the options listed there are practicable and most methods have been tried at least at laboratory scale, if not at commercial level. In the next few paragraphs the principles, advantages and drawbacks of each option will be discussed.

There are two very distinct routes, as identifiable in fig 5.1, which can be followed to convert the heat of the sun into ice. The first involves the conversion of solar energy into electrical energy which can then be used, directly or indirectly, to power the refrigeration devices. Alternatively the second route could be followed where solar energy is converted into thermal energy which can then be utilized to run a refrigeration unit.

5.3.1 Solar-photovoltaic refrigeration systems

First we consider the options where the electrical output from photovoltaic cells can be used. As the photovoltaic panels are widely used in space applications they are in commercial production. Manufacturing of these cells involve silicon-chip high technology. Initial capital cost is very high compared to the basic refrigeration system cost. A complete photovoltaic panel assembled in a developing country (i.e. Egypt) utilizing 'cheap' local labour costs about $8.0 per peak watt (at 1984 prices) [3]. High capital cost of photovoltaic panels and low efficiency of conversion process

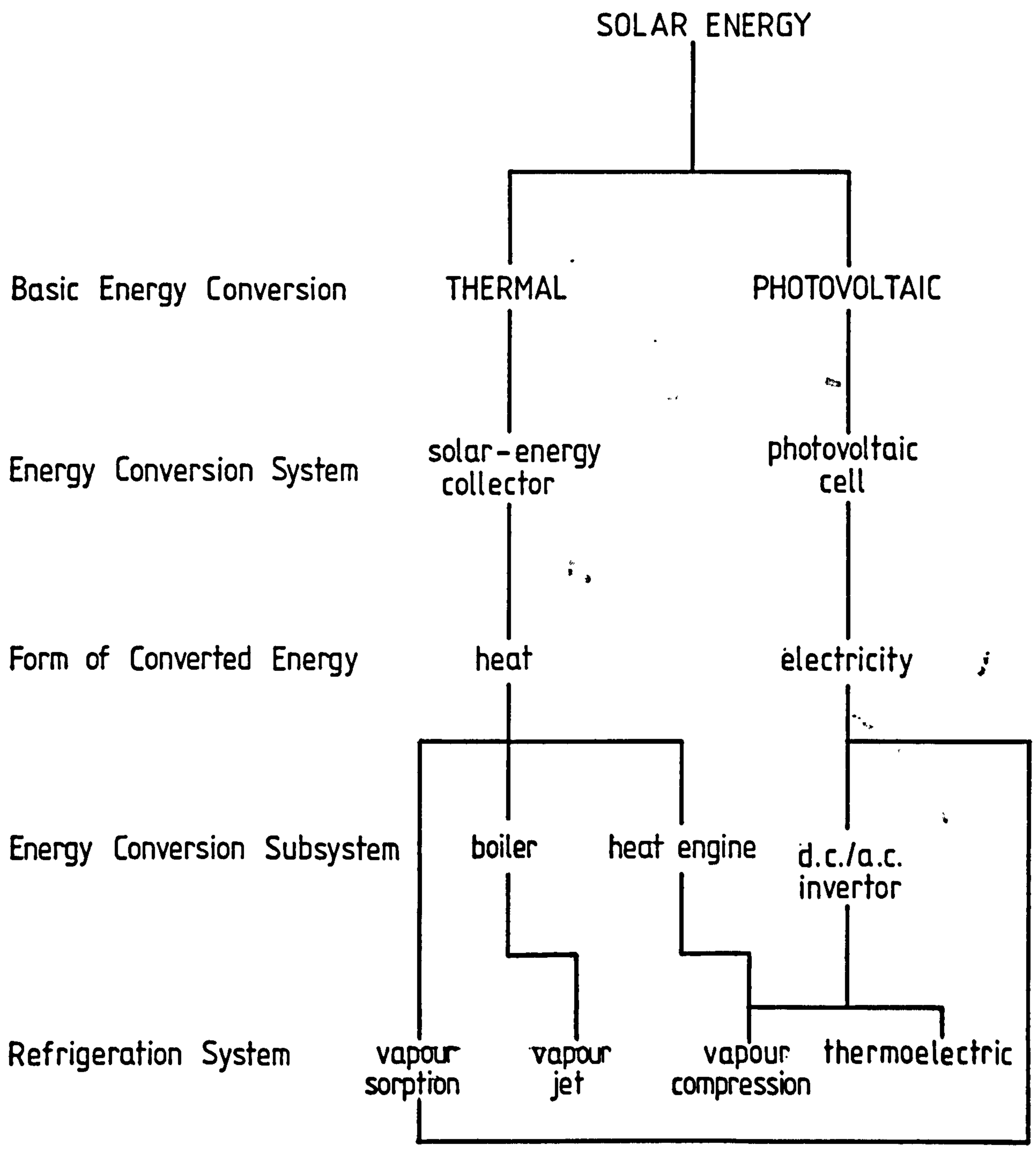

Fig 5.1 Options for building a solar refrigeration system

(0.1-0.15 at 25°C [4]), have been prohibitive in competing with the conventional sources of electricity. If the commercially available refrigerators, which are cheap because of mass production, can be coupled to photovoltaic panels it may result in a feasible option.

5.3.1.1 Photovoltaic-vapour compression refrigeration

One way of producing cold from d.c. electricity generated by photovoltaic panels is to run a vapour compression refrigerator on it. Small refrigeration units which require a 12 V d.c. power are already marketed for use in boats and caravans [4,5]. The normal household refrigerator is designed to run on 110/or 240 V a.c. This can be powered by a 12 V d.c. source through an inverter. Figure 5.2 gives a general appreciation of the overall arrangement of different components involved in such a system.

This option has a big attraction that the solar operated unit can be made from 'off-the-shelf' items already in mass production. This would help reducing the cost of the new system. A major disadvantage of the system, however, would be the photocells whose production cannot be undertaken, at present, in the developing countries which are the ultimate target of this application. But photocells are very rugged piece of equipment and these are not likely to fail during the life time of the equipment.

Thus it is considered worth looking in detail. An elaborate analysis of the option is presented in the next chapter where this system is compared with other options as well.

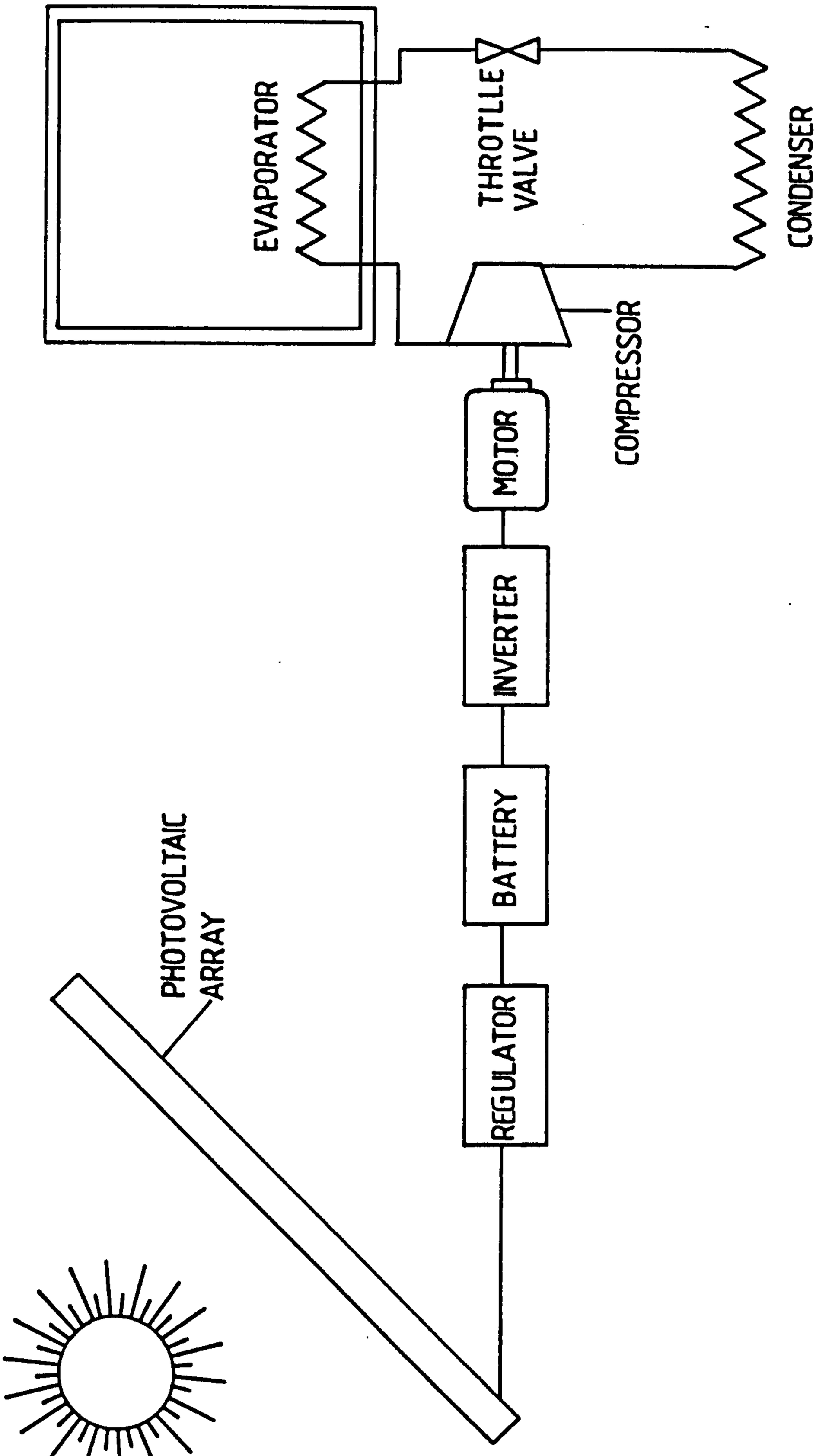

Fig 5.2 Essential components of a photovoltaic vapour compression refrigerator

5.3.1.2 Photovoltaic-thermoelectric refrigeration

A thermoelectric refrigerator can be powered directly with the electricity produced by photovoltaic panels. As mentioned in the previous chapter the process of thermoelectric cooling is inherently inefficient. The efficiency of conversion of electrical input into 'cold' is only 0.1. The continuous operation of the unit would require a massive storage of energy in a battery bank for the periods of zero or low insolation. The major problem in the design of an intermittent operation unit (i.e., which produce cold during the sunshine hours only) is the heat leak into the cabinet through the Peltier unit under zero insolation conditions [5].

The capital cost is ten times, and the storage battery requirement is five times, that of a photovoltaic-vapour compression system [6]. Hence with overall efficiency of 0.015 [5], a high initial cost and with the above mentioned technical limitations, this system cannot be regarded feasible.

5.3.1.3 Photovoltaic-vapour absorption refrigeration

This option would be feasible if the mass produced refrigerators could be coupled to the photovoltaic arrays. As mentioned in the previous chapter the commercially available domestic absorption refrigerators are inherently inefficient (typical COP of 0.2-0.25). Their response to change in cooling load is slow and thus large fluctuations in the internal temperature could be expected. Compared to vapour compression systems these systems would require a four

times larger panel area and four times bigger battery storage. All this means a four times initial capital cost.

Therefore on the basis of performance limitations and higher capital cost this option is not considered feasible.

5.3.2 Solar-thermal refrigeration systems

Vapour compression, continuous vapour absorption, and intermittent vapour sorption refrigerators are the three systems which can be driven by the thermal energy derived from the sun. Among the commercially available systems are vapour compression and continuous vapour absorption refrigerators. One brand of solar operated intermittent vapour sorption refrigerator have very recently appeared in the market. But being very simple in construction and reliable due to the absence of moving parts, it has the potential of being competitive with other mass produced systems.

Vapour compression and continuous vapour absorption systems would need either a heat storage to keep them running during no and low insolation periods, or these would have a cold storage which could balance the heat gains during the period of inactivity (i.e. after sunset). On the other hand intermittent sorption refrigerators would have the benefit that these would remain working during the longer period of no/low insolation hours. Therefore a smaller cold store for the period of effective insolation hours would be required.

5.3.2.1 Solar-thermal-vapour compression refrigerators

An arrangement of solar-thermal conversion device and a vapour compression refrigerator(VCR) combined into one system is shown in fig 5.3. There are three main components of the system, i.e. a solar energy collector, a heat engine and a refrigerator. The thermal energy available from solar collector is used to run the heat engine which produce a mechanical power working on a Rankine cycle. The compressor of the refrigerator is fed that mechanical power through a mechanical coupling and so the cooling is produced by the refrigerator.

For low temperature systems, employing flat-plate collectors, an organic Rankine engine seems to be the most suitable (i.e. R11, R22, R113 and R114 as the working fluid). The performance characteristics of heat engine and solar energy collector are opposed to each other. The efficiency of heat engine improves at high operating temperatures whereas the collector's efficiency declines. This opposing requirement of the two components renders the combined machine unable to perform at higher efficiency. Use of some prototypes and their performance characteristics are reported in references [7-10].

Solar-operated heat engines are still at development stages. The major factors which are not favourable to them are the lubrication problems due to excessive friction, need for balancing the reciprocating masses, high cost and maintenance efforts [11]. Typical variation of overall coefficient of performance values [10]

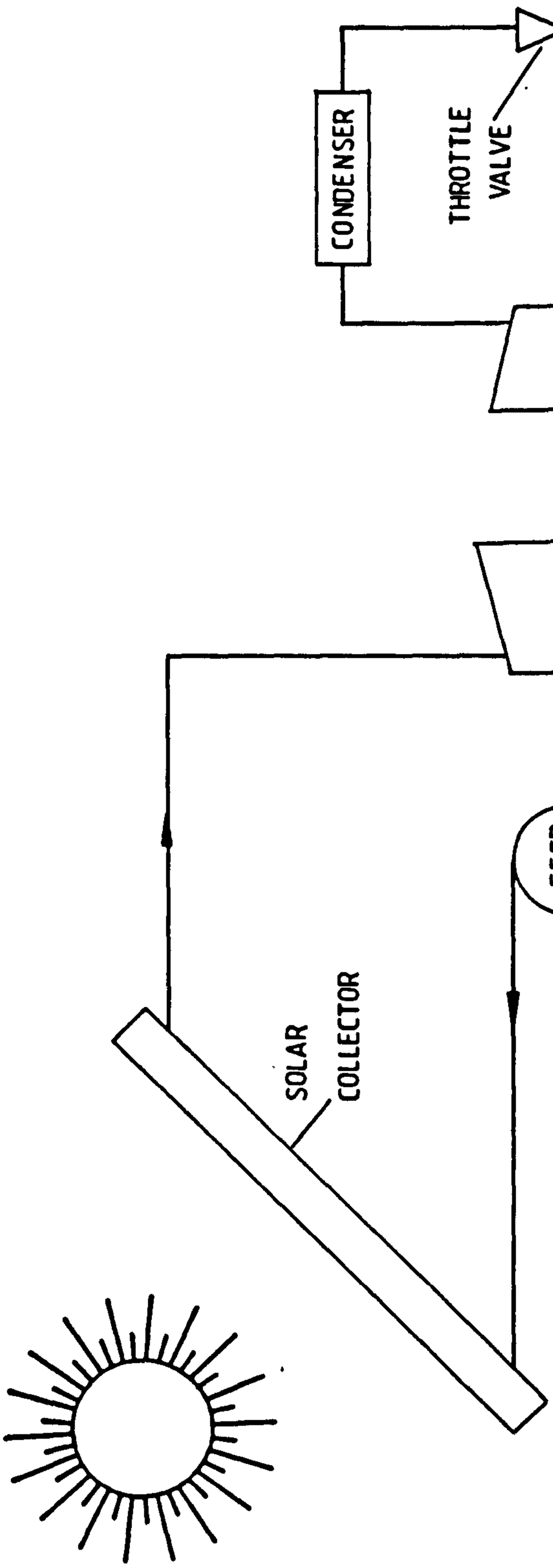

Fig 5.3 A schematic representation of a solar-thermal vapour compression refrigerator

shown in fig 5.4 indicate the expected trend of improved performance with boiler outlet temperature. The high sensitivity to condenser temperature is due to dependence of both heat engine and refrigerator performance on the condenser temperature.

However because of low component efficiencies (i.e less than 0.1 [12]) due to the small scale of the considered application a solar operated heat engine-driven VCR is not feasible. A detailed study concerning the application of Rankine cycle engine at such a small power level can be found in [12].

5.3.2.2 Solar-thermal-continuous vapour absorption refrigerator

Continuous vapour absorption refrigerators (CVAR) generally have COP values less than unity. CVAR can be driven thermally if the solution pump in the circuit is replaced by a bubble pump. This imposes a serious limitation on the pressure difference between the low and high sides. A successful domestic unit built on this principle is the Platen-Munters design (usually known as Electrolux refrigerator after its first commercial developers). These refrigerators are both totally thermal power driven and are widely available.

Due to the absence of any moving parts, these refrigerators are very quiet and reliable. Although the COP of these machines is in the range of 0.2-0.25 but these can perform well for their lifetime without any special attention. The thermal energy from a solar energy collector can be transfered easily to the generator of an Electrolux refrigerator through a 'simple' heat exchanger. The

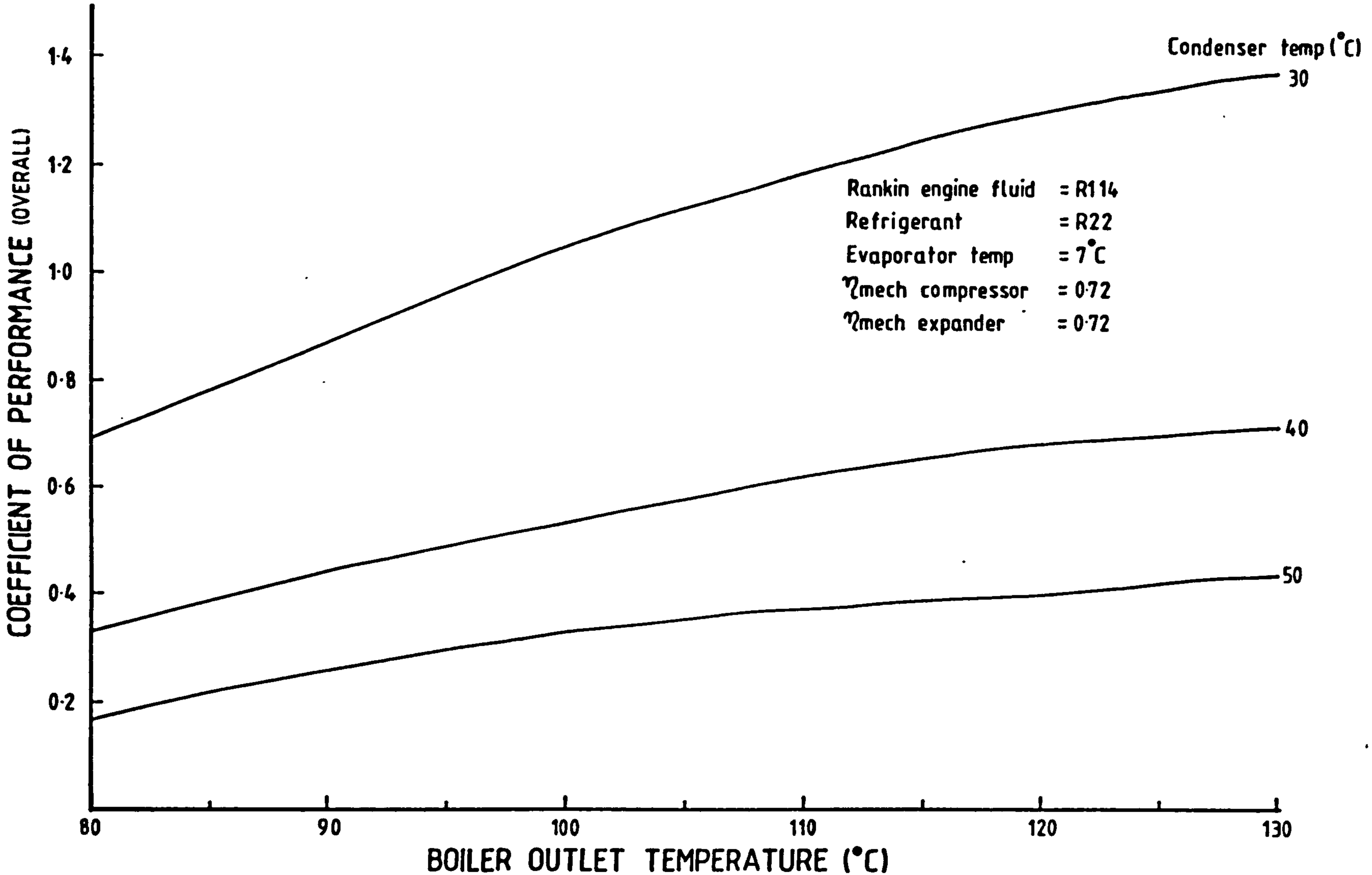

Fig 5.4 Variation in overall COP of a Rankine engine driven vapour compression refrigerator with changing condenser and boiler temperatures

theory of operating the unit on solar power is long been proven practicable since 1958 [13,14].

On the basis of our feasibility criterion, a solar-Electrolux refrigerator could be feasible and thus a detailed analysis of this option is carried out in the next chapter.

5.3.2.3 Solar-thermal-intermittent vapour sorption systems

The process of vapour sorption can be classified generally into two catagories, i.e. absorption and adsorption. The detailed discussion of the subject can be found in chapter 4. In general absorption results in a change in chemistry and lattice structure of the sorbent whereas during adsorption no such change happens and it remains a physical phenomenon.

An intermittent vapour sorption refrigerator(IVSR) is very rugged and simple in construction. It does not incorporate any moving parts and thus very reliable. The COP is generally below 0.6. The sun is a cyclic source of energy and the intermittent operation of these refrigerators is very well suited to their solar operation. As discussed in the previous chapter generator acts as sorber during the refrigeration part of the cycle. This opens up the possibility of using generator/sorber vessel as a solar collector by it absorbing the solar insolation directly. In short the solar-thermal-IVSR has a lot of potential to be a preferred option.

5.3.2.3.1 Initial screening of sorption pairs

There is a variety of sorption pairs which has been proved successful at a laboratory scale. Some of them has been employed in commercial and prototype units built successfully so far. There are three types of sorbent-refrigerant pairs:

1 the sorbent is fully miscible liquid (e.g. water in sulphuric acid). Concentration of refrigerant in the sorbent can vary from 0 to 1 and vapour pressure is dependent on temperature and concentration, i.e. it is a bivariant system.

2 the sorbent is a partially soluble solid (e.g. sodium hydroxide in water). m_s is maximum solubility at temperature T. If the concentration is less than m_s the system is bivariant, but if concentration is greater than m_s then it is monovariant i.e. the vapour pressure only depends on the temperature.

3 the sorbent is an unsoluble solid (e.g. activated carbon) which adsorbs the refrigerant. The system is usually bivariant and vapour pressure is dependent on the temperature and concentration of the 'mixture'.

Table 5.2 enlists some 37 of all three types of those sorption pairs which has been cited in the literature.

TABLE 5.2

Sorption pairs for use
in intermittent vapour sorption refrigerators

TYPE		NO	REFRIGERANTS	SORBENTS	REFERENCES
TYPE 1	Bivariant	1	water	sulphuric acid	22,28
		2	water	ethyleneglycol	23
		3	methanol	ethyleneglycol	23
		4	ammonia	water	24,31,51
		5	ammonia	water + lithium bromide	25
		6	methylamine	water	25
		7	methylamine	water + lithium bromide	25
		8	R-22	DEG	26
		9	R-22	DMF	27
		10	R-22	DMETEG	27,28,51
		11	R-21	DMF	27
		12	R-21	DMETEG	28
		13	methylamine	water	28
		14	ethylamine	water	28
TYPE 2	Bivariant	15	water	lithium brimide	29,35,51
		16	water	sodium hydroxide	22,28
		17	water	potassium hydroxide	28
		18	methanol	lithium & zinc bromides	30,31,51
		19	methanol	lithium thiocyanate	31
		20	ammonia	lithium thiocyanate	32
		21	methylamine	lithium thiocyanate	33
		22	ammonia	sodium thiocyanate	34,51
		23	ammonia	lithium nitrate	34,28
		24	methanol	lithium bromide	28
		25	ammonia	water + lithium nitrate	36
		26	ammonia	Ammonium thiocyanate	28
	Monovariant	27	water	sodium sulphide	37
		28	methanol	calcium chloride	38,39
		29	ammonia	calcium chloride	40,41,18
		30	ammonia	strontium chloride	42
		31	methylamine	lithium chloride	43
TYPE 3	Bivariant	32	water	zeolite-13X	44,45,46
		33	methanol	zeolite-13X	47
		34	methanol	activated carbon	48
		35	ammonia	activated carbons	49
		36	freons	zeolite-13X, 5A	50
		37	freons	activated carbons	51

DEG = diethylene glycol
DMF = dimethyl formamide
DMETEG = dimethyl ether of tetraethylene glycol

Due to the intermittent operation of the refrigerator the thermal capacity of the system becomes very important. Higher thermal capacity will mean more time to reach the operating temperature level. Thus this will be one of the deciding factors while choosing a pair for use in a solar-thermal-IVSR.

A corollary of low thermal mass requirement is to use refrigerants which have higher latent heat of evaporation to reduce their total mass (thermal capacity = mass x specific heat) required for a specific cooling capacity. But an exploration of a property data book would reveal that higher specific heats are generally associated with the materials having high latent heat of evaporation (see table 5.3 for comparison of a few of the more common refrigerants). This leaves us with the other option of reducing the thermal capacity of sorbent and that of the sorption equipment.

First we consider the ways of reducing the thermal capacity of sorbent. Again a careful look into the properties of applicable sorbents would reveal that solid sorbents have lower specific heats than the liquid sorbents (e.g. compare 0.7 of activated carbon or 0.92 of zeolite with 4.18 for water). Further it was observed that during the generation process liquid absorbents, for instance water, tend to evaporate along with the refrigerant. The absorbent vapours have to be removed from the desorbed refrigerant before it reaches the condenser. This means wasted energy and additional equipment. All this evidence suggests that solid sorbents are favourable.

TABLE 5.3

Physical and thermodynamic properties
of common refrigerants

REFRIGERANT	DENSITY kg/m^3	SPECIFIC HEAT kJ/kg-K	LATENT HEAT kJ/kg	VAPOUR PRESSURE bars	
				$-10^{o}C$	$50^{o}C$
Methanol	792	2.53	1200	0.0226	0.533
Water	917	4.187	2500	0.0029	0.123
Sulpher dioxide	1923	1.36	388	1.023	5.827
Ammonia	607	4.72	1298	2.91	20.33
Freon-12	1311	0.974	156.3	2.19	12.19
Freon-21	1366	1.062	240	0.454	4.43
Freon-22	1194	1.36	213.2	3.54	19.42
Ethanol	789	2.45	842+	0.0076	0.296
Ethylamine	689	2.68	622	0.296	3.43
Methylamine	699	3.34	827	0.96	7.8

Density at $25^{o}C$

Specific heat at $25^{o}C$

Latent heat at $-10^{o}C$

+ at normal boiling point

For reducing the thermal capacity of sorption equipment one has to use metals which have low specific heat and low density. But there is not a greater choice between copper, aluminium and mild steel; the three most commonly used materials. Another important factor which affects the total mass of the metal used is the system pressure. For higher working pressures (e.g. ammonia condensing at 20 bars at 50^{o}C) the equipment has to be fabricated from thicker sheets of metals. Thus a sorption pair with a lower working pressure (or vacuum) is perhaps more desirable. This will help reducing the overall mass and hence the thermal capacity of the equipment.

Sorbents with larger sorption capacity and lower heat of sorption will tend to generate more refrigerant per unit weight of the sorbent and therefore help reduce the overall size of the plant.

Lastly, the thermodynamic COP of the sorption pair is very important. As the lower COP will demand a higher heat input to the system. Which in turn would require a larger solar collection equipment. The implication would be in terms of higher capital cost which is undesirable again. In reference [15] a comparison of solar operated liquid and solid absorption refrigerators concluded that the solid absorbents had performed better than the liquid absorbents. The results from [15] and [16-18], shown in fig 5.5, indicate the superior performance of solid sorbents over the liquid sorbents.

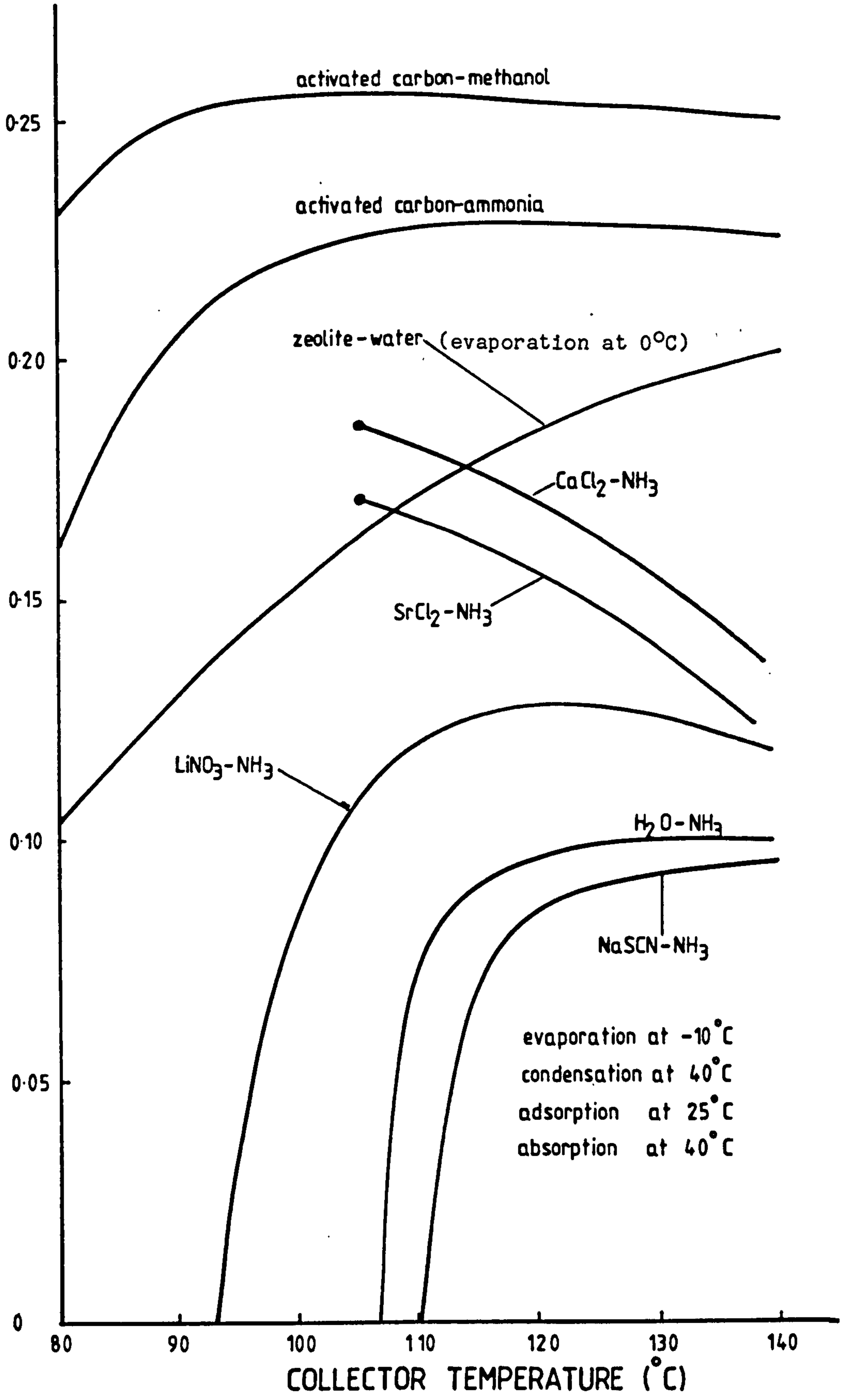

Fig 5.5 Solar COP of IVSR system for various sorption pairs using a double glazed selective surface flat plate collector

Summarizing the discussion so far it can be concluded that

(1) solid sorbents are better than liquid sorbents.

(2) a solid sorbent with larger sorption capacity is preferable.

(3) thermodynamic cycle COP of the sorption pair should be high.

(4) the refrigerants with low condensation pressure, low specific heat, and high heat of vaporization are preferable.

From the list of sorption pairs cited in table 5.2 activated carbon, calcium chloride and zeolite emerge as the suitable sorbents. Whereas water, ammonia and methanol, all of which possess high latent heat of evaporation, are preferred refrigerants. Water is excluded from further investigation as sub-zero temperatures cannot be achieved when water is a refrigerant. Detailed assessment of these pairs will be carried out in the next chapter.

5.4 An up-to-date survey of solar refrigerators

In United States of America an application for a patent was filed on 10th April 1933. It was a design for a 'Solar Operated Refrigerating System' and the patentee was A.T. Bremser [52]. The designed plant is shown in fig 5.6. The working principle and the components, except the generator, were similar to those in a classic Platen-Munters' refrigerator. The heater was a solar-energy collector (1) and the rich ammonia mixture while passing through it was heated to the temperature of vaporization. This heated mixture was fed to a boiler chamber indicated by number 2, where the ammonia bubbles would lift the solution through the tube, indicated by number 3, into the generator (4). The ammonia vapours from (4) were fed into the condenser (5). The weak solution from (4) was partly fed back to the solar collector and remaining went to the absorber (6). The remaining circuit was identical to a classic Platen-Munters' unit. No evidence has been found that the unit was ever constructed.

In a first detailed study, at the University of Florida in 1936, on the subject of utilizing solar energy for air conditioning and refrigeration, Green [53], used a cylindro-parabolic reflector (concentration ratio of 11 to 1) to heat water which flowed through a pipe which was placed at its focal line. Two weight driven alarm clocks were used to keep the collector track the sun. The steam produced was used to provide heating during winter. For summer cooling a steam jet refrigerator or an 'Electrolux' type unit was proposed.

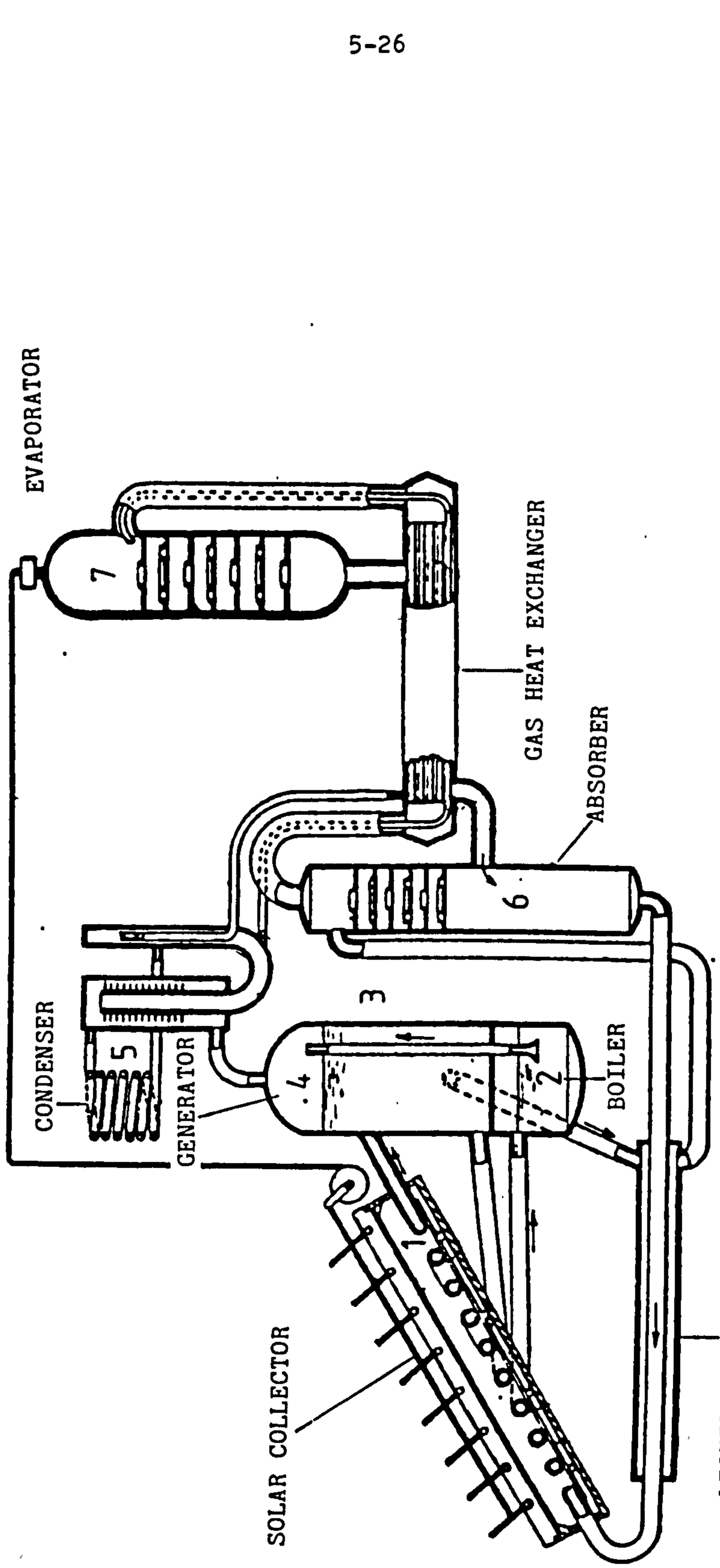

Fig 5.6 Proposed design of a solar refrigerator patented in the name of Bremser [52]

It was in 1954 that two Russian researchers, Kirpichev and Baum [54], reported a successful attempt to run a set of vapour compression refrigerator by solar energy. The refrigerators were driven by steam engines fed from a boiler placed at the focus of a large parabolic mirror. Very high cost of equipment and the low efficiency of heat engines and of solar collection has been the factors for discouraging any further developments in this direction.

In 1957 Williams and others [55,56] used the principle of an intermittent refrigeration cycle. A simple apparatus consisting of a generator-absorber and a condenser-evaporator, was used with the generator-absorber placed at the focus of a parabolic mirror. The mirror was constructed from a 1.27 mm polystyrene-moulded parabolic shell. This was lined with aluminized mylar polyester film and stiffened at the rim by metal tubing. The 106.7 cm aperture presented an area of 0.773 m^2 to the sun. Focal length of the paraboloid was 45.7 cm. The cooling space of 0.064 m^3 was maintained at 19.4^{o}C below ambient.

In the two publications cited they have discussed the desirable characteristics of refrigerants and absorbents. The systems with aqua-ammonia and dimethyl ether of tetraethylene glycol (DMETEG) with R12 as absorption pairs had been compared. Evaporator temperature had been kept constant while the solution concentration, final generation temperature and the condensing temperature had been varied. The two systems of aqua-ammonia and DMETEG-R12 had been reported to have a cooling ratio of 0.32 and 0.26 respectively. The overall solar COP was reported as 0.14 for aqua-ammonia and 0.08 for

DMETEG-R12. The reason for lower performance of DMETEG-R12 pair had been the low thermal conductivity of the solution. R12 also needed large quantity of DMETEG which was to be heated and cooled.

As stated by Swartman et al [57] ' the first major project on an all solar absorption refrigeration system was undertaken by Trombe and Foex [58] of France in 1957'. They claimed that a commercial refrigerator manufactured by Ets Pierre Mengin, Montargis, France was a modified version of Trombe and Foex's design.

As shown in fig 5.7 the apparatus consisted of a cold reservoir or absorber, A, containing the ammonia solution, a generator, D, placed higher than the absorber, and a pipe, C, connecting the two which was placed at the focal line of a cylindro-parabolic reflector. Ammonia solution was heated upto the generation temperature in that pipe; ammonia was driven off into the generator and weak ammonia solution returned via the heat exchanger, B, to the absorber under gravity. Ammonia was subsequently condensed in a cooling coil, G, and was collected inside a collection vessel, H, in the cold chamber. Evaporator coil, I, was wrapped around a container, J, in which ammonia from the reserve was evaporated during refrigeration period.

The cylindro-parabolic reflector measured 1.5 m^2. Daily production of the prototype was 6 kg of ice. By reducing the thermal inertia of the system Trombe and Foex were able to reduce heat absorbed, from 9.0 MJ to 3.6 MJ, to produce one kg of ice.

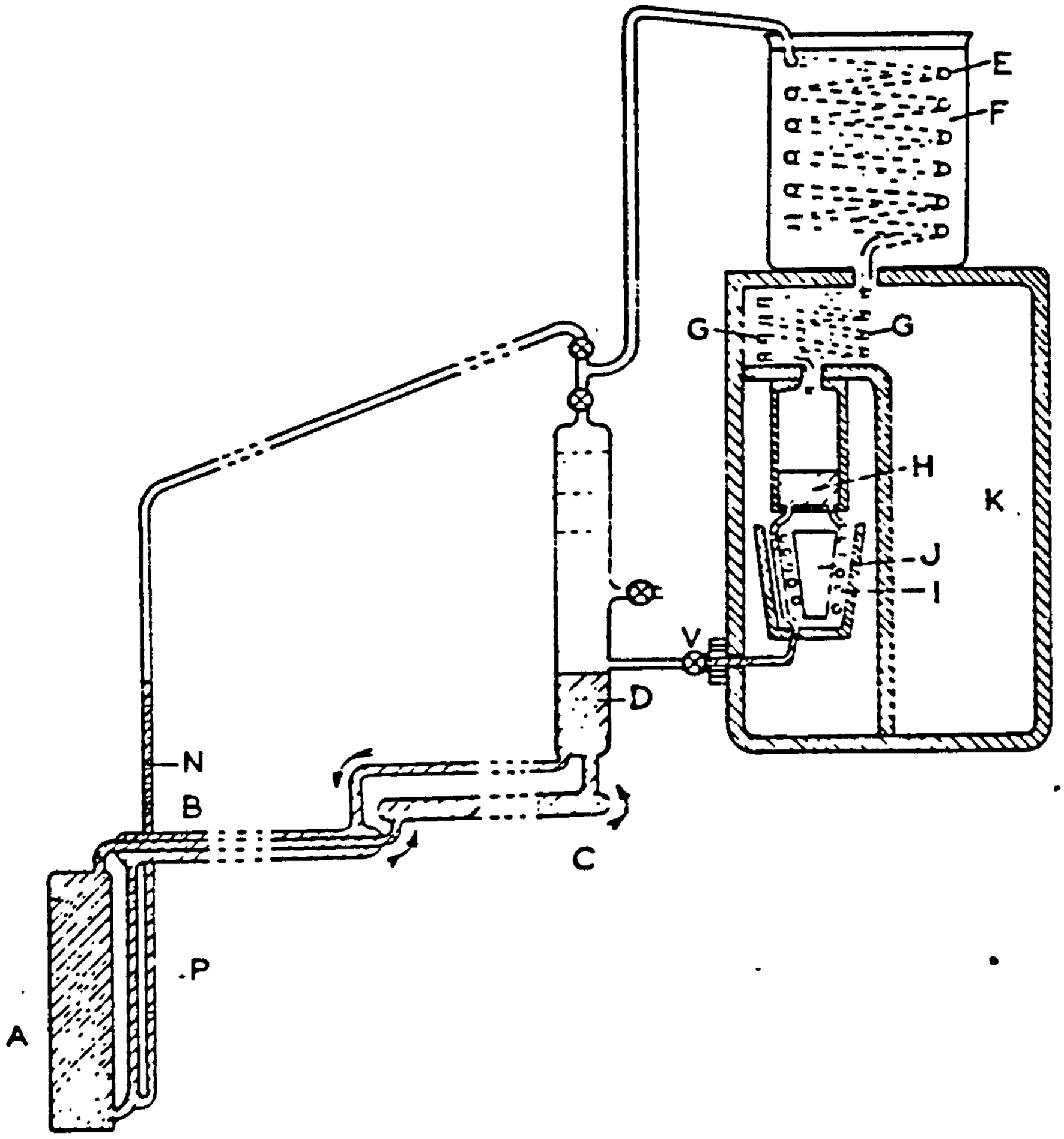

A ammonia reservoir
B liquid heat exchanger
C heating tube placed at the focus of the cylindro-parabolic collector
D boiler
E condenser
F water tank
G cooling coil for the condensate
H ammonia collection vessel
I evaporator coil
J ice container
K cold chamber

Fig 5.7 A diagramatic sketch of the absorption refrigerator designed and tested by Trombe & Foex [57]

At University of Florida, in 1958, an Electrolux Servel (Platen-Munters type) refrigerator was modified to use solar energy for generation [13,14]. The generator received heat through a heat exchanger in which hot oil from a cylindero-parabolic reflector was flowing. A storage tank for hot oil was also connected to the solar collector for night running of the unit. A flat plat collector was also connected in the circuit which preheated the oil entering the cylindero-parabolic collector. The generator of the refrigerator was heated and maintained at 180^{o}C by the circulating hot oil from the solar collectors. It worked successfully for several weeks.

Chinnappa [59], at Colombo in Sri Lanka, designed and operated with success an intermittent aqua-ammonia refrigerator. The design was different from those mentioned so far as the four components namely generator, absorber, condenser and evaporator were not present separately (fig 5.8). The generator was combined into the solar collector. The collector was a 0.76 cm copper sheet of 152.4 cm by 106.7 cm, painted black. There were three glass covers supported by cork strips and the back was insulated with cork board. Six steel pipes of 6.35 cm diameter, welded to headers and soldered to the collector sheet, made the generator. The absorber and condenser were water cooled. Working fluid was aqua-ammonia solution.

The results were tabulated and some were presented in graphical form. Despite results being not very spectacular, nevertheless they indicated that flat plate solar-energy collector incorporated with the generator could be used to produce temperatures as low as

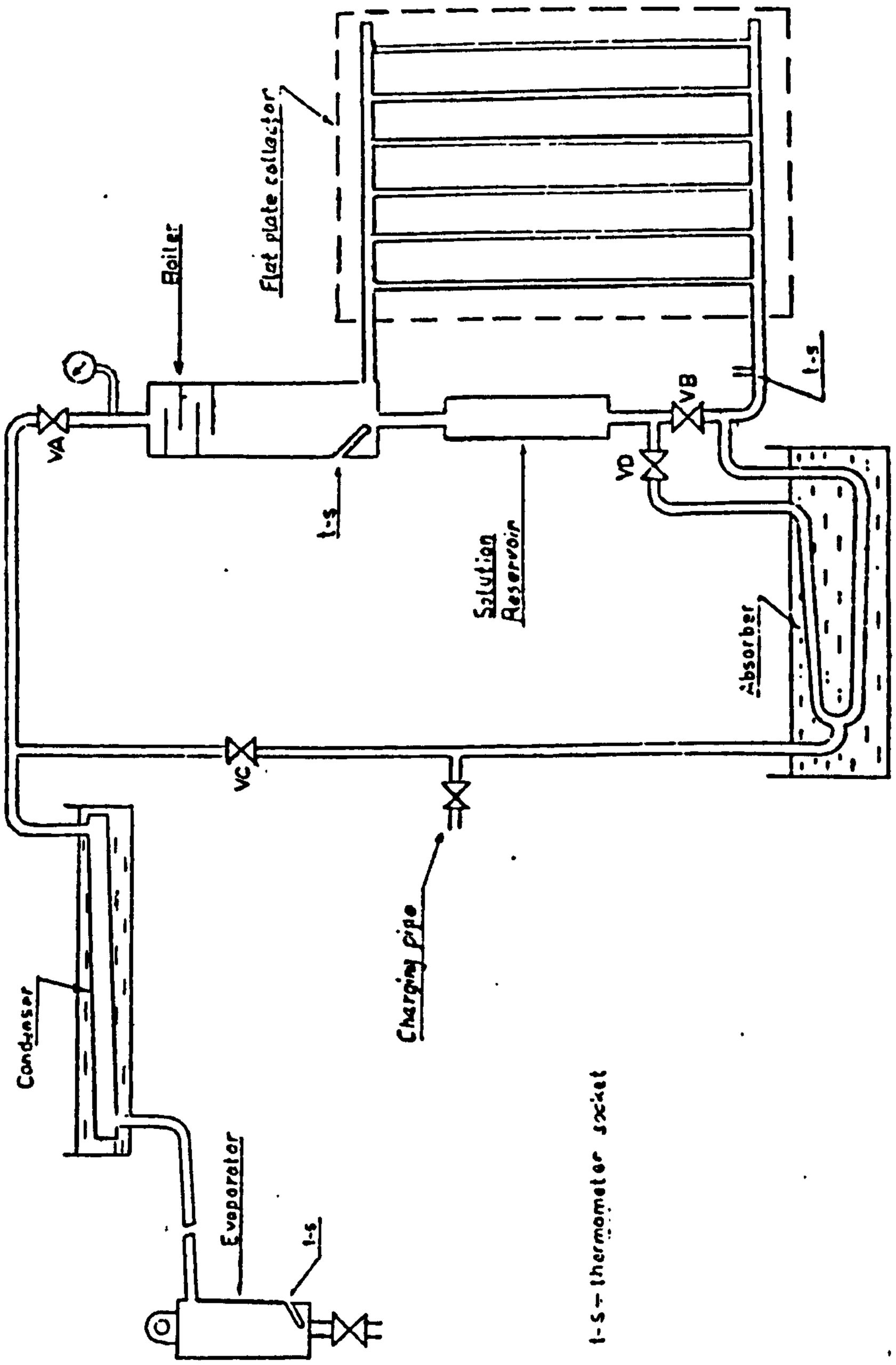

Fig 5.8 A schematic representation of water ammonia refrigerator having a combined collector/generator/absorber [59]

-12 ^{o}C. Ice at a rate of one kg a day per 0.7 m^2 of solar collecting area was produced.

Oniga [60] in his paper described an " all-solar" aqua-ammonia intermittent refrigerator. His design included some very interesting features which resulted into 24 hour refrigeration ability. Fig 5.9 gives a schematic of the apparatus. The condenser had two parts joined through a non-return valve. The first part was air-cooled to 50 ^{o}C while the second part was placed inside the refrigerating chamber. The end of this opened out into a container for concentrated ammonia also placed inside the refrigerating chamber. Evaporator was maintained at a pressure of 3.6 bar and ammonia from the container evaporated into it through a throttle-valve. The evaporated ammonia was absorbed continuously by the weak solution in the absorber at a pressure of 3.0 bar. When the sun set the generator cooled down gradually and the pressure dropped from 8.0 bar to 3.0 bar. At this point valves between generator and absorber opened and the rich solution transfered to the generator for another generation period. It was claimed that the unit had a capacity of 194 W per day with a cooling ratio of 0.58. The proposal did not progressed beyond the prototype stage.

de Sa [61] built a small and very simple aqua-ammonia refrigerating unit. It consisted of two vessels linked together by a pipe. One vessel placed at at the focus of a 1.37 m parabolic reflector acted as a generator-absorber. The other one was a condenser/evaporator. The condenser was water-cooled or air-cooled. Evaporation temperatures of 10 ^{o}C were achieved and sub-zero temperatures were

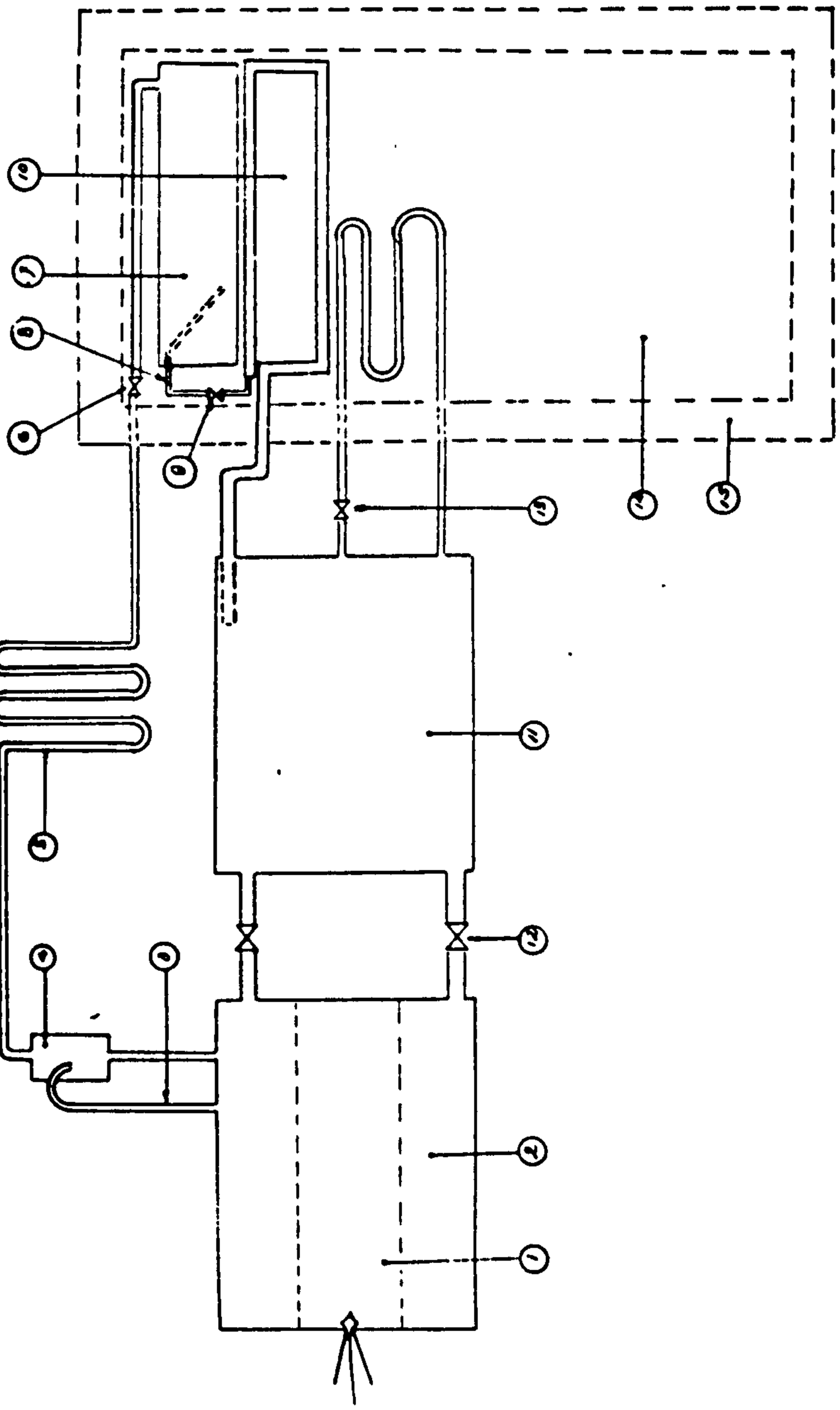

Fig 5.9 Schematic diagram of a refrigerator proposed by Oniga [60]

possible if the absorber was constantly shook. This indicates the critical importance of absorption process. It was claimed that two kg of 53 % concentrated solution generated 0.25 kg of ammonia.

Fig 5.10 shows a schematic drawing of a compact solar refrigerator developed and tested by Farber [60,61]. The flat-plate solar energy collector also serves as an ammonia generator. Area of the collector was 1.5 m^2. 12 steel pipes of 25 mm diameter were soldered to a 20 gauge galvanized iron sheet and welded at top and bottom to two headers of 63.5 mm and 32 mm diameter respectively. The assembly was placed into a box of galvanized iron sheet with a 25 mm styrofoam insulation at its back and covered with a sheet of glass. Condenser, evaporator and absorber were all shell and tube type construction. Condenser and absorber were water cooled. The evaporator absorbed heat from a solution coming from a cold box through a pump. A more detailed discussion of solar energy collector's design and construction is available in [61].

It worked on a continuous cycle and was designed to produce the maximum amount of ice during the day. The generation temperature was about 65 ^{o}C and evaporation temperature varied between -9.5 ^{o}C and -6.7 ^{o}C. On a sunny day the unit was reported to have collected 42,200 kJ of solar energy and produced 19 kg of ice, from water at 24 ^{o}C, with an over-all COP of 0.1. The system worked on cloudy days proving the ability of flat-plate solar collectors to absorb the diffused solar radiation. Despite being a very successful solar refrigeration system (12.5 kg of ice per m^2) the unit cannot work without electricity because of the two electrically operated solution pumps.

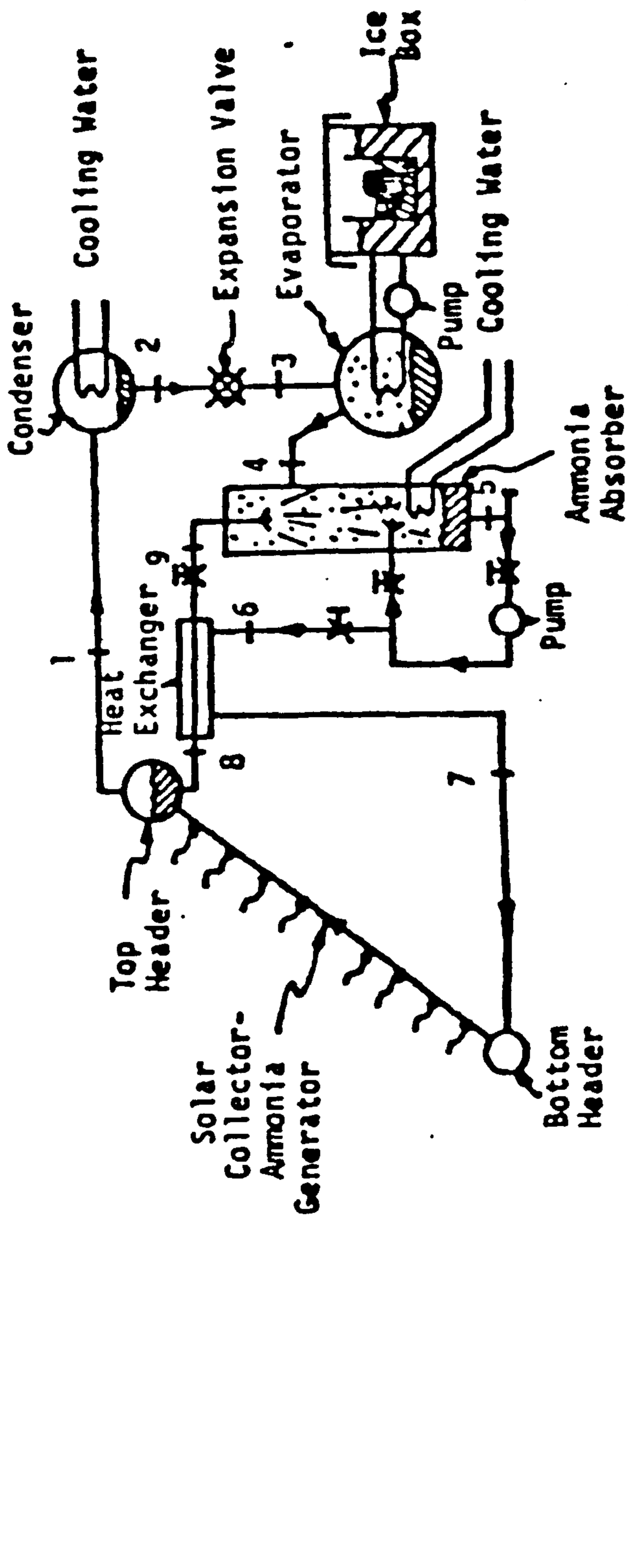

Fig 5.10 A line diagram of refrigerator tested at Florida University [62]

An aqua-ammonia intermittent refrigeration unit was built and tested in the University of Western Ontario [64,65] in 1967. The design featured a 1.4 m^2 flat-plate solar energy collector in which were combined the generator and the absorber. It consisted of 12.7 mm steel pipes connected to a 51 mm feeder at the bottom and 152 mm header at the top (see fig 5.11). Thin copper sheet was soldered to the tubes and the whole assembly was placed into a wooden box with a two-layered glass cover on top. The condenser-evaporator section was a vessel 152 mm in diameter and 559 mm in height. It was surrounded by a steel jacket of 508 mm in diameter with stagnant water for cooling the condenser. 58% to 70% solution concentrations were tested. Tests were relatively successful, evaporator temperatures were as low as -12 ^{o}C, but due to poor absorption, the evaporation rate of ammonia in the evaporator was low demanding an improved design for the absorber.

In another study, on the same unit described above, ammonia-sodium thiocyanate was used [66,67]. The results reported in the publications indicated that COP of system was better when sodium thiocyanate was used as absorbent instead of water. Maximum solar-COP for ammonia-water system and ammonia-sodium thiocyanate was 0.07 and 0.26 respectively. The system with Sodium thiocyanate did not require a rectifying column as the absorbent had low volatility. This could result in lower manufacturing cost.

Muradov and Shadiev [68,69,70] through their continuous research built an improved intermittent sodium chloride-ammonia solar refrigerator. It was of welded construction and consisted of a

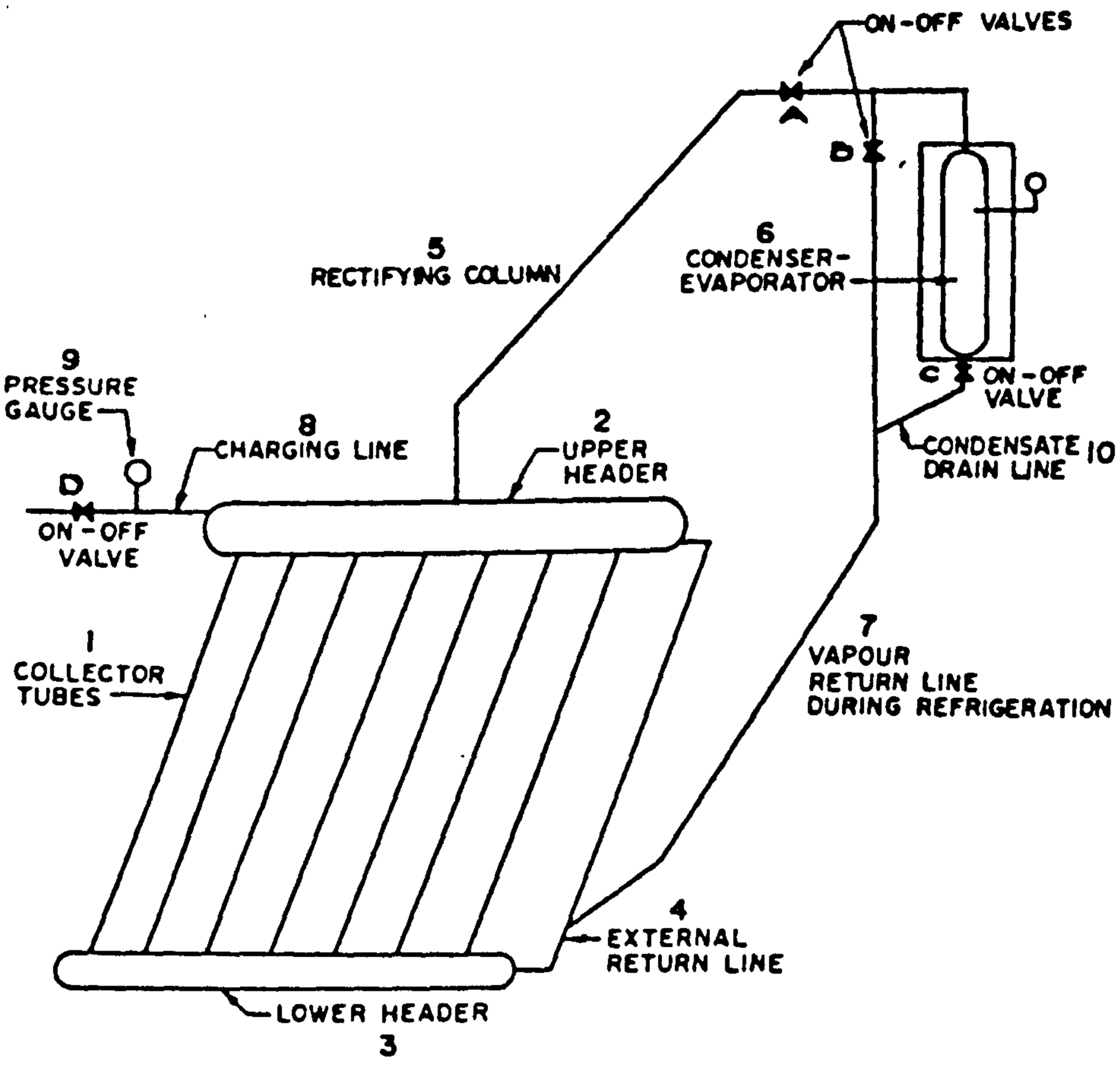

Fig 5.11 A line diagram of the system tested at University of Western Ontario [64-67]

generator, condenser and evaporator. Generator was a flat-plate solar energy collector of 2 m^2 of area enclosed into a double glazed hot box. The unit was tested in summer 1970 and the results indicated that freezing temperatures were attained in the evaporator within half an hour of the refrigeration period. It was reported that 2 kg of ice was produced. It was concluded from the study that the system was successful to function as an ice maker, was reliable, sturdy and did not need constant attention.

Eggers-Lura et al [72] in this paper discussed the solid absorption refrigeration cycle. After discussing the theory a survey of solid absorption intermittent refrigeration systems was presented. Then a design for a refrigeration plant with a production capacity of 500 kg of ice per day was described.

The plant worked with calcium chloride-ammonia as the absorption pair. The solar energy collector, which was also acting as the absorber-cum-generator, had an area of 156 m^2. The condenser was cooled in a water basin to keep the condensing temperature of 40 ^oC. The evaporator, whose area was kept large for natural convection heat transfer, was placed into the ice generator. Two problems were encountered at the design stage. Due to low thermal conductivity the temperature of the generator had to be elevated to achieve sufficient generation rates. Secondly it was found difficult to cool absorber at a good rate, by convection heat transfer, to complete the process of absorption within 12 hours.

An ordinary household Electrolux absorption refrigerator was modified by Khalil et al [74] to work on solar energy. A line-focus concentrating solar energy collector was used to heat up glycerin which while passing through a heat exchanger transfered heat to the generator of the refrigerator at a temperature of 120 ^{o}C. The circulation was attained by an electrically driven pump. Solar energy collector area was 0.5 m^2 whereas the area needed to produce sufficient cold for 24 hours was 2 m^2. The paper is very brief and no other information is provided.

Giri and Barve [75] designed and tested a 3.5 kW refrigeration capacity continuous cycle unit. The absorption pair used was water-ammonia. The unit consisted of a generator, an absorber, a condenser, an evaporator and a rectifying column. Eighteen flat-plate double-glazed solar energy collectors, of total area 36 m^2, were used. The hot water was produced at a temperature of 93 ^{o}C to give a generation temperature of 85 ^{o}C. A hot water storage tank was introduced in between the solar energy collectors and the generator for continuous operation of the plant.

The condenser, the absorber and the rectifier were water cooled and the heat from the cooling water circuit was removed through a cooling tower. The cold chamber, specially built to store potatoes, was 16 m^3 and the plant was designed to maintain a temperature of 5 ^{o}C in there.

Three pumps were used in the system: one to circulate hot water in the solar energy collector circuit; another to circulate cooling

water from the cooling tower and the third to pump the rich solution to the generator. Together with an air circulation fan in the cold chamber, these consumed an electric power of 886 W.

The plant was tested in April and May 1977. It took 2 hours to cool the cold chamber from 26 ^{o}C to 5 ^{o}C when the ambient temperature was between 35 to 40 ^{o}C. It was reported that with solar insolation of 778 W/m^2 the efficiency of the system was 0.28.

Prigmore and Barber [8] described a solar operated Rankine cycle vapour compression air conditioning unit installed in a 'Mobile Solar Research Lab'. Flat-plat collectors of 58 m^2 area and refrigeration equipment of 10.6 kW cooling capacity was installed on a trailer. The Rankine engine fluid was R-113 and refrigeration circuit used R-12. Water at 101^{o}C from the solar collectors was used to heat up R-113 to run a high speed turbine and cooling water at 29^{o}C circulated in the condenser. A conventional 12 piston compressor produced a COP of 7.4 at 7^{o}C evaporator temperature. The overall COP of the plant, taking into account an efficiency of 11% for the Rankine engine and 40% for the solar collector, was 0.2.

Alloush and Gosney [30] reported the successful operation of a solar operated continuous absorption refrigerator working with methanol and lithium and zinc bromide. It was completely autonomous in the sense that it did not require any auxilary power. Circulation of the strong solution between the absorber and the generator had been achieved through gravity by placing the absorber 1.2 m higher than the generator. The week solution was fed to the absober by a bubble

pump. This imposed serious limitation on the working pressure of the system which was kept under designed limits by reducing the condensing and absorbing temperatures to 20 and 25°C respectively. That in turn called for the water cooling of both the components.

The refrigerator worked well at low generator temperatures e.g. at a generation temperature of 90°C and evaporation proceeded at -7°C with a cycle COP of 0.4. Despite the very good performance the design required water circulation which rendered it unsuitable for areas where water is scarce. For the optimum operation of the bubble pump a receiver was introduced between the absorber and the generator whose height was varied to achieve the required head at the generator. In a practical plant, under varying operating conditions, absence of this flexibility would affect the performance of the bubble pump seriously and may even stop it functioning. This is a very serious limitation.

At Asian Institute of Technology in Thailand a continued research on water-ammonia absorption refrigeration is going on [24, 76-80]. The ultimate aim of the team lead by R.H.B. Exell was to develop a solar operated village-size refrigerator with a collecting area of 20 to 25 m^2 that can provide 0.5 m^3 of food storage cooled below 10°C, or make about 100 kg of ice per day. The reports and papers cited above describe the progression to reach the final design.

The latest plant, which had been tested and reported in [79], is shown fig 5.12. It had a solar collector area of 25 m^2 consisting of 12 solar collectors of 2.1 m^2 each. The collectors were placed in

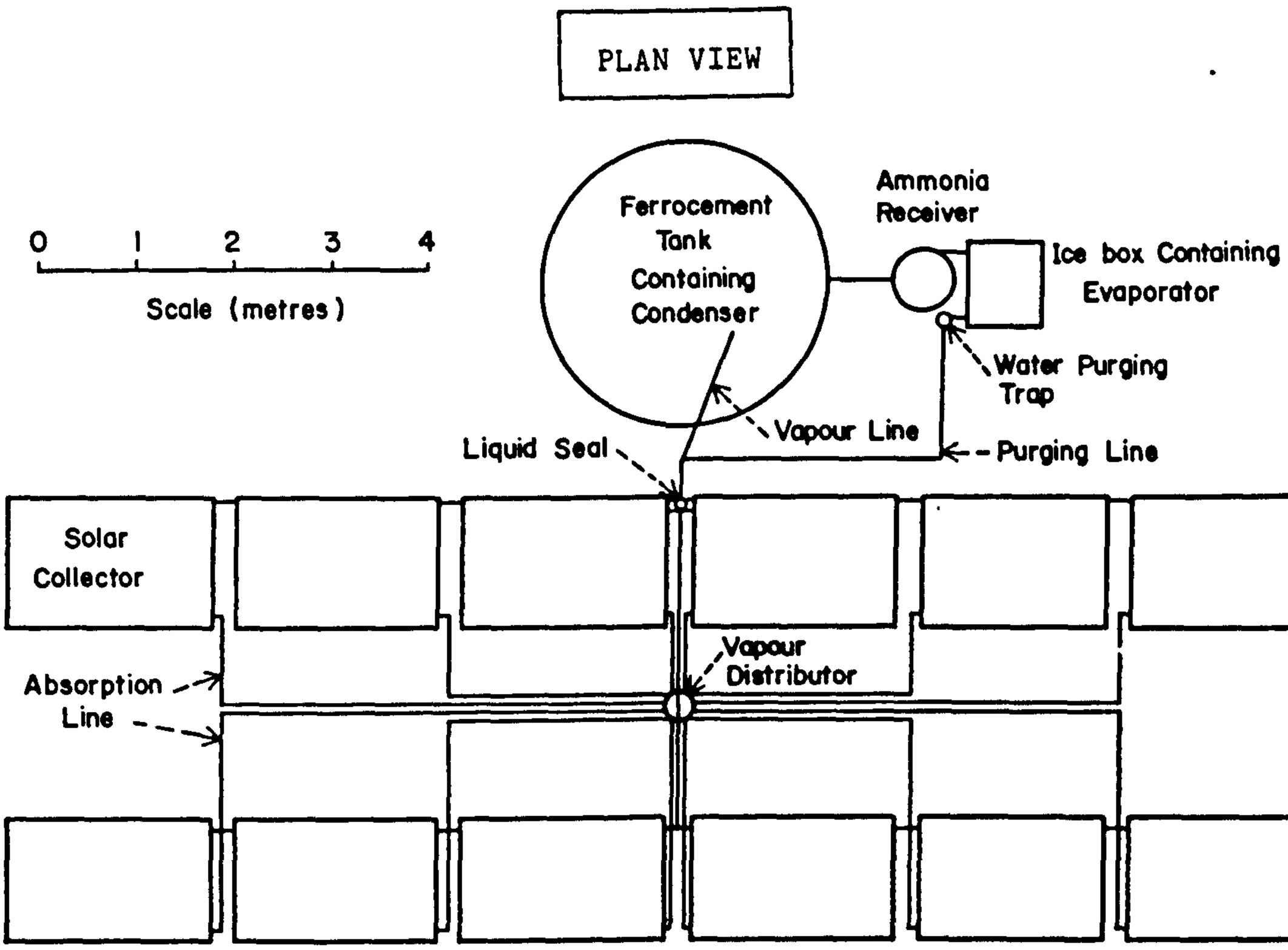

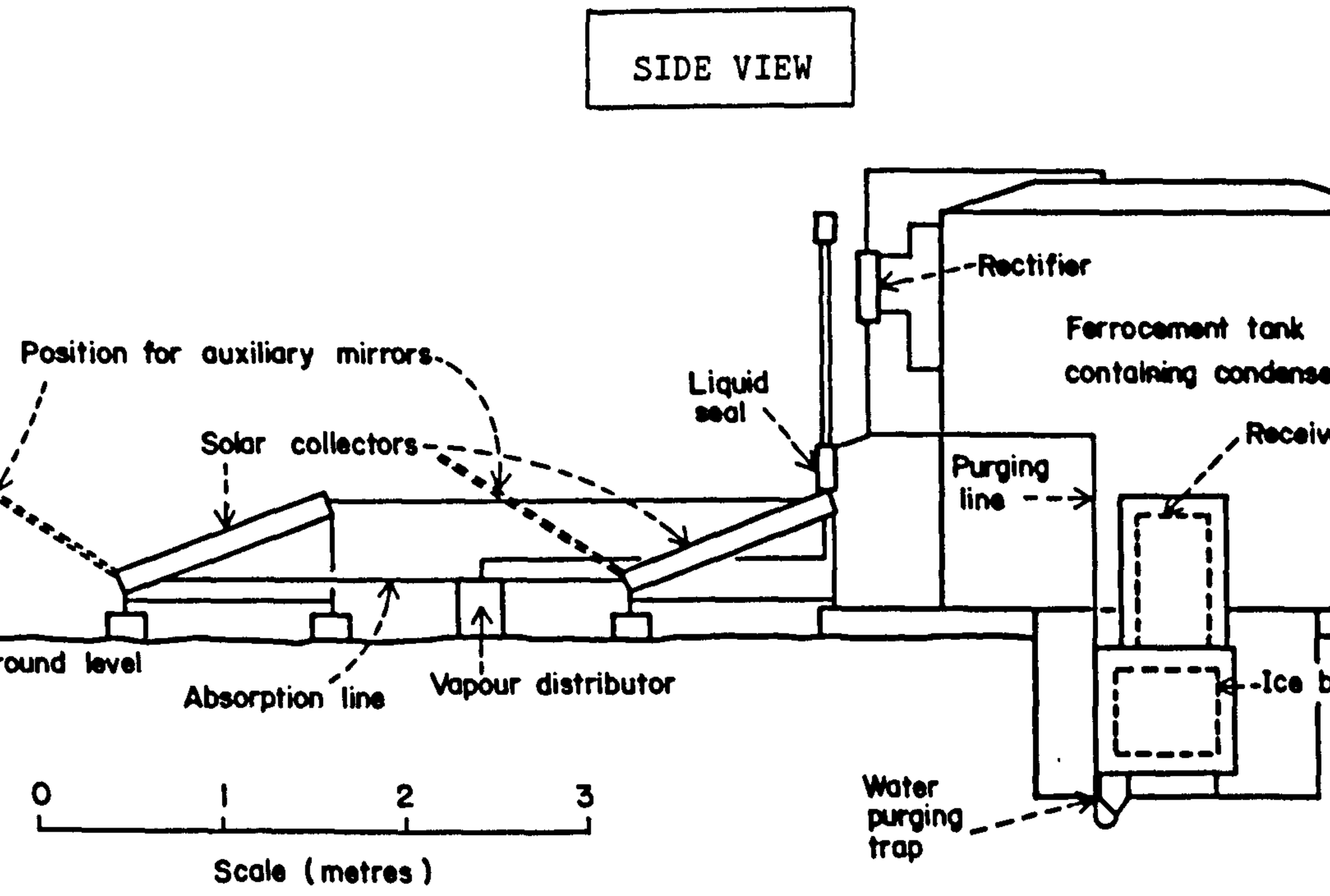

Fig 5.12 A village size solar operated refrigeration plant built at AIT Bangkok [79]

two rows. The concentration of the strong solution was 46% and its total volume was 338 litres. The condenser was enclosed in a stagnant water tank. The evaporator coil was immersed in a brine solution which acted as heat transfer medium between the evaporator coil and the ice cans. The operation of the plant was intermittent; generated ammonia during the day and produced cold at night.

The plant worked automatically except that the insulation at the back of the collectors had to be lowered in the evening to facilitate cooling during absorption and put back early next morning. Although the designed capacity of the plant was 100 kg of ice but it could produce only 31 kg. The reason pointed out were poor heat transfer between evaporating ammonia and freezing water. Despite this discrepancy this was a successful design which had room for further development.

Energy Concepts Company [81] has completed a development program on their intermittent solar ammonia absorption cycle (ISAAC) icemaker in 1988. ISAAC utilized conventional water-ammonia pair and the solar collector (which acted as generator and absorber as well) had been designed as non-tracking type. It has been claimed to produce 7 kg of ice per square meter of collector area. The units are produced in three sizes, i.e.25, 50, and 100 kg ice per day and their respective prices are $3500, $5700, and $8000 (1988 prices).

A lot of work had been reported regarding the use of metal halides in solar absorption refrigeration cycles, e.g. calcium chloride/ ammonia [15,18,40,41,72], calcium chloride/methanol [38,39],

strontium chloride/ammonia [41,42]. At the Technical University of Denmark, Worsoe-Schmidt and co-workers [16,17,82-86] had been working on solid absorption refrigeration utilizing the reaction of calcium chloride and ammonia. They had succeeded in converting the academic research into a commercial product . A danish company Kaptan A/S market the product for making block ice, chilling milk and as an ice pack freezer/refrigerator[85].

The basic components of the plant are shown in a schematic representation in fig 5.13. The collector tubes contained specially prepared porous granules of calcium chloride. The collector acted both as the generator and the absorber for the refrigeration circuit. The condenser was a placed in a tank of stagnant water. The cooling cabinet consisted of two parts; a 40 litres compartment surrounded by a water jacket for storage of vaccines and a 9 litres compartment for freezing ice packs.

The combined generator/absober tubes were made from extruded aluminium profiles as shown in fig 5.14. The flat fin attached to the outer tube had a selective surface and absorbed solar energy. The inner tube with 6 longitudinal fins helped to carry away the heat of absorption. This was achieved by connecting an air cooled condenser with the tubes and filling them with R-114. The air cooled condenser was placed at the top of the collector as could be seen in fig 5.15. A thermostatic valve operated by the solar heat controlled the automatic cooling of absorber.

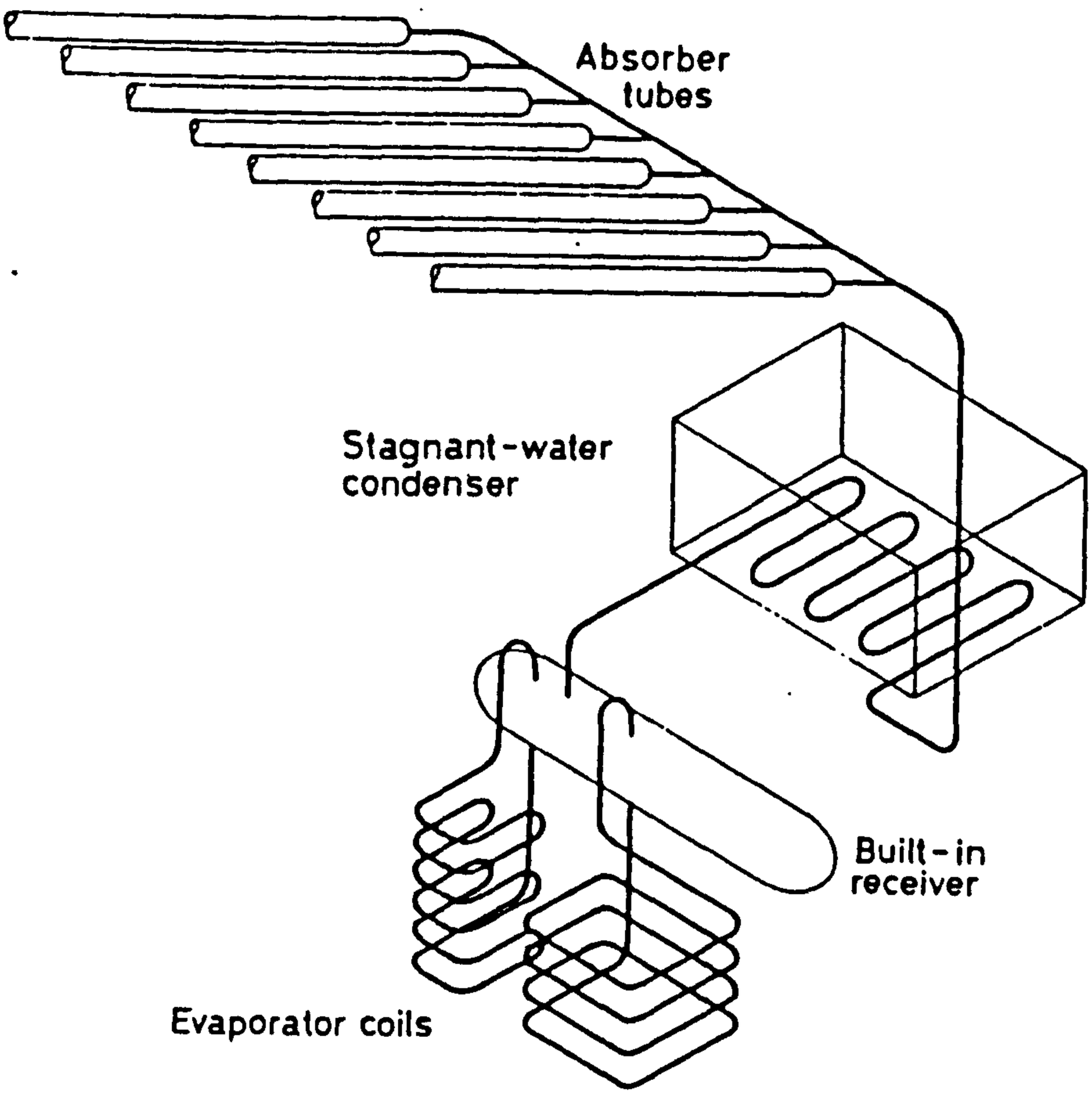

Fig 5.13 A schematic diagram showing the different components of calcium chloride ammonia absorption refrigerator designed at The Technical University of Denmark and manufactured by Kaptan ApS, Denmark [83]

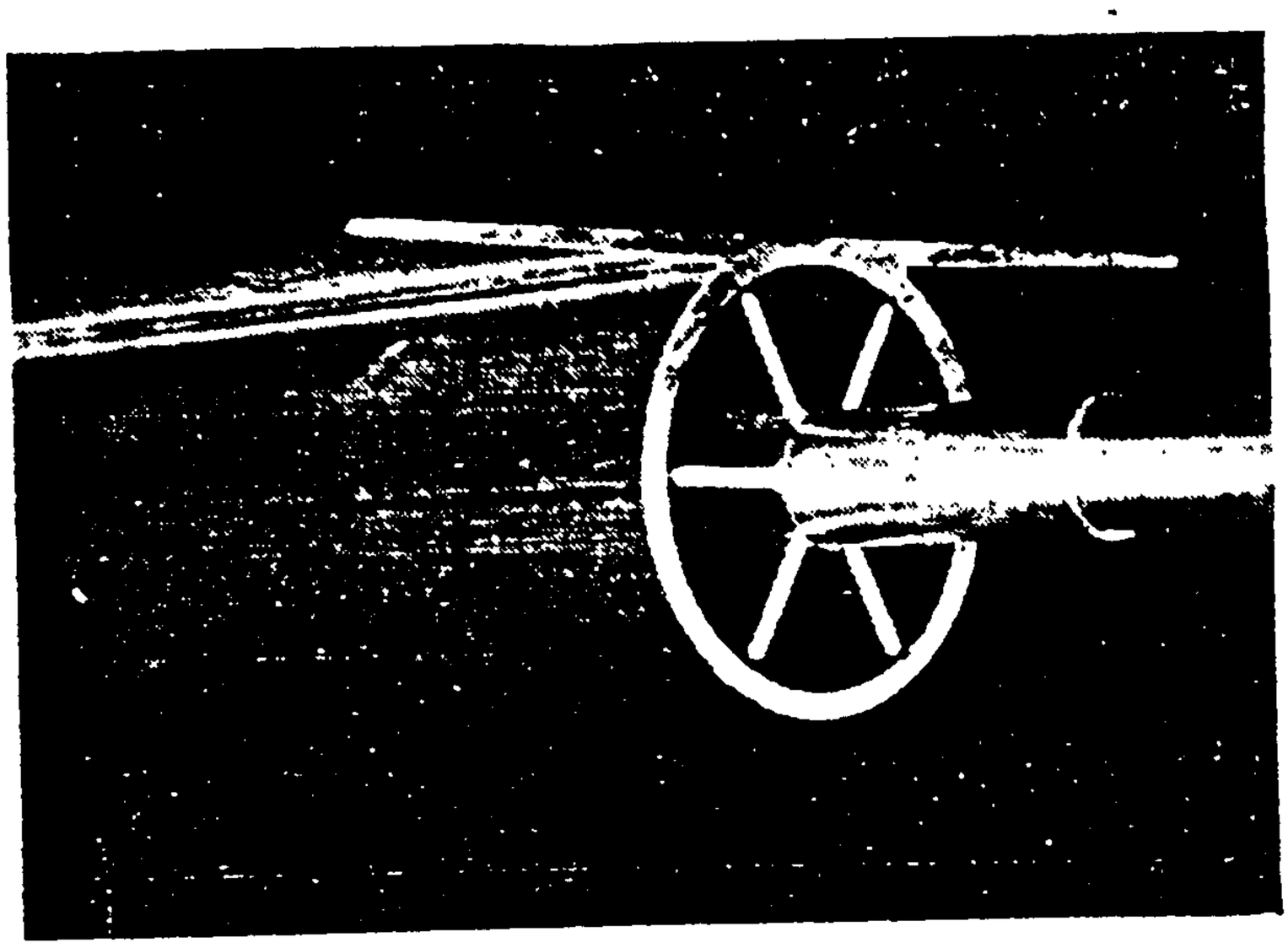

Fig 5.14 Photograph of extruded aluminium absorber tube

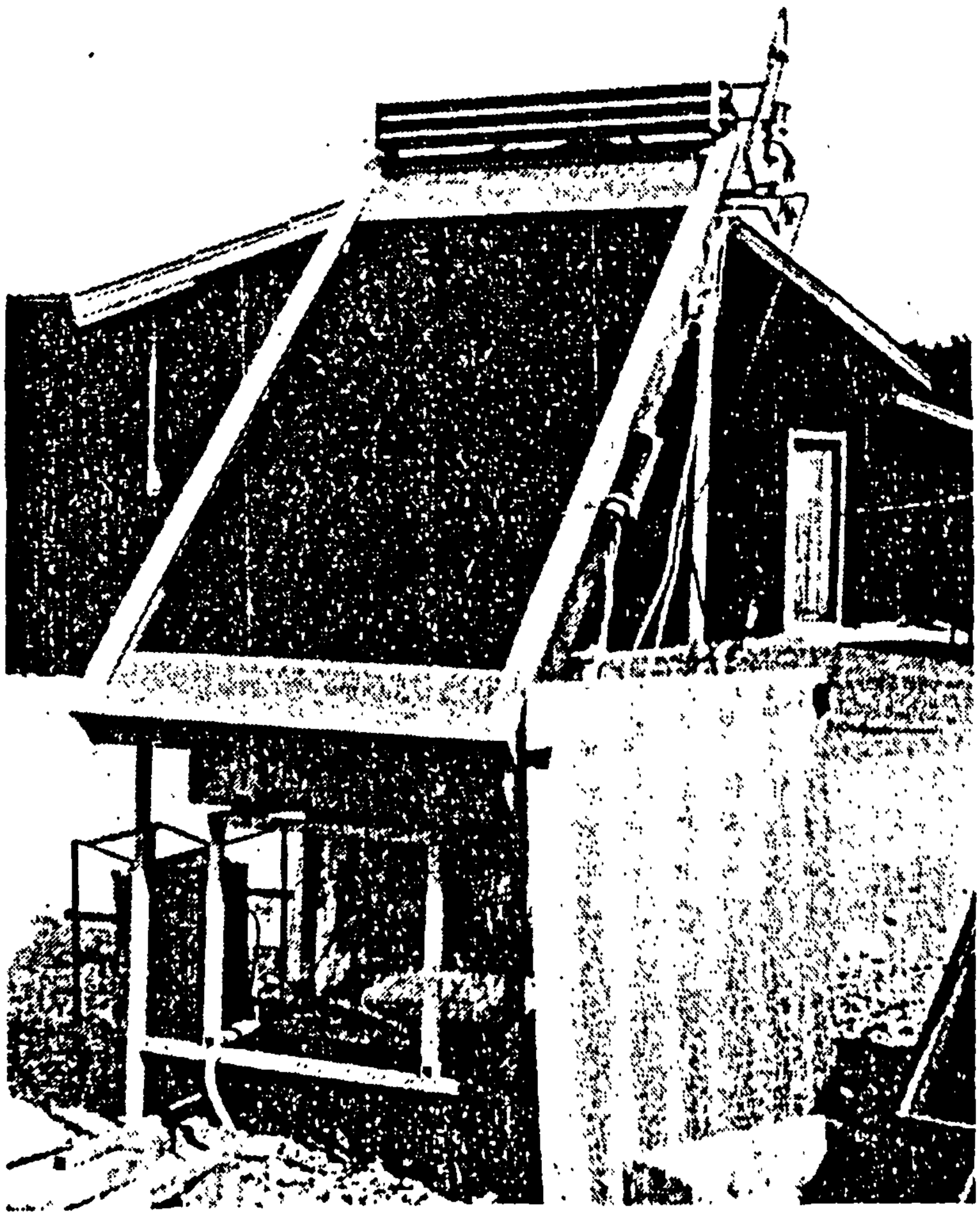

Fig 5.15 Photograph of the commercial refrigerator showing the air cooled condenser for the absorber at the top of the collector

The COP of the refrigerating cycle was found to be 0.34 and the overall COP was 0.096 which gave an average collector efficiency of 0.28 [84]. The major drawback of the design is the inability control the internal temperature as the evaporation process is dependent on the night time ambient conditions.

Another refrigerator using the same pair is manufactured by a French company Comesse Soudure S.A. under a licence from the University of Nancy. The refrigerator has been designed on a modular basis so as to facilitate building of plants of various sizes and capacities. The price varied according the type and capacity of the unit and was claimed to be cheaper than the photovoltaic powered vapour compression units [87]. Different components of the unit are shown in fig 5.16. There are three main parts of the the device:

1) The Collector-absorber-generator: it consisted of steel tubes of 60 mm diameter and 2 meter long designed to withstand a pressure upto 50 bars; they were placed at the focal axis of cylindero-parabolic collector fixed in an east west orientation. The tubes were filled with calcium chloride granules and ammonia and covered with a selective surface. Single glazing reduced the radiation losses. Aperture area of one collector was 0.6 m^2.

2) The condenser: it was an air cooled type consisting of a finned tube designed to give a condensation temperature of 10^{o}C maximum above ambient.

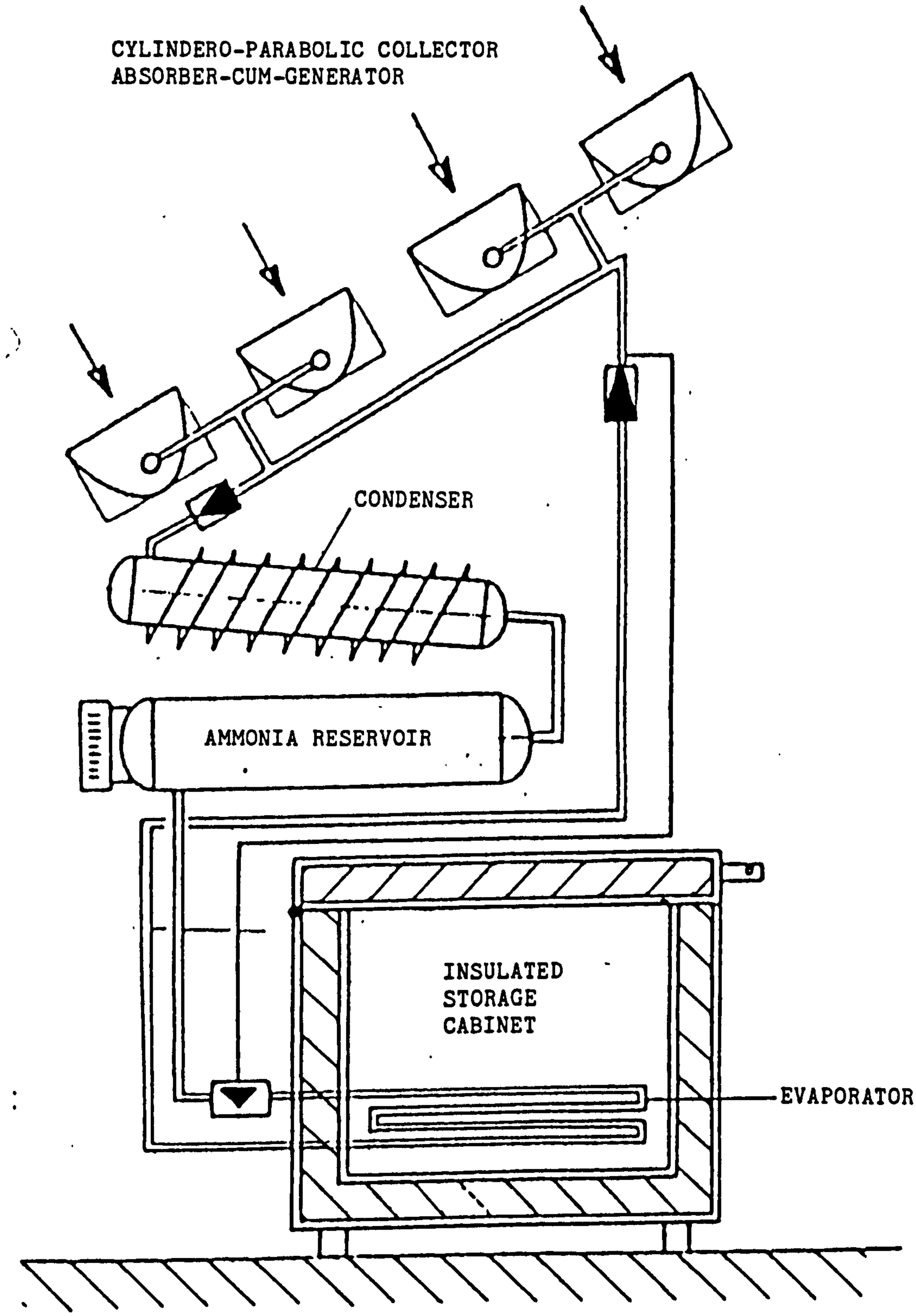

Fig 5.16 Calcium chloride ammonia absorption refrigerator manufactured by Comesse Soudure S.A., France [87]

3) The evaporator: it consisted of steel tubes of diameter suitable for the particular application. It was enclosed in an insulated box to preserve the vaccines and other perishable stuff.

The refrigerators are produced to perform either of the two functions: a) the ice production; about 10kg per 24 hours with 4.8 m^2 aperture area, b) maintain a temperature between -3 and +8°C of about 30 kg perishable stuff. The latter was achieved through a utectic mixture being cooled by the evaporator which acted as a cold storage.

The test results conducted at Madagascar Island showed that the refrigerator reduced the temperature of 75 litres of water at 18°C to 8°C in 16 hours when the ambient temperature was 28°C. The temperature of the cold storage utectic mixture fluctuated between -32°C and -29°C. This indicate a need to improve the heat transfer from the walls of the cold storage.

This is again a story of successful liaison between the industry and an academic institution. The basic research into the design of the unit had been conducted by Flechon and co-workers [88,89] at the Laboratoire de Physique de Depots Metalliques, University of Nancy, France.

Solar operated refrigeration units based on adsorption of water by zeolite had attracted many researchers. Many prototypes had been developed and reported [44-46,90,91]. A small commercial refrigerator produced by Tchernev [91] utilized zeolite water pair.

It had a solar collector area 0.74 m^2, contained 36 kg of natural zeolite (zeosarb 5.0 A) and made 6.8 kg of ice after a sunny day ($20MJm^{-2}$). The ice produced was inaccessable for the user as it was contained in a hermetically sealed system. It melted slowly during the day and cooled an insulated box of 113 dm^3. The refrigerator worked on a cloudy day as well, though ice formation did not occur .

The refrigerator was not suitable for producing ice. The temperature regulation was not possible. Due to these limitations it did not receive any popular acceptance. The production of these units was ceased about four years ago [92].

Activated carbon and methanol adsorption pair had been the focus of activity for the development of a solar operated refrigerator for quite some time. Many theoretical [19,21,94-96] and experimental [20,97,98] have been published. Pons and Guilleminot [97] reported a successful ice maker which had a solar collector area 6 m^2 which contained 130 kg of activated carbon. A sketch of the plant is shown in fig 5.17. The main parts of the ice maker were:

1) Four solar energy collectors, in the shape of a metal box, which contained a bed of activated carbon and were made of copper sheet. The front of the collectors was furnished with a selective coating (maxorb). Fins, to enhance the heat transfer from the front into the carbon bed, were attached on the inside of the front. To facilitate the transport of methanol vapours through the activated carbon bed, a false bottom was introduced to create a vapour space at the rear

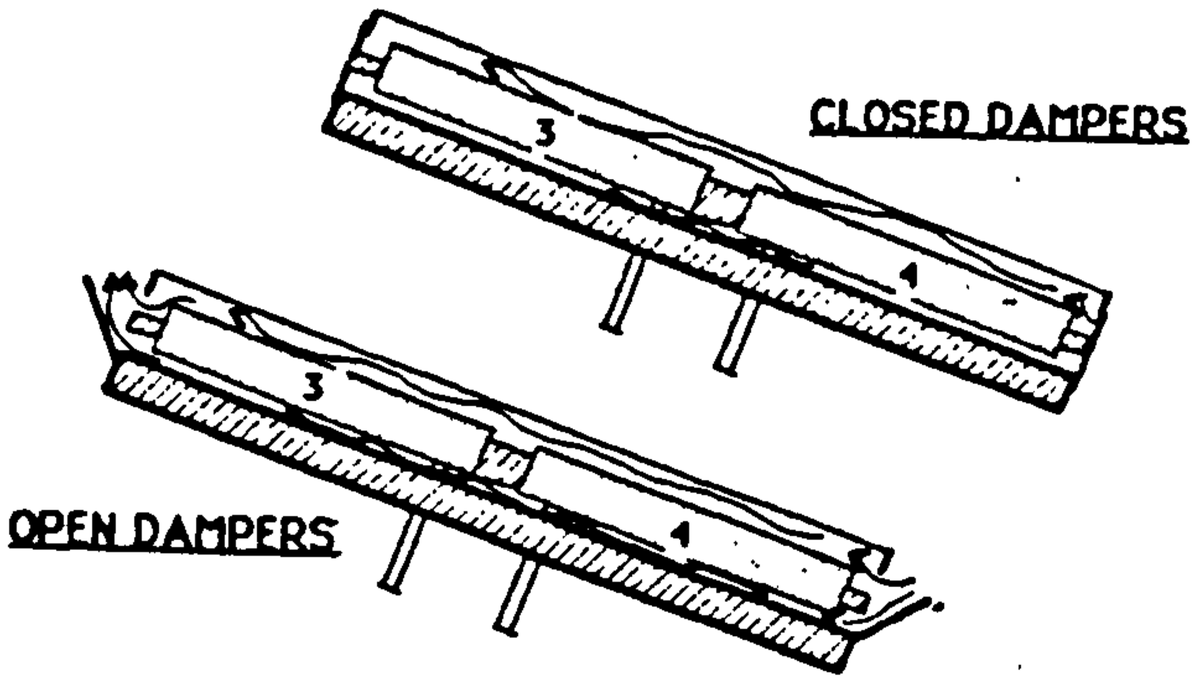

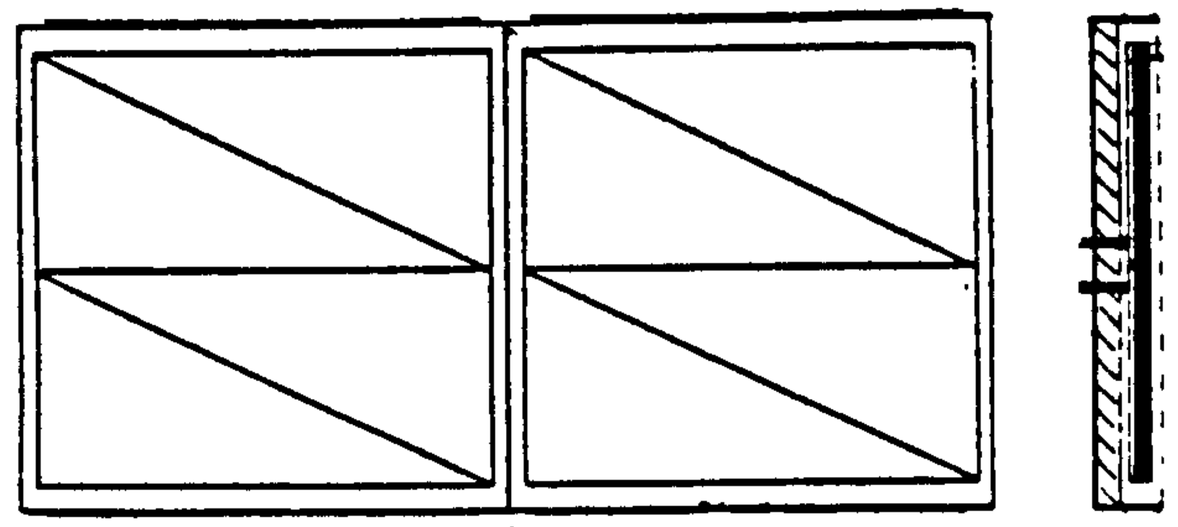

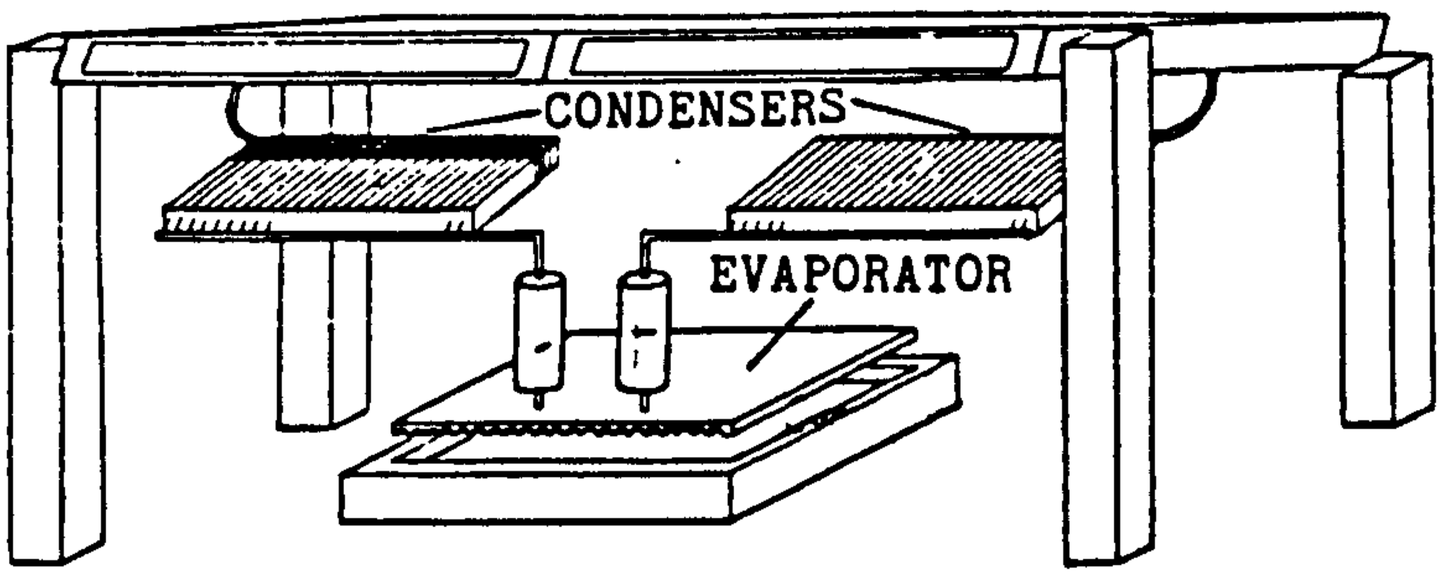

Fig 5.17 Schematic drawing of the experimental icemaker [97]

of the box. The box was placed in an insulated casing covered with single glazing.

2) Two air cooled condensers were part of the ice maker circuit each communicating with two of the four solar collectors. These were made from copper tubes with rectangular aluminium fins and designed to condense methanol at 5^{o}C above the ambient temperature.

3) The evaporator was designed and shaped to produce ice blocks. It had enough volume to contain all the methanol desorbed during the day. The methanol inside the evaporator boiled and absorbed heat from the water to be frozen. Every morning the ice was removed.

The results from the tests on the experimental ice maker were discussed in [98]. The data presented for the collector number 3 showed that when the front of the collector reached its maximum of 107^{o}C the adsorbent was at 92^{o}C. This indicate the high value of contact resistance between the front wall and the activated carbon granules. The maximum ambient temperature on the test day was 23^{o}C and condenser temperature recorded was 38^{o}C. For an air cooled condenser 15^{o}C temperature difference was a bit higher. The explanation given was improper convection due to fins being too close (3 mm apart).

The average efficiency of the collectors was reported to be 30 to 40 percent and the maximum insolation on the day of the test was recorded as 870 Wm^{-2}. This means the maximum rate of heat transfer across the front wall was 261 Wm^{-2}. The temperature difference

between the wall and the adsorbent at that instance was 15°C which gave a value of 17.4 $Wm^{-2}K^{-1}$ for heat transfer.

The reported tests were conducted in an ambient of 23°C and looked encouraging. But in tropical climates ambient temperatures of 40°C are common. In such a situation condensation and consequently the desorption would take place at much higher temperatures which would seriously affect the performance of the ice maker.

A commercial refrigerator based on the activated carbon methanol pair had been manufactured by a french company BLM [99]. It was very similar in design to the experimental ice maker discussed in [97]. Fig 5.18 shows the essential parts and general layout of the plant. Due to take over of the company by new management it is out of production now [100].

Fig 5.18 Photograph of adsorption refrigerator by BLM [99]

REFERENCES

1 World Health Organization, 'A guide to estimating capacity of equipment required for storage and transporting EPI vaccines', Document no WHO/EPI/CCIS/86.3, Geneva, 1986.

2 World Health Organization, 'Guide on Implementation of Solar Energy for EPI' WHO/UNICEF EPI technical Series, Document no WHO/UNICEF/EPI.TS/86.3, Geneva, 1986.

3 Anis, W.R., Mertens, R.P., and von Overstraeten, R., 'Economic feasibility of photoelectric systems in the developing countries', Solar and Wind Technology, vol 2, no 1, pp 9-14, 1982.

4 Sheradin, N.R., 'Solar air conditioning', in Solar Energy Applications in Tropics, D Reidel Publishing Company, pp 57-89, 1983.

5 Harris, D.J., Norton, B. and Smith, I.E., 'Design and performance of a novel Peltier effect solar-powered refrigerator', Proceedings of UK-ISES conference, Solar Electricity for Development, University of Reading, UK, pp 89-95, 1988.

6 Field, R.L., 'Review of photovoltaic-powered refrigeration for medicine use in developing countries', Solar Cells, vol 6, pp 309-316, 1982.

7 Sargent, S.L. and Teagen, W.P., 'Compression refrigeration from a solar powered organic Rankine cycle engine', ASME paper no 73-WA/Sol08, 1973.

8 Prigmore, D. and Barber, R., 'Cooling with sun's heat, design considerations and test data for a Rankine cycle prototype', Solar Energy, vol 17, pp 185-192, 1975

9 Vokaer, D. and Bougard, J., 'Autonomous Rankine cycle solar cooling unit', International Institute of Refrigeration, Poceedings of commissions E1 and E2, Jerusalem, Israel, 1982/3.

10 Eckard, S.E. and Bendd, J.A., 'Performance characteristics of a 3 ton Rankine powered vapour compression airconditioner', Proceedings of Second Workshop on Use of Solar Energy for the cooling of buildings, University of California, USA, 1976.

11 Murthy, M.V.K. and Murthy, S.S., 'Solar cooling systems: An overview', in Active Solar Cooling, Proceedings of Solar cooling Workshop, Indian Institute of Technology, Madras, India, 1984.

12 Provost, E.T., 'Solar Powered Refrigeration', PhD thesis, University of Liverpool, UK, 1980.

13 Chari, R.K., 'An Investigation of the Use of Solar Energy for Absorption Refrigeration', MS thesis, College of Engineering, University of Florida, 1958.

14 Farber, E.A., 'The direct use of solar energy to operate refrigeration and airconditioning systems', Revista de Colegio de Ingeneros, Argenitetos y Agrimensores de Puerto Rico, vol 15, no 3, pp 59, 1965.

15 Eggers-Lura, E., Nielsen, P.B., Stubkier, B. and Worsoe-Schmidt, P., 'Potential use of solar powered refrigeration by an intermittent solid absorption system', COMPLES international meeting, Heliotechnique and Development, University of Petroleum and Minerals, Dahran, Saudi Arabia, pp 83-104, 1975.

16 Worsoe-Schmidt, P. and Nielsen, P.B., 'Design of a combined solar collector/absorber/desorber for a solid-absorption refrigerating system', ASME paper 78-HT-35, presented at the AIAA/ASME Thermophysics and Heat Transfer conference, Palo Alto, California, USA, 1978.

17 Nielsen, P.B. and Worsoe-Schmidt, P., Development of a solar powered solid absorption refrigeration system. Part I: Experimental investigation if the generation and absorption processes. Report F30-77.01, Refrigeration Laboratory, The Technical University of Denmark, Lynby, Denmark, 1977.

18 Iloeje, O.C., 'Quantitative comparison of treated $CaCl_2$ absorbent for solar refrigeration', Solar Energy, vol 37, no 4, pp 253-260, 1986.

19 Delgado, R., Choisier, A., Grenier, P., Ismail, I., Meunier, F. and Pons, M., 'Etude du cycle intermittent charbon actif-methanol en vue de la realisation d'une machine a fabriquer de la glace fonctionnant a l'energie solaire', International Institute of Refrigeration, Proceedings of Commissions E1 and E2, Jerusalem, Israel, 1982/3.

20 Grenier, Ph. and Pons, M., 'Experimental and theoretical results on the use of an activated carbon CH_3OH intermittent cycle for the application to a solar powered ice maker', Proceedings of ISES conference, Solar WOrld Forum, Perth, Australia, pp 500-506, 1983.

21 Critoph, R.E., 'Activated carbon adsorption cycles for refrigeration and heat pumping', Proceedings of IoP, RSC conference, Porosity in Carbons, Bath, UK, 1987.

22 Perry, R.H. and Chilton, C.H., Chemical Engineers' Handbook, 5th edition, MacGraw Hill, N.Y., USA, 1973.

23 Gmehlin, J., Chemistry Data Series, vol III, part I, Dechema, Frankfurt, W. Germany, 1984.

24 Exell, R.H.B. and Kornsakoo, S., Design and Testing of a Solar Powered Refrigerator, AIT research report no 126, Asian Institute of Technology, Bangkok, Thailand, 1981.

25 Radermacher, R. and Alefeld, G., 'Lithiumbromid-Wsser-Losengen abs Absorber fur Ammoniak oder Methylamin', Brennst-Warme-Kraft, vol 34, no 1, pp 31-38, 1982.

26 Bhaduri, S.C. and Varma, H.K., 'P-T-X behaviour of R 22 with five different absorbents', International Journal Of Refrigeration, vol 9, pp 362-366, 1986.

27 Iyer, P.S.A., Murthy, S.S. and Murthy, M.V.K., 'Thermodynamic properties of some vapour absorption system refrigerant-absorbent pairs', Active Solar Cooling Systems, Proceedings of Solar Cooling Workshop, India, pp 165-185, 1984.

28 Durgunov, N. Ch., Maksudov, T.M. and Vakhidov, A.T., 'Choice of coolants and absorbents for absorption-type solar refrigerators', Applied Solar Energy, vol 17, no 1, pp 32-34, 1981.

29 Renz, M. and Pfeiffenberger, U., 'Thermodynamic properties of binary system water-lithium bromide', Solar Energy for Refrigeration and Air Conditioning, Proceedings of meetings of commissions E1 & E2, International Institute of Refrigeration, Paris, France, pp 69-74, 1982/83.

30 Alloush, A. and Gosney, W.B., 'An absorption system using methanol plus lithium and zinc bromides for refrigeration using solar heat', Proceedings of 16th International Congress of Refrigeration, Paris, France, pp 339-345, 1982/3.

31 Bokelmann, H., Ehmke, H.J. and Renz, M., 'Working fluid for a sorption heat pump', Proceedings of four contractors meetings on heat pumps, Commission of the European Community, Brussels, 1982.

32 Macriss, R.A., Punwani, D., Rush, W.F. and Biermann, W.J., 'Thermodynamic and physical properties of ammonia-lithium thiocyanate system', Journal of Chemical and Engineering Data, vol 17, no 4, pp 443-446, 1972.

33 Macriss, R.A., Punwani, D., Rush, W.F. and Biermann, W.J., 'Thermodynamic and physical properties of monomethyleamine-lithium thiocyanate system', Journal of Chemical and Engineering Data, vol 15, no 4, pp 466-470, 1970.

34 Infante Ferreira, C.A., 'Thermodynamic and physical property data equations for ammonia-lithium nitrate and ammonia-sodium thiocyanate solutions', Solar Energy, vol 32, no 2, pp 231-236, 1984.

35 Wendel, D.R. and Biermann, W.J., Solid Absorbents; High Latent Heat Refrigerants, Carrier Corporation, N.Y., USA, 1978.

36 Bokelmann, H. and Ehmke, H.J., 'Erstellung von Enthalpie - Konzentrations - diagrammen fur Stoffsysteme fur Warmepumpen', Ki Klima - Kalte-Heizung, vo 6, pp 241-244, 1985.

37 Bakken, K., 'Syatem Tepidus; high capacity thermochemical storage/heat pump Tepidus AB', International Conference on Energy Storage, Brighton, UK, 1981.

38 Offenhartz, P.O'D, Brown, F.C., Mar, R.W. and Carling, R.W., 'A heat pump and thermal storage system for solar heating and cooling based on the reaction of calcium chloride and methanol vapour', ASME Journal of Solar Energy Engineering, vol 102, pp 59-65, 1980.

39 Ravelet, R., 'Methanol-calcium chloride absorption cycles' Proceedings CEC Absorption Heat Pump Congress, Paris, France, pp 239-249, 1985.

40 Flechon, J. and Machizaud, F., 'Solar refrigeration : study of dry absorption', Alternative Energy Sources Two: Proceedings of 2nd Miami International Conference, Miami Beach, USA, Vol 2, pp 749-760, 1981.

41 Stanish, M.A. and Perlmutter, D.D., 'Salt hydrates as absorbents in heat pumps', Solar Energy, vol 26, pp 333-339, 1981.

42 Buffington, R.M., 'Absorption refrigeration with solid absorbents', Refrigeration Engineering, vol 26, pp 137-152, 1933.

43 Balat, M. and Crozat, G., 'Solar refrigeration by solid-gas reactions: physical-chemistry feasibility tests on a laboratory device', International Journal of Refrigeration, vol 11, pp 33-40, 1988.

44 Hinotani, K., Kanatani, K., Matsumoto, K. and Kume, M., 'Development of solar actuated zeolite refrigeration system', Solar World Forum, ISES conference, Perth, Australia, pp 527-531, 1983.

45 Meunier, F., Mischler, B., Guilleminot, J.J. and Simonot, M.H., 'On the use of a zeolite 13X-H_2O intermittent cycle for the application to solar climatization of buildings', SUN II, Proceedings ISES conference, Atlanta, USA, pp 739-743, 1979.

46 Tchernev, D.I., 'The use of zeolites for solar cooling', Proceedings 5th International Conference on Zeolites, Naples, Italy, pp 788-794, 1980.

47 Aittomaki, A. and Harkonen, M., 'Zeolite-methanol adsorption heat pump', Proceedings International Workshop on Research Activities on Heat Pumps, Graz, pp 421-434, 1986.

48 Pons, M. and Grenier, Ph., 'Solar ice maker working with activated carbon-methanol adsorbent-adsorbate pair', INTERSOL 85, Proceedings of ISES conference, Montreal, Canada, pp 731-734, 1985.

49 Bougard, J., 'Thermodynamical and technical problems in solar adsorption refrigeration', Proceedings of the meetings of commissions B1, B2, E1, E2, (Purdue, USA), International Institute of Refrigeration, Paris, France, pp 25-33, 1986.

50 Critoph, R.E. and Vogel, R., 'Possible adsorption pairs for use in solar cooling', International Journal of Ambient Energy, vol 7, no 4, pp 183-190, 1986.

51 Renz, M. and Steimle, F., 'Comparison of thermodynamic properties of working fluids for absorption systems', Solar Energy for Refrigeration and Air Conditioning, Proceedings of meetings of commissions E1 and E2, International Institute of Refrigeration, Paris, France, pp 61-68, 1982/3.

52 Bremser, A.T., 'Solar Operated Refrigeration System', US Patent no 2,030,350, February 11, 1936 (Filed April 10, 1933).

53 Green, W.P., 'The Utilization of Solar Energy for Air Conditioning and Refrigeration in Florida', Master's Thesis, College of Engineering, University of Florida, USA, 1936.

54 Kirpichev, M.V. and Baum, V.A., 'Exploitation of sun's rays', (in Russian), Perivoda, vol 43, p 54, 1954.

55 Williams, D.A. et al, 'Intermittent absorption cooling systems with solar regeneration', ASME Paper no 57-A-260, 1957.

56 Williams, D.A. et al, 'Cooling systems based on solar regeneration', Refrigeration Engineering, pp 33-37,64-66, November 1958.

57 Swartman, R.K., 'Survey of solar-powered refrigeration', ASME Paper no 73-WA/SOL-6, 1973.

58 Trombe, T. and Foex, M., 'The production of cold by means of solar radiation', Solar Energy, vol 1, no 1, pp 51-52, 1957.

59 Chinnappa, J.C.V., 'Performance of an intermittent refrigerator operated by a flat-Plate collector',Solar Energy, vol 6, no 4, pp 143-150, 1962.

60 Oniga, T., 'Absorption cooling unit with fixed conoidal reflectors', New Sources of Energy, Proceedings of the United Nations Conference, Italy, vol 6, pp 41-50, 1961.

61 de Sa, V.G., 'Experiments with solar energy utilization at Dacca', Solar Energy, vol 8, no 3, pp 83-90, 1964.

62 Farber, E.A., 'Design and performance of a compact solar refrigeration system', Proceedings ISES conference, Melbourn, Australia, Paper no 6/58, 1970.

63 Farber, E.A. and Moore, G.L., 'Combining the collector and generator of a solar refrigeration system', ASME Paper no 67-WA/Sol-4, 1967.

64 Alward, R., 'Solar Powered Intermittent Absorption Refrigerator', M.E.Sc. Thesis, The University of Western Ontario, Canada, 1967.

65 Swaminathan, C. and Swartman, R.K., 'Further studies on solar powered intermittent absorption refrigeration', Proceedings ISES Conference, Melbourne, Australia, Paper no 6/114, 1970.

66 Swartman, R.K. and Ha, V., 'Performance of a solar refrigeration system using ammonia-sodium thiocyanate', ASME Paper no 72-WA/Sol-3, 1972.

67 Swartman, R.K., Swaminathan, C. and Ha, V., 'Comparison of ammonia-water and ammonia-sodium thiocyanate as the refrigerant-absorbent in a solar refrigeration system', Solar Energy, 17, pp 123-127, 1975.

68 Muradov, D. and Shadiev, O., 'Experimental investigation of the operation of an intermittent solar refrigerator', Proceedings All Union Conference on the Utilization of Solar Energy (in Russian), VNIIT, Moscow, 1969.

69 Muradov, D. and Shadiev, O., 'Intermittent solar refrigerator with solid absorbent', Problems of Natural Science (in Russian), izd. TashGU i BGPI, Tashkent, 1969.

70 Muradov, D. and Shadiev, O., 'Testing of a solar adsorption refrigerator', Geliotekhnika, vol 7, no 3, pp 33-35, 1971.

71 Sargent, S.L. and Beckman, W.A., 'Theoretical performance of an ammonia-sodium thiocyanate intermittent absorption refrigeration cycle', Solar Energy, 12, pp 137-146, 1968.

72 Eggers-Lura, A., Nielson, P.B., Stubkier, P. and Worsoe-Schmidt, P., 'Solar-powered refrigeration by intermittent solid absorption systems', Proc. International Conference on Heliotechnique and Development, Dahran, Saudi Arabia, vol 2, pp 83-104, 1975.

73 Eggers-Lura, A., 'Solar Energy in Developing Countries', Pergamon Press, 1979.

74 Khalil, K.H. et al, 'Factors affecting the use of solar energy for cooling', Proc. International Conference on Heliotechnique and Development', Dahran, Saudi Arabia, vol 2, 1975.

75 Giri, N.K. and Barve, K.M., 'Solar ammonia-water absorption system for cold storage application', Proc. ISES Congress , New Delhi, India, vol 3, pp 1183-1187, 1978.

76 Exell, R.H.B. et al, 'Experiments on a prototype solar powered refrigerator for remote areas', Proc. ISES congress, New Delhi, India, vol. 3, 1978, pp 2114-2117.

78 Exell, R.H.B., Kornsakoo, S., Oeapipatanakul, S. and Chanchaona, S., A Village-size Solar Refrigerator, Research Report no 172, Asian Institute of Technology, Bangkok, Thailand, 1984.

79 Exell, R.H.B., 'A village size solar refrigerator', paper presented at Workshop on Physics of Solar Energy, New Delhi, India, 1986.

80 Exell, R.H.B., Bhattacharya, S.C. and Upadhyaya, Y.R., 'Solar cooling for cold-storage applications using solid desiccant and adsorbents', paper presented at Workshop on Physics of Solar Energy, New Delhi, India, 1986.

81 Personal communication with D.C. Erickson, President, Energy Concepts Company, Annapolis, Madison, USA, April, 1988.

82 Worsoe-Schmidt, P., 'A solar-powered solid-absorption refrigeration system', International Journal of Refrigeration, vol 2, no 2, pp 75-84, 1979.

83 Clausen, N. and Worsoe-Schmidt, P., Indoor Testing of a Solar-powered Solid-absorption Refrigerator/ Ice-pack Freezer, Report no F77-01, The Technical University of Denmark, 1983.

84 Worsoe-Schmidt, P., 'Solar refrigeration for developing countries using a solid-absorption cycle', International Journal of Ambient Energy, vol 4, no 3, pp 115-124, 1983.

85 Worsoe-Schmidt, P., 'Solar refrigeration at the village level based on a solid-absorption cycle', paper presented at the National Solar Energy Convention 1984 of the Solar Energy Society of India, Bhopal, 1985.

86 Worsoe-Schmidt, P., 'Some results from the development of a solid-absorption refrigeration system', paper presented at Council of European Community Absorption Heat Pump Congress, Paris, France, 1985.

87 Sales literature, Comesse Soudure S.A., France

88 Flechon, J., Machizaud, F., Benhammon, K. and Godmel, G., 'Refrigeration solaire par photothermic: premiers resultats d'un appareil reel', Journal of Power Sources, vol 13, no 3, pp 197-216, 1984

89 Flechon, J., Kotowski, A., Machizaud, F. and Deczynski, M., 'Capteur solaire a surface absorbante en forme de jalousie', Journal of Power Sources, vol 13, no 3, pp 245-257, 1984.

90 Ulku, S., 'Adsorption heat pumps', Journal of Heat Recovery Systems, vol 6, no 4, pp 277-284, 1986.

91 Ragot, Ph., Berger, M., Lebuhotel, C. and Serra, J.M., 'Solar sanitary case for vaccine conservation at +4°C', INTERSOL 85, Proceedings of ISES congress, Montreal, Canada, 1985.

92 Tchernev, D.I., 'Solar energy application of natural zeolites', in Natural Zeolites: Occurance, Properties, Use, Ed: Sand, L.B. and Mumpton, F.A., Pergamon Press, Oxford, UK, pp 479-485, 1978.

93 Personal communication with Mr. Peter Downing, the Business Manager, The Zeopower Company, Natick, Massachusetts, USA, May, 1988.

94 Passos, E., Meunier, F. and Gianola, J.C., 'Thermodynamic performance improvement of an intermittent solar-powered refrigeration cycle using adsorption of methanol on activated carbon', Journal of Heat Recovery Systems, vol 6, no 3, pp 259-264, 1986.

95 Pons, M. and Grenier, Ph., 'A phenomenological adsorption equilibrium law extracted from experimental and theoretical considerations applied to the activated carbon + methanol pair', Carbon, vol 24, no 5 pp 615-625, 1986.

96 Guilleminot, J.J., Meunier, F. and Paklesa, J., 'Heat and mass transfer in a non-isothermal fixed bed solid adsorbent reactor: a uniform pressure-non-uniform temperature case', International Journal of Heat and Mass Transfer, vol 30 no 8 pp 1595-1606, 1987.

97 Pons, M. and Guilleminot, J.J., 'Design of an experimental solar powered, solid adsorption ice maker', ASME Journal of Solar Energy Engineering, vol 108, pp 332-337, 1986.

98 Pons, M. and Grenier, Ph., 'Experimental data on a solar powered ice maker using activated carbon methanol adsorption pair', ASME Journal of Solar Energy Engineering, vol 109, pp 303-310, 1987.

99 Sales literature BLM, France.

100 Personal communication with Prof F. Meunier, France, March 1989.

CHAPTER SIX

Solar Refrigeration : Detailed Study of Selected Options

PART I

Photovoltaic refrigerators

6.1 The purpose of this chapter

In the previous chapter three feasible options for a solar operated vaccine store were selected. In this chapter their performance limitations be evaluated and compared so as to choose the most desirable one. For this purpose the size of the plant and area of the solar collector, for a prescribed cooling load, will be determined and compared. So the first step is to determine the cooling load of the vaccine storage cabinet.

6.2 Cooling capacity of the refrigerator

The cooling capacity of the unit was calculated assuming the cabinet to be cubical. Although a cuboid is the most practical shape for a storage cabinet, a cube, being the closest practical shape to a sphere, offers the least surface area per unit volume. The cabinet is assumed to be a double walled metallic box and the cavity is filled with insulation. A cabinet of 30 litres volume is recommended for a typical rural health clinic as defined in section 5.1.1. The assumption here is that the cabinet will store some life-saving drugs in addition to the prescribed load of vaccines and ice-packs. Further parametric assumption were made to simplify the calculations which were:

(i) All the six walls of the cabinet had the same thickness

(ii) All the cabinet walls had the same heat transfer characteristics

(iii) Internal temperature of the cabinet was uniform at $0^{o}C$

(iv) Ambient temperature was $32^{o}C$ and $43^{o}C$ (night & day)

(v) Heat transfer resistance through metal cases was neglected

(vi) Radiation exchange at the inner surface was neglected

6.2.1 Environmental heat gains

Heat transfer to the cabinet takes place through all the three mechanisms i.e. conduction, convection, and radiation. The internal and external surfaces are characterized by heat transfer coefficients h_i and h_o, respectively, representing both convection and radiation at these surfaces and the insulation by its thermal conductivity k.

The heat transfer which takes place from the external to the internal surfaces is conducted across the insulation through a varying area. Thus the conduction area is taken as the mean of internal and external areas. Therefore,

Internal surface area, A_i $= 6 \times L^2$

External surface area, A_o $= 6 \times (L+2t)^2$

Mean conduction area, A_m $=6 \times (L+t)^2$

It is very fair to assume that the cabinet is always placed at some sheltered place. Thus the system is analyzed assuming heat gains through natural convection. There are four vertical and two horizontal faces of the cabinet. Simplified correlations for natural convection to air given by McAdam [1] are used. These are;

(a) for vertical plates

for 10^9 <R_a> 10^{13} $h_c = 1.31\ (\Delta T)^{1/3}$
for 10^4 <R_a> 10^9 $h_c = 1.42\ (\Delta T/L)^{0.25}$

(b) for horizontal plates with lower surface cold

for $2x10^7$ <R_a> $3x10^{10}$ $h_c = 1.52\ (\Delta T)^{1/3}$
for 10^5 <R_a> $2x10^7$ $h_c = 1.32\ (\Delta T/L)^{0.25}$

(c) for horizontal plates with upper surface cold

for $3x10^5$ <R_a> $3x10^{10}$ $h_c = 0.59\ (\Delta T/L)^{0.25}$

where ΔT is the difference between the surface and air temperatures. The radiation at the inner surface was neglected but at the outer surface was simply calculated assuming it to be a grey body enclosed in black environment. As the temperature difference between the cabinet surface and the ambient was less than 50^oC the radiative heat transfer coefficient was approximated by

$$h_r = \sigma \epsilon 4T_{av}^3$$

The overall heat transfer across the cabinet walls was then calculated by the equation

$$Q_{env} = UA(T_o - T_i)$$

and $$UA = [(1/h_iA_i) + (t/kA_m) + (1/h_oA_o)]^{-1}$$

A computer program listed in appendix C was used to calculate the heat gains at different ambient temperatures and for different insulation thicknesses. The result for a 30 litre capacity cabinet with closed cell polyurethane foam (thermal conductivity 0.022 $Wm^{-1}K^{-1}$) is presented in graphical form in fig 6.1. It is evident from the graph that by increasing the thickness of insulation beyond

6-5

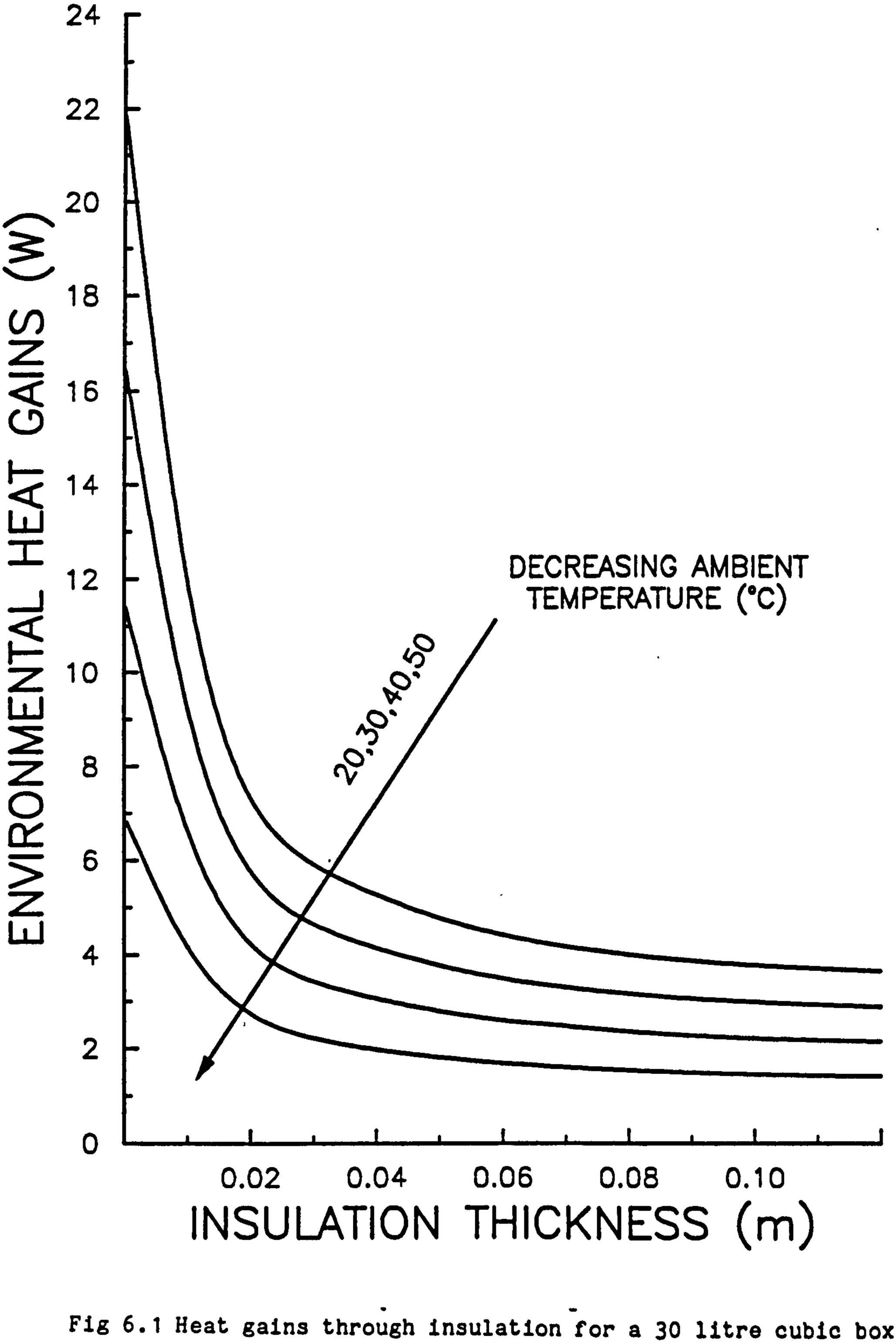

Fig 6.1 Heat gains through insulation for a 30 litre cubic box

70mm the corresponding change in the amount of heat transfered is not substantial. Thus under ambient temperature of 40°C and with an insulation thickness of 7.0 mm the heat gained from the environment would be 3.3 W.

6.2.2 Cooling load of vaccines

A primary health centre holds a six weeks' stock of 15 litres of vaccine. This gives a daily consumption (assuming a six day working week) of 0.417 litre of vaccines. The actual pattern of vaccine administration would vary from clinic to clinic. As an average it is assumed that the quarter of the daily stock consumed is allowed to be heated upto ambient of 30°C and is then replaced in the refrigerator. Taking the specific heat and density of vaccines as equal to water i.e 4.18 kJ/kg and 1 kg/l respectively, the cooling load of the vaccines would be

$$Q_{vac} = 4.18 \times 0.417 \times 0.25 \times (40 - 0) \times 1000 / 24 / 3600$$

$$= 0.2 \text{ W}$$

6.2.3 Cooling load due to intermittent door opening

Whenever the door of a refrigerator is opened some of the cold inside air is replaced with the warm and humid outside air. To quantify the load imposed by the warm air is again difficult because it depends on the pattern of use. Considering the worst scenario that a) the door is opened every half an hour b) the working day is 6 hours long c) the refrigerator is 3/4 empty and d) half the cold

is replaced by warm saturated air every time the door is opened and e) the warm air is cooled to 0°C in half an hour, the cooling load would be calculated as follows.

Volume of air inside the refrigerator = 0.75 x 30
= 22.5 l

Volume of warm saturated air = 0.5 x 22.5
= 11.25 l

Moisture contents of saturated air at 40°C = 0.042 g l^{-1}

Latent heat of condensation of water = 2250 J g^{-1}

Neglecting the heat contents of air compared to water the cooling load due to the ingressed warm moist air would be

$$Q_{air} = 11.25 \times 0.042 \times (2250 + 4.18 \times 40) \times 2 / 3600$$

$$= 6.4 \text{ W}$$

6.2.4 Cooling load of ice packs

For the case of a typical health centre considered there is a need for 3 kg of ice to be produced per day. As per WHO's specifications, referred to above, This ice is to be produced from water at 32°C. Thus to produce 3 kg of ice from 3 kg of water at 32°C in 24 hours the required cooling capacity would be

$$Q_{ice} = 3 \times (4.18 \times 32 + 333) \times 1000 /24 / 3600$$

$$= 16.21 \text{ W}$$

6.2.5 Cooling load of other drugs

Out of total capacity of 30 litres, 20% (i.e. 6 litres) is assumed to be unoccupied (to leave some room to manoeuvre the stored items) and about 3.75 litres would be occupied by 3 kg of ice packs. Thus the remaining 5.25 litres would be available for storage of other drugs. The 'worst case' that of a whole stock of new drugs, is considered. The contents of drugs are assumed to have thermal properties equivalent to that of water and are further assumed to cool down in 2 hours, therefore the cooling load due to 5.25 litres of drugs at 40°C would be

$$Q_{drugs} = 5.25 \times 4.18 \times 40 \times 1000 / 24 / 3600$$
$$= 10.2 \text{ W}$$

6.2.6 Total cooling capacity

The total cooling capacity of the 30 litre refrigerator suitable for a typical primary health centre would be the sum of all the cooling loads considered in sections 6.2.1 to 6.2.5 above. The calculations show that under the assumed practices and environmental conditions the refrigerator would have to have a cooling capacity of 38.5 Watts. For calculation purposes in the next sections, a cooling capacity of 100 Watts will be considered which is assumed to have a 85 watt icepack freezing load.

6.3 Photovoltaic (PV) vapour-compression refrigerator

The components of PV refrigerator, as described earlier in chapter five, are (i) a photovoltaic array, (ii) a dc-to-ac inverter, (iii) a lead acid battery storage, and (iv) a vapour compression refrigerator. Although, in theory, a normal household refrigerator, incorporating a dc motor or coupled with a dc-to-ac inverter, can be directly energized by a PV array without a parallel connection to a battery, its inclusion in the circuit is necessitated for the following reasons.

(1) The starting current of a motor-compressor assembly is higher than the normal operational current. PV-arrays, for the reasons of economy, are always selected to meet the normal operational load. The extra power required at the start of a compression system is provided by the battery.

(2) Due to fluctuations in insolation, the output of the PV-array changes. The battery acts like as a reservoir to dampen these fluctuations in the output. Thus the refrigerator, which requires a stabilized power supply, can receive a constant power input through the battery.

(3) The battery stores the extra energy available during the high insolation periods to keep the system running during the low insolation periods and after the sunset.

6.3.1 System performance

The overall system response is a collective behaviour of individual components in the system. Thus to determine the required size of the system for a particular requirement, a knowledge of the performance of each individual system component is necessary.

Fig 6.2 shows a block diagram of the system components. The average values of the efficiencies are also shown in the diagram. The notations used in the analysis are defined below:

η_c = Efficiency of PV array

η_b = Efficiency of the battery

η_i = Efficiency of the inverter

η_m = Efficiency of the motor

COP_{vc} = Thermodynamic efficiency of the vapour compression refrigerator

The overall efficiency or coefficient of performance of a PV-vapour compression refrigerator, denoted by $COP_{overall}$, is then given by

$$COP_{overall} = \eta_c x \eta_b x \eta_i x \eta_m x COP_{vc}$$

6.3.1.1 Performance of a photovoltaic array

Performance of a photovoltaic array is described in the shape of current-voltage(I-V) characteristic curve. I-V characteristics of a typical commercial PV array are shown in fig 6.3 [2]. It can be

6-11

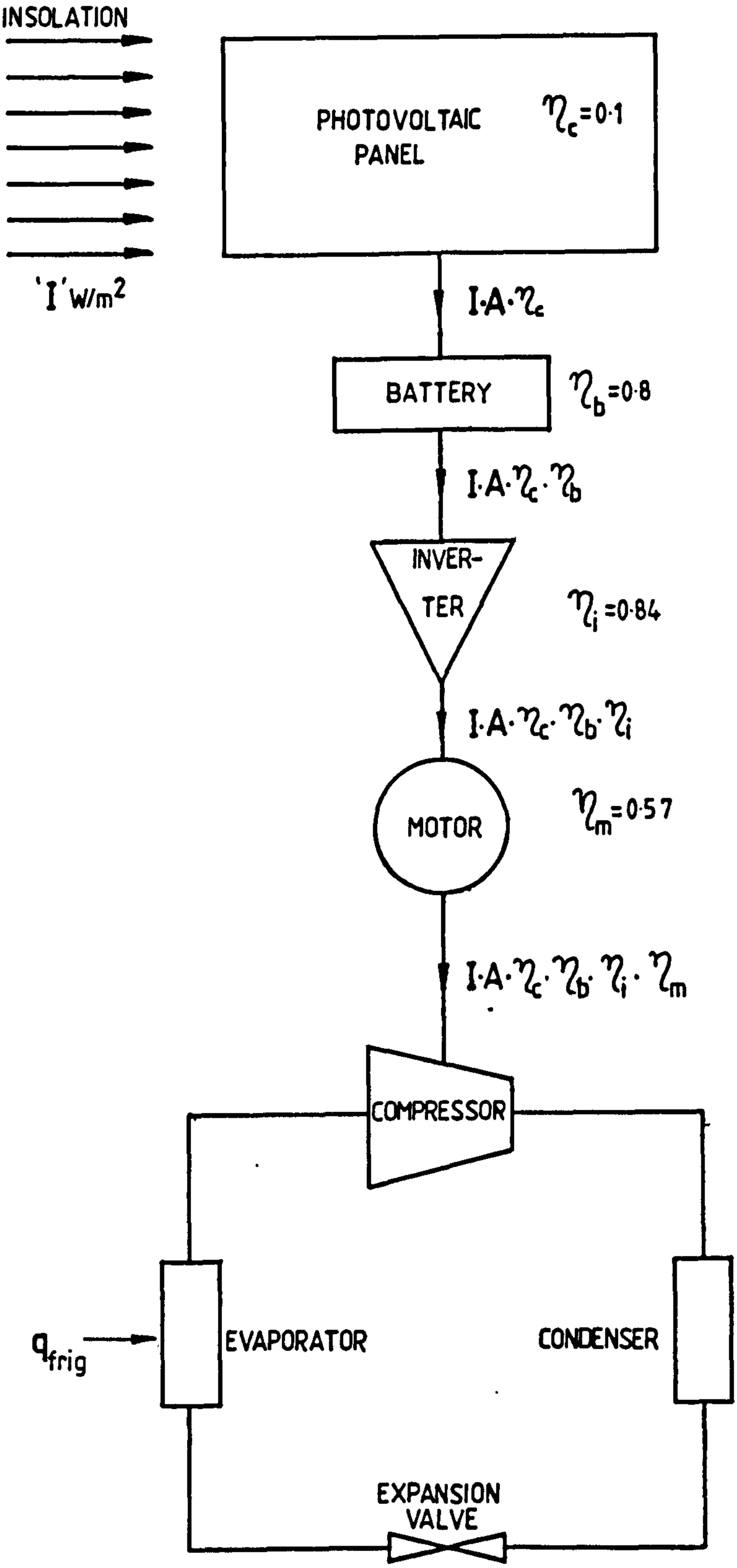

Fig 6.2 Block diagram showing components and their efficiencies in a photovoltaic refrigerator

observed that I-V characteristics vary in response to changes in insolation (see the left hand side set of curves) and operating temperature of the array (see the right hand side set of curves).

The curves in fig 6.3 show that the output of the array is directly proportional to the insolation intensity i.e the efficiency of a PV array does not vary with change in insolation levels. In response to changes in operating temperature the output power of the array is affected. The peak power of the PV array cited in fig 6.3 decreases with the increase in operating temperature of the array at the rate of 0.4% per degree celsius.

Each I-V curve has a maximum-power point (see fig 6.4) at which the the product of array voltage and current is maximized. It is clearly evident that operation at the maximum-power-point is advantageous but would require the load to operate at different voltages. In practice a vapour compression refrigerator work at a fixed operating voltage and fairly steady power. Thus a refrigerator directly powered by the PV-array cannot always work at the maximum-power-point.

In fig 6.4 a battery voltage is superimposed on the I-V characteristic curve. The battery voltage is chosen such that the array operates at maximum-power-point at noon (in solar time) on a clear day (i.e. clearness index > 0.7). At other times or when sky is not clear, the chosen battery voltage would cause the array to deliver less, but not far less, than the maximum possible power. This observation means that in the case under consideration (i.e. a

6-13

Electrical Characteristics

	SX-100	SX-110	SX-120
Peak power (Pp)	32	36	40
Voltage at peak power (Vpp)	17	17.25	17.5
Current at peak power (Ipp)	1.9	2.1	2.3
Short-circuit current (Isc)	2.2	2.35	2.5
Open-circuit voltage (Voc)	22	22.25	22.5

NOTES.

1. Panels are measured under full sun illumination (1kW/m^2) at 25°C ± 3°C cell temperature. Minimum performance is 2 watts less than peak. The ruling specification is peak watts. For a more detailed explanation, see our *Electrical Performance Measurements* bulletin.
2. Electrical characteristics vary with temperature.

Voltage (Voc)	increases by decreases by	2.4mV/°C/cell	below above	25°C
Current (Isc)	increases by decreases by	25uA/°C/cm^2	above below	25°C
Power (peak)	increases by decreases by	0.4%/°C	below above	25°C

SX-110
Performance at Various Light Intensities, T = 25°C

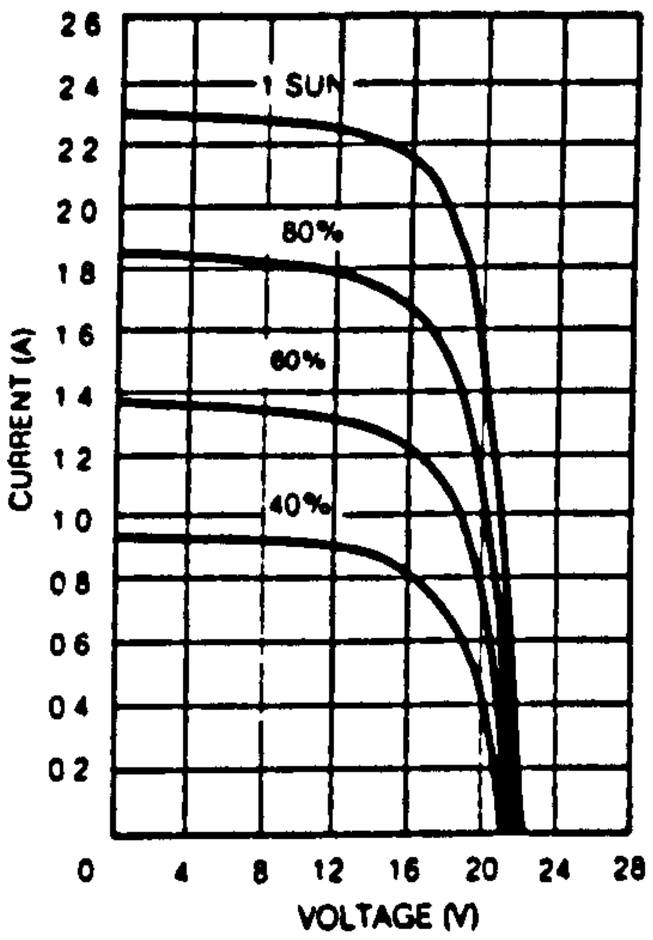

SX-110
Performance at Various Temperatu
at AM1 (1kW/m^2)

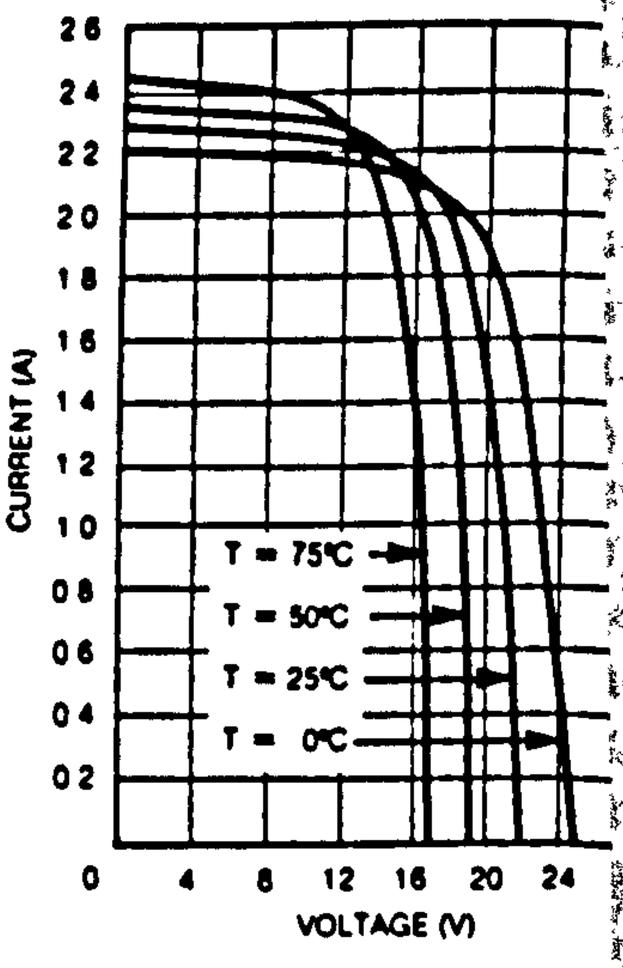

NOTE: These curves are representative of the performance of typical panels at the terminals, without any additional equipment such as diodes, cabling, etc. These curves are intended for reference only. Curves for the SX-100 and SX-120 panels are available from Solarex Marketing.

Mechanical Specifications

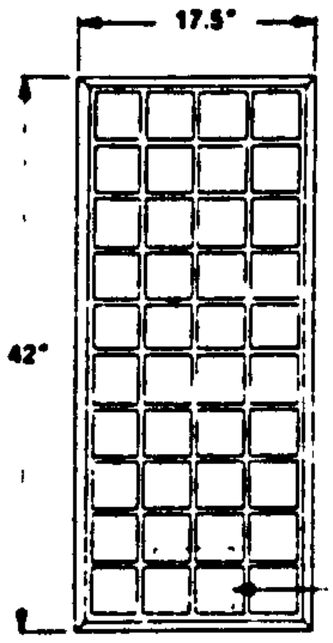

Weight:
17.5 lbs (7.9 kg)

Dimensions:
17.5" x 42" x 2.1"
(44.5cm) x (106.7cm) x (5.4cm)

Cross Section of Panel

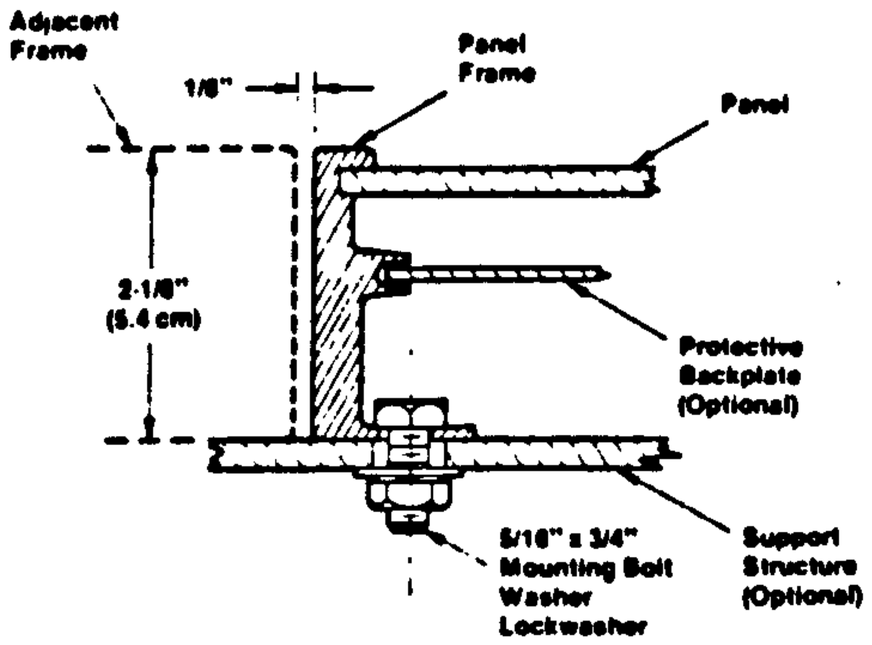

Reliability and Environmental Specifications

These panels are subjected to intensive quality control during manufacture and rigorous testing before shipment. They are designed to meet or exceed the following tests with no performance degradation:

- Repetitive cycling between −40°C and 100°C.
- Prolonged exposure to 90-95% humidity at 70°C.
- Wind loading of over 160 m.p.h.

All SX Series panels are covered by the standard Solarex 5 year limited warranty.

Options and Accessories

Backplates — Anodized aluminum backplate protects the panel in harsh environments. Backplates are available either mounted inside the panel frame at the factory or as components to be mounted onto the panels during field assembly.

Diodes — In-line blocking diode prevents reverse current flow from the panel to the battery during darkness. Bypass diode is available for high voltage systems to provide alternate current path protection.

For multiple panel arrays and large power regulation, contact Solarex Marketing.

Specifications are subject to change without notice. 8024-1 5/82

Fig 6.3 Specification sheet for a typical silicon solar panel [2]

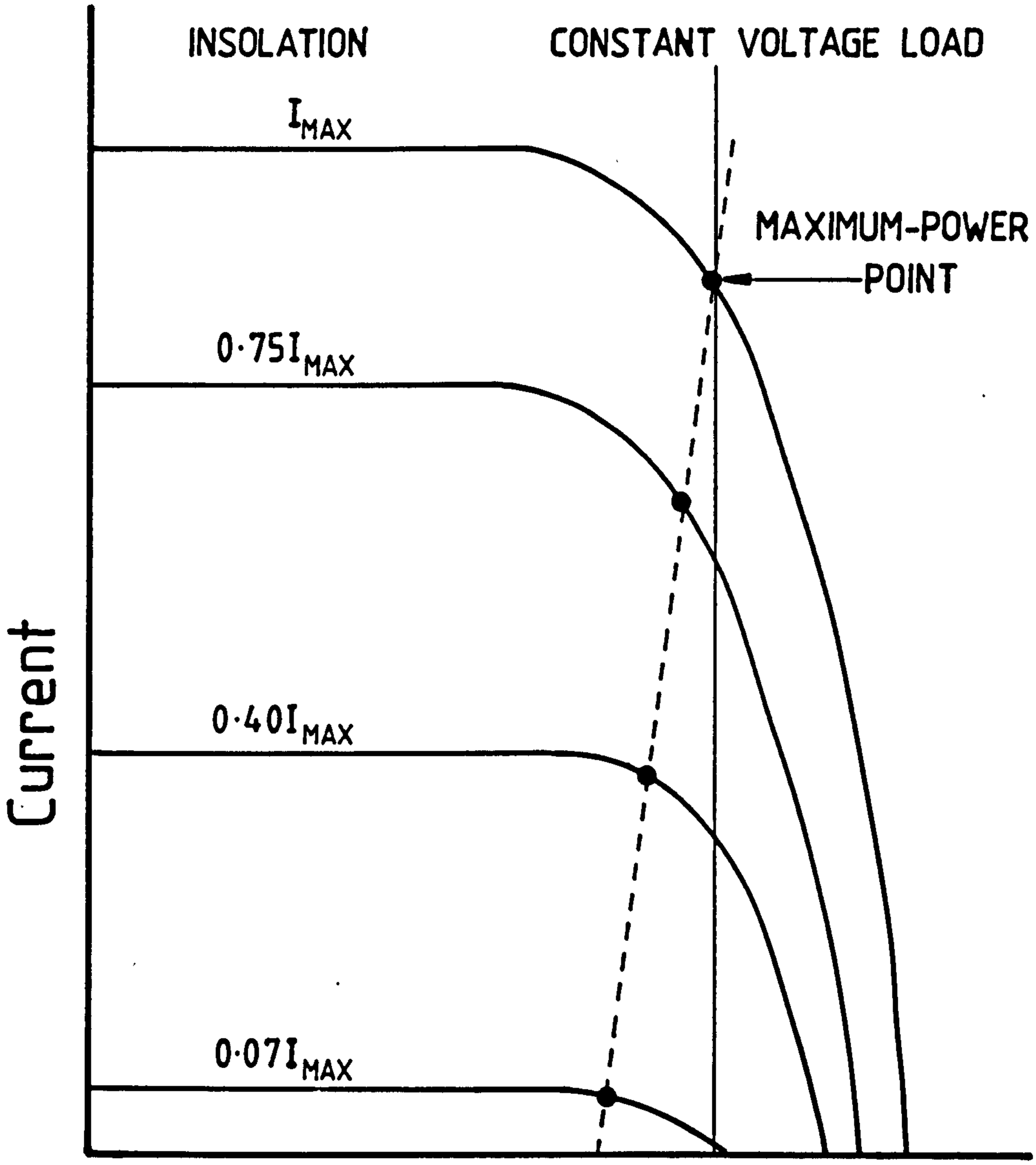

Fig 6.4 Typical I-V characteristics of a PV-array showing the variation of maximum-power-point in relation to the constant battery voltage

vapour compression refrigerator powered by PV-array through a battery) the assumption that the PV array always operates at the maximum-power-point would be justified.

Thus for the purpose of this analysis the efficiency of the PV array can be treated as a function of the array temperature only and can be represented, for this particular [2], but, typical flat plate silicon array, by

$$\eta_c = \eta_{c,ST} \times (1-0.004(T-T_{ST})) \qquad 6.1$$

where $\eta_{c,ST}$ is efficiency of the PV array at a standard temperature, T_{ST} (usually at 25°C) and T is the operating temperature of the array.

6.3.1.2 Determination of operating temperature of the array

Monocrystalline silicon PV arrays have a protective coating of glass on the top and bottom surfaces which are exposed to the ambient environment. Insolation on this glass layer is transmitted through it and absorbed by the array (except for a small portion which is reflected). Thus for the thermal analysis of the array, its surface, at its boundary with the environment, can be assigned the properties of glass. The following is assumed:

Reflectance of the array surface = 0.1

Emittance of the array surface = 0.9

inclination of the array = 30° with vertical

The efficiency of silicon PV arrays is of the order of 0.1, owing to reflective losses and to inactive areas between cells and where structural members are located. In the solar spectrum 26 percent of photons have energy less than 1.1 eV (the band gap for silicon) and will be reflected from silicon surface. The rest will be absorbed by silicon, part of which will be converted to electricity and the remaining will appear as heat rejected to atmosphere. If 20 percent of total area is considered as inactive then the energy balance sheet for a typical silicon array will be as follows:

total insolation falling on the array surface	= I
energy reflected from the glass surface	= 0.1xI
energy reaching silicon surface	= (1-0.2)x0.9xI
energy reflected from silicon surface	= 0.26x0.8x0.9xI
total unused energy	= 0.29xI
net energy available for convertion to electricity	= 0.71xI

This means that with increasing level of insolation there will be increasing heat dissipation as well. The heat transfer is only possible through higher than the ambient array temperature. Thus despite the array efficiency being independent of the insolation levels (see section 6.3.1.1) it has an indirect dependency on the insolation level.

This rise of array temperature reaches a dynamic equilibrium when the heat transfer rate from the array equals the energy rejected by

it. The heat transfer mechanism involved are convection and radiation. It is assumed further that the temperature of both faces of the array is equal and uniform all over the surface area.

The radiative heat transfer from the array is estimated by the following equation which applies to both sides.

$$Q_r = A.\sigma.\epsilon.(T_s^4 - T_a^4) \qquad 6.2$$

Natural convection heat transfer from the array surface is assumed. For the lower face of the array the relation used, given by Ozisik [3], to evaluate the heat transfer coefficient is

$$Nu = 0.56(Gr\ Pr\ \cos\theta)^{1/4} \qquad 6.3$$

For the upper surface of the array the relation used, given by Wong [4], is

$$Nu = 0.8(Gr\ Pr\ \cos\theta)^{1/4}\ [\cos 0/(1+(1+1/Pr^{0.5})^2)]^{1/4} \qquad 6.4$$

These relations are used to calculate the operating temperature of PV array and forms part of the final model discussed in section 6.3.1.6.

6.3.1.3 Performance of lead-acid batteries

Lead acid batteries, due to their widespread global availability, are considered suitable for this system. Energy is stored chemically

in a lead-acid battery, on passing charging current through it, by converting the lead sulphate on the battery electrodes into a mixture of pure lead, lead dioxide, and sulphuric acid. The reaction is reversed when the battery is discharged while being used.

The lead-acid batteries used in electric vehicles (i.e. milk floats and forklift trucks) are heavy duty batteries which can last upto 1500 deep discharge-charge cycles (i.e. discharged upto 50% of their capacity). Therefore this type is chosen for the proposed system. These batteries, as a part of a photovoltaic system, have shown a discharge-charge cycle efficiency of about 80 percent [5].

6.3.1.3 Energy efficiency of an inverter

An inverter is an electronic device which converts the dc electricity to ac electricity. This dc-to-ac conversion is necessary as a normal household refrigerator incorporates an ac-motor to drive the compressor. Brushless dc-motors are being substituted into the refrigerators produced for special recreational markets for use in boats, caravans etc, but these are not available widely or at competitive prices. Most of the PV refrigerators marketed employ 12 V dc-motors but the bulk of the household refrigerators are produced for 115/240 V ac use. Thus to cover the more general case of an ac-powered refrigerator an inverter is considered as part of the circuit.

The performance of an inverter depends on its size. The efficiency of the stand-alone inverters required by the system under consideration will be about 84% [6].

6.3.1.4 Performance of an ac induction motor

The small capacity compressors used in domestic refrigerators are designed to operate from single-phase power supplies. Domestic refrigerators employ a capillary tube as the expansion device. This makes it possible to use low starting torque induction motors. Such motors, due to their small size, are not very efficient. Efficiency of such a motor, which forms part of a hermetically sealed compressor unit was measured by Adell [7] to be equal to 57% Thus this figure was used as an average value in this analysis.

6.3.1.5 Performance of a vapour compression refrigerator

The aim of developing this model was to be able to size different components of a PV vapour compression unit; a vapour compression refrigerator is one of them. Thus a simple but accurate method was required. It was decided to use Carnot coefficient of performance as the basis to work out the actual COP of the refrigerator. As described by Gosney [8] the two performances can be related by the relation

$$COP_{vc} = R x \eta_{isen} x COP_{carnot} \qquad 6.5$$

where R is the efficiency of the refrigeration cycle related to the Carnot coefficient of performance calculated using refrigerant evaporation and condensation temperatures (T_e and T_c respectively) for low and high temperatures respectively. An approximate expression for the value of R for ammonia is given by Linge [9] (which is applicable to R-12 and R-22 as well [8]) in evaporation temperature range of -50 to 40°C. The expression for saturated liquid at expansion valve is

$$R = 1 - (t_c - t_e)/265 \qquad 6.6$$

If the condensed refrigerant is subcooled to t_u then R is multiplied by a factor

$$1 + (t_c - t_u)/250 \qquad 6.7$$

η_{isen} is the isentropic efficiency of the compressor which is often in the range 0.5 to 0.8. Due to the small size of the compressors used in refrigerators their mechanical efficiency is low and it needs to be taken into account as well. Thus the value of isentropic efficiency of compression (taken to be 0.9 [7]) is modified by mutiplying it with the mechanical efficiency (taken to be 0.8 [7]). The equation 6.5 can be written as

$$COP_{vc} = 0.72xRxCOP_{carnot} \qquad 6.8$$

Values of COP predicted by equation 6.8 were compared to those from the actual values published by Danfoss for their compressors. The

predicted values were slightly higher and the disagreement was within 10% of the actual values.

6.3.1.6 Construction and resolution of the model

The set of equations 6.1 to 6.8, developed in the previous sections, constitute the basis for the numerical model which was used to determine the parameters which could affect the size of the refrigerator and the PV array.

There are six input variables to the model, (a) the refrigeration capacity, q_{frig} (in watts), (b) the ice pack freezing load, q_{ice} (in watts), (c) the monthly-average insolation on the plane of the PV array, I, (d) the monthly-average ambient temperature, T_a, (e) the number of sunshine hours (monthly average), n, and (f) the nominal operating voltage of the compressor-motor assembly.

The final output of the model is the size of the PV array and the battery storage required for three days of continuous operation without solar input.

Some intermediate calculations are necessary to reach the final result. These involve the determination of array surface (operating) temperature, its efficiency, and the overall COP of the PV refrigeration system.

Strictly speaking the efficiencies of batteries, dc-to-ac inverters and motors are variable under varying operating conditions. But the variations being small, average values over the operating regime have been used for the purpose of sizing the system.

The product of array efficiency and the total insolation on the plane of array will give the amount of generated electricity. When this amount is subtracted from the net energy available for conversion to electricity, the energy rejected to the ambient, as heat, is obtained

$$Q_{rej} = (0.71 - \eta_c) x I \qquad 6.9$$

This rejected heat is dissipated to the ambient through a temperature gradient by convection and radiation. Equations 6.2 to 6.4 give the coefficient of heat transfer by radiation and convection.

A guess is made of the array surface temperature and its efficiency determined from equation 6.1. Heat transfered from the surface, through convection and radiation, is then found The amount is compared with the heat rejected found by applying equation 6.9. If the difference between the two values is greater than the required accuracy a new value of the surface temperature is assumed. The procedure is repeated until the two values of the rejected heat match to the required accuracy. When a satisfactory value of the array surface temperature is obtained its efficiency is determined by applying equation 6.1.

COP of the refrigerator is determined, next, by using equations 6.6 & 6.8 which is then multiplied by the efficiencies of the motor, the inverter, the battery and the PV-array to evaluate the overall coefficient of performance, $COP_{overall}$, of the PV refrigerator.

Dividing the required refrigeration capacity q_{frig} by the $COP_{overall}$ gives the required power rating of the PV array. This information along with the array efficiency determines the area of the array, sufficient to power the refrigerator during the day, according to relation

$$A_{array} = q_{frig}/COP_{overall}/I \qquad 6.10$$

Battery-storage is required to fulfil two duties;

(a) provide a three-days autonomy to the system in the absence of sun or under very low insolation conditions, and

(b) to meet the daily load after sunset.

The refrigeration capacity of q_{frig} (in Watts) involves a cooling load of q_{ice} (in Watts) for the ice-packs. If this load is taken off the refrigerator during the low or no insolation periods then the battery storage requirement can be reduced to a great extent. On the basis of this assumption the total energy, which will be drained in three days out of the batteries, will be

$$E_{drain,\ 3day} = (q_{frig} - q_{ice})/COP_{bat} x24x3 \quad \text{(in Wh)} \qquad 6.11$$

Where $COP_{bat} = COP_{vc} x \eta_m x \eta_i$. Assuming further that the battery system is of V volt nominal output then the drained capacity will be

$$C_{drain,\ 3day} = E_{drain,\ 3day}/V \qquad \text{(in Ah)} \quad 6.12$$

The charging current will be much higher for a deeply discharged battery. The higher current demand would inevitably increase the size of the array. On the other hand for reducing the charging current, battery capacity has to be increased. Thus there would exist an optimum balance between the array area and battery capacity which would be decided on the grounds of economics. For the purpose of this analysis a heavy duty battery mentioned in section 6.3.1.3 is considered. To keep the model simple it is assumed that the battery would be drained to 50% of its full capacity. Thus the total storage capacity of the battery will be

$$C_{store,\ 3day} = C_{drain,\ 3day}/(1 - 0.5) \qquad \text{(in Ah)} \quad 6.13$$

The amount of daily energy required after sunset will vary with the sunshine hours. If we assume a minimum of n hours of effective sunshine then for (24 - n) hours the battery will be drained. It has to meet a load of q_{frig} (in Watts) through this period. Thus the daily drained capacity of the batteries will be

$$C_{drain,\ daily} = q_{frig}/COP_{bat} x(24 - n)/V \qquad \text{(in Ah)} \quad 6.14$$

Again the 50 percent rule applies for maximum drain and therefore the total storage capacity the batteries to meet the daily drain will be

$$C_{store,\ daily} = C_{drain,\ daily}/(1 - 0.5) \qquad \text{(in Ah)} \quad 6.15$$

The PV array should meet the daily load of q_{frig} (in Watts) and top up the overnight drained battery capacity (assuming that the overnight drain is greater than the drain during 3 days of no or low insolation conditions) as well. Thus the array size determined by equation 6.10 needs modification to include the additional top-up load. This additional area is

$$A_{array,\ add} = C_{drain,\ daily} xV/(Ix\eta_c xn) \qquad 6.16$$

If the daily drain is less than the energy drain during three days of no- or low-insolation then the $A_{array,\ add}$ will be determined by the following equation

$$A_{array,\ add} = C_{drain,\ 3day} xV/(Ix\eta_c xn) \qquad 6.17$$

Thus the total array area required to meet the total system demand will be

$$A_{array,\ total} = A_{array} + A_{array,\ add} \qquad 6.18$$

6.3.2 Discussion of results

A the wind effects were not considered while calculating the heat transfer from the array, the model would predict a higher estimate of the array temperature. Thus the efficiency of the array ascertained through the application of this model would be pessimistic in absolute terms. Curves for variation in the PV-array

efficiency were plotted against the solar insolation for various ambient temperatures in fig 6.5. The relation between the efficiency and insolation was linear and the two were related by the expression

$$\eta_c = \eta_{c,ref} + 0.001(I_{ref} - I) \qquad 6.19$$

where $\eta_{c,ref}$ is the array efficiency at a reference insolation, I_{ref}. As the relation 6.19 is based on the relative difference thus the accuracy of the result would be same as that of the reference figures.

The relation between operating temperature and the ambient temperature turned out to be linear (see fig 6.6). Consequently the PV-array efficiency, which had a linear dependency on the operating temperature, would decline linearly with the rising insolation. Fig 6.5 confirmed that it was true.

In fig 6.7 the overall coefficient of performance of the total system is plotted against the ambient temperature for various insolations. It was evidently clear from the graph that the COP was highly sensitive to the ambient temperature and the variation in the insolation had a minimal effect (i.e. 0.074% decrease per 100 Wm^{-2} increase in insolation). Increase in ambient temperature increase the operating temperature of the array and decrease its efficiency. Likewise higher ambient temperatures result in higher condensation pressures which subsequently reduce the COP of the refrigerator.

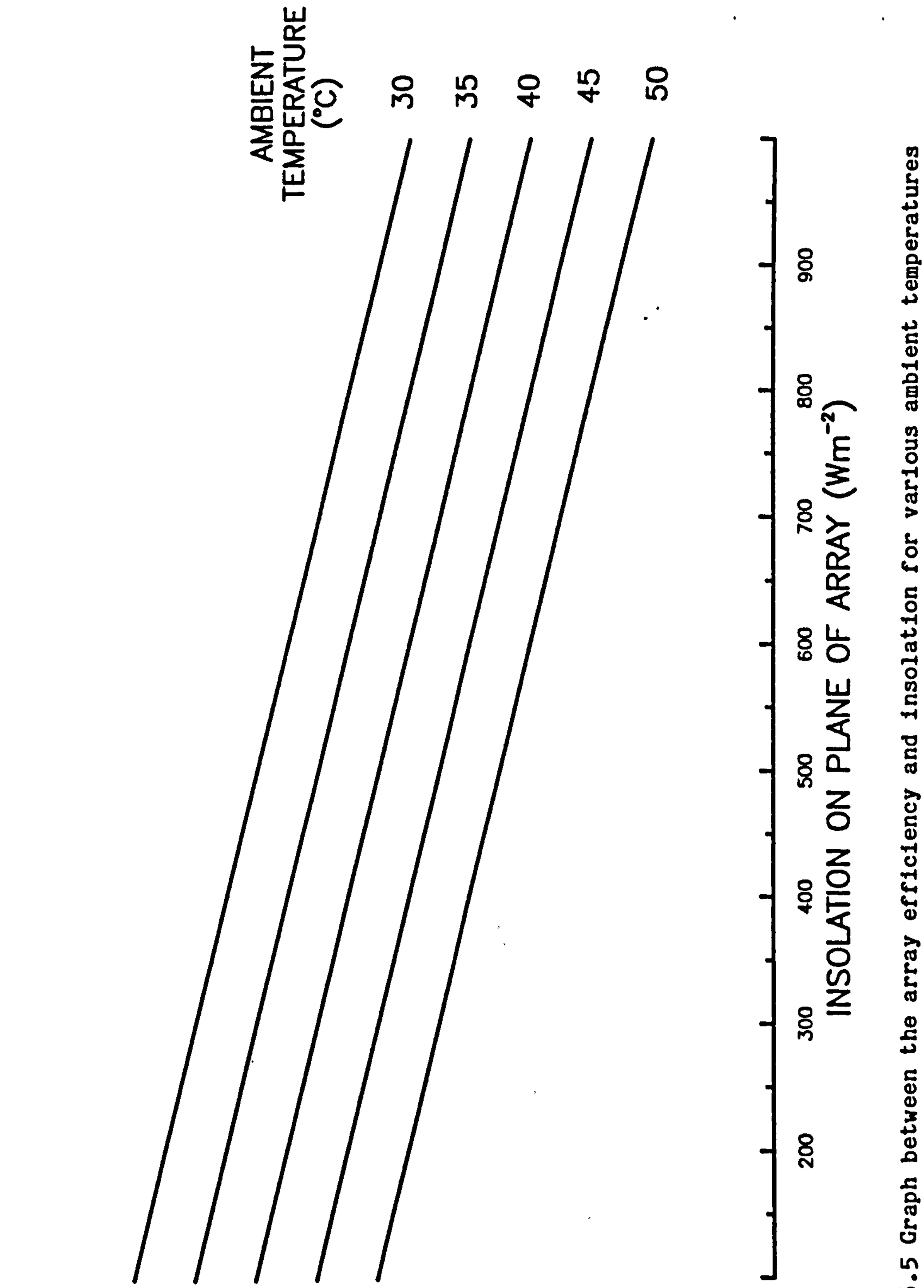

Fig 6.5 Graph between the array efficiency and insolation for various ambient temperatures

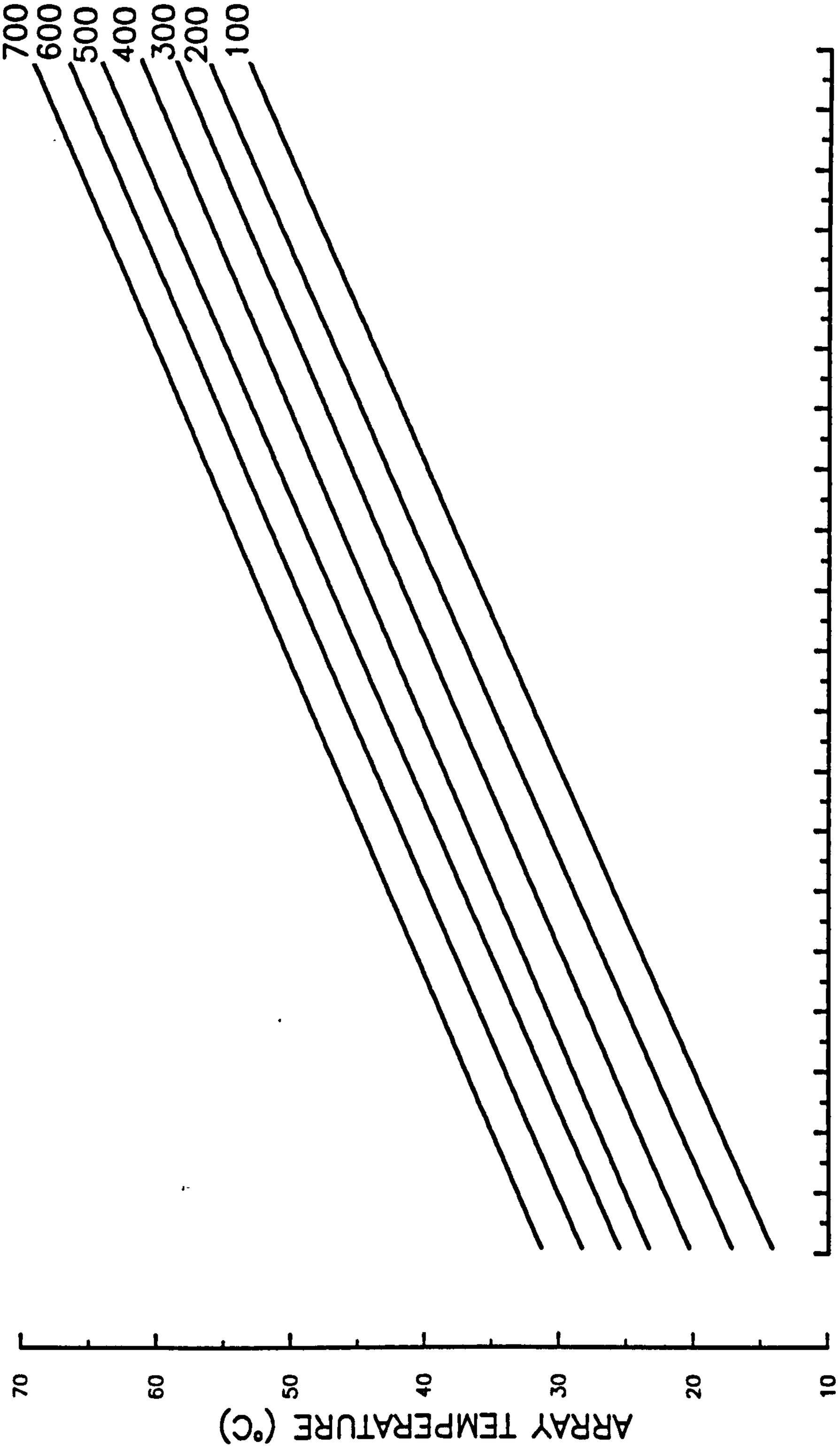

Fig 6.6 Graph showing the variation in array temperature corresponding to a change in ambient temperature for various insolations

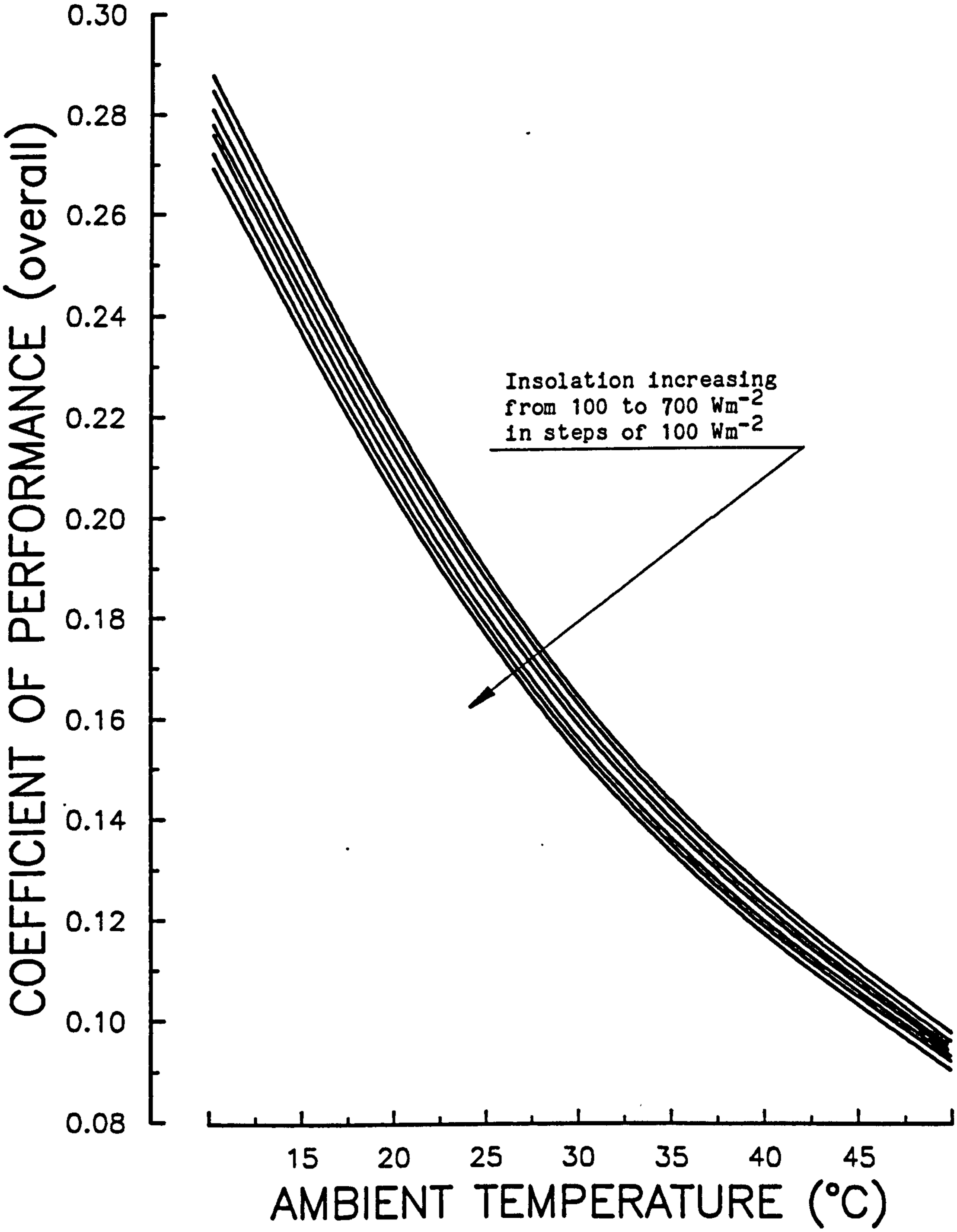

Fig 6.7 Variation in overall COP of PV-refrigerator with the change in ambient temperature at various insolations

As the overall COP is a product of component efficiencies, it can be made independent of ambient effects if both the array efficiency and the COP of the refrigerator can be made independent of it. This could be achieved through the use of a constant temperature cooling media (e.g. water) which would add more complexity to the system and add towards the cost. Thus it can be said in conclusion that there is no straightforward and simple solution to reduce the sensitivity of the overall COP to the changes in the ambient temperature.

The array area required to energize a PV-vapour compression refrigerator would depend primarily on its size, insolation conditions and the array efficiency. In fig 6.8 the array area required for a 100 watt refrigerator was plotted against the ambient temperature at various insolations and for 7 hours of average sunshine. There was an exponential decrease in the size of the array with the increase in insolation. While the effect of ambient temperature was quite pronouced at low insolations, it diminished at higher values of it. A similar trend was observed for varying sunshine hours, as could be seen in fig 6.9.

The battery capacity (storage) showed its dependence on the sunshine hours and the ambient temperature. The requirement diminished linearly with the increase in number of sunshine hours. The trend is depicted by fig 6.10 for the proposed 100 watt vaccine store. Fig 6.11 was drawn for a refrigerator of 110 W which had lesser insulation and so the environmental heat gains increased by 10

6-32

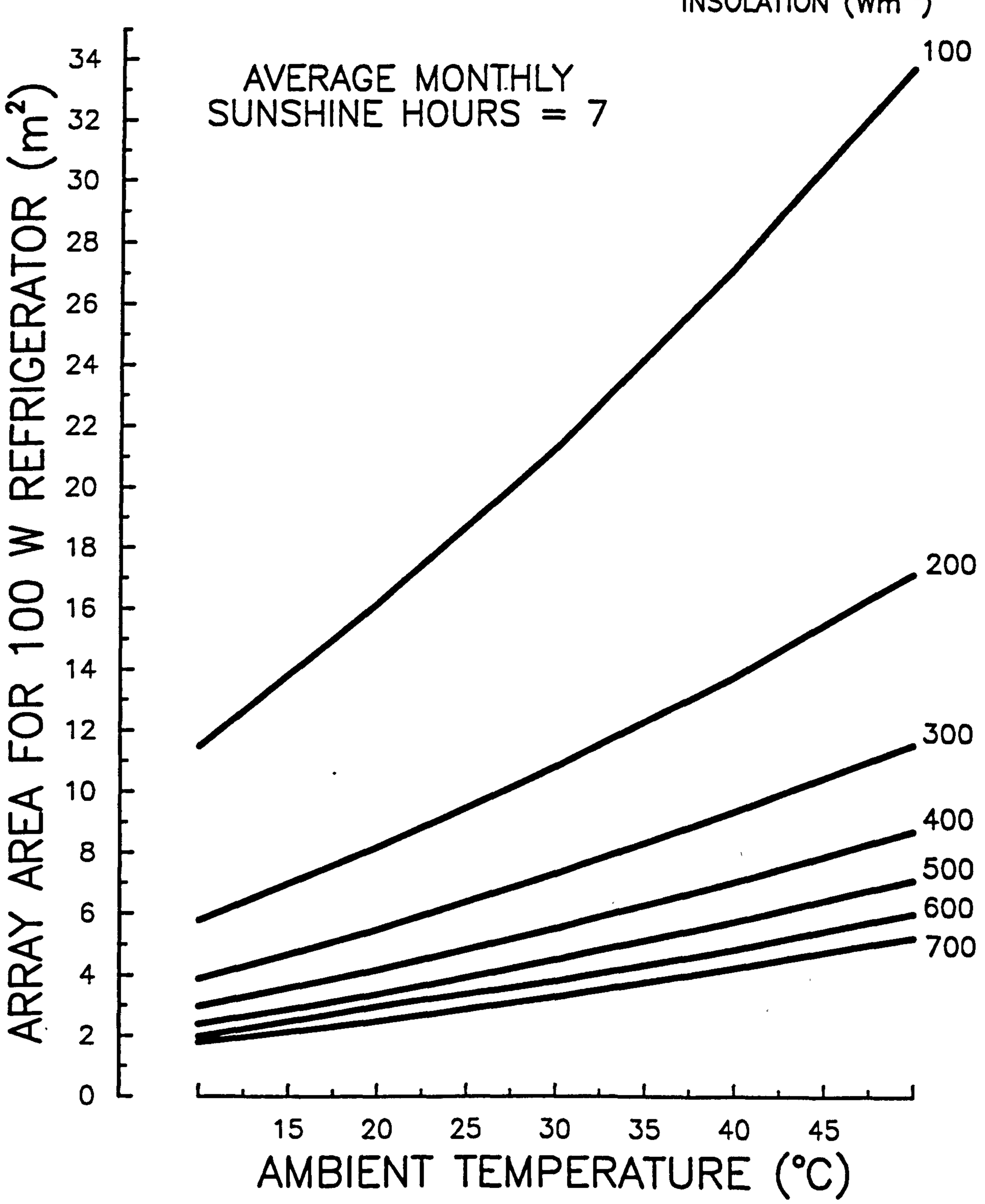

Fig 6.8 Graph of array area against ambient temperature under various insolation conditions

6-33

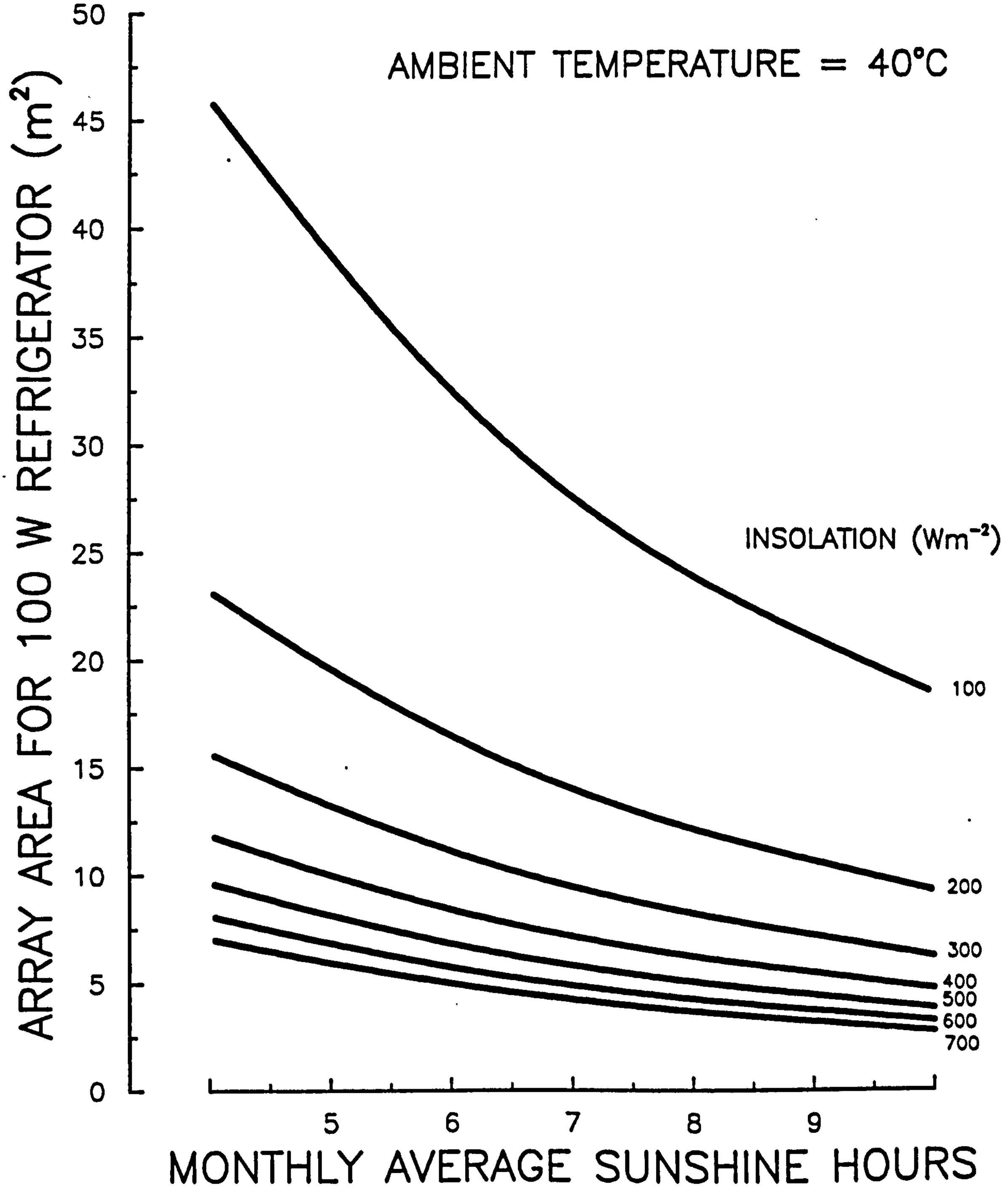

Fig 6.9 Variation in array area with change in sunshine hours for different insolation condition

watts. When the figures 6.10 and 6.11 were compared, it was observed that the required battery capacity decreased with the increase in sunshine hours upto six hours but further increase in the sunshine hour had not affected it.

The observation made in the previous paragraph can be explained by recalling the purpose of the battery storage. The storage was required to meet (a) the daily energy demand after sunset, which would decrease with the increase in the number of sunshine hours, and (b) the energy required to run the refrigerator, without ice packs, for 3 days in the absence of sunshine. With the increase in environmental heat gains the battery duty at (b), which was independent of the sunshine hours, was more than the diminishing daily demand for six or more hours of sunshine. This also highlighted the importance of insulation to reduce the environmental heat gains.

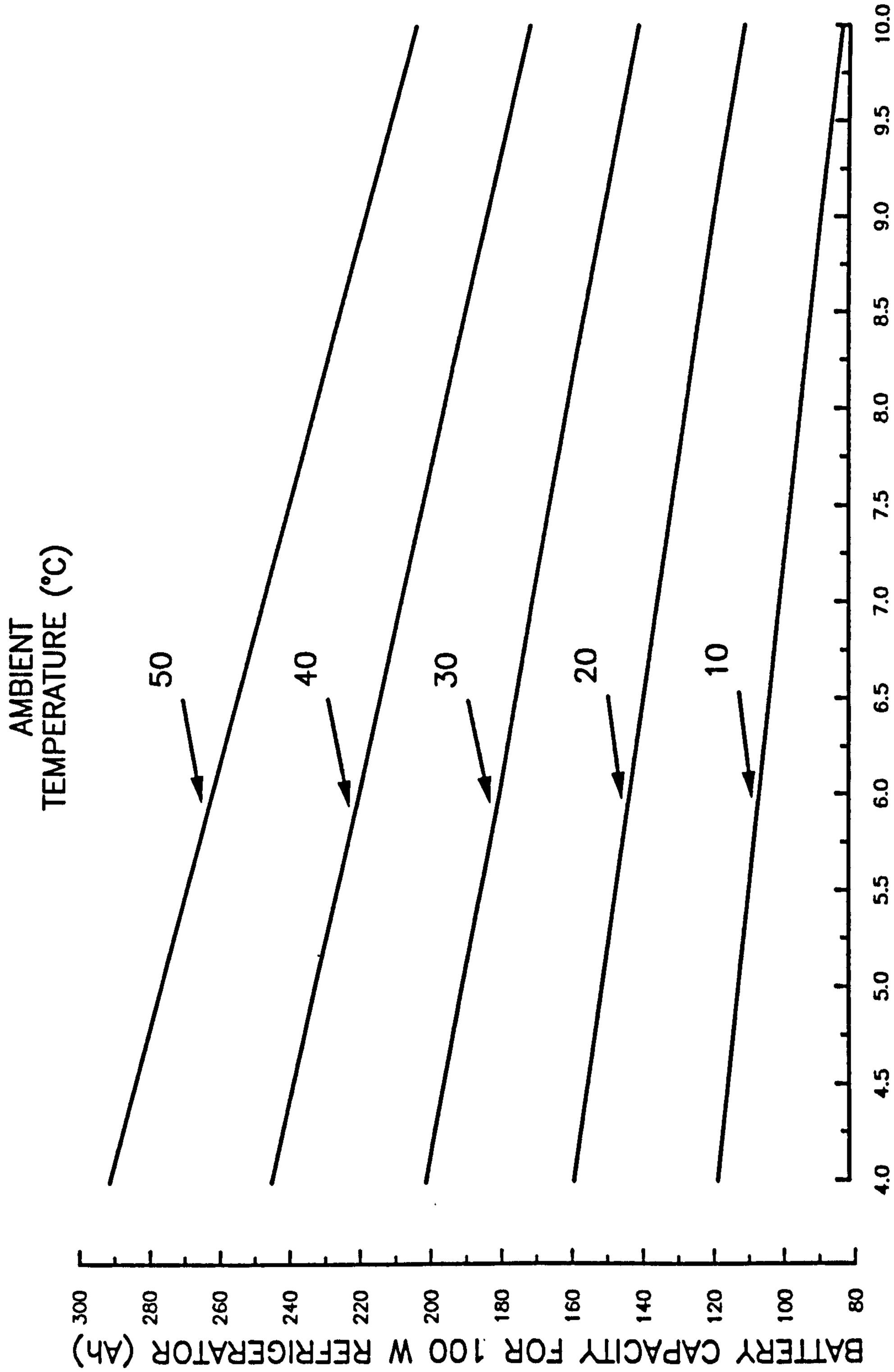

Fig 6.10 Battery capacity for a 100 watt refrigerator for varying conditions

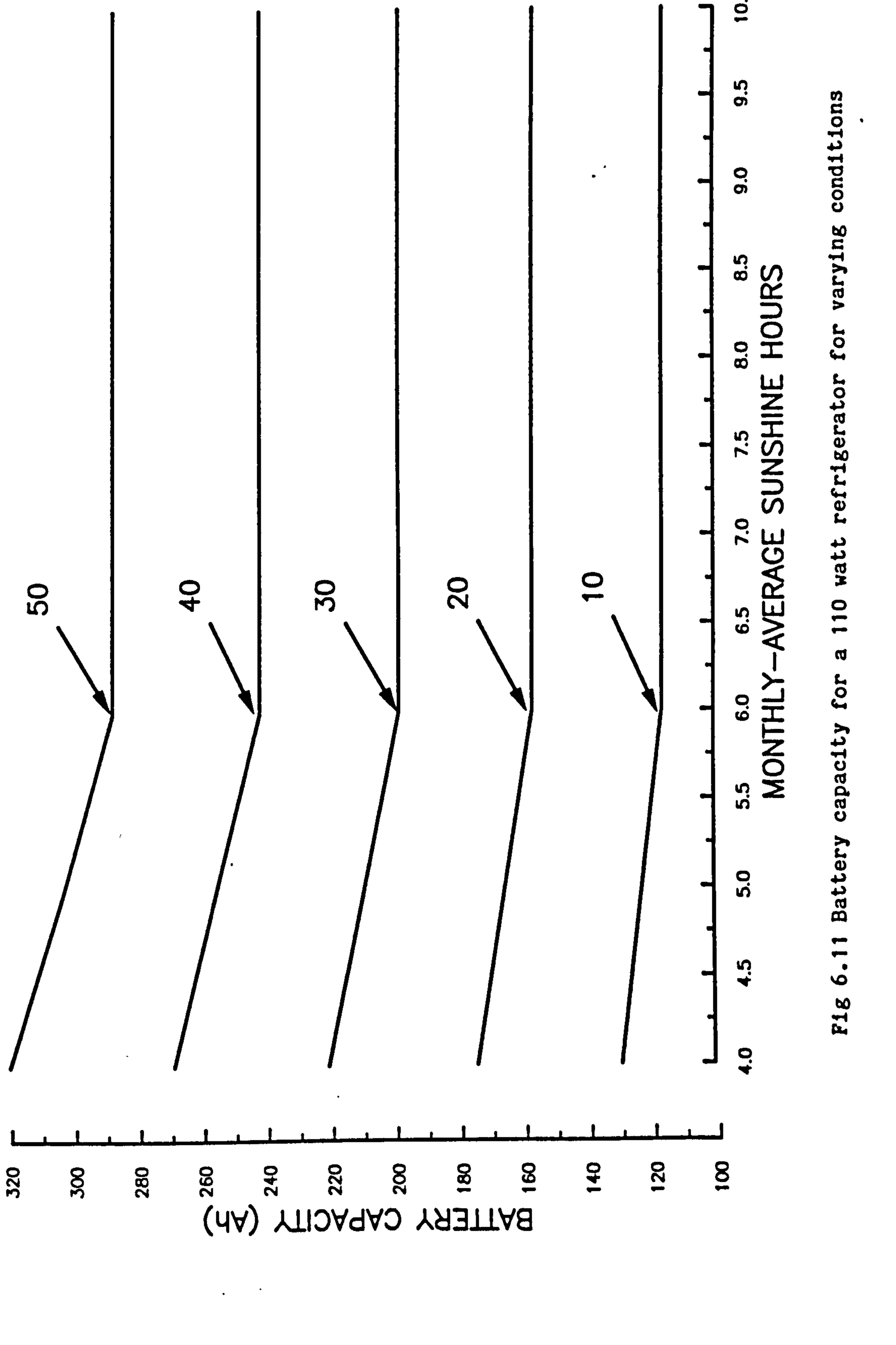

Fig 6.11 Battery capacity for a 110 watt refrigerator for varying conditions

6.3.3 Conclusions

The major conclusion drawn from the analysis were as follows:

(a) A smaller PV-array and battery storage would be required for the refrigeration system to be operated in the areas where the average insolation was high and the average sunshine hours were long (e.g. near the equator or in tropics).

(b) Increased thickness of insulation would reduce the required size of the PV-array and the battery storage which would subsequently lower the initial capital and running costs.

(c) The size of the array could be reduced further by employing more efficient solar cell (which would be expensive). Although its impact on the overall price of the system can only be appreciated after an economic analysis.

(d) The battery storage represent about 15% of the initial capital cost and incurs a recurring expenditure every 2-3 years. Alternative methods of energy storage (e.g. a cold storage) may reduce the cost of the system, making it more competitive.

This has so far been the only system which is being used by WHO to fulfil its EPI requirements. Its overall performance is very low which means large size PV-arrays but same is true of the thermal

refrigeration systems. It uses established technologies and mass produced equipment. But silicon arrays are inherently expensive. The electronic regulation devices and dc-to-ac inverters add further to the total cost and introduce unreliability in the system. Many researchers have reported failure of these electronic devices (e.g [7]). Cooling of these devices at high ambient temperatures involve additional energy consumption for cooling fans which subsequently increase the size of the array and the battery storage and increase the initial capital and running costs.

There has been a considerable reduction in the price of these units over the past few years. For example the price of a PV refrigerator in 1985 was more than £4500 [10] and now in 1989 these units can be purchased for about £3000 [11] i.e. a reduction of 33% over a period of four years. But there remains a major hinderance in the way of proliferation of these systems into third world countries where these are most needed. The hinderance is the requirement of high technology for the production of PV-arrays and electronic control and regulation units.

Summarizing, it can be concluded that, though, this system is acceptable on technical grounds, it lacks ground for transfer of technology to the third world countries. These countries would always find it difficult to accept a product which would mean a long term foreign currency drain. Thus alternative systems need to be developed which can be manufactured with the kind of basic technological skills and materials available in the developing countries.

PART II

Solar 'Electrolux' refrigerator

6.4 Solar-thermal 'Electrolux' refrigerator

Both the standard 'Electrolux' refrigerators and flat plate solar collectors are mass produced. It is an attractive option, as pointed out earlier in chapter 5, to manufacture solar operated vaccine stores from these mass produced (and therefore cheap) products. In this section the technical feasibility of this option will be studied.

A complete analytical analysis of a diffusion type 'Electrolux' absorption refrigerator is possible though quite complicated and involved [11]. The aim of the analysis which will be carried out in this section is to determine whether a commercially available unit can be driven by the thermal energy collected by a solar collector without any major design changes. This can be ascertained by a simpler approach using pressure enthalpy diagram for the water ammonia pair.

There are two distinct cycles working in the diffusion absorption refrigerator; the ammonia-water cycle and the ammonia-hydrogen cycle. The latter is limited to the evaporator and absorber parts. Our analysis is related to the solar operation of the refrigerator. It will, therefore, involve the quality of thermal energy available, i.e. its temperature, and the ambient temperature. These parameters will affect, directly, the working and performance of generator, absorber, and condenser and consequently the performance of evaporator. The analysis of ammonia-water circuit will be performed with the help of pressure-enthalpy (logP-h) diagram developed by

Backstrom [13] for such a system. It is a diagram describing the variation of enthalpy of liquid (h) and of vapours (h") against logarithm of pressure for various concentrations of vapours (k") and solution (k). There are lines of constant temperature as well drawn on the diagram.

In a previous investigation [14,10], here at Cranfield, a standard Electrolux refrigerator was run by the heat energy collected by Thermomax evacuated tubular collectors (see fig 6.12). The results were reported as encouraging although the water inside the evaporator box never attained a sub-zero temperature even under an ambient temperature of 30°C. The standard and modified systems used in the above mentioned investigation is analyzed in the next section.

Fig 6.12 Photograph showing the Electrolux absorption refrigerator working with Thermomax evacuated tube heat pipe collectors [10]

6.4.1. Analysis of the standard Electrolux refrigerator

The standard refrigerator (i.e. as supplied by the manufacturer) had a strong solution concentration of 35% and a hydrogen pressure of 25 bars. The manufacturer quoted a COP was 0.23. The analysis of the system is performed with the help of a logP-h diagram.

Allowing a 10°C temperature difference at the absorber and condenser and assuming an ambient temperature of 43°C (as specified by WHO [15]) the analysis can be started by marking the points on the logP-h diagram as shown in fig 6.13.

A concentration of 35% and a temperature of 53°C gives the absorber state marked by point A on the diagram. The partial pressure of ammonia in the absorber can be read against this point which is 3.5 bars. The partial pressure of ammonia in the evaporator must be 1 bar higher than this [16] to allow a reasonable rate of circulation of ammonia-hydrogen mixture from evaporator to the absorber. Thus the point E on the pure ammonia line at a pressure of 4.5 bars will give the maximum evaporation temperature in the evaporator.

The evaporator in the Electrolux refrigerator is an integerated evaporator-cum-heat exchanger (gas-to-gas). It is a double tube in which the cold hydrogen is enriched with evaporating ammonia, while flowing towards the absorber through the annulus, and the warm hydrogen -weak in ammonia- flows from the absorber, in the centre tube, towards the evaporator. This way the heat is exchanged between the hot and cold streams of hydrogen. As the concentration of

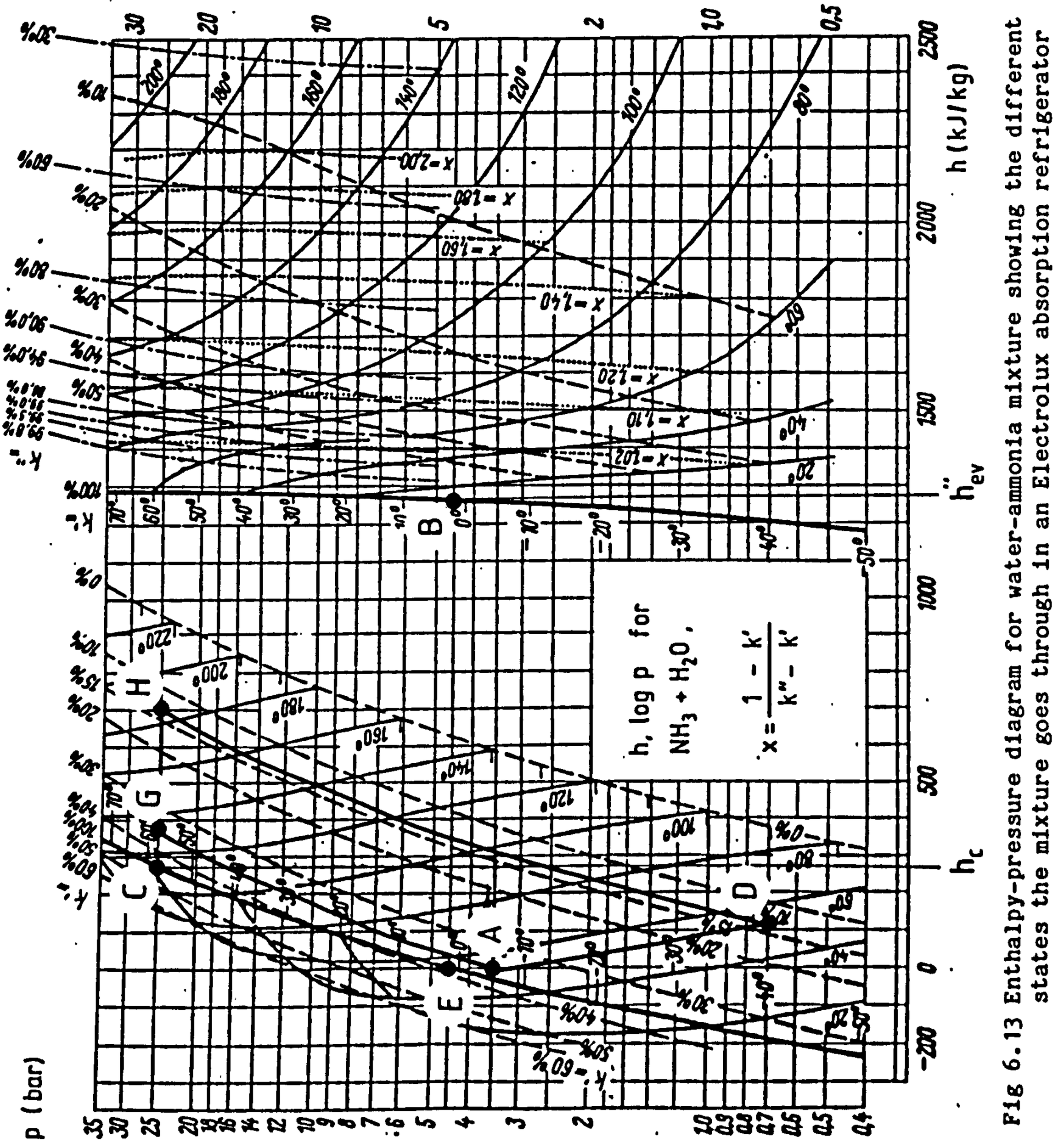

Fig 6.13 Enthalpy-pressure diagram for water-ammonia mixture showing the different states the mixture goes through in an Electrolux absorption refrigerator

ammonia in hydrogen gas increases as the mixture flows along the evaporator, the temperature distribution along it varies continuously. Under the assumed conditions maximum evaporation temperature at the exit of evaporator will be 1°C.

The total pressure of system is 25 bars, at which the saturation pressure of ammonia is 58°C. Therefore under 43°C ambient temperature the condenser will perform properly. Point C on the pure ammonia line represent this state. The point G, marked by 35% concentration and the total pressure of 25 bars, gives the minimum generation temperature of 135°C. This is the temperature below which no generation is possible and so the refrigerator will not work.

At this point it is clear that the refrigerator with the standard specifications is not suitable for solar energy operation as it demands a generator temperature of more than 130°C which cannot be achieved with simple flat plate collectors. Hence the system needs modification so as to lower its generation temperature. Before considering the required modifications, the expected cooling capacity and the bubble pump circulation ratio in standard configuration will be, however, calculated.

The maximum generator temperature measured [14,10] on the standard model was 186°C. The point H on the intersection of total pressure line and 186°C temperature line gives a 13% concentration of the weak solution. The weak solution concentration and the absorption temperature of 53°C then defines the state of solution at the entry to the absorber. This state is marked by point D in fig 6.13 which

corresponds to a partial pressure of 0.7 bar.

The flow of weak solution from the generator to the absorber per kilogram of ammonia is given by [13]

$$Y = (1 - k_r)/(k_r - k_w)$$

$$= (1 - 0.35)/(0.35 - 0.13) = 2.95 \text{ kg/kg of } NH_3$$

The corresponding amount of rich solution will be (Y + 1) i.e 3.95 kg per kg of ammonia generated. Thus the bubble pump in the standard refrigerator will at the most circulate 3.95 kg of rich solution per kg of ammonia generated.

Finally a calculation of refrigeration effect can be made. The enthalpy of vapours emerging from the evaporator is determined by the point B on the vapour side corresponding to point E (see fig 6.13). Thus the refrigeration effect per kg of ammonia generated is equal to enthalpy difference between points B and C. Because of the hydrogen circulation the useful refrigeration effect is reduced by [13]

$$Q_{gas} = \frac{(1 - v_{rg})(28.7 + 9xv_{wg})}{17(v_{rg} - v_{wg})} x\Delta T \quad kJ/kg \quad NH_3 \qquad 6.19$$

The ammonia vapours have to diffuse through hydrogen atmosphere in the evaporator and absorber. Thus the ammonia-hydrogen mixture in the evaporator is never saturated with ammonia and as such its partial pressure should be reduced in the rich gas mixture. Similarly ammonia cannot be washed out to the mixture to the partial

pressure of weak solution in the absorber and so the partial pressure of ammonia in the weak gas mixture should be increased.

After consultation with Green [16] the value for the difference in partial pressure was assumed as 0.2 bar. Thus the partial pressures of rich and weak ammonia-hydrogen gas mixture are

$$p_{rg} = 4.7 - 0.2 = 4.5 \text{ bar}$$

$$p_{wg} = 0.7 + 0.2 = 0.9 \text{ bar}$$

The corresponding volumetric concentrations are

$$v_{rg} = p_{rg}/p = 4.5/25 = 0.18$$

$$v_{wg} = p_{wg}/p = 0.9/25 = 0.036$$

Thus the cooling lost due to gas circulation with an assumed temperature difference, across the two streams, of 10°C is

$$Q_{gas} = (1 - 0.18)x(28.7 + 9x0.036)/17/(0.18 - 0.036)x10$$

$$= 97.2 \text{ kJ/kg } NH_3$$

Thus the net refrigeration effect will be

$$Q_{ref} = h''_{ev} - h_{con} - Q_{gas}$$

$$= 1270 - 270 - 97.2 = 902.8 \text{ kJ/kg } NH_3$$

6.4.2 Analysis of modified Electrolux refrigerator

In the research previously conducted at Cranfield [14,10] the concentration and pressure of the system was changed to 55% and 18 bars in order to lower the generator temperature. The Thermomax evacuated tube heat pipe collector used in the research could deliver heat at a maximum temperature of 140°C [14]. Allowing a total temperature difference across the heat exchanger and the thermosyphon of 15°C the maximum generation temperature could be 125°C.

Assuming the 43°C ambient conditions the pressure in the absorber will be 9 bars. This implies that the maximum evaporation pressure will be 10.2 bar which correspond to a temperature of 20°C. At maximum pressure of 18 bars ammonia will condense at 45°C. This implies that under an ambient of 43°C, and hence a condensation temperature of 53°C the operating pressure of the refrigerator will rise to 22 bars. Therefore at maximum generation temperature of 125°C the concentration of the weak solution will be about 36%.

The duty of the bubble pump can now be calculated

$$Y = (1 - 0.55)/(0.55 - 0.36) = 2.37 \text{ kg/kg of } NH_3$$

or 3.37 kg of strong solution per kg of ammonia desorbed. This is lower than what it was doing in a standard configuration but is compatable with the lower operating temperature.

The partial pressure of ammonia in the weak solution at the entry to the absorber will be around 0.7 bars which indicate that the partial pressure of ammonia in the weak ammonia-hydrogen gas entering the evaporator will be 0.9 bars. This gives a minimum temperature of -35°C at the start of evaporation gradually increasing to 20°C at the exit from the evaporator. Assuming the temperature distribution along the evaporator to be linear, the temperature of more than a third of the evaporator length is above 0°C. This will seriously reduce its capacity.

As the cabinet temperature is to be maintained below 8°C the highest evaporation temperature should not be above 0°C. The partial pressure of ammonia at 0°C is 4.3 bars. The partial pressure at the evaporator exit was calculated as 10.2 bars. This means that the amount of ammonia which evaporates at or below 0°C is only 0.42 (i.e. 4.3/10.2 = 0.42) of that available after condensation. The effective refrigeration effect can thus be calculated as

$$h_{ev} = 1270 \text{ kJ/kg } NH_3$$

$$h_{con} = 250 \text{ kJ/kg } NH_3$$

$$Q_{gas} = 21.7 \text{ kJ/kg } NH_3$$

and $$Q_{ref} = 0.42x(1270 - 250) - 21.7 = 406.7 \text{ kJ/kg } NH_3$$

This is some 44.8% of the value which the standard refrigerator produced. Thus it can be said that the modifications carried out are not suited to its optimum operation under envisaged conditions.

6.4.3. Modified system for optimum operation with solar input

For optimum operation of the refrigerator all the condensed ammonia should evaporate completely below 0°C. This means that rich mixture in the absorber cannot have a partial pressure of more than 3.1 bars. Thus without improving heat transfer characteristics of the absorber the maximum concentration at absorption temperature of 53°C will be 33%. The minimum generation temperature at a total pressure of 22 bars is around 130°C. This clearly means that a higher concentration is to be allowed in the absorber.

Keeping the higher evaporation temperature as 0°C, the only way to raise the concentration of rich solution is to lower the absorption temperature. By increasing the heat transfer area by the use of fins on the absorber surface, absorption temperature can be reduced to 5°C above ambient i.e. 48°C. A maximum concentration of 36% will then be possible.

For a 10% reduction in the concentration of rich solution at 125°C, the system pressure cannot exceed 20 bars. This imposes a limit on the maximum condensation temperature of 49°C. This would again involve improving the heat-transfer design of the condenser.

Now the bubble pump duty can be calculated. The amount of weak solution circulated per kg of ammonia will be

$$Y = (1 - 0.36)/(0.36 - 0.32.4) = 18.82$$

which gives a rich solution circulation of 19.82 kg/kg NH_3. This is about five times what the pump was circulating under standard refrigerator configuration. The effect of change in operating temperature and tube diameter on the performance of a bubble pump can be studied from Cattaneo's [17] experiments presented in appendix D. It is clear from his work that at reduced operating temperature a five times higher circulation is not possible unless the design of the bubble pump is radically changed.

6.4.4 Conclusion

It can, thus, be concluded that optimum operation of a commercially available refrigerator with solar input at 140°C is not possible without major modification to its circuit. Designing and production of a completely new system of enormous complexity for such a limited market is not economically feasible.

A recent study by Gutierrez [18] substantiates the observations made above. In this study a 250 litre capacity SERVEL brand refrigerator was used as a prototype. A schematic view of the prototype is shown in fig 6.14. The high temperature flat plate collector replaced the generator. A larger heat exchanger and a new bubble pump was installed to cope with larger circulation rate of the weak solution.

He reported that freezing temperatures could not be produced under ambient temperatures of greater than 28°C. Below 28°C ambient the thermodynamic COP of the refrigerator was 0.11 and solar collector efficiency was 23%, giving an overall COP of 0.0253.

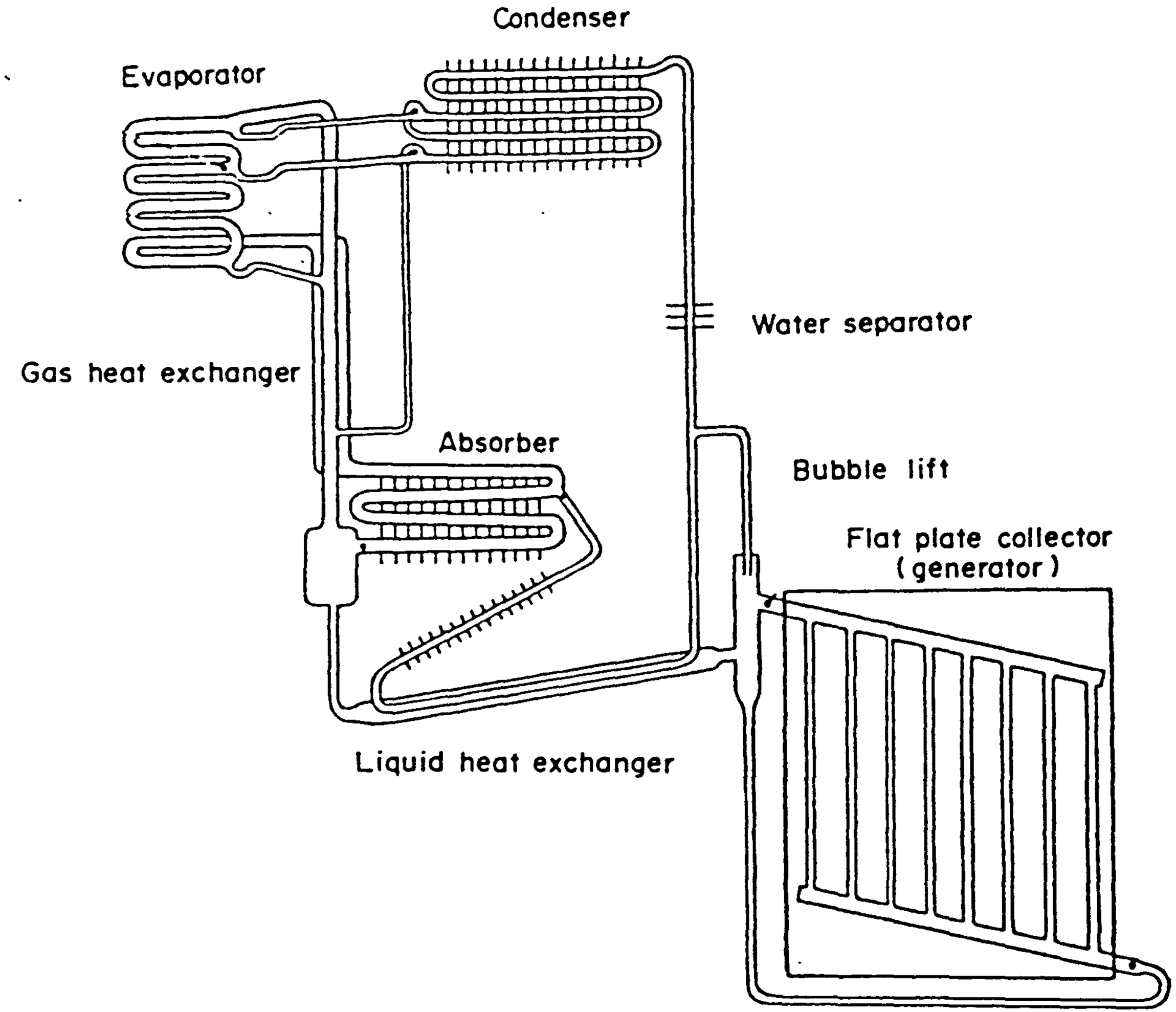

Fig 6.14 Schematic of a modified SERVEL brand refrigerator with trapezoidal collector

Continuous absorption refrigerators can produce cooling while the heat is supplied to the generator. Thus for the period when there is no insolation, either a heat storage or a cold storage would have to be provided. In either case it would be a massive store. The heat storage would have to maintain a temperature above the generation temperature. This would result into a very large and inefficient solar collector . In the case of a cold storage the refrigerator would have to be oversized by a factor of upto 4.

Summarizing, it can be concluded, on the basis of these technical limitations, that it is not possible to construct a solar thermal absorption refrigerator by using "off-the-shelf" mass-produced components.

PART III

Solar intermittent vapour sorption refrigerators

6.5 Solar-thermal intermittent solid sorption refrigerator

In chapter 5 it was noted that intermittent solid sorption refrigerators were simple and rugged. Sun being a diurnal source of energy is well compatible with their intermittent operation. Therefore these have the potential to be a better option. It was further concluded that activated carbon, calcium chloride, and zeolite were good sorbents whereas ammonia and methanol were suggested to be good refrigerants for the sorbents. In this section, firstly, performance of these different sorption pairs will be determined and compared to choose the best. Then the overall performance of the system using the best pair will be ascertained and compared with the other options.

6.5.1 Suitability criterion for a refrigerant

In the context of solar stimulated sorption refrigerators the thermodynamic cycle temperatures are very important. For a specific application the evaporation temperature, T_e, the condensation temperature, T_c, and the sorption temperature, T_a are known. The maximum cycle temperature is limited by the type of solar energy collection device, which for a flat plate collector is 120°C. A sorption refrigeration cycle on a Clapeyron diagram is shown in fig 6.15. The chosen refrigerant defines the saturation line, while the high and the low concentration lines represent the equilibrium of the refrigerant in the sorbed state. The required evaporation temperature fixes the pressure, P_e, for the chosen refrigerant and the sorption temperature, subsequently, marks the point 1 on the

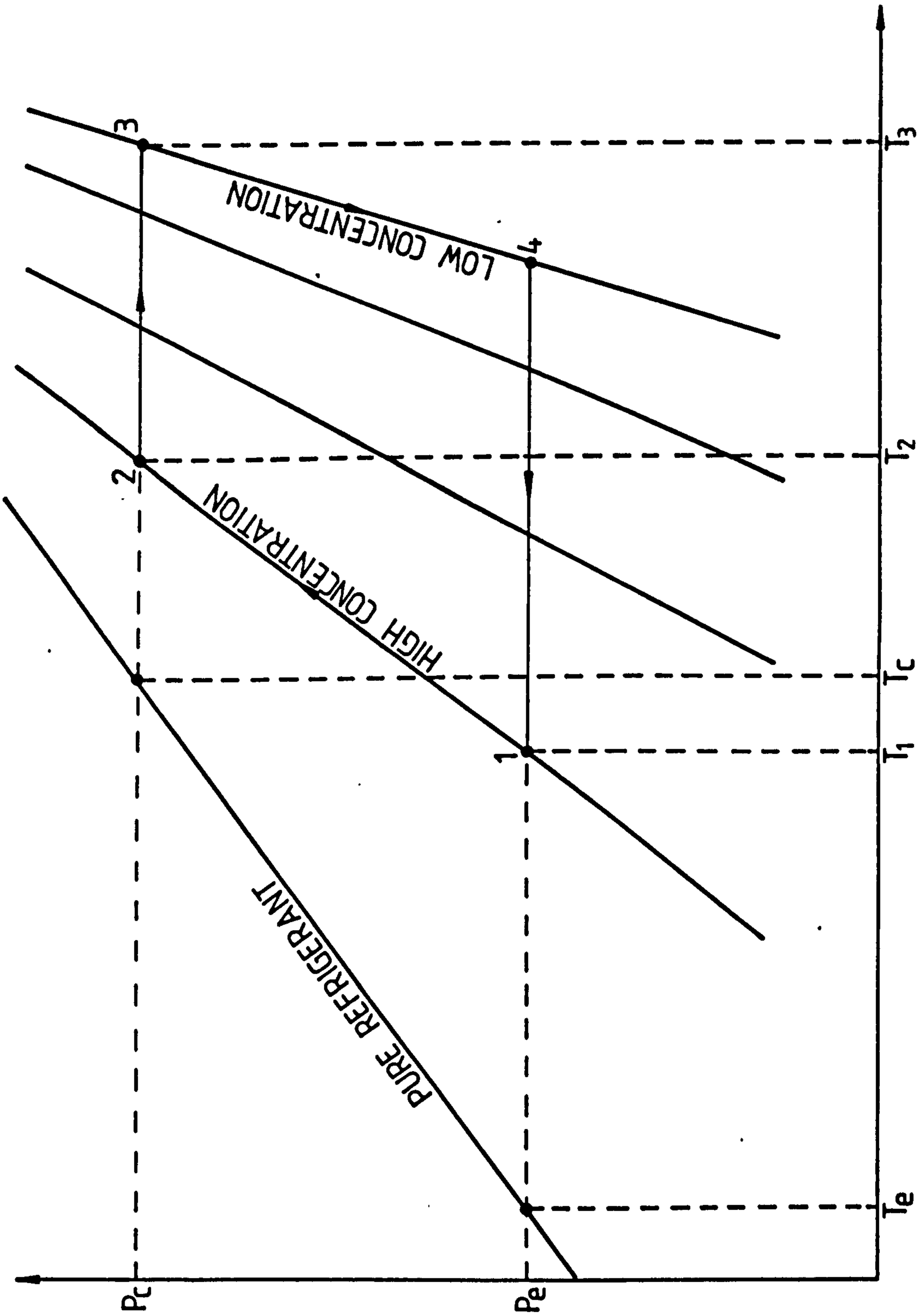

Fig 6.15 A sorption refrigeration cycle represented on a Clapeyron diagram

high concentration line. The point 2, which gives the minimum generation temperature, is controlled by the condensation temperature.

Assuming the refrigerant vapours behave as an ideal gas, the change in Gibbs free energy of the adsorbed molecule at temperature T and pressure p, with reference to its free saturation state at the same temperature, is given by

$$\Delta G = RT\ln[p/p_s(T)] \qquad 6.20$$

which, after Dubinin [19], is equal in magnitude to the molar adsorption work, D. The adsorption equilibrium is defined by the D-A equation (which is equally applicable to bivariant absorption equilibrium)

$$m = m_0 \exp[D/E]^n \qquad 6.21$$

The characteristic adsorption energy, E, is constant for a particular adsorption pair, which implies a constant value of D for a constant concentration m. Thus along an isostere the value of ΔG will be constant, e.g. along the high concentration isostere

$$\Delta G = RT_a\ln[p_e/ps(T_a)] = RT_2\ln[p_c/p_s(T_2)] \qquad 6.22$$

Expressing the evaporation and condensation pressures in terms of respective temperatures and rearranging equation 6.22 yields

$$T_2 = T_a \frac{\ln[p_s(T_e)/p_s(T_a)]}{\ln[p_s(T_c)/p_s(T_2)]} \qquad 6.23$$

Thus the above equation 6.23 provides one with a method to determine the minimum generation temperature, T_2, when one can define the function $p_s(T)$, i.e. selects the refrigerant. It is further evident from equation 6.23 that for a specific operating environment, i.e. a known evaporation, sorption and condensation temperature, the required minimum generation temperature is only a function of the refrigerant and is independent of the sorbent. This is a very important, rather overriding, point with regard to the selection of a refrigerant for a sorption cycle when the maximum cycle temperature is restricted (such as in solar operated refrigerators). This lays a new foundation for the selection of refrigerants to be used in solar operated (or when the maximum cycle temperature is limited) vapour sorption refrigerators.

Thus, knowing the refrigerator's operating temperatures and the maximum temperature achievable in the solar energy collection device, one can ascertain, by applying equation 6.23, the suitability of the chosen refrigerant for the envisaged application. In the next section, this new found basis for the suitability of a refrigerant was applied to some, otherwise suitable, refrigerants to ascertain if those could be used in a solar operated vapour sorption refrigeration cycle.

6.5.2 Evaluation of refrigerants

The proposal being considered in this report is the design of solar operated vaccine store conforming to the WHO specifications (see appendix B). This would mean a day time temperature of 43°C and a night time temperature of 32°C. Therefore in an air-cooled condenser and sorber the condensation and sorption temperatures would be 53 and 43°C respectively. To freeze the ice-packs the evaporation temperature should be at least -10°C.

It was concluded in chapter 5 that methanol and ammonia are good refrigerants for sorption cycles. Using the suitability criterion, developed in the previous section, charts for methanol and ammonia (shown in fig 6.16 and 6.17 respectively) were prepared which depict the variation of minimum generation temperature under varying sorption and condensation temperatures for evaporation taking place at -10°C.

In an intermittent sorption refrigerator, performing under the WHO specified (discussed above, and see appendix B) operating conditions, the minimum generation temperature, when methanol or ammonia is the refrigerant, is 124.6 or 118.6°C respectively. This makes it very clear that any sorption refrigerator with air-cooled condenser and absorber using methanol or ammonia as refrigerant cannot operate, under WHO specified conditions, with a flat plate collector (operating temperature in a flat plate collector is limited to 120°C).

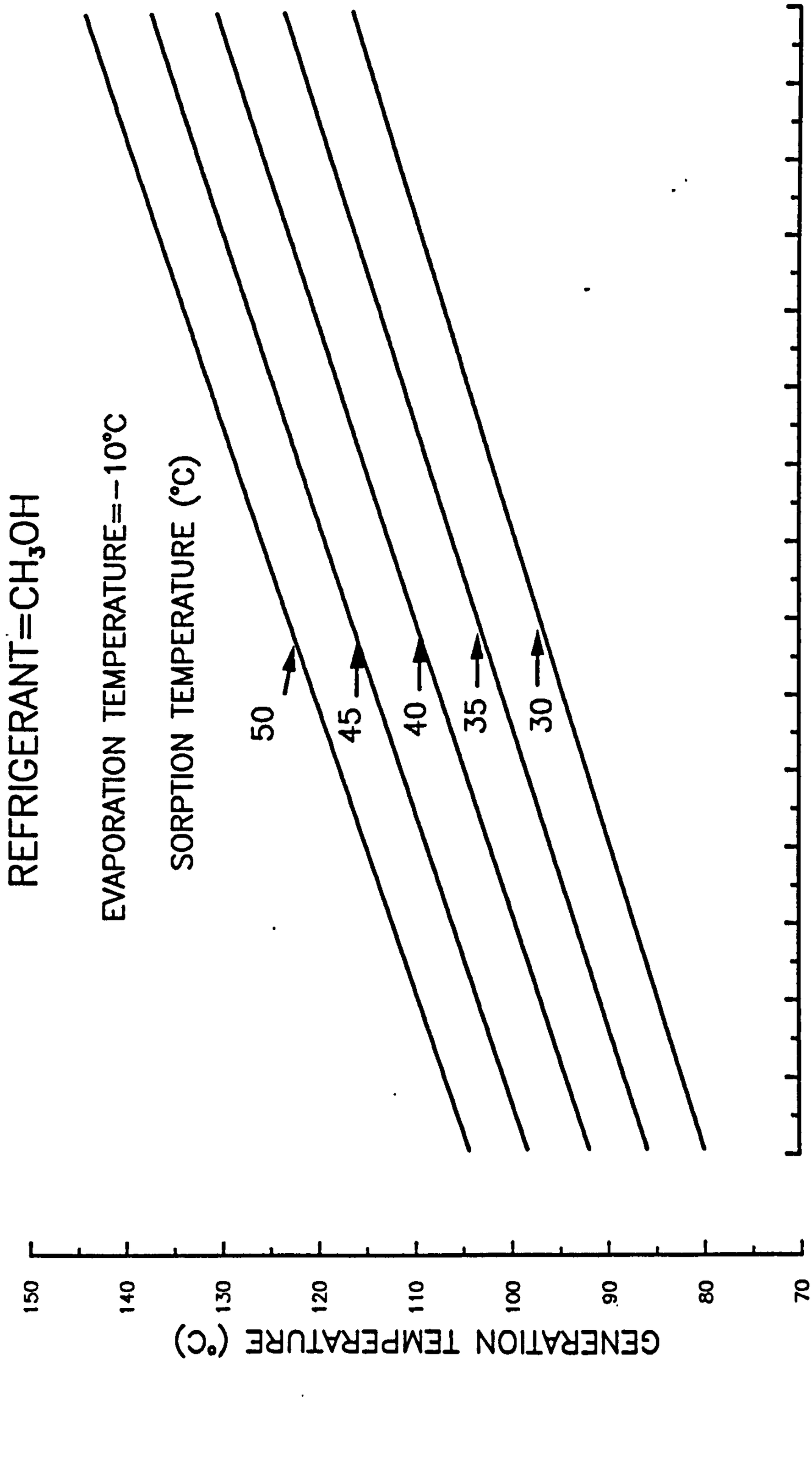

Fig 6.16 Graph showing the variation of generation temperature of methanol in an adsorption refrigeration cycle

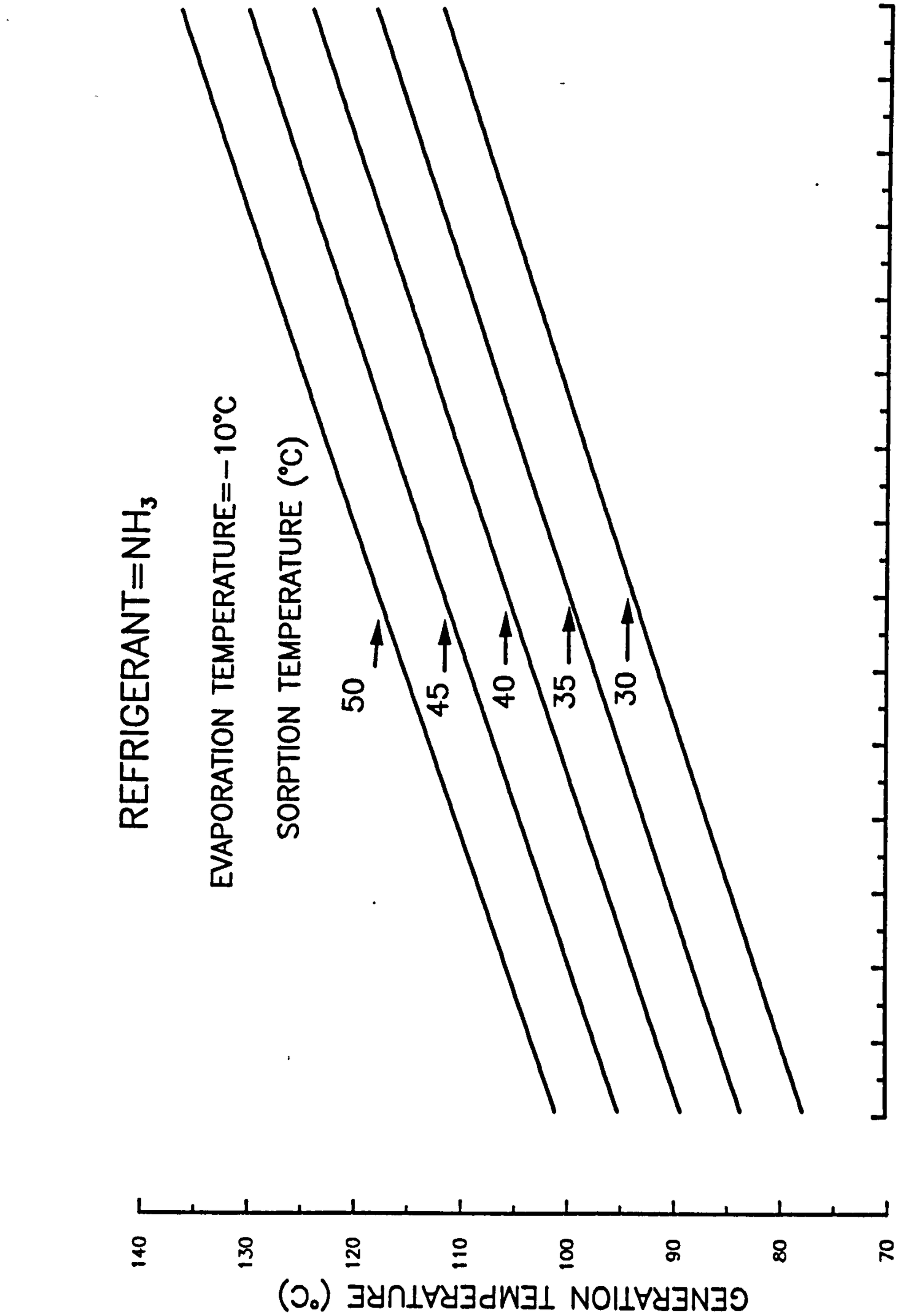

Fig 6.17 Graph showing the variation of generation temperature of ammonia in an adsorption refrigeration cycle

The problem with the concentrating collectors -the alternative for higher operating temperatures of upto 150°C- is that they would need frequent adjustment and would not perform well under diffuse insolation conditions. So the operating temperatures of the refrigeration unit would have to be altered. Ice packs cannot be frozen if evaporation temperature is raised but condensation temperature can be lowered easily by water-cooling the condenser. This can be achieved by placing the condenser in a stagnant pool of water. Under an ambient temperature of 43°C and 50% humidity, stagnant water would be at a temperature of 32°C. Therefore having a water-cooled condenser can reduce the condensation temperature to 40°C.

Using the graphs presented in fig 6.16 and fig 6.17 one can see that by lowering the condensation temperature to 40°C (while sorption and evaporation are taking place at 40 and -10°C respectively) the generation temperature of methanol and ammonia is lowered to 107 and 103°C respectively. This is very much in the range of a flat plate collector. Hence it becomes clear that both methanol and ammonia would need water-cooled condenser to operate under WHO specified operating conditions.

Some other more common refrigerants were also examined on the basis of this newly established suitability criterion. The result of the evaluation exercise is presented in table 6.1. Methanol and ammonia are also listed in the table and one can see that all but sulphur trioxide have their minimum generation temperature fall between that

TABLE 6.1

Minimum generation temperature of various refrigerants

REFRIGERANT	MINIMUM GENERATION TEMPERATURE (°C)		HEAT OF * VAPORIZATION (kJ/kg)
	air-cooled condenser	water-cooled condenser	
METHANOL	124.6	107.2	1102
AMMONIA	118.6	103.2	1374
SULPHUR DIOXIDE	120.8	105.0	390
SULPHUR TRIOXIDE	134.3	114.6	508
METHYL AMINE	122.1	106.0	839
ETHYL AMINE	123.5	107.0	623
WATER	122.1	105.4	2260
NITROGEN DIOXIDE	120.2	105.0	415

Evaporation temperature = -10°C

Sorption temperature = 42°C

* at normal boiling point

of ammonia and methanol. Sulphur trioxide indicated a higher temperature of 114.6^{o}C even when the condenser was water cooled.

Thus methanol and ammonia, because of their higher heat of vaporization, stand out as better refrigerants for solar operated vapour sorption units. Table 6.2 compares the pressure and specific volume of saturated vapours of both the refrigerants at -10 and 50^{o}C. It can be seen that the vapour pressure of methanol is very low compared to ammonia. The specific volume of methanol at -10^{o}C is 90 times that of ammonia which evidently mean that the evaporator pipes would have to be much larger for methanol to avoid the excessive pressure drop due to high velocity. On the other hand, because of very high condensation pressure (37 times that of methanol) and corrosive nature, the ammonia equipment would have to be built from very heavy gauge steel sheet.

The final choice between the two cannot be made in isolation. For example, one would have to take into consideration the corresponding sorbent, its performance with the particular sorbent and the design of the collector-cum-generator.

TABLE 6.2

Comparison of some physical properties
of methanol and ammonia

TEMPERATURE (°C)	SATURATION PRESSURE (bar)		SPECIFIC VOLUME (m^3/kg)	
	Methanol	Ammonia	Methanol	Ammonia
-10	0.018	2.91	37.95	0.418
50	0.556	20.3	1.529	0.063

6.5.3 Evaluation of sorbent pairs

It was concluded, on the basis of their performance, that calcium chloride, activated carbon and zeolite were better sorbents. The performance and the suitability of each one of them for solar refrigeration, with methanol and ammonia as refrigerants, is ascertained in the next few sections.

6.5.3.1 Calcium chloride/methanol

Calcium chloride absorbs methanol and the reaction is chemical in nature. Two interesting studies had been carried out on the equilibrium reaction between the salt and methanol [20,21]. The reaction is represented by the following chemical equation;

$$CaCl_2.2CH_3OH \text{ ==== } CaCl_2 + 2CH_3OH \pm 1700 \text{ kJ/kg } CH_3OH \qquad 6.24$$

which is follows the following pressure-temperature curve [20];

$$\ln p(\text{mbar}) = -6540/T + 22.99 \qquad 6.25$$

The latent heat of vaporization of methanol at -10°C is 1260 kJ/kg (estimated from the value at normal boiling point, using the Watson relation [22]) which means that, ignoring the sensible heat of the absorbent and the equipment, the pair can show maximum COP of 0.74. This is a very reasonable figure but one has to see if the reaction kinetics allow the cycle to take place within 24 hours.

Equation 6.25 represent a reaction equilibrium at 68°C above that of pure methanol. Therefore, in theory, for condensation to take place at 42°C (assuming a water-cooled condenser), a bed temperature of 110°C would be required. In practice after 8 hours, with heating fluid at 142°C, 95% demethanolation occured [20]. In ref [21] 1.5 moles of methanol had been reported desorbed after 4 hours when the heating fluid was at 140°C. These temperatures are within the limits of evacuated tube heat-pipe collectors. The reactions kinetics are reasonable. But one has to look into the sorption process as well.

It was reported in ref [20] that, for methanolation reaction to take place, a divergence in pressure between methanol and the equilibrium pressure of the salt mixture must be more than 23 mbar. The reaction kinetics were observed to slow down at lower evaporation temperatures. For instance, only 45% methanolation occured in 16 hours for an evaporation temperature of -0.9°C and the bed temperature of 37.7°C.

For the envisaged conditions of 32°C ambient temperature (i.e. a bed temperature of 42°C) the equilibrium pressure of the salt mixture (from equation 6.25) would be 2.23 mbar. For evaporation taking place at -10°C, the vapour pressure of methanol would be 18 mbar. This would create a pressure difference of less than 23 mbar (which is necessary to start methanolation) and therefore the reaction would not take place. Thus it was concluded that the calcium chloride/methanol absorption reaction was not suitable for to build a refrigerator to meet WHO/EPI requirements.

6.5.3.2 Calcium chloride/ammonia

The equilibrium reaction between calcium chloride and ammonia is represented by the following chemical equations;

$$CaCl_2.8NH_3 ==== CaCl_2.4NH_3 + 4NH_3 \pm Q_1 \quad 6.26$$

$$CaCl_2.4NH_3 ==== CaCl_2.2NH_3 + 2NH_3 \pm Q_2 \quad 6.27$$

$$CaCl_2.2NH_3 ==== CaCl_2.NH_3 + NH_3 \pm Q_3 \quad 6.28$$

The reactions represented by equations 6.26 and 6.27 take place at temperatures of 97°C and 114°C respectively under a pressure of 20 bars. The reaction represented by equation 6.28 takes place at temperature of 185°C which cannot take effect by solar heat. Thus 6 moles or 102 g of ammonia are available for refrigeration purposes per mole or 111 g of calcium chloride. This is a plus point of the system as the mass of available refrigerant per unit mass of absorbent is considerably large. But to complete the reaction within the limited available sunshine period the kinetics of the system has to be accelerated. This demanded a surface temperature in excess of the equilibrium temperature by about 10-15°C [23]. With a flat-plate collector-cum-generator a maximum degree of generation of 70% was achieved after a period of 6 hours [24]. When evaporation took place at -10°C, cooling of the mixture through convection and night sky radiation was not enough to achieve the desired rate of reaction (to complete the reaction within 16 hours) [23].

The heats of reaction Q_1 and Q_2 are about equal and vary between 2200 and 2500 kJ/kg NH_3 [23], which is approximately twice the latent heat of vaporization of ammonia. This is a bit on the high side and indicate that the thermodynamic cycle COP of this pair can never be more than 0.5.

One crucial problem associated with solid absorption is the swelling of absorbent during absorption. Calcium chloride swells by about 400% on absorbing ammonia [23,24]. The result is compacting of absorbent and reduction in its capacity to absorb more refrigerant. Solution to this problem had been found [23,24] by adding some other binding materials and salts. Up to 20% of binding material had been used in successful units. This represents a wasteful addition to the thermal capacity and decreases the overall COP.

Fig 6.18 shows the equilibrium of calcium chloride/ammonia reaction represented on a Clapeyron diagram. It can be clearly seen from it that equilibrium temperatures during absorption and desorption are determined solely by the evaporation and condensation temperatures, respectively. This is because the solid absorption systems are monovariant and one does not have the freedom of choosing the concentration of the mixture of absorbent and refrigerant as in liquid absorption. This is a serious limitation which leaves one with no straightforward temperature control.

A commercial refrigerator, based on this reaction, produced by Comesse Soudure of France (see chapter 5 for details) has recently

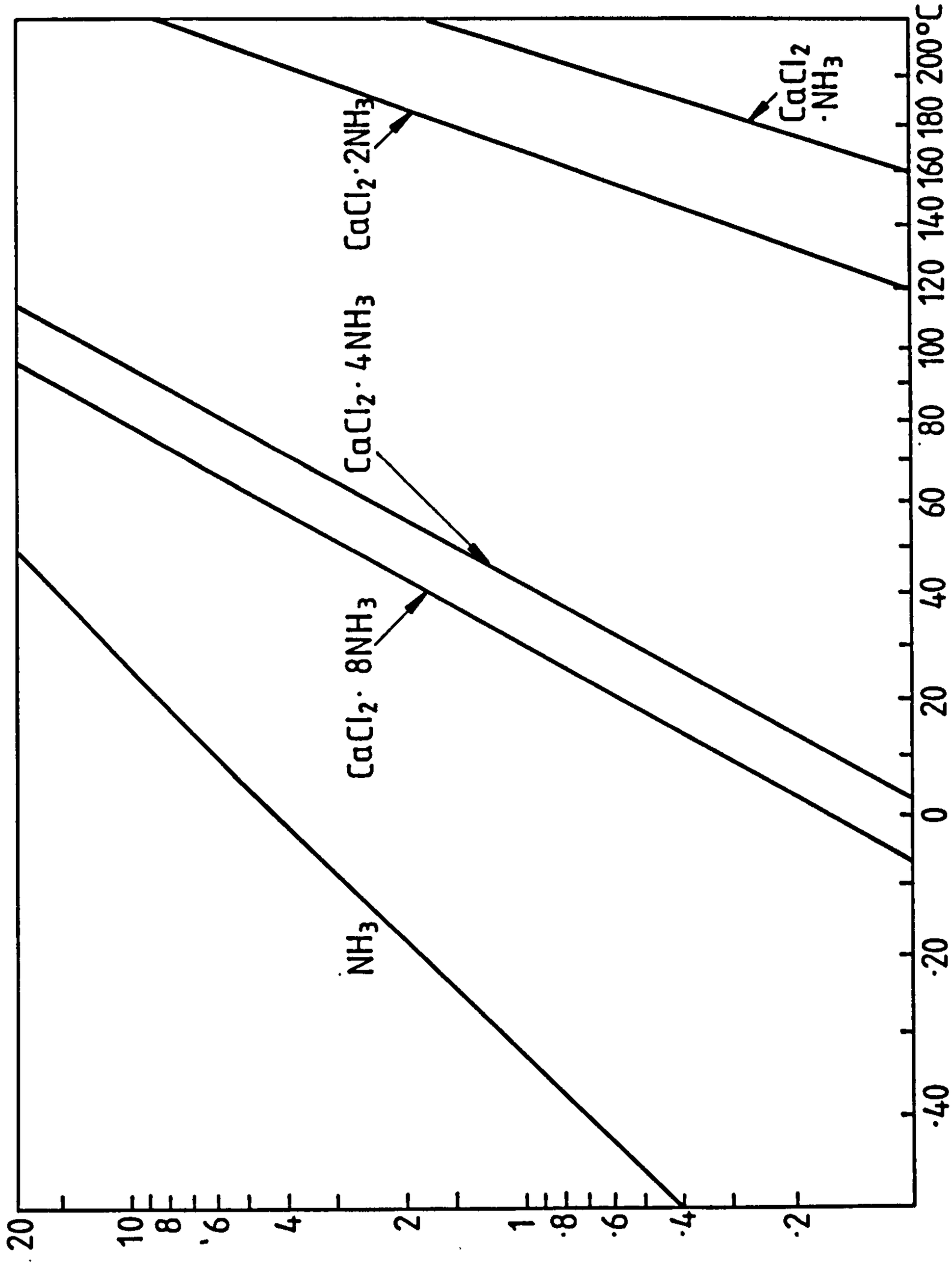

Fig 6.18 Clapeyron diagram for the pair calcium chloride-ammonia

been reported to perform satisfactorily and meet WHO/EPI requirements [25]. The price of US$ 6,000 is very high and reflects the complexity of the circuitry required for maintaining the temperature within the prescribed limits.

6.5.3.3 Activated carbon and zeolite-13X

The two solids, activated carbon and zeolite-13X adsorb the refrigerants. As explained earlier (see chapter 4), adsorption is a physical phenomenon and thus is not accompanied by any changes in the lattice structure of the adsorbent. Therefore the serious problem of swelling exhibited by solid absorbents is not experienced by solid adsorbents. Adsorption systems are bivariant and therefore more freedom is available in the choice of working pressure or temperature. The desired evaporation or condensation temperature can be achieved by varying the concentration of refrigerants into adsorbents.

In order to determine which adsorption pair was better suited to the envisaged application (i.e. a solar operated vaccine store) a model, constructed by using equations 4.19-4.28 (see chapter 4), was employed. The listing of the computer program incorporating the model is included in appendix H. The adsorption equilibrium for the two, with ammonia and methanol, was established experimentally. Table 7.1 (see chapter 7) enlists the characteristic constants for the pairs.

The COP calculations, at various generation temperatures, were done for zeolite/ammonia, activated carbon-208C/ammonia and activated carbon-208C/methanol. The results shown in fig 6.19-6.20 are for the following conditions.

Evaporation temperature	-10°C
Adsorption temperature	45°C
Condensation temperature	40 & 50°C
Generation temperature	100-150°C

The evaluation has been done at two condensation temperatures 40 and 50°C (representing the expected condensation temperature in a water-cooled and an air-cooled condenser respectively) under WHO/EPI specified conditions. Both the refrigerants imposed minimum generation temperatures below which the cycle would not perform. The COP at these temperatures was zero. It can be observed that all the three pairs showed improved performance at higher temperatures. Activated carbon-208C/methanol combination showed the best performance of all with water-cooled condenser. At 120°C generation temperature (which is the upper limit in a flat plate collector) methanol combination cannot work with air-cooled condenser and, although, ammonia worked, its COP was very low (0.045).

The COP so calculated did not take into account the energy which would be lost in heating up the metal box containing the mixture of adsorbent/refrigerant. Ammonia being very corrosive and the system pressure being high, the equipment is usually made of heavy gauge duralumin or mild steel sheets. Therefore the sensible heat loss

6-70

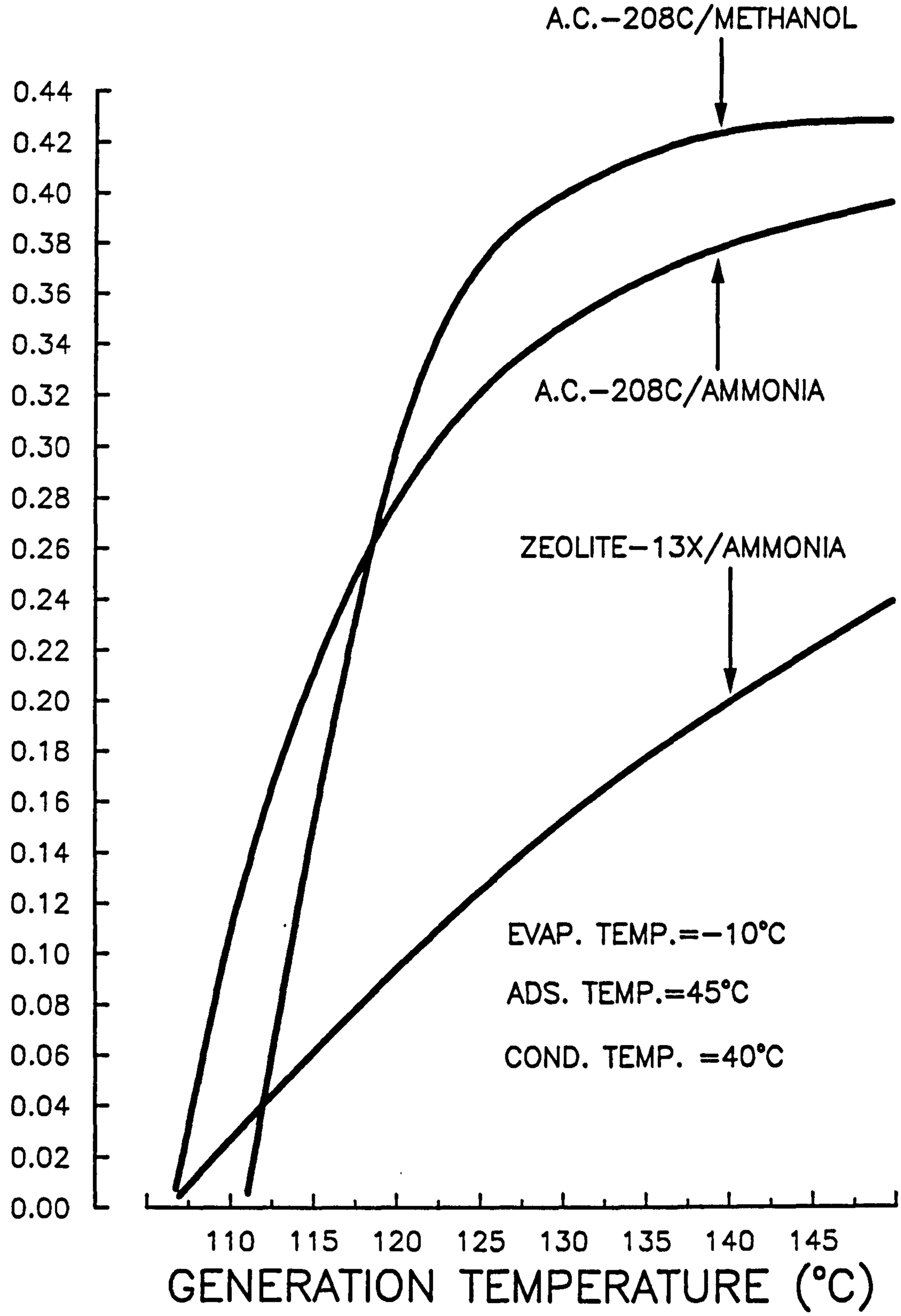

Fig 6.19 COP of various adsorption pairs in an intermittent cycle over a range of generation temperatures (water-cooled condenser)

6-71

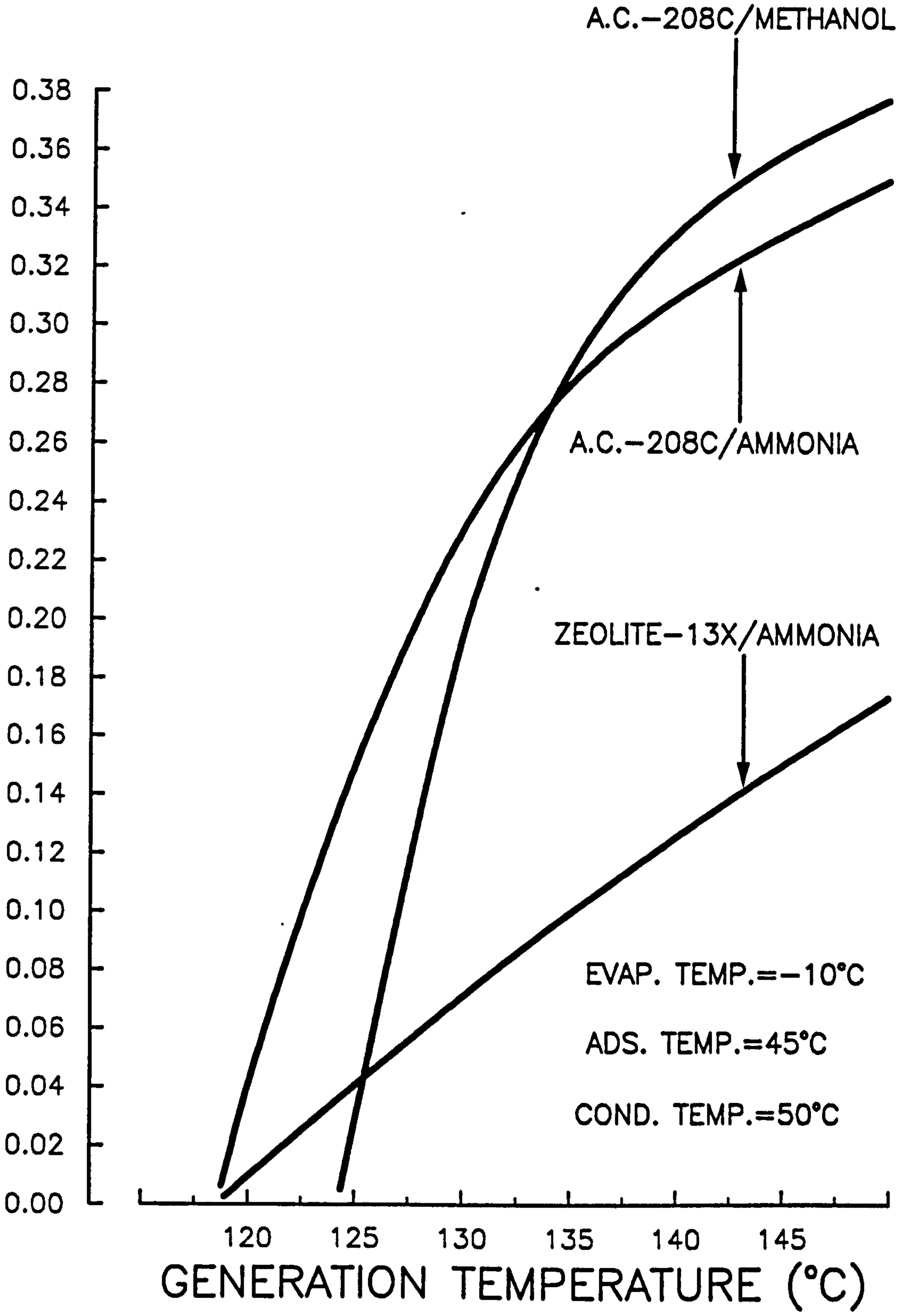

Fig 6.20 COP of various adsorption pairs in an intermittent cycle over a range of generation temperatures (air-cooled condenser)

would be greater in ammonia equipment as both the materials have higher specific heat than copper which can be used in methanol system. This means that the COP of ammonia system would lowered in larger proportion in comparison with methanol system. Thus, on the basis of higher COP, it was concluded that activated carbon-208C/methanol pair is the best suited for the intended application of a solar operated vaccine store.

6.6 The final conclusion

In this chapter three major options were studied in detail. The first one was the photovoltaic vapour compression refrigerator. It was concluded in the part I of this chapter that it was a technically feasible option. It fulfilled the minimum criterion for feasibility but failed to meet the requirements of a feasible option as defined in section 5.2. The major drawbacks of the system can be summarized as below.

(i) Photovoltaic panels are expensive and the technology is not within the reach of developing countries. Thus in case of damage (e.g. as a result of hailstorm) the repairs may take months.

(ii) The electronic control circuitry is prone to failure at high operating temperatures (common in many developing countries). The replacement circuits, therefore, would have to be kept in spare stock at an additional investment.

(iii) The storage batteries have a normal life of 2-3 years. This is a source of recurring expenditure. As the failure of this component renders the system inoperable, additional investment on spare batteries is required as well.

(iv) The storage batteries need a regular attention and maintenance.

Thus the final word about this system would be that it is an expensive system. Its reliability need to be improved either by improving the design of the components that fail or finding alternatives which would dispense with those unreliable parts. The manufacturing and maintenance technology is not available readily in most of the countries expected to use it. It is providing currently an alternative to equip the health centres in remote areas of the developing world. But cheaper and 'low' technology equipment is needed for the promotion of WHO/EPI objectives.

The second option was operating an 'Electrolux' refrigerator by the heat produced from evacuated tube heat-pipe collectors. It looked attractive as both the major components were mass produced already. But in part II of the chapter it was found that to adapt the system to solar operation required major design changes. The changes would have called for a new manufacturing line, which for such a limited market could not be economical. Thus the option was technically knocked out of the competition.

Alternative fuels such as biogas can be produced locally and may be used to meet other energy requirements as well. If the burner design (which is the major cause of failure in kerosene fueled systems) could be improved and made reliable 'Electrolux' type refrigerators could prove to be a good alternative.

The last option considered was a thermally operated intermittent solid sorption refrigerator. This was dealt with in part III of this chapter. Ammonia and methanol were found to be suitable refrigerants

for such a plant. It was further established that under the WHO specified operating conditions both the refrigerants required a water-cooled condenser unless a high temperature concentrating collector was employed as the generator. Two absorption and three adsorption pairs were evaluated.

Calcium chloride/methanol system could not produce ice-producing temperature under 32°C night time ambient temperature and was not in the race any more. Calcium chloride ammonia systems were found to suffer from inherent problems of swelling and no straightforward temperature control. The commercial systems produced were expensive compared to photovoltaic units. The factors contributing towards the high price were (a) the special treatment of calcium chloride to produce stable porous granular material, (b) introduction of thermostatic valves for the temperature control and (c) cooling circuits introduced to cool the absorber.

Heat of absorption is usually much higher than the heat of adsorption. Thus a higher heat input per unit mass of refrigerant would be required for calcium chloride system. Specific heat of calcium chloride is larger compared with zeolite or activated carbon and thermal conductivity is much less than activated carbon (see table 6.3). This would slow down the response of the system under transient conditions and make the heat transfer in the sorbent bed difficult. Owing to these reasons the thermodynamic COP of the cycle under the WHO/EPI specified conditions cannot exceed 0.25. Therefore it was decided to focus attention on adsorption systems which are much simpler and do not require special treatment for the adsorbents.

TABLE 6.3

Physical properties of some sorbents

SOLID SORBENT	BULK DENSITY (kgm^{-3})	SPECIFIC HEAT CAPACITY ($kJkg^{-1}K^{-1}$)	THERMAL CONDUCTIVITY ($Wm^{-1}K^{-1}$)
Calcium chloride	870	2.47	0.12
Zeolite	670	0.92	0.12
activated carbon	500	0.67	0.61

Out of the three adsorption pairs evaluated activated carbon-208C/methanol was considered the best on the grounds of better performance. There are other advantages, too, of using activated carbon as adsorbent, for instant;

(a) activated carbon has the lowest specific heat and the highest thermal conductivity of the three solid sorbents considered (see table 6.3). This means that the response time, under transient conditons, of an activated carbon bed will be lesser and the heat transfer in it will be better in comparison with both the other sorbents;

(b) activated carbon is already manufactured in many developing countries and is a widely used industrial material. It is mass produced from cheap raw material (e.g. coconut shell) and is, therefore, inexpensive; and,

(c) activated carbon properties can be varied easily, by controlling the activation process and treating it with special chemicals, to suit the particular system requirements.

Thus the whole of this excercise proved that a solar stimulated activated carbon-208C/methanol intermittent vapour adsorption refrigerator would meet the WHO/EPI requirements for an autonomous refrigerated vaccine store. Its design was studied in detail and the findings presented in the next chapter.

REFERENCES

1 McAdams, W.H., Heat Transmission, Kogakusha Company, Ltd. Tokyo, Japan, 1954.

2 Sales literature Solarex Corporation USA.

3 Ozisik, M.N., Heat Transfer: A basic approach, McGraw-Hill Book Company, Sigapore, 1985.

4 Wong, H.Y., Heat Transfer for Engineers, Longman, London, 1977.

5 Vincent, C.A., Modern Batteries: An introduction to electrochemical power sources, Edward Arnold, 1984.

6 Kelsey, E.L. and Holt, H.H., Development and Evaluation of A High-Efficiency Power Inverter, NASA technical note NASA TN D-5881, 1970.

7 Adell, A., 'Comparison obtained in a tropical country, of a solid adsorption, solar-driven refrigerator and photovoltaic refrigerator', Journal of Power Sources, vol 15, no 1, pp 1-12, 1985.

8 Goseny, W.B., Principles of Refrigeration, Cambridge University Press, 1982.

9 Linge, K., In Handbuch der Kaltetechnik, by Niebergall, W., Editor Plank, R., Springer-Verlag, Berlin, vol5, p 81, 1966.

10 Uppal, A.H., Norton, B. and Probert, S.D., 'A low-cost solar-energy stimulated absorption refrigerator for vaccine storage', Applied Energy, vol 25, pp 167-174, 1986.

11 Personal communication with BP Solar International, UK, August 1989.

12 Makiya, G.A.A.S., Experimental and Theoretical Investigation of the Behaviour and Heat Energy Distribution In a Diffusion-Absorption Refrigerator, PhD Thesis, University of Strathclyde, Glasgow, UK, 1983.

13 Backstrom, M., Svenska Kyltekniska Foreningens Handbok 1, Third Edition, Almqvist & Wiksell, Uppsala, Sweeden, 1970.

14 Cullimore, D.A., A Solar Operated Absorption Refrigerator, MSc Thesis, Cranfield Institute of Technology, Bedford, UK, 1985.

15 World Health Organization, 'Guide on Implementation of Solar Energy for EPI', WHO/UNICEF technical series, document no WHO/UNICEF/EPI.TS/86.3, Geneva, 1986.

16 Personal communication with Mr. Green at Electrolux, Luton, U.K.

17 Cattaneo, A.G., In Handbuch der Kaltetechnick (Handbook of Refrigeration), by Niebergall, W., Editor Plank, R., Springer-Verlag, Berlin, vol 7, pp 289-291, 1959.

18 Gutierrez, F., 'Behavior of a household absorption-diffusion refrigerator adapted to autonomous solar operation', Solar Energy, vol 40, no 1, pp 17-23, 1988.

19 Dubinin, M.M., 'Porous structure and adsorption properties of activated carbons', in Chemistry and Physics of Carbon, volume 2, Ed: Walker, P.L. Jr., Marcel Dekker Inc., New York, pp 51-120, 1966.

20 Ravelet, R., 'Methanol calcium chloride absorption cycles', paper presented at Commission of the European Community, Absorption Heat Pump Congress, Paris, France, 1985.

21 Offenhartz, P.O'D., Brown, F.C., Mar, R.W. and Carling, R.W., 'A heat pump and thermal storage system for solar heating and cooling based on the reaction of calcium chloride and methanol vapor', Journal of Solar Energy Engineering, vol 102, pp 59-65, 1980.

22 Reid, R.C., Prausnitz, J.M. and Sherwood, T.K., The Properties of Gases and Liquids, Third Edition, McGraw-Hill Book Company, p 210, 1976.

23 Nielsen, P.B. and Worsoe-Schmidt, P., Development of A Solar-Powered Solid-Absorption Refrigeration system, Part I, Report no F30-77.01, Refrigeration Laboratory, The Technical University of Denmark, Denmark, 1977.

24 Eloeje, O.C., 'Design construction and test run of a solar powered solid absorption refrigerator', Solar Energy, vol 23, no 5, pp 447-455, 1985.

25 World Health Organization, Cold Chain Newsletter, no 89.2, August 1989.